Bound By
Blissett Bookbinders
020 8992 3965
www.blissetts.com

Investigation into the application of adult human Müller stem cells in retinal ganglion cell replacement therapy

Shweta Singhal
M.B.B.S.

This thesis is submitted to University College London
for the degree of Doctor of Philosophy

UCL Institute of Ophthalmology
University College London
November 2008

ProQuest LLC
789 East Eisenhower Parkway
P.O. Box 1346
Ann Arbor, MI 48106-1346

Declaration

I, Shweta Singhal, confirm that the work presented in this thesis is my own. Where information has been derived from other sources, I confirm that this has been indicated in the thesis.

London, November 2008

Acknowledgements

I must begin by thanking Dr. Astrid Limb for giving me the chance to do this PhD. This thesis could not have come about without her faith in me at our first meeting and her constant encouragement, support and enthusiasm over the last 3 years. She let me fly solo but was always there to guide when the ride got shaky. I consider myself very fortunate to have had the chance to study science under her supervision. Thank you Astrid, for making this such an enjoyable and exciting research experience.

This PhD could also not have come about without Peng and Peggy Khaw. Peng, thanks for giving me the chance to do this, for all your guidance and advice through this work and especially for teaching me about clinical translation of research. Watching you work in the clinic and outside of it has been an honour. Peggy, thanks for making me feel so welcome when I first came to the Institute and for all your concern and care over the last 3 years. Tackling administrative hurdles is not my forte but you were always an unwavering confidence inspiring ally in these situations. Thank you also for all the delicious food you kept a constant supply of, to feed us hungry students.

This PhD was funded by the Inlaks foundation, India (maintenance); ORSAS UK and UCL fee awards (fees); the Henry Smith Charity, UK and the Arthur and Mildred Slater award (consumables). I am very grateful to all these funding bodies for their support.

Thanks to Jean (Lawrence) for teaching me everything I know about *in vivo* research and Tony Kwan for initiating me into the world of retinal stem cell transplantation. Alison Cambrey and Anna Tsapara were my adopted post docs and I am grateful to them for letting me pick their brains and for teaching me the basics of molecular biology and cloning. Thank you Tom (Prof.Tom Salt) for allowing me into the dark and mysterious world of electroretinography and Anne (Georgiou) and Becca (Longbottom) for teaching me how to make my way through it. Thank you Ant (Antony Vugler) and Mitali (Patel) for the generous donation of your time and expertise with immunostaining and QPCR; Wendy,

Nicky, Amy and all the BRU staff for their constant support and guidance during the *in vivo* experiments; and Grazyna for all her help with the FACS analysis. Thanks also to Steve Griffiths, Claire Cox and Aida for all their help with ordering and maintenance of lab supplies and equipment.

I'd like to thank Bhairavi for being one of 'Astrid's girls' with me. This PhD was half as traumatic and twice as much fun because you were around. Lux and Maria, thank you for being the friends I have missed here in my home away from home, for making sure I ate lunch and for always being handy with an ear or a shoulder when I needed one. Thanks to Jenny Murray, Laurence Dufaur, Stelios Georgoulas and Hari Jayaram for all the fond memories of our fun times together during these last 3 years.

To my parents who have always believed in me even when the going was tough, thank you for letting me go and follow my dreams and for being the wonderful loving people you are. Thanks to my dear brother Saurabh for his touching and unfailing vote of confidence in his big sister. To Amma, Appa, Rashmi and Patti, when I got married, I acquired another mother, father, sister and grandmother. Thank you for making me a part of the family and for your pride and joy in my work.

And to Anand, my husband...thank you for helping me with cloning, calcium imaging and microscopy, for feeding me while I was writing this thesis, for bailing me out numerous times when I was stuck for ideas, for teaching me how to think critically, for all the times when you had more confidence in my work than I did and kept me going; and for being the kindest person I know. I could not have done this without you by my side, rooting for me all the way.

Finally, there would be nothing to put in this thesis, if it hadn't been for Sally, her family and friends and everything they gave up. This piece of work is therefore dedicated to them. To Sally, her family and her many many friends...

Abstract

This work investigated the potential of adult human Müller stem cells to differentiate towards a retinal ganglion cell (RGC) fate *in vitro* and their ability to replace damaged RGC *in vivo*. Müller stem cells isolated from the adult human retina were examined for their expression of RGC developmental markers ATOH7, BRN3B, ISL1 and HUD, and extracellular matrix proteins and growth factors were used to modulate the expression of these RGC makers by these cells *in vitro*. The role of the Notch signalling pathway in Müller stem cell proliferation and differentiation was also examined and it was found that inhibition of Notch activity using gamma secretase inhibitor DAPT could further promote differentiation of these cells towards RGC fate *in vitro*. Cell preparations enriched for RGC developmental markers demonstrated neural morphology with extensive neurite formation. More significantly Müller stem cells differentiated into the RGC phenotype were able to demonstrate neuronal function as elicited by changes in their cytosolic calcium in response to neurotransmitter stimulation with nicotinic agonists.

To further confirm the RGC phenotype, a BRN3B GFP transcriptional reporter was designed and transfected into the Müller stem cells to specifically identify the BRN3B expressing committed RGC precursors. Transduced cells expressing GFP were found to be post mitotic, expressed high levels of differentiated RGC markers and increased in numbers when cultured in the RGC differentiating conditions mentioned above.

Transplantation of Müller stem cells *in vivo* into models of retinal degeneration revealed that microglia and chondroitin sulphate proteoglycans (CSPG) present a significant barrier to transplant cell migration. Use of enhanced immunosuppression and the CSPG degrading enzyme Chondroitinase ABC significantly improved transplant cell survival and migration of Müller stem cells in degenerating RCS rat retinae. These transplant conditions were used in eyes depleted of RGC by NMDA in the presence of Triamcinolone, to study the ability of differentiated Müller stem cells differentiated into RGC to replace these cells *in vivo*. The RGC differentiated Müller stem cells were able to migrate and integrate into the RGC depleted rat retina. More significantly they were able to partially restore lost retinal ganglion cell

function as demonstrated by an improvement in the negative scotopic threshold response on the ERG.

These results suggest that adult human Müller stem cells are similar to embryonic retinal progenitors in their intrinsic programming and can be directed using the same developmental cues to differentiate towards an RGC fate *in vitro*. Müller stem cells differentiated into RGC are also able to integrate and partially restore function in models of RGC depletion *in vivo*. They may therefore constitute a potential source of RGC for replacement therapy in glaucoma.

Table of Contents

List of figures

Chapter 1

Chapter 2

Chapter 3

Chapter 4

Chapter 5

Chapter 6

Chapter 7

Chapter 9

List of Abbreviations

AchE	Acetylcholinesterase
AMPA	α-amino-3-hydroxy-5-methyl-4-isoxazolepropionic acid
AMV	Avian Myeloblastosis Virus
ATOH7	Atonal Homologue 7
BAC	Bacterial Artificial Chromosome
Brm	Brahma
CBF-1	C-promoter binding factor-1
CDK2	Cyclin-dependent kinase 1
ChABC	Chondroitinase ABC
Chx10	Ceh-10 homeo domain containing homolog
CNS	Central Nervous System
CNTF	Ciliary Neurotrophic Factor
CSL	CBF-1, Suppressor of Hairless, Lag1
CS stub	Chondroitin Sulphate stub
CSPG	Chondroitin Sulphate Proteoglycan
DAPT	N-[N-(3,5-Difluorophenacetyl)-L-alanyl]-S-phenylglycine t-butyl ester
DART-PCR	Data Analysis for Real Time PCR
DMSO	Dimethyl Sulfoxide
DMEM	Dulbecco's Modified Eagle's Medium
DNA	Deoxyribonulceic Acid
dNTP	Deoxyribonucleotide Triphosphate
DSHB	Developmental Studies Hybridoma Bank
DTT	Dithiothreitol
DZ	Debris Zone
ECM	Extracellular matrix proteins
EDTA	Ethylenediaminetetraacetic acid
EGF	Epidermal Growth Factor
ELAVL4	Embryonic Lethal, Abnormal Vision, L4

ERG	Electroretinogram
ESC	Embryonic Stem Cells
FACS	Fluorescence Assisted Cell Sorting
FBS	Fetal Bovine Serum
FGF	Fibroblast Growth Factor
GAP-43	Growth Associated Protein-43
GAPDH	Glyceraldehyde 3-phosphate dehydrogenase
GCL	Ganglion cell layer
GFP	Green fluorescent protein
GSI	Gamma Secretase Inhibitors
HD	Homeodomain
Hes1	Hairy and enhancer of split-1
Hes5	Hairy and enhancer of split-5
Hey2	Hairy/enhancer-of-split related with YRPW motif 2
HESCs	Human Embryonic Stem Cells
HUD	Human antigen D
ICD	Intracytoplasmic Domain
ILGF	Insulin-Like Growth Factor
IOP	Intra ocular pressure
INL	Inner nuclear layer
ISL1	Islet 1
Isl2	Islet 2
KA	Kainic Acid
KO	Knock out
LB	Luria-Bertani
LIM	Protein structural domain named after Lin11, Isl-1 & Mec-3
LH	Lister Hooded
Math3	Mouse Atonal Homologue 3
Math5	Mouse Atonal Homolgue 5
MERTK	MER Receptor Tyrosine Kinase
MG	Matrigel
MIO	Moorfields Institute of Ophthalmology
mRNA	messenger Ribonucleic Acid

NMDA	N-methyl D-Aspartate
NF-L	Neurofilament-Light
Nrl	Neural retinal leucine zipper
NR	Neural retina
nSTR	negative Scotopic Threshold Response
Oct1,2	Octamer-binding transcription factor 1/2
OCT	Optimum cutting temperature
ON	Optic nerve
OPL	Outer plexiform layer
OS	Outer Segments
Otx2	Orthodenticle homeobox 2
Pax6	Paired box gene 6
PFA	Para formaldehyde
Pit1	POU domain, class 1, transcription factor 1
PMSF	Phenyl Methyl Sulfonyl Fluoride
PN	Post natal
POU	Pit1, Oct1, Unc86
PVDF	Polyvinylidene Fluoride
QPCR	Quantitative Polymerase Chain Reaction
RA	Retinoic Acid
RARE	Retinoic Acid Response Elements
RCS	Royal College of Surgeons
RGC	Retinal Ganglion Cells
RIPA	Radio Immuno Precipitation Assay
RP	Retinitis Pigmentosa
RPE	Retinal Pigment Epithelium
RT PCR	Reverse Transcriptase Polymerase Chain Reaction
Rx	Retinal Homeobox
SDS	Sodium dodecyl Sulphate
Six-3	Sine oculis-related homeobox 3 homolog
siRNA	small interfering Ribonucleic Acid
Shh	Sonic Hedgehog
SRS	Sub retinal space

Sox2	SRY-box containing gene 2
STR	Scotopic Threshold Response
TA	Triamcinolone Acetate
TBS	Tris Buffered Saline
TGFβ	Transforming Growth Factor-β
TLE1	Transducin like enhancer of split 1
TF	Transcription Factor
TUNEL	Terminal deoxynucleotidyl Transferase Biotin-dUTP Nick End Labeling
Unc-86	UNCoordinated-86
VEP	Visual Evoked Potential
Xath5	*Xenopus* atonal homologue 5

Chapter 1: General Introduction and Objectives

1.1 Müller glial stem cells

The adult human body has the ability to repair and regenerate. Although this is true of most organ systems, the central nervous system (CNS) was thought to be impossible to regenerate until recently. The presence of constantly regenerating neurons in the adult olfactory epithelium was the earliest evidence that there are areas of the CNS capable of self renewal (Graziadei & Grasiadei 1979;Graziadei, Levine, & Graziadei 1978). Since then a lot of progress has been made in the field of neural repair and regeneration and it is now possible to grow neurons *in vitro* from various areas of the embryonic/ neonatal and adult brain. In this context, it is of interest that neural glia have been found to be an important cell source for regenerating neurons. Glial cells were previously thought to play a purely supportive role, but compelling evidence has now shown that they retain the ability to divide and differentiate into cells of various neuronal phenotypes in response to insult and injury (Anthony et al. 2004;Campbell & Gotz 2002;Doetsch 2003;Ever & Gaiano 2005;Hartfuss et al. 2001;Merkle et al. 2004;Mori, Buffo, & Gotz 2005).

The eye, viewed as an extension of the central nervous system, works on similar principles of development. The same neurectoderm that forms the major portion of the cerebral cortex also gives rise to the neuroretina. Joe Hollyfield in 1968 described the presence of actively dividing cells in the ciliary marginal zone of the peripheral retina of frog tadpoles (Hollyfield 1968). This work described the role of this zone of dividing cells in the circumferential enlargement of the tadpole retina and the thickening of its inner nuclear layer of cells with progressive development. This region was later found to maintain mitotic activity even in adult eyes where the developmental process was completed, and this was later confirmed in post-hatch chick eyes as well (Fischer & Reh 2001;Ghai, Stanke, & Fischer 2008;Perron & Harris 2000). The mammalian eyes are not known to have a ciliary marginal zone but populations of retinal progenitors in the ciliary body have been described in adult mice (Tropepe et al. 2000), pigs (Gu et al. 2007;MacNeil et al. 2007) as well as humans (Coles et al. 2004).

It has since been established that as in the CNS, the glial population of the retina namely the Müller cells also possessed the ability to divide in response to injury. Müller cells form the glial population of the retina and are responsible not only for

the structural organisation of the various cellular layers present in this tissue, but also perform important metabolic functions. They are responsible for the uptake and mopping up of the neurotransmitter glutamate in the retina, thereby preventing toxicity through its accumulation (Ramon & Cajal 1972).The role of Müller glia in retinal regeneration was first described in the zebrafish which are known for their retinal regenerative capacity. The zebrafish retina has the ability to repair and regenerate all its layers following full thickness retinal injury. This remarkable ability has now been categorically shown to be the result of Müller cell dedifferentiation, re entry into the cell cycle and production of a progeny that subsequently differentiates into retinal neurons. Together the ciliary marginal zone and the Müller glia have now been shown to be the stem cell niches of the zebrafish retina (Fausett & Goldman 2006;Raymond et al. 2006;Yurco & Cameron 2005). Evidence of similar behaviour of Müller glia in the chick retina has also been found with the Müller glia dividing and differentiating into retinal progenitors in response to factors associated with retinal injury like insulin and FGF (Fischer & Reh 2001). Recent work has suggested that mammalian Müller cells have similar properties, although mammals greatly differ in their ability to regenerate their retinae compared to the zebrafish. The Müller glia of rat eyes have been shown to respond to an injurious stimulus and proliferate *in vivo* and *in vitro* demonstrating the characteristics of retinal progenitors (Das et al. 2006). Rat Müller cells are activated *in situ* in the presence of injury as demonstrated by the expression of neural progenitor markers like nestin, and an increase in their rate of division and proliferation. Further, when transplanted into an eye with damaged or degenerating retina these cells show the ability to integrate and differentiate into retinal neurons (Das, Mallya, Zhao, Ahmad, Bhattacharya, Thoreson, Hegde, & Ahmad 2006). Most recently, it has also been shown that persisting retinal progenitors in the central neural retina of mice with a Chx10 mutation also exhibit Müller glial characterisitics adding further support to the role of Müller glia as retinal progenitors (Kokkinopoulos et al. 2008).

Given this background, establishing the stem cell role of Müller glial cells in the human eye became considerably significant. Behaviour of Müller cells in the human eye *in vivo* is more difficult to study. The response of these cells to injury can not be easily examined given the obvious ethical impracticality of performing the necessary *in situ* experiments. It is however possible to study human retinae in organ culture

systems and to isolate the Müller cells *in vitro* for culture. Using these methods, a spontaneously immortalised Müller cell line was first isolated from an adult human eye and characterised at the Institute of Ophthalmology, London. The cell line was called the MIO (Moorfields Institute of Ophthalmology) cell line, named after the research institute and the affiliate eye hospital (Limb et al. 2002d). Since the isolation of this first cell line, similar cells have been isolated from other post mortem retinae and each of these are able to expand indefinitely in culture without any genetic manipulation or the help of additional growth factors. On this basis they are considered to be immortal. Karyotyping analysis revealed that the MIO M1 cell line showed considerable levels of polyploidy, but 4 other cell lines tested upto passage 4 had less than 10% polyploid cells. However despite the polyploidism of these cell lines, there has been no evidence of tumorogenecity when the cells were transplanted into experimental animals (Limb GA unpublished work). Spontaneous acquisition of extra chromosomes has been widely observed with several types of stem cells *in vitro*; including embryonic cells (Baker et al. 2007) and this process is not well understood.

A stem cell is defined by its ability to continually self renew and by the ability of its progeny to differentiate into a number of different cell types (multipotency). Haematopoietic stem cells for example are derived from the adult bone marrow, can indefinitely self renew and have the ability to give rise to progeny that can differentiate into all the various blood cell types. The stem nature of these cells is well established and transplantation of these cells (bone marrow transplants) can be used to replace a various blood cell types in haematological deficiencies. The cells from the MIO cell lines exhibit Müller glial characteristics *in vitro* (morphological and electrophysiological), can continually self renew in culture, express major retinal progenitor markers like Sox2 and Pax6, form neurospheres with actively dividing cells when placed in differentiating conditions and express markers of differentiated retinal neurons like rhodopsin, peripherin and HUD (albeit in small numbers) (Fig1.1). When transplanted into rat models of retinal degeneration, these cells showed limited migration into the retina (better in neonatal eyes compared to adult), but cells that migrated expressed markers of retinal neurons (Lawrence et al. 2007c). It is believed therefore that unlike retinal progenitors which have restricted proliferation potential and limited potency, the Müller cells are more akin to retinal

stem cells. Based on this evidence they were designated stem cells of Müller glial origin and in this thesis the long term human Müller glial cultures are referred to as Müller stem cell lines. There is however no evidence so far that these human Müller stem cells are able to regenerate retinal tissue by giving rise to functional retinal neurons. Nevertheless, the above evidence suggests some similarity in the behaviour of human Müller glial stem cells to those of zebrafish and rat retina. These cells could form an invaluable source of retinal neurons for treatment in a wide variety of retinal diseases. Not only would they offer an adult source of stem cells which could potentially be used for transplantation, it may be possible that the patients' own Müller cells could become the source of new retinal neurons to replace their damaged retinae.

There is no evidence of human Müller glial proliferation *in vivo*, and while this is difficult to test, it is thought unlikely that Müller glia demonstrate any stem cell behaviour in a diseased human retina. With progressing evolution the ability of the central nervous system to repair itself is seen to decline and it is likely that the human retinal Müller glia do not have the inherent ability or the right environmental signals necessary to perform such repair spontaneously in response to injury *in vivo*. If however the signals that stimulate the activation of a Müller glial cell into a stem cell could be identified, it may be possible to apply these signals intraocularly and achieve such activation *in vivo*. In other words, given the right signals, it may eventually be possible to switch on the stem cell behaviour of the human Müller glia in patients with retinal disease. This could then potentially enable them to regenerate their own damaged retina without the need for transplantation.

1.2 Müller stem cells are a potential source of stem cells for retinal regeneration

In order for stem cells to repopulate a given tissue, they must possess the ability to differentiate into the target tissue type, be amenable to integration into the host tissue without being rejected by the host immune response and ultimately be able to perform the functions of the intended target tissue (Lund et al. 2001a;Taupin 2006).

The ability of a stem cell to differentiate towards a particular cell fate is obviously crucial to successful tissue repair. The differentiation may be achieved *in vitro* or *in*

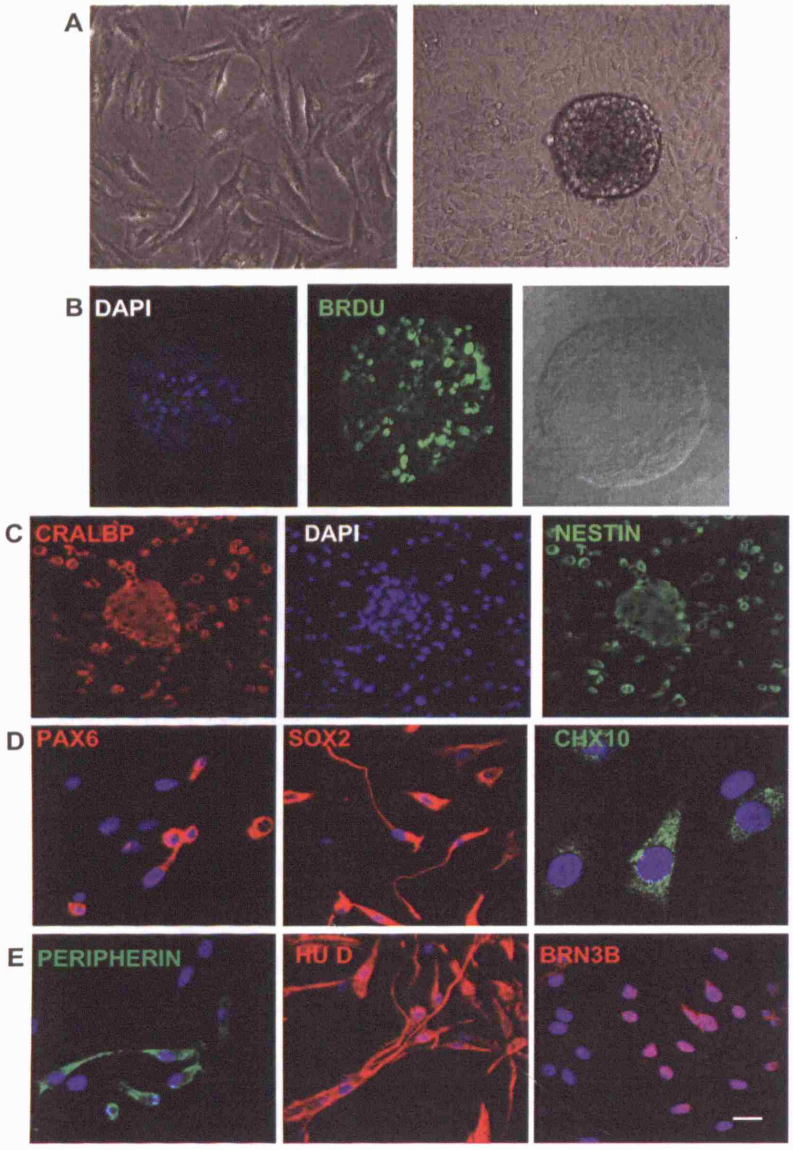

Figure1.1: Retinal progenitor nature of Müller stem cells

Müller stem cells isolated from the adult human retina can be cultured as monolayers (A). They can be induced to form actively dividing neurospheres as shown by BrdU staining (B). The neurospheres give rise to cells expressing Müller glial markers like CRALBP as well as neural progenitor markers like Nestin (C). Müller stem cells have the ability to express retinal progenitor markers like Pax6, Sox2 and Chx10 (D). When induced to differentiate they can also express markers of differentiated retinal neurons like peripherin, HuD and Brn3b (E). C,D,E derived from Lawrence et al, 2007.

vivo but the potential ability to differentiate is required. Embryonic stem cells are believed to differentiate in to numerous cell types and for this reason they are considered to be a very good source of cells for tissue regeneration. It would be ideal if stem cells could directly differentiate into the target cell type once transplanted but no evidence of this has been seen and much research is currently being undertaken to identify the conditions in which these cells can be differentiated prior to transplantation (Yao et al. 2006). It therefore becomes desirable that the differentiation be achieved with as few treatments as possible. The chances of achieving differentiation *in vitro* may improve with the ontogenic proximity of the intended cell fate to the source stem cell during development, i.e. the closer the stem cell source is developmentally to the intended differentiated cell type the easier it should be to achieve differentiation *in vitro*. For example a limbal stem cell is pre-destined to form corneal epithelial cells and would require lesser manipulation to form a corneal epithelial cell from it than a neural progenitor (Shortt et al. 2007;Zhao et al. 2008). Similarly, if one was to derive a retinal neuron from an embryonic stem (ES) cell, the ES cell would first need signals to convert into a neural progenitor, then signals to make retinal progenitors and finally signals to differentiate into the specific retinal neuron of interest (Lamba et al. 2006). By contrast Müller stem cells are already retinal neural progenitors and express all the markers an ES biologist would be looking for in order to achieve retinal progenitor status (Fischer & Reh 2003b;Lawrence et al. 2007f;Ooto et al. 2004). The only manipulations required in this case would be signals to direct them towards a specific retinal neuronal fate. In terms of the ability to differentiate towards a neural retinal phenotype, research has indicated that Müller stem cells are ideally placed developmentally.

Integration into the host tissue has proved to be a difficult problem to solve. Retinal transplant biologists all over the world have found that stem cells transplanted into the diseased retina either die as a result of the host immune response or if they survive, fail to integrate into the host tissues. Several means of immune suppression have been used to prevent host rejection of transplanted tissue, but the failure of transplanted cells to integrate despite this immune suppression suggests that other factors are at play preventing this integration. Factors attributed to this failure include the lack of plasticity of the mature host tissue, the presence of

physical barriers, such as scarring, absence of developmental signals that allow tissue repair or a function of the transplanted cells themselves. Recent work has emphasised the importance of the stage of differentiation of the transplanted cells in integration. McLaren and Pearson et al showed that the ontogenic stage of the transplanted cell is important in achieving successful integration into the degenerated retina. They transplanted rod precursors at various stages of development into adult mice retinae and showed that cells in a particular stage of rod differentiation, just after cell cycle exit possessed the best ability to integrate into the mouse retina and restore function (MacLaren et al. 2006b). In order to successfully repair retinal tissue, it is important that these barriers to integration, both physical and developmental, are identified and overcome.

Ultimately the functional success of retinal cell transplantation may depend on the successful achievement of the above goals. In addition, once transplanted cells achieve complete neural differentiation, they will need to function as such and will be required to form the right synaptic connections with adjacent, proximal as well as distal neurons to re-establish the retinal neuronal network.

Various sources of retinal stem cells have previously been studied and all pose the problem of limited migration or failure to integrate. Most of these tissues are also xeno and allografts and face additional problems of immune rejection. Embryonic progenitors, retinal progenitors, central nervous system progenitors and even Schwann cells are among the various cell types that have been studied and the only human cells used so far include the embryonic stem cells (Banin et al. 2006b) the ciliary body cells and the RPE cells (Little et al. 1996a;Lund et al. 2001b;Lund et al. 2007a;Mizumoto et al. 2001;Sakaguchi, Van Hoffelen, & Young 2003b;Takahashi et al. 1998b;Wojciechowski et al. 2002b;Young et al. 2000a). However there is no categorical evidence to suggest that any one of these cells fully achieve an ideal outcome after transplantation, and while there is some evidence for the differentiation of some cells into mature retinal neurons, very little evidence for their ability to form functional synapses with the existing neuronal circuitry has been shown.

It may be possible to suggest that Müller stem cells exist in the retina for the specific purpose of replacing retinal neurons and it is therefore likely that they possess the intrinsic programming that retinal progenitors possess during development.

However, transplantation of undifferentiated Müller stem cells only achieves a minute degree of differentiation and integration; not sufficient to be of good therapeutic use at present (Lawrence et al. 2007e). Further understanding of the signals that direct their differentiation into retinal neurons is required and this work was aimed at identifying the developmental signals that might be used to effect differentiation of Müller stem cells into retinal neurons *in vitro*. Upon transplantation, xenogeneic Müller stem cells seem to induce a considerable immune response from the host and while this could in part be due to the fact that human tissue was being transplanted into rat models, there are other physical barriers that need to be considered. This investigation therefore attempted to examine these barriers and identify methods to overcome them thereby promoting integration of stem cells upon transplantation.

1.3 Potential of stem cell based therapies in the treatment of advanced glaucoma

Clinically defined as optic nerve damage and visual field loss arising as a result of raised intra ocular pressure (IOP), glaucoma is one of the most common causes of blindness second only to cataract worldwide. Retinal ganglion cells (RGCs) carry signals from the retina to the brain. Their axons form the nerve fibre layer of the retina and leave the eye in the form of the optic nerve. The optic nerve head is the point of exit of these nerve fibres from the eye and this is where the nerve fibres are believed to be damaged during glaucoma. Unlike cataracts which are easily treated surgically, visual loss due to glaucoma is irreversible and cannot be corrected. The current means of treatment is preventative control of IOP and involves the use of either topical medication or filtration surgery. This regulates the amount of aqueous humor being either produced or drained from the eye thereby controlling the IOP. Detected early and treated in this manner it is possible to control the disease and vision can be preserved for considerable periods of time with careful monitoring and timely intervention. However such care is not always possible and there are several instances when the disease is either not picked up until very late in its history, progresses rapidly or is resistant to existing treatments. Control of IOP can be

extremely difficult in these cases and retinal ganglion cell damage is inevitable (Alward 1999).

The loss of vision associated with glaucoma is progressive and proportional to the amount of ganglion cell damage. The predominant and early visual manifestation of glaucoma is peripheral field defects which progress centrally as the extent of the nerve damage worsens. Eventually all of the nerve fibres are damaged or dead and vision is lost completely and irreversibly. The only possible means of restoring vision in such a case would be to replace the damaged RGC with healthy functional RGCs. These should possess the ability to restore synaptic connections with the retinal neurons as well as the brain. While sourcing healthy RGC to replace the damaged ones in an eye seems a challenging task in itself, identifying the signals responsible for directing RGC axons and achieving accurate synapse formation with the brain once these cells have potentially been transplanted into the eye has often been deemed too ambitious, given our current understanding of visual pathway development. Testimonial to this is borne by the fact that most of the current research in retinal stem cell biology focuses on the differentiation of retinal stem cells into photoreceptors and not retinal ganglion cells. The significant visual disability caused by photoreceptor disease and the lack of any comprehensive treatments in this field certainly warrants the attention photoreceptors receive from stem cell biologist. In addition the fact that RGCs would be much more difficult to integrate into the host tissue post transplantation compared to photoreceptors has proved a deterrent to retinal stem cell biologists pursuing this field. Clinically however the need for RGC replacement does exist and the numbers of glaucoma patients facing blindness increases everyday with no current hope of treatment.

The degree of nerve damage an eye with glaucoma has undergone can be depicted numerically to a certain extent and this measure (the cup: disc ratio) is used clinically to follow disease progression in a patient. As the RGC nerve fibres pour out from the outlet in the back of the eye (the lamina cribrosa), like strings through a ring, they leave in the centre of the 'ring' a space referred to clinically as the cup. The ring itself is referred to as the optic disc. With increasing RGC damage, fewer nerve fibres pass through the disc, leaving a larger space in the centre of the disc. In other words as glaucoma progresses the cup becomes larger (Fig 1.2). The ratio of the cup and the disc sizes is used as an indicator of the amount of glaucomatous

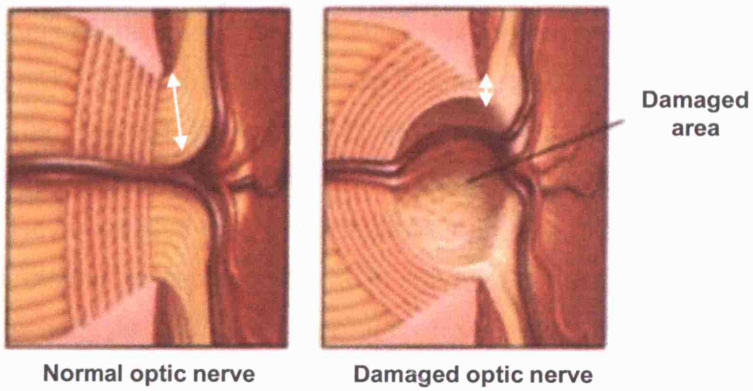

Figure1.2: Glaucomatous damage to the retinal ganglion cell axons

In a normal retina the axons of the retinal ganglion cells leave the retina through the optic nerve and form a thick layer of nerve fibres (shown by the long white arrow in the normal optic nerve). In glaucoma as a result of raised intra ocular pressure, the axons of the retinal ganglion cells are damaged and this results in death and subsequently thinning of the nerves (as seen by the short white arrown in the damaged optic nerve. It is this loss that would potentially require replacement by the neural stem cells. Image modified from www.intecheye.com/Upload/glaucoma1.jpg

nerve fibre damage an eye has undergone. Normal cup to disc ratio (C:D ratio) is in the range of 0.3 to 0.4 while patients with advanced glaucoma can have cup disc ratio of as high as 0.9- 0.99 which means that these patients have lost 90- 99% of their nerve fibres (Alward 1999). However despite such an evident loss of nerve fibres, a considerable percentage of patients with advanced glaucoma possess enough central vision to be able to look after themselves and maintain a reasonable quality of life right up to the point where they lose all of their nerve fibres and finally become blind. What this suggests is that less than 10% of the optic nerve fibres are sufficient to maintain reasonable central vision and that perhaps even 1% of RGCs might be sufficient to enable processing of visual signals that make the difference between preserved central vision in advanced glaucoma and debilitating blindness. With loss of the remaining 1% complete irreversible blindness ensues. It might therefore be possible to replace only a very small proportion of all of the damaged RGCs in glaucoma. If just this small percentage of RGCs could be functionally replaced, it might restore the minimal central vision that is so invaluable to these patients in maintaining their quality of life. The challenge at this point is simple as only a few RGCs need to be sourced to effect this change and is arguably likely to be a significant step towards preventing blindness in glaucoma. These clinical observations must at this point be considered subjective as they have not been formally studied. However they lead us to believe that it might be possible to use stem cell transplantation to replace RGCs in advanced cases of glaucoma and make a real difference to the quality of life of patients who would otherwise eventually and inevitably become irreversibly blind. With this in mind this research has pursued the investigation of Müller stem cells as a potential source of RGCs.

Formation of synaptic connections of new neurons within the host brain *in vivo* is a difficult problem and at present much research is being undertaken in the field. Numerous transcription factors and signalling molecules have been identified to date which direct the formation of synaptic connections between the optic nerve fibres and the brain during development (Haupt & Huber 2008). It has been proposed however that it might not be necessary for the transplanted retinal ganglion cells to form too may connections with the brain. This suggestion derives from evidence that surviving RGC post axotomy can form intra retinal axons and thereby re-establish some synaptic connections to the colliculus (Watanbe, Sawai,

& Fukuda 1997). It might therefore be possible that parallel synaptic connections with surviving retinal ganglion cells might be sufficient to restore function.
While the answers to these questions still remain unknown, this work has primarily addressed the problem of achieving functional differentiation of retinal ganglion cells *in vitro* using Müller stem cells as the source.

1.4 Potential of Müller stem cells to differentiate into RGC

1.4.1 Developmental cues in the study of Müller stem cells in vitro

In order to delineate the signals that might affect Müller stem cell differentiation, examination of retinal development is essential. It is possible to suggest that Müller glial cells, like the neural glia, were pre-destined to replace retinal neurons when required. It is likely that they have an intrinsic programming similar to that of retinal progenitors during development. This programming along with external environmental cues directs the complex pattern of retinal differentiation in the embryo. Every retinal neuron is born at a particular stage of retinal development and this timing is well conserved across species. The retinal ganglion cells are the first to be born followed by the photoreceptors (cones in species that possess them).The last cells to be born are the Müller glia. It has been suggested that Müller stem cells are a population of late retinal progenitors that did not fully differentiate into Müller glia thereby retaining some Müller glial characteristics as well as the ability to divide and behave as progenitor cells(Furukawa et al. 2000e). If this were true then one would assume that Müller stem cells would be limited in their ability to differentiate into late retinal neurons only. However it has been found that Müller stem cells express markers of early (RGC) as well as late (rods) retinal neurons, suggesting that they possess the ability to form all types of retinal neurons and are not limited in their progenitor ability (Lawrence et al. 2007d).

1.4.1.1 Transcription factors in RGC development

Specific transcription factors (TFs) and signalling pathways together orchestrate the different periods of development and this network maintains the tightly coordinated process of differentiation of particular retinal neurons in the correct spatiotemporal pattern (Mu & Klein 2004). Given their function, these transcription factors

themselves have a distinct spatiotemporal pattern of expression in the developing retina. For example members of the achaete scute homologue family of transcription factors are expressed early during RGC development while members of the neurogenin family of TFs are expressed later during terminal RGC differentiation by which time the late retinal neurons are just beginning to form and other photoreceptor specific TFs like Nrl are being expressed alongside (Matter-Sadzinski et al. 2005a). Transcription factors can therefore be used as developmental cues with which to study the progenitor nature of the human Müller stem cells *in vitro*. Not only do they impart information on the ability of the stem cells to differentiate down a particular cell fate, they can also be used as markers to follow the differentiation process.

RGC development is putatively divided into 3 main stages (Fig 1.3). The first is referred to as the stage of 'competence' and describes the time when retinal progenitors first acquire the ability to develop into fully functional RGC. They may not all form RGC but they are able to do so if they are committed to the fate. This stage distinguishes those progenitors which can form RGC from those that can not. The next stage is referred to as the stage of specification. This is believed to define from among the competent progenitors those that will definitely go onto become RGC. They acquire markers that signify their commitment to the RGC fate but are not fully differentiated RGC yet. The final stage is the stage of differentiation when the committed progenitors exit the cell cycle and undergo the necessary phenotypic changes that would convert them to fully differentiated and functional RGC (Mu & Klein 2004a) and Fig 1.3). It is possible therefore to use expression of transcription factors as markers to identify each of these stages and study the process of RGC differentiation.

1.4.1.2 Extracellular matrix proteins and growth factors in RGC development

Factors that influence the differentiation of retinal progenitors towards the various retinal neuronal cell fates during early development have been widely investigated in fish, amphibians and small mammals. Amongst the various models proposed to explain how the retinal progenitors are able to decide what retinal cell type they must form at a precise stage of retinal development, the best supported is the

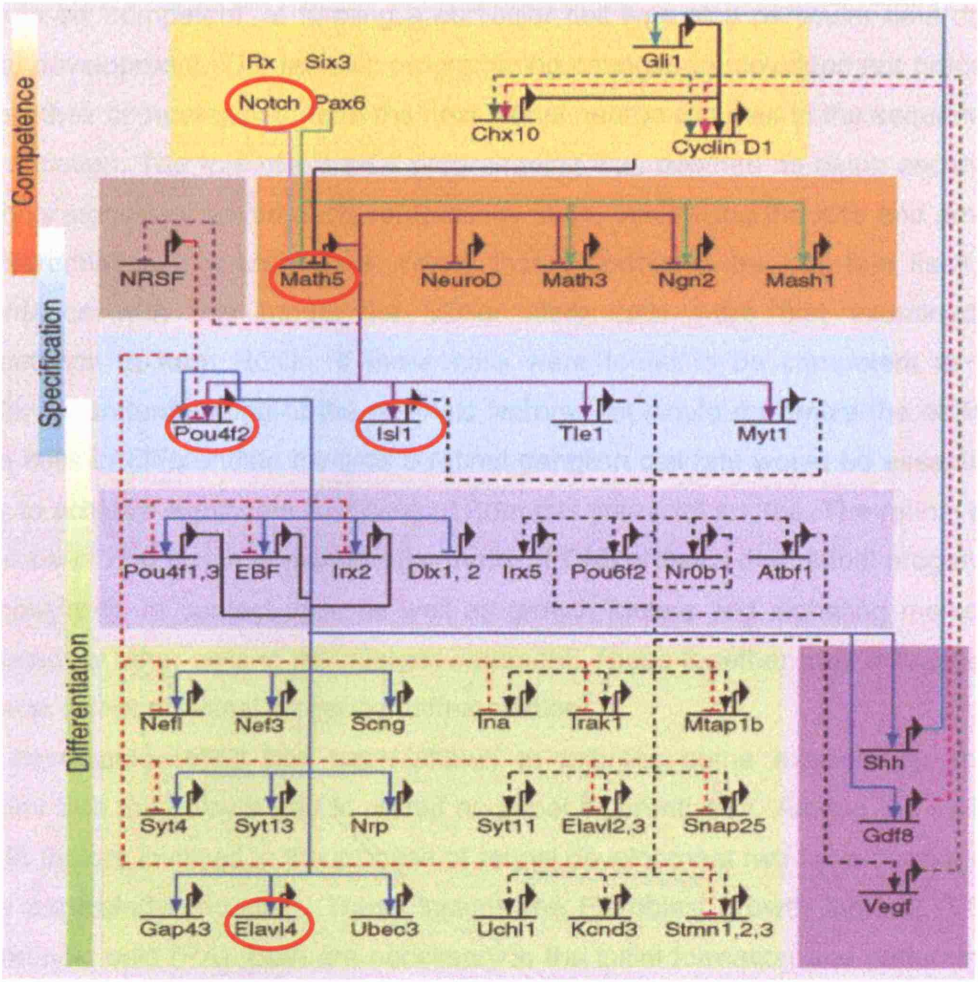

Figure1.3: Stages of RGC differentiation.

Retinal ganglion cell differentiation is putatively divided into three stages. The stage of competence is when the retinal progenitors acquire the ability to form RGC. The stage of specification is when the competent progenitors are committed to an RGC fate. The final stage of differentiation is when the process of terminal differentiation resulting in the formation of a functional RGC takes place. This model was proposed by Mu et al in 2005. The above figure illustrates the various transcription factors and signalling molecules are believed to characterise each of these stages. (Mu et al, Dev.Biology, 2005) Signalling pathway Notch and significant transcription factors at each of these stages, studied in this work, are highlighted by the red circles. This figure uses the correct nomenclature for the various genes. However, through this thesis some of the highlighted genes are referred to by their alternative or more commonly used names- Math5 is referred to as ATOH7, Pou4f2 as BRN3B and Elavl4 as HUD.

competence model first proposed by Cepko et al in 1996 (Cepko et al. 1996). They proposed that the retinal progenitors contain intrinsic programming that allows for them to be 'competent' at forming a particular cell type at a particular time during retinal development. The intrinsic programming changes as development proceeds to alter their competency to form the next retinal neuron required in the sequence of differentiation. The role of extrinsic programming was deemed as being secondary and only significant within each competency state, influencing the rate and amount of differentiation that took place, rather than determining the cell fate itself. In accordance with this model the Müller stem cells were first examined for competence to form RGCs. If these cells were found to be competent to form RGCs, an understanding of the extrinsic factors that would maximize the ability of these cells to differentiate towards a retinal ganglion cell fate would be essential in order to achieve significant RGC output from this stem cell source. The retinal stem cell niche *in vivo* is rich in extracellular matrix (ECM) proteins that retinal progenitors are constantly in contact with, as well as growth factors and signaling molecules produced by other cells in the microenvironment. These together may influence the rate and extent of retinal progenitor differentiation.

The developing retina has been shown to express some extracellular matrix proteins that may play a role in retinal neuronal differentiation. Among the multiple growth factors involved in the process of retinal development two have been shown to be particularly important. These include the Fibroblast growth factor-2 (FGF2) and retinoic acid (RA). Both are necessary in the initial formation and patterning of the eye field but more importantly, both have an effect on the actual differentiation of the various retinal neuronal cell types (Esteve & Bovolenta 2006b;Hyatt & Dowling 1997a;Stenkamp, Gregory, & Adler 1993b).

1.4.1.3 Notch signaling in RGC development

Signalling pathways directly and indirectly regulate the expression of transcription factors and influence the cell fate of progenitors. Of particular relevance to the differentiation of RGC is the Notch signalling pathway which is known to be important in maintenance of retinal progenitor populations and has a strong temporal correlation with RGC development. The Notch pathway was first identified for its role in *Drosophila* wing patterning and has since been known as a cell

signaling mechanism that is conserved across species and crucial to development. Notch regulates stem cell fate determination and proliferation and is involved in maintaining the undifferentiated status of progenitor cells (Louvi & Artavanis-Tsakonas 2006a). It is expressed in almost every developing tissue type and is responsible for renewal of the progenitor population until differentiation is initiated. Notch is expressed in early development throughout the neural retina (Bao & Cepko 1997a) and it has been postulated that retinal progenitors are required to escape Notch inhibition in order to be able to differentiate towards a retinal ganglion cell fate (Austin et al. 1995a). Stem and progenitor cells *in vitro* have also been shown to be regulated by Notch signalling (Carlson & Conboy 2007b) and in the context of retinal progenitors it was of interest to this work to investigate if the differentiation of Müller stem cells too was under the influence of Notch activity.

1.5 Objectives of this thesis

Based on the current knowledge and in view of the characteristics of Müller stem cells, the research presented in this thesis aimed to examine the potential of the adult human Müller stem cells to differentiate towards a retinal ganglion cell (RGC) fate *in vitro* and to explore their application in the regeneration of RGC function *in vivo*. The following objectives were therefore formulated.

1. To investigate the expression of various developmental markers of RGC by Müller stem cells and to examine the environmental conditions that may influence their differentiation towards this retinal neuronal phenotype.
2. To investigate the role of Notch signalling in the Müller stem cell proliferation and differentiation and to determine the effect of Notch inhibition on Müller stem cell differentiation into RGC.
3. To analyse the neural functionality of Müller stem cells differentiated towards an RGC phenotype *in vitro.*
4. To investigate mechanisms that prevent graft migration and integration following transplantation of Müller stem cells into experimental models of retinal degeneration.

5. To establish an *in vivo* model of RGC depletion and study the migration, integration and functional behaviour of Müller stem cells differentiated into RGC phenotype and transplanted into this model.

Chapter 2: Expression of markers of developing and mature RGC by Müller stem cells *in vitro*

2.1 Introduction

2.1.1 Established markers of RGC development

2.1.1.1 ATOH7 (Math5) is expressed in RGC competent retinal progenitors

The vertebrate homologue of *Drosophila* atonal (known as Ath5 in the chick, Math5 in the mouse and ATOH7 in humans) is the earliest transcription factor to be expressed among retinal progenitors heading towards a retinal ganglion cell fate (Brown et al. 1998). Other members of the atonal family include Math3, Neuro D, Neuro M and Neurogenins. In *Drosophila*, atonal is necessary for the formation of R8 neurons equivalent of the vertebrate RGCs. In the chick and the mouse Math5 demonstrates similar function. Math5 null mice do not form retinal ganglion cells or optic nerves(Brown et al. 2001). Targeted deletion of Math5 in mice results in loss of more than 80% of ganglion cells and virtually all BRN3B expressing ganglion cells, which represents a more differentiated state of ganglion cell development (Wang et al. 2001a). Math5 is also necessary for the expression of important downstream transcription factors like Brn3 and ISL1 which are essential for RGC specification and differentiation and null mice completely lack expression of these markers (Yang et al. 2003d). While these observations suggest that Math5 is essential for the formation of RGC, not all Math5 expressing cells form RGCs. Yang et al also followed the fate of Math5 expressing cells using a cre-loxP recombination system and found that Math5 expressing cells form not just ganglion cells but also photoreceptors, amacrine cells and occasionally horizontal cells. It seems therefore that Math5 alone is not sufficient for RGC fate determination. This factor seems to be required for RGC formation and confers competence to the progenitors but is not responsible for directing the terminal differentiation of these cells. Nevertheless it is necessary for RGC formation due to its role in activation of a downstream transcriptional network that is necessary for RGC specification and terminal differentiation. Given this direct and significant involvement of Math5 in progenitor competence and commitment to an RGC cell fate, it was important to investigate

the level of expression of ATOH7 by Müller stem cells as a way of estimating the RGC competent population among these cells.

2.1.1.2 BRN3B is expressed in committed RGC precursors during retinal development

Of the class IV POU (Pit1, Oct1,2, Unc-86) domain transcription factors found in the retina, BRN3B (otherwise referred to as POU4f2) was the first to be described (Xiang et al. 1993). Like the other POU domain transcription factors, it consists of a bipartite DNA binding domain i.e. one POU-specific domain and one POU-homeo domain separated by a variable linker (Xiang et al. 1995b). The earliest works described BRN3B as being expressed only in a subset of developing retinal ganglion cells. Subsequent generation of BRN3B knockout mice revealed the importance of this gene in development of RGCs. Knockout mice lose more than 70% of their differentiated RGC population (Gan et al. 1996b). In the developing mouse eye BRN3B is expressed around e11.5 soon after the retinal progenitors exit the cell cycle and are committed to a retinal ganglion cell fate (Gan et al. 1996a;Turner, Jenne, & Rosenfeld 1994). Initially it was believed that BRN3B might be responsible for this specification. However cell fate commitment and migration of the committed progenitors remains unaltered in BRN3B null mice, suggesting that its involvement is during the later stages of ganglion cell differentiation. Lack of BRN3B is also associated with enhanced apoptosis of ganglion progenitor cells at late developmental stages when they would otherwise have become mature RGC, suggesting a more supportive role in ganglion cell differentiation and maturation (Xiang et al. 1998). One possible function of BRN3B might be in assisting axon formation and establishment of retinal ganglion cell polarity as demonstrated by the dendritic nature of RGC axon formation and the thinner, poorly formed optic nerves of BRN3B null mice (Gan et al. 1999b;Wang et al. 2000).

Brn3a and Brn3c are very closely linked to BRN3B structurally and functionally. Spatially their expression pattern is also similar to that of BRN3B, although fewer cells are positive for these genes than for BRN3B (Xiang et al. 1995a). Brn3a null mice selectively lose neurons in their somatosensory ganglia and selective brainstem nuclei, causing loss of coordinated limb movement and suckling

capabilities (Xiang et al. 1996). Brn3c null mice lack auditory and vestibular hair cells of the inner ear and have impaired hearing and balance as a result (Keithley et al. 1999). However knockouts of Brn3a/Brn3c do not produce as severe a defect in the RGC layer as does the BRN3B knockout. Interestingly replacement of BRN3B knockouts with Brn3a results in functional restoration of normal development and survival of RGC. In these animals expression of Brn3a is spatiotemporally identical to that of BRN3B. These observations in accordance with the fact that not all RGCs are lost in the absence of BRN3B have led to the postulate that perhaps Brn3a and BRN3B have functional equivalence and the difference in their effect on RGC differentiation is as a result of differing temporal expression (Pan et al. 2005).

These observations suggested that the Brn3 group of genes are crucial to retinal ganglion cell differentiation from retinal progenitors. They also indicated that cells that express BRN3B are committed to retinal ganglion cell fate and in the process of undergoing final maturation and differentiation towards adult RGC.

2.1.1.3 Islet 1 is required for maintenance of differentiating RGC precursors

Islet1 (ISL1) is a LIM homeodomain transcription factor known to be involved in the development of various tissues in the body, particularly pancreas and motor neurons. The structure of LIM homeodomain transcription factors consists of 2 zinc finger (LIM) domains present within the N-terminal of the homeodomain itself. The LIM homeodomains (HD) distinguish these transcription factors (TFs) from other TFs in their ability to bind proteins. Most other TFs only bind proteins at the HD and any other domains that might exist outside of the homeodomain usually bind DNA. This ability allows the LIM TFs to bind to other TFs and play a significant role in various developmental processes (Hobert & Westphal 2000).

The Islet family of LIM HD transcription factors are particularly important in motor neuron development as well as development of pancreatic islets. While in *Drosophila*, Islet nulls have abnormal axon development and lose dopaminergic and serotonergic neurons, in the rat, loss of ISL1 results in complete loss of motor neurons (Pfaff et al. 1996). Of note is the fact that in *Drosophila*, the null phenotype can be reversed by expression of Islet in postmitotic neurons, indicating that Islet

plays a more significant role in terminal differentiation of the neurons, rather than their cell fate determination (Thor & Thomas 1997).

In the developing vertebrate retina ISL1 is expressed by cells in the outer part of the inner nuclear layer (bipolar cells, specifically ON-bipolar cells), scattered cells in the inner part of the inner nuclear layer (the cholinergic amacrine cells), as well as in the ganglion cell layer (Elshatory et al. 2007a). Conditional knockout of ISL1 results in loss of ON bipolar, cholinergic amacrine and a significant proportion (71%) of ganglion cells suggesting that ISL1 is involved in the development of these cell types (Elshatory et al. 2007b).

The role of ISL1in RGC differentiation in particular has been further delineated in recent work by Mu and colleagues in the conditional knock out mice model of ISL1 (Mu et al. 2008a). They conditionally knock out ISL1 in retinal progenitors using floxed exon3 of ISL1 crossed with Six-3: Cre resulting in a selective loss of ISL1 in retinal progenitors. At E14.5 in these knock outs, there was no significant difference in the number of cells expressing BRN3B, as indicated above, a marker expressed in committed retinal ganglion cell precursors. However at E17.5, the number of BRN3B positive cells fell compared to wild type controls suggesting that ISL1 played a role not in cell fate determination of RGC but in the maintenance of differentiated RGC once they had been formed. Mu et al further corroborated these findings by examining the optic nerves of the KO mice at P20, which were much thinner than the wild types and showed empty or partially filled myelin sheaths. Since myelin sheaths are only formed in the presence of axons (Michailov et al. 2004), it was likely that RGCs axons had been formed but later degenerated in the absence of ISL1 thereby suggesting that this factor has a role in axon maintenance (Mu et al. 2008b).

BRN3B knock outs as described previously also seem to play some role in maintenance of RGC precursors and it would seem that ISL1 and BRN3B work together or at least at the same stage of RGC development to mediate RGC differentiation. In this context, Mu et al suggested as much in this paper and performed microarrays in ISL1 nulls and compared them with results from BRN3B nulls. Their results identified several genes that both BRN3B and ISL1 were regulating together, along with a set of genes that each regulated independently. Like in the Brn3 knock outs they found that several genes regulated by ISL1 were

necessary for neuronal structural integrity and function. ISL1 also seemed to regulate other transcription factors important in retinal neuronal differentiation. Mu et al suggested that it was likely that ISL1 formed a distinct branch in the gene regulation network of RGCs that they earlier proposed (Mu et al. 2005). Their results implicate that this distinct branch may overlap in some ways with the BRN3B branch and these together regulate other downstream transcription factors and neuron specific genes required for RGC differentiation.

These observations were further supported by the work of Pan et al (Pan et al. 2008c), who used BRN3B ISL1 double knock outs to show a more severe phenotype with almost complete loss of RGCs. Using chromatin immunoprecipitation assays and Isl2 and Shh as target genes (immediately downstream of BRN3B and ISL1 expression during RGC development), they also showed that both ISL1 and BRN3B proteins bind to the promoter regions of these genes, suggesting that in some cases ISL1 and BRN3B act together to regulate RGC differentiation.

While there is a very limited body of work on the role of ISL1 in RGC differentiation, what little there is, points to an important role of ISL1 in maintenance of RGC precursors that have begun the process of differentiation into RGCs, as well as assistance in the actual process of differentiation including axon formation.

2.1.1.4 Hu antigen D (HUD) is expressed by terminally differentiated RGC

Human antigen D (HUD) or Embryonic Lethal Abnormal Vision L4 (ELAVL4) is an RNA binding protein. RNA binding proteins bind to the 3' untranslated region of mRNA and through this binding affect the stability of the mRNA. HUD is able to bind to several transcripts important in neural differentiation in this manner and thereby regulates neural differentiation. More specifically it is known to affect the stability, transport and ultimate translation of transcripts like GAP-43, Tau and acetylcholinesterase (AchE) which play an important role in the formation of neuronal processes. Studies have shown that HUD is able to effect the export of these transcripts from the nucleus to the cytoplasm, following which it is able to then target these transcripts to cellular compartments, like the axons or the growth cones, where they ultimately need to be translated. They therefore play an

important role in affecting terminal differentiation of neural progenitors following exit from the cell cycle and are one of the earliest markers of differentiated neurons(Deschenes-Furry, Perrone-Bezzozero, & Jasmin 2006).

In the retina, HUD expression is observed in retinal ganglion cells as well as in amacrine cells but not in photoreceptors. The expression pattern of HUD in the developing retina has been studied in *Xenopus laevis*, chick and rats and despite some discrepancy in the data obtained from these three species, it is largely observed that HUD is expressed in newly differentiating ganglion and amacrine cells which have exit the cell cycle (Amato et al. 2004;Ekstrom & Johansson 2003d).

With this data in mind HUD can be used as a marker of early differentiated RGC within a given retinal stem/progenitor cell population. While it would be incorrect to describe all cells expressing HUD within the progenitor population as differentiated RGC, the expression of this gene could be used as a good indication of post mitotic cells undergoing neural differentiation.

2.1.2 Role of extrinsic factors in retinal development

2.1.2.1 Extra cellular matrix proteins

Amongst the various components of the Bruch's membrane known to be important in retinal progenitor development and differentiation (Hiscott et al. 1999a), the role of vitronectin in retinal differentiation is best known. Vitronectin is a secreted glycoprotein that was long believed to be solely produced in the liver and found in the blood. In 1999 Anderson et al showed that vitronectin was expressed in the adult human retina where it was specifically seen in cone photoreceptors, RPE and retinal ganglion cells (Anderson et al. 1999). The role of vitronectin in retinal development has been established through work with the developing chick retina. It was found that vitronectin expression was localised to areas of synapse formation (ie the plexiform layers of the retina) and as development progressed it moved towards the nerve fibre layer where it persisted after completion of differentiation. This pattern of localisation suggested that vitronectin may function as a substrate for the initial development of neuronal processes and subsequently help in the survival of and axon/dendrite formation by these cells. Of note was the fact that

vitronectin expression coincided with that of α5integrins suggesting that a possible mechanism by which vitronectin is able to affect cellular differentiation is by binding to the cells via the integrins, thereby effecting the matrix protein- cellular interaction (Martinez-Morales et al. 1995).

Fibronectin and laminin are also believed to interact with cells in a similar fashion, although via different integrins – fibronectin through α5β1 and laminin through α6β1 (Braam et al. 2008). Both these proteins are also believed to play a role in axon guidance and fibronectin is also known to constitute a proangiogenic matrix component. However their role in retinal neuronal differentiation is less well defined.

Matrigel is a complex ECM protein derived from the Engelbreth-Holm-Swarm (EHS) mouse sarcoma and is made up of a combination of laminin, collagen IV, heparan sulphate proteoglycans, as well as growth factors like TGFβ, EGF, insulin like growth factor (ILGF), FGF and tissue plasminogen activator (TPA). While each of the ECM proteins present in Matrigel might individually play a role in retinal development, together they possess a combination of proteins present in the Bruch's membrane during development (Hiscott et al. 1999b). Matrigel is used widely by stem cell biologists to promote cell adhesion *in vitro* and often to maintain self renewal and pluripotent properties of stem cells of various origins. Some investigators have used ECM proteins to study differentiation of stem cells towards a retinal progenitor fate. Human embryonic stem cells (HESCs) form retinal progenitors when cultured on human Bruch's membrane. They adopt neuronal morphology on laminin and develop tight junctions characteristic of RPE when grown on matrigel (Gong et al. 2008b). All of these observations suggest that the ECM proteins are able to influence the differentiation of retinal progenitors.

2.1.2.2 Growth factors

2.1.2.2.1 Fibroblast growth factor (FGF)

Formation of the eye field on the anterior neural plate requires that the presumptive retinal progenitors, as identified by their expression of transcription factors Otx2, Pax6 and Rx, move away from the midline of the anterior neural plate in either direction. This movement is the earliest decision that separates the retinal progenitors from other neural progenitors in the anterior neural plate and is

influenced by the interaction between FGF2 and ephrinB1 (Moore et al. 2004). This is the earliest among several different roles ascribed to Fibroblastic growth factor (FGF) in the process of retinal neuronal differentiation. Following the formation of the eye field and eventually the optic stalk and cup, FGF signaling begins the actual process of retinal neuronal differentiation in the optic cup. In the chick and fish, FGF3 and FGF 8 are essential for the beginning of retinal ganglion cell differentiation. In the absence of these two factors there is no expression of Ath5 which is a hallmark of retinal progenitors competent to form retinal ganglion cells (Esteve & Bovolenta 2006a). Addition of FGF8 induces an increase in RGC differentiation (measured by the number of ISL1 positive cells) in embryonic retinal explant cultures, without any apparent increase in cell proliferation (Martinez-Morales et al. 2005). The same group also showed that blockage of the FGF receptor results in a reduction of ISL1 positive cells, without increase in cell death. Additionally removal of the optic stalk prevents initiation of RGC differentiation and can be corrected with administration of FGF8 suggesting that the optic stalk is the source of the crucial initiating FGF signal. In the embryonic chick and fish retina therefore it is well established that FGF is necessary for RGC differentiation.

In the post natal retinal progenitor populations, FGF has also been shown to have an effect on cell proliferation and differentiation, in a manner similar to that seen in embryonic retinal progenitors. Fischer described the effect of insulin and FGF2 on the various presumptive post natal retinal progenitor populations in the damaged chick retina. He showed that both the ciliary margin progenitors as well as the Müller cells are able to proliferate in response to these signals (Fischer 2005). Müller cells have also been shown to be responsive to FGF 2 in other species including the rabbit (Lewis et al. 1992) and the bovine retina (Mascarelli, Tassin, & Courtois 1991). The effect of FGF2 on Müller glial cells in the retina is not restricted to proliferation alone and a combination of insulin and FGF2 can initiate neuronal differentiation among proliferating Müller cells. (Fischer et al. 2002) If these signals are provided in an eye where RGCs are previously damaged (NMDA, kaianate, colchicine induced RGC death) Müller cells are also able to specifically generate retinal ganglion cells during early post natal life *in vivo* (Fischer & Reh 2002).

Given the importance of FGF in retinal neuronal differentiation during embryonic development *in vivo* and its effect on Müller cell proliferation and differentiation, this

growth factor is an ideal candidate to use in attempts to enhance RGC differentiation of human Müller stem cells *in vitro*.

2.1.2.2.2 Retinoic Acid (RA)

The earliest contribution that Retinoic acid (RA) makes to retinal development is the determination and maintenance of the dorsoventral axis of the retina. During early formation of the optic cup, levels of RA are much higher in the ventral retina compared to the dorsal retina and this gradient is believed to contribute towards the patterning of the dorsoventral retinal axis (McCaffery et al. 1992b). Following this stage, during the process of retinal neuronal differentiation, RA is believed to have a significant effect on rod photoreceptor differentiation. RA is expressed by retinal progenitor cells (RPC) as well as differentiated retinal neurons and this pattern of expression changes with progressive retinal development (Levine, Fuhrmann, & Reh 2000). Initially the expression is confined to the RPC. Once the retinal ganglion cells have differentiated they begin to express RA in high amounts and as differentiation proceeds, the expression moves outward toward the RPE. Indeed in the early post natal stages it is the RPE that continues to express the highest amounts of RA(McCaffery et al. 1992a). This pattern of expression is believed to be directed towards providing the differentiating photoreceptors with maximum RA signaling. Further evidence of the role of RA in photoreceptor differentiation also comes from work in the chick retinal progenitor cultures *in vitro* which respond in a dose dependent fashion to addition of RA by differentiating into rod photoreceptors (Stenkamp, Gregory, & Adler 1993a). In the zebrafish, addition of RA *in vivo* during retinal development causes precocious development of rod photoreceptors (Hyatt et al. 1996). RA therefore appears to have predominant function in rod photoreceptor development. However RA is also known to affect the expression of other growth factors like ciliary neurotrophic factor (CNTF) as well as FGF in other tissues in the body and it is possible that indirectly, it has an effect on differentiation of other retinal neuronal cell types. RA through it response elements (RARE) also affects the expression of other retinal transcription factors (for example Pax2 and Msh-c in zebrafish) involved in retinal development and differentiation (Hyatt & Dowling 1997b), but no direct evidence suggests an effect of RA on RGC differentiation or Müller cell proliferation.

2.2 Objectives and experimental plan

This chapter aimed at answering the question - Do Müller stem cells possess the same intrinsic programming seen in embryonic retinal progenitors during development that is necessary for retinal ganglion cell (RGC) differentiation? Markers of different stages of RGC development in the embryo were therefore used as cues to answer this question. The objectives of this chapter were -

1. To examine the *in vitro* expression by Müller stem cells of the genes ATOH7, BRN3B, ISL1 and HUD, normally expressed by embryonic retinal progenitors at different times during RGC development.
2. To investigate of the effect of matrix substrates and growth factors on the expression of these genes by Müller stem cells in culture, given the significance of the stem cell niche in influencing the differentiation of tissue specific stem cells,. Using these additional factors the culture conditions best suited to expression of differentiated RGC markers were identified.

The experiments performed to fulfil the above objectives were as follows-

1. Müller stem cells were cultured under baseline conditions and on laminin, matrigel, fibronectin and vitronectin for 7 days. RNA and proteins were isolated from these cells and RT PCR and western blots performed on these samples.
2. Cells cultured in this way on glass chamberwell slides were fixed after 7 days in culture with 4% PFA and immunostained for BRN3B, ISL1 and HUD antibodies.
3. Müller stem cells were also cultured with RA and FGF for 7 days and cell pellets collected for RNA and protein isolation. These samples were examined for ATOH7, BRN3B, ISL1 and HUD RNA and protein expression.
4. The relative protein and RNA expression of these genes was then compared among the 4 different matrix culture conditions and the 2 growth factors to decide upon the best culture conditions to maximize RGC marker expression.

The results described below are the results of experiments performed on the cell line MIO-M1. These experiments were intended as preliminary work to gain an

estimate of the ability of these cells to express RGC markers and their response to various matrix proteins and growth factors. Hence only one cell line was analyzed in this instance. Subsequent experiments were then performed on multiple cell lines to confirm that the effects seen were a true characteristic of human Müller stem cells and not one single cell line alone. Unless other wise mentioned all cells were cultured under the described culture condition for 7 days before being analyzed for protein and mRNA expression of the transcription factors under investigation.

2.3 Results

2.3.1 ATOH7 expression by human Müller stem cells

In the absence of a reliable antibody to human ATOH7, it was only possible to study its mRNA expression in Müller stem cells. Previous studies have shown that Müller stem cells express several transcription factors expressed by retinal progenitors including Pax6 and Chx10 (Lawrence, Singhal, Bhatia, Keegan, Reh, Luthert, Khaw, & Limb 2007d). The present experiments revealed that Müller stem cells expressed detectable levels of ATOH7 mRNA as well. Müller stem cells expressed ATOH7 mRNA under baseline conditions without the addition of matrix substrates and/or growth factors. Detection of ATOH7 mRNA in these cells suggested to us that the human Müller stem cells may contain some degree of competence to form retinal ganglion cells. The baseline expression was detectable but in small amounts and indicated that the level of competency was quite low too (Fig 2.1A).

When the cells were cultured with laminin, matrigel, fibronectin or vitronectin, the levels of ATOH7 expression varied (Fig 2.1A). The variation in expression with matrices was detectable with semi quantitative RT PCR and showed that when compared to the control (cells cultured without any matrix substrate) some of the matrices caused an upregulation of ATOH7 mRNA. Since mRNA detection was the only tool to study ATOH7 expression in Müller stem cells (in the absence of a reliable antibody) we use quantitative real time PCR (QPCR) to obtain a more

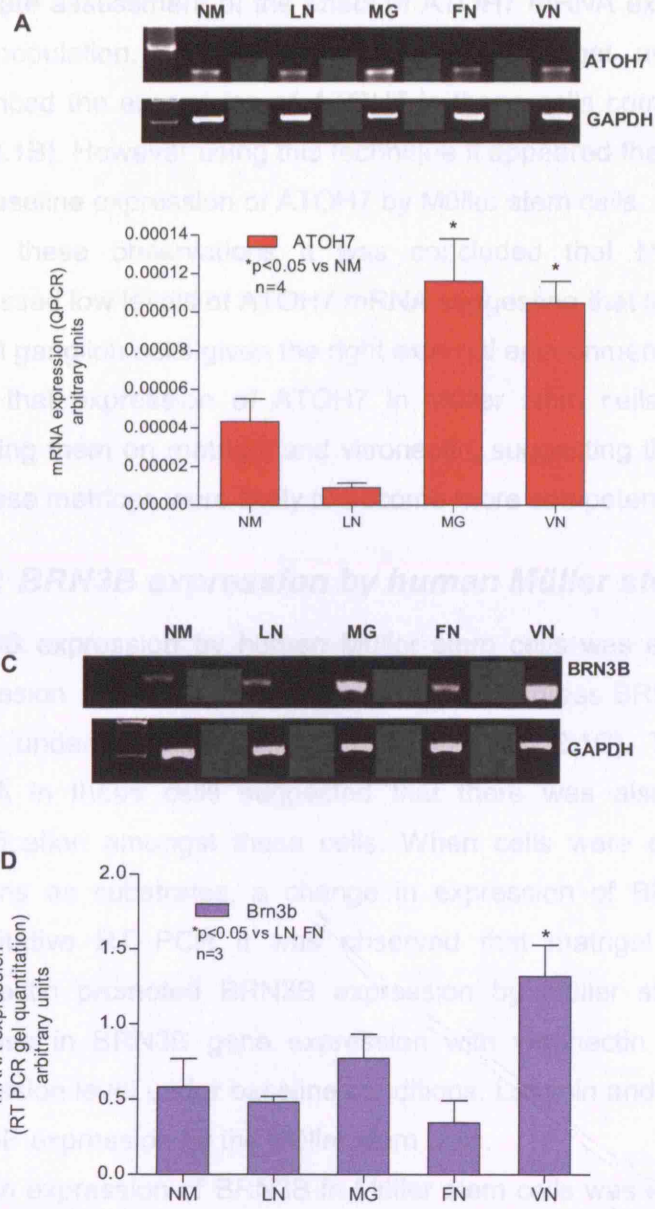

Figure 2.1: Expression of ATOH7 and BRN3B in Müller stem cells and effect of extracellular matrices on this expression. (A)ATOH7 mRNA expression in Müller stem cells after 7 days in culture under baseline conditions or on various extracellular matrix proteins. GAPDH was used as house keeping gene to control loading.(B) Quantitative PCR showed high levels of Atoh7mRNA expression in Müller stem cells cultured with MG and VN. (C) BRN3B mRNA expression by Müller stem cells after 7 days in culture with or without various matrices, GAPDH was used to control loading as with ATOH7. (D) Histogram depicting BRN3B mRNA expression by Müller stem cells cultured on different matrices. In each case 'n' refers to the number of independent measurements. NM=no matrix, LN=laminin, MG=matrigel, FN=Fibronectin, VN=Vitronectin

accurate assessment of the effect of ATOH7 mRNA expression in the Müller stem cell population. QPCRs confirmed that matrigel and vitronectin significantly enhanced the expression of ATOH7 in these cells compared to control conditions (Fig 2.1B). However using this technique it appeared that laminin was not modifying the baseline expression of ATOH7 by Müller stem cells.

From these observations it was concluded that Müller stem cells normally expressed low levels of ATOH7 mRNA suggesting that they were competent to form retinal ganglion cells given the right external environment to differentiate. It was also seen that expression of ATOH7 in Müller stem cells could be upregulated by culturing them on matrigel and vitronectin, suggesting that Müller stem cells grown on these matrices were likely to become more competent to form RGCs.

2.3.2 BRN3B expression by human Müller stem cells

BRN3B expression by human Müller stem cells was also analysed using mRNA expression. Müller stem cells were found to express BRN3B mRNA at considerable levels under baseline culture conditions (Fig 2.1C). The expression of BRN3B mRNA in these cells suggested that there was also a certain level of RGC specification amongst these cells. When cells were cultured with various ECM proteins as substrates, a change in expression of BRN3B was seen. By semi quantitative RT PCR it was observed that matrigel and to a greater extent vitronectin promoted BRN3B expression by Müller stem cells (Fig 2.1D). The increase in BRN3B gene expression with vitronectin was nearly 2.5 times the expression level under baseline conditions. Laminin and fibronectin did not improve BRN3B expression by the Müller stem cells.

Protein expression of BRN3B in Müller stem cells was examined using the BRN3B N-15 antibody (Santa Cruz Biotechnology) (Fig 2.2A). Müller stem cells expressed a 55kD band as identified by western blotting using this antibody. In our hands immunostaining of Müller stem cells with the BRN3B antibody did not reveal a specific expression pattern. While there were occasional instances of nuclear immunostaining of Müller stem cells, often there was considerable background staining, particularly in the cytoplasm (Fig 2.2B). Several different titrations of the antibody and immunostaining conditions were tested. In the light of variable results,

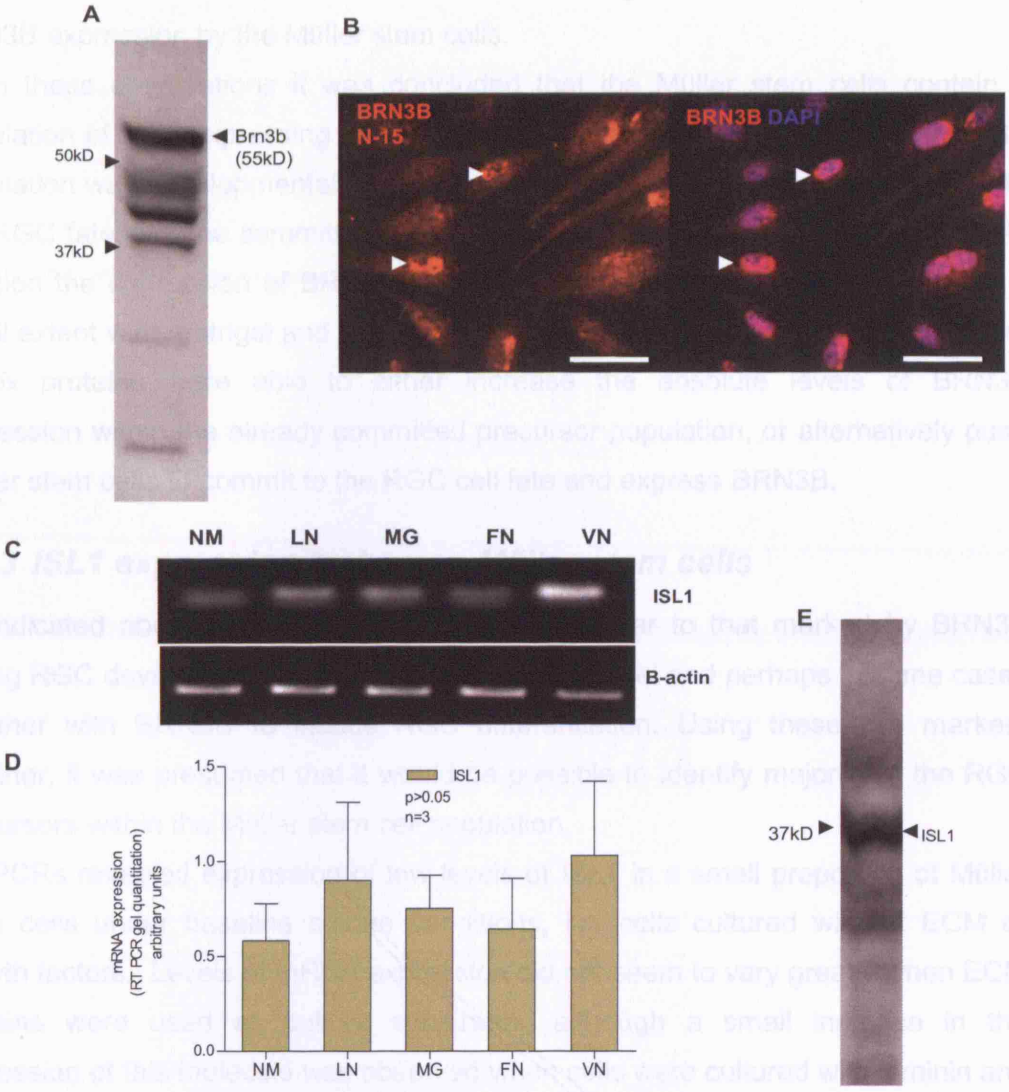

Figure 2.2: Brn3b protein and ISL1 gene expression by Müller stem cells and effect of matrices on their expression. (A) Western blot showing expression of BRN3B protein by Müller stem cells with a characteristic band of 55kD. Non-specific smaller bands were also seen occasionally which appeared to identify immuoglobulins as suggested by the molecular weight of these proteins. (B) Immunostaining of Müller stem cells cultured on matrigel, showing occasional nuclear staining (white arrowheads) but excessive background staining in the cytoplasm. Counterstain with DAPI is shown to delineate the cell nuclei. Scale bars= 20µm (C) Representative RT PCR gel showing results of ISL1 mRNA expression by Müller stem cells after 7 days in culture on various ECM proteins. (D) Histogram depicting difference in Isl1 expression by Müller stem cells using various ECM proteins. Although LN and VN were found to induce slightly higher expression of the gene, no statistically significant difference was observed. (E) Western blot with 39.4D5 antibody showing expression of ISL1 by Müller stem cells. A characteristic band of 36kD is seen. In each case 'n' refers to the number of independent measurements. NM=No Matrix, LN=Laminin, MG=Matrigel, FN=Fibronectin, VN=Vitronectin

it was decided to use RT PCR and western blotting to conduct further studies on BRN3B expression by the Müller stem cells.

From these observations it was concluded that the Müller stem cells contain a population of cells expressing BRN3B mRNA and protein and it was likely that this population was developmentally at a stage where the cells have been committed to the RGC fate, like the committed RPCs during embryonic retinal developmental. In addition the expression of BRN3B in Müller stem cells could be upregulated to a small extent with matrigel and to a significant extent with vitronectin suggesting that matrix proteins were able to either increase the absolute levels of BRN3B expression within the already committed precursor population, or alternatively push Müller stem cells to commit to the RGC cell fate and express BRN3B.

2.3.3 ISL1 expression by human Müller stem cells

As indicated above, ISL1 also marks a stage similar to that marked by BRN3B during RGC development and seems to work in parallel and perhaps in some cases together with BRN3B to induce RGC differentiation. Using these two markers together, it was presumed that it would be possible to identify majority of the RGC precursors within the Müller stem cell population.

RT PCRs revealed expression of low levels of ISL1 in a small proportion of Müller stem cells under baseline culture conditions, i.e. cells cultured without ECM or growth factors. Levels of mRNA expression did not seem to vary greatly when ECM proteins were used as culture substrates, although a small increase in the expression of this molecule was observed when cells were cultured with laminin and vitronectin. (Fig 2.2 C&D)

Unlike ATOH7 and BRN3B, a reliable antibody was available to study the protein expression of this molecule by human Müller stem cells. The Developmental Studies Hybridoma Bank (DSHB) antibody to ISL1 (39.4D5) has been widely used by other researchers and is known to distinctly mark the nuclei of cells expressing this LIM homeodomain transcription factor. To confirm this, immunostaining of cryosections of adult lister hooded rat eyes was performed. The results showed that the antibody stained clearly cell nuclei in the ganglion cell layer (GCL) and outer nuclei of the inner nuclear layer (INL) of the retina (Fig 2.3A). A similar pattern of expression was also seen in sections of adult human retina (Fig 2.3B).

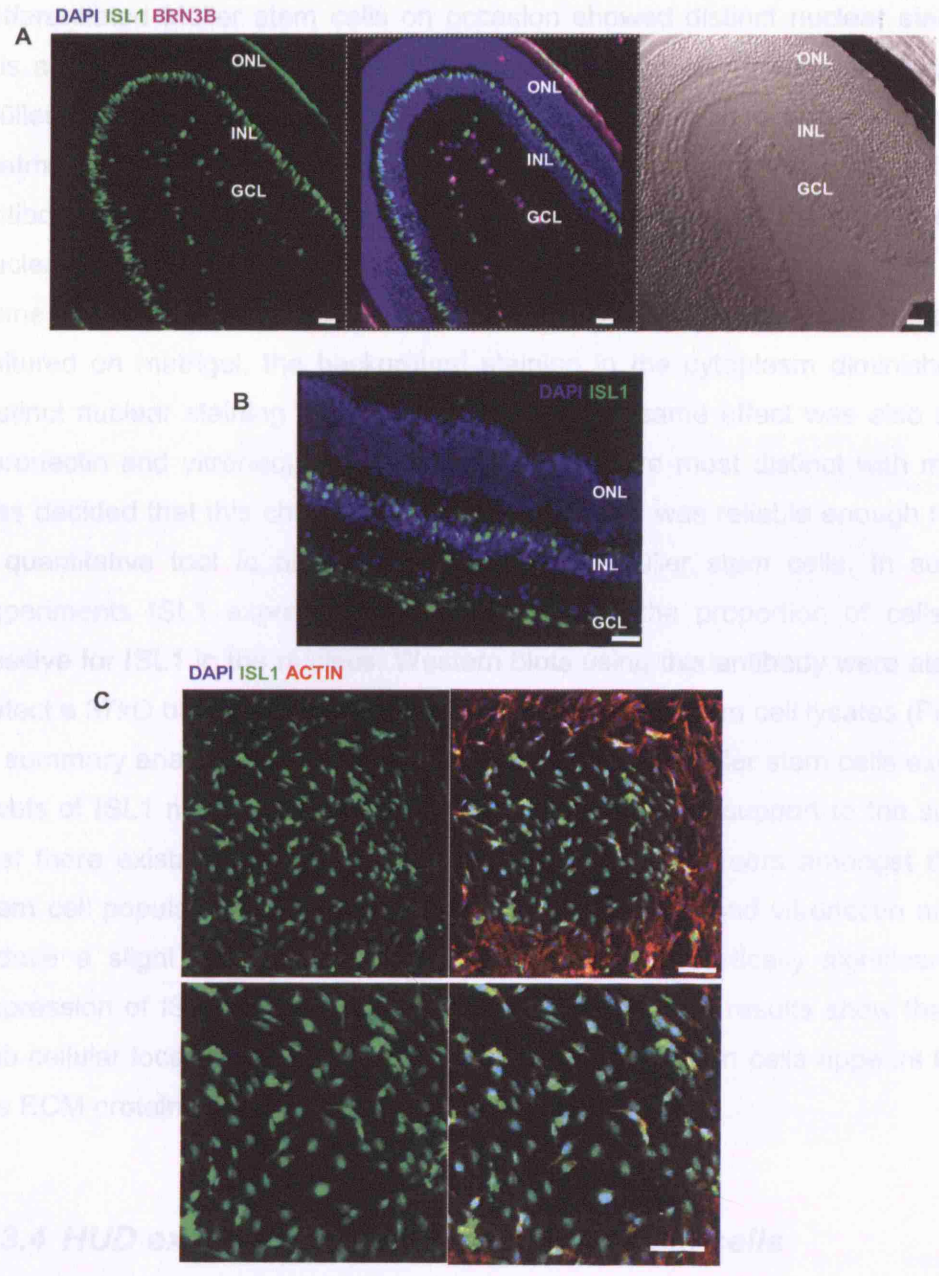

Figure 2.3: Characterisation of the ISL1 39.4D5 antibody from DSHB - using the rat and human retina as well as the human Müller stem cells. (A) ISL1 expression in the 3-4 week old lister-hooded rat retina is seen in the outer part of the inner nuclear layer as well as the ganglion cell layer, where it also occasionally co-localises with BRN3B. (B) In the adult human retina ISL1 immunoreactivity is also observed in the outer part of the inner nuclear and the ganglion cell layers. (C) Human Müller stem cells *in vitro* also express ISL1 when cultured with matrix substrates and growth factors. When positive the cells express ISL1 specifically in the nucleus, similar to that seen in the rat and human retina. Actin was used to delineate the cellular architecture and in the ISL1 positive cells in the centre of the field, the fine cell processes show very little actin staining compared to the surrounding cells which have a more glial morphology and stain extensively for actin. Scale bars=20µm

Differentiated Müller stem cells on occasion showed distinct nuclear staining with this antibody (Fig 2.3C). When this was studied formally it was seen that human Müller stem cells cultured *in vitro* on tissue culture plastic without extra cellular matrix, failed to show a distinct nuclear staining pattern when stained with the antibody. Instead background staining in the cytoplasm and a slightly enhanced nuclear staining accompanying this cytoplasmic distribution was seen (Fig 2.4). The same pattern was seen with cells cultured on laminin. However when the cells were cultured on matrigel, the background staining in the cytoplasm diminished and a distinct nuclear staining pattern was visible. The same effect was also seen with fibronectin and vitronectin, although the nuclei were most distinct with matrigel. It was decided that this characteristic staining pattern was reliable enough for use as a quantitative tool to assess ISL1 staining of Müller stem cells. In subsequent experiments ISL1 expression was quantified by the proportion of cells staining positive for ISL1 in the nucleus. Western blots using this antibody were also able to detect a 37kD band characteristic of ISL1 in the Müller stem cell lysates (Fig 2.2E).
In summary analysis of ISL1 expression revealed that Müller stem cells express low levels of ISL1 mRNA and protein *in vitro*, adding further support to the suggestion that there exists a population of committed RGC precursors amongst the Müller stem cell population *in vitro*. The ECM proteins laminin and vitronectin are able to induce a slight upregulation (although this is not statistically significant) in the expression of ISL1 by Müller stem cells. In addition the results show that precise sub cellular localization of ISL1 proteins in the Müller stem cells appears to require the ECM proteins matrigel, fibronectin or vitronectin.

2.3.4 HUD expression by human Müller stem cells

HUD is expressed in early differentiated RGC and therefore expression of this marker in Müller stem cells should suggest the existence of a population of cells that have achieved the transition from RGC precursor to differentiated RGC. However it is not plausible to make such a suggestion based on the expression of this marker alone and in this case HUD was used as another marker that indicates the extent of RGC differentiation among Müller stem cells without postulating that any cells positive for this marker may be fully differentiated RGC.

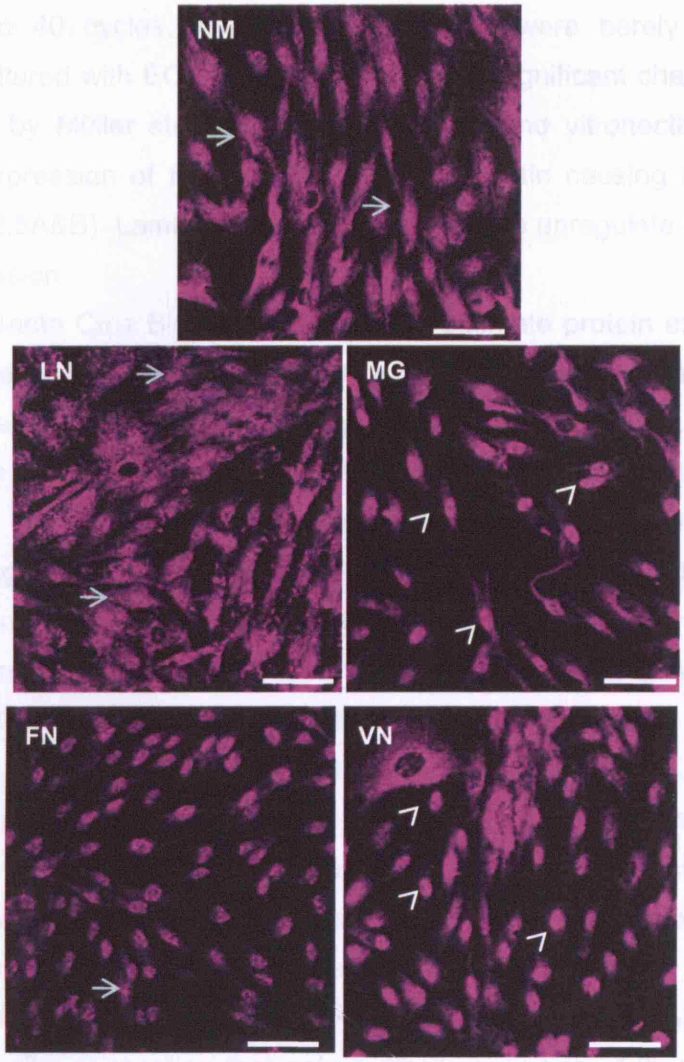

Figure 2.4: ISL1 protein expression by human Müller stem cells cultured on different ECM. Müller stem cells express nuclear Isl1 when cultured on matrigel and vitronectin (white arrow heads highlight cells with nuclear staining of ISL1). When cultured on the other matrices, the expression pattern is less discrete with faint nuclear as well as some background cytoplasmic staining (white arrows highlight some examples of cells with granular staining of ISL1). Scale bar = 20μm

It was difficult to detect HUD mRNA in Müller stem cells at baseline culture conditions using the 36 cycles normally used in this study for PCR reactions. Even upon increasing to 40 cycles, levels of HUD mRNA were barely detectable. However, when cultured with ECM proteins there was a significant change in HUD mRNA expression by Müller stem cells. Both matrigel and vitronectin, markedly upregulated the expression of HUD mRNA, with vitronectin causing a significant upregulation. (Fig 2.5A&B) Laminin and fibronectin failed to upregulate the levels of HUD mRNA expression.

A HUD antibody (Santa Cruz Biotech.) was used to estimate protein expression of this gene in Müller stem cells. This HUD antibody has also been used for immunostaining previously and predominantly stains nuclei in the GCL of adult rat and human retinae (Ekstrom & Johansson 2003c). The staining pattern of Müller stem cells under baseline conditions *in vitro* showed predominantly granular cytoplasmic staining with only the occasional cell positive for HUD in the nucleus. Laminin and fibronectin failed to change this staining pattern significantly. In contrast, in the presence of matrigel and vitronectin, a predominantly nuclear staining pattern with very little cytoplasmic staining was observed in a significantly higher percentage of cells (Fig 2.5D). Western blotting using this HUD antibody showed a 40kD band specific for this protein in Müller stem cell lysates (Fig 2.5C). This HUD antibody with its precise expression pattern was therefore established as being useful to quantify levels of HUD expression among the Müller stem cells and was used for this purpose in subsequent experiments.

In summary it was found that very few cells amongst the Müller stem cell population expressed HUD *in vitro* suggesting that only a small proportion of these cells had reached the stage of near complete differentiation towards an RGC fate. In addition, the expression of HUD mRNA could be significantly up regulated by matrigel and vitronectin which correlates with all the other previous analyses that show that these ECM proteins are the best suited to provide the signals that Müller stem cells need to differentiate towards an RGC fate.

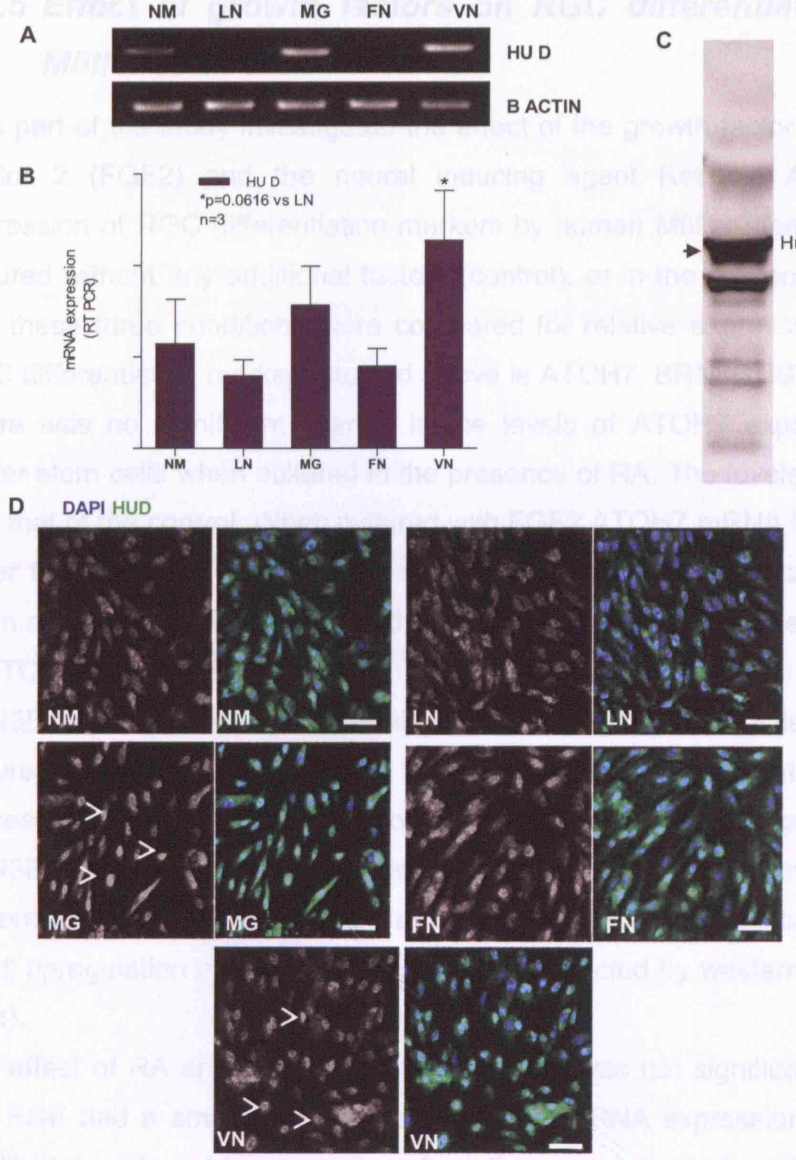

Figure 2.5: HUD expression by Müller stem cells. (A) RT PCR on Müller stem cells grown on various matrices shows that HUD is expressed in small amounts under baseline culture conditions but upregulated when cells are cultured on matrigel and vitronectin. (B) Histogram showing relative HUD gene expression by Müller stem cells cultured on different matrices, with the highest expression seen with vitronectin, followed by matrigel (although not significantly higher). 'n' refers to the number of independent measurements. (C) Western blot for HUD showing expression of a characteristic 40kD band by Müller stem cells. (D) Müller stem cells immunostained with the HUD antibody rarely showed positivity when cultured in the absence of ECM. The characteristic nuclear staining pattern was best seen with matrigel and vitronectin (arrow heads highlight some examples of nuclear staining). On the other matrices only background cytoplasmic staining was observed, with only occasional nuclear positivity. For each condition, the grey scale image of HuD staining and the colour image of HuD in green and DAPI in blue is shown. Scale bars= 20µm, NM=No Matrix, LN=Laminin, MG=Matrigel, FN=Fibronectin, VN=Vitronectin

2.3.5 Effect of growth factors on RGC differentiation of human Müller stem cells

This part of the study investigated the effect of the growth factor Fibroblast Growth Factor 2 (FGF2) and the neural inducing agent Retinoic Acid (RA) on the expression of RGC differentiation markers by human Müller stem cells. Cells were cultured without any additional factors (control), or in the presence of FGF2 or RA and these three conditions were compared for relative expression of each of the RGC differentiation markers studied above ie ATOH7, BRN3B, ISL1 and HUD.

There was no significant change in the levels of ATOH7 expression by human Müller stem cells when cultured in the presence of RA. The levels were comparable with that of the control. When cultured with FGF2 ATOH7 mRNA levels were slightly lower than those of control cells, but not at statistically significant levels. Overall when cultured with RA and FGF, there was no significant change in the expression of ATOH7 (Fig 2.6A&C).

BRN3B expression was considerably altered when human Müller stem cells were cultured with FGF2. This growth factor was able to significantly up-regulate the expression of BRN3B mRNA compared to baseline conditions (Fig 2.6A&C). BRN3B protein expression was also significantly up regulated by FGF2 compared to controls. RA had no apparent effect on the mRNA expression of BRN3B but a small upregulation in protein expression was detected by western blot analysis (Fig 2.6B).

The effect of RA and FGF on ISL1 expression was not significant. We saw again that FGF had a small positive effect on ISL1 mRNA expression but this was not significantly different in some cases from the expression at baseline levels. (Fig 2.6 A&C)

HUD mRNA expression by human Müller stem cells was slightly elevated when FGF was added to the culture but not to a level that was statistically significant. Western blots corroborated these results, showing a small increase in levels of HUD expression when cells were cultured with FGF2. In the presence of RA on the other hand, levels of HUD declined (Fig 2.6A, B&C).

From the above results it was concluded that addition of RA or FGF does not offer any particular advantage to the levels of RGC competence by Müller stem cells *in*

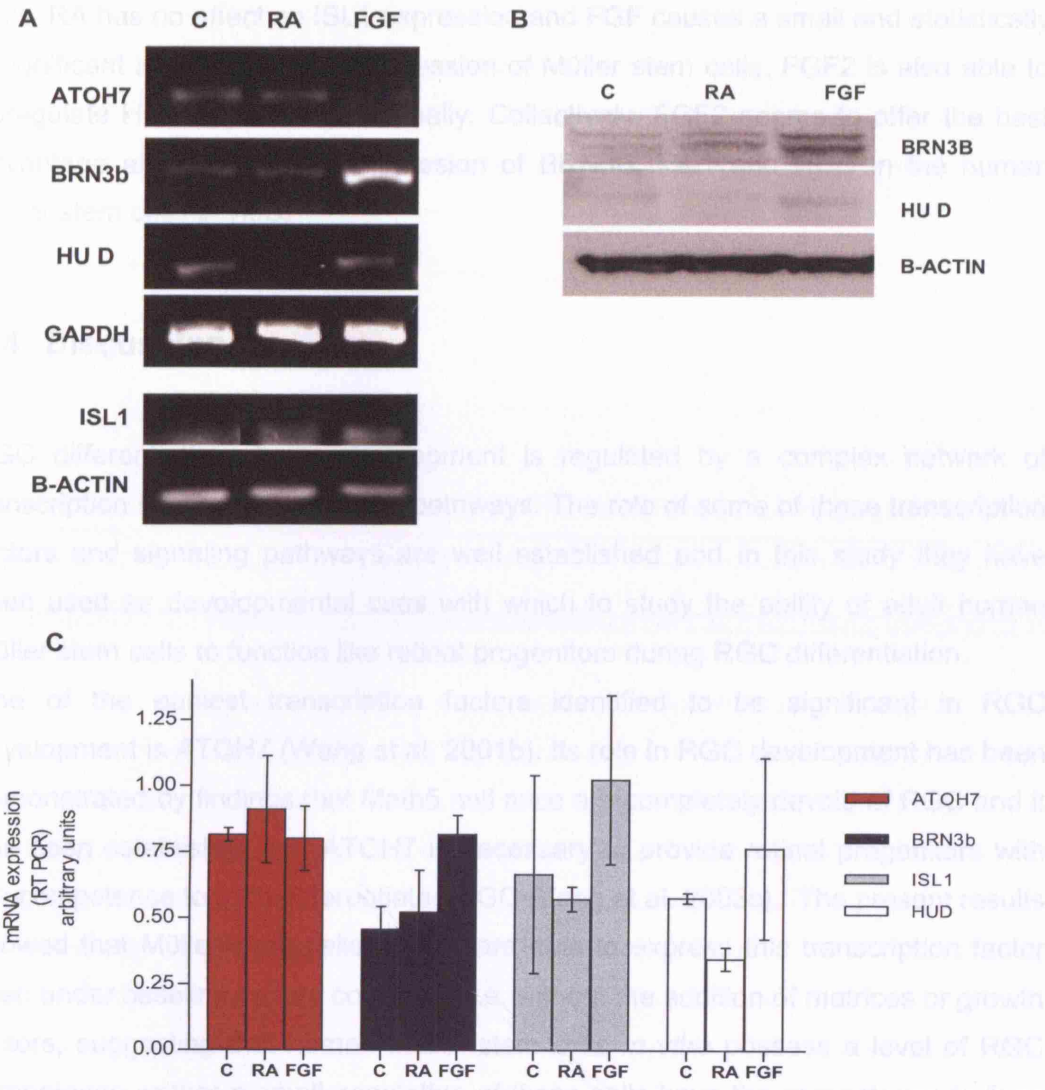

Figure 2.6: Effect of FGF and RA on expression of RGC markers in Müller stem cells *in vitro*. (A) Expression of mRNA coding for Atoh7, Brn3b, Isl1 and HuD by Müller stem cells cultured in the presence of FGF or RA (B) Brn3B and HuD expression by the Müller stem cells in the presence of FGF or RA as examined by western blots. (C) Cumulative histogram of RGC gene expression in Müller stem cells cultured with FGF or RA. FGF up regulates the expression of all genes investigated except ATOH7. Although individually the difference in expression amongst the three culture conditions for each gene was not significantly different, cumulatively it appeared that the highest expression of RGC precursor genes in each case was seen with FGF2. This graph was generated from the cumulative results of 2 different experiments and is depicted here to show a trend. As already stated the differences are not individually statistically significant. RA=Retinoic Acid, FGF=Fibroblast growth factor

vitro. FGF2 significantly up regulates BRN3B expression by human Müller stem cells. RA has no effect on ISL1 expression and FGF causes a small and statistically insignificant increase in ISL1 expression of Müller stem cells. FGF2 is also able to upregulate HUD expression minimally. Collectively, FGF2 seems to offer the best advantage at up regulating expression of BRN3B, ISL1 and HUD in the human Müller stem cells *in vitro.*

2.4 Discussion

RGC differentiation during development is regulated by a complex network of transcription factors and signaling pathways. The role of some of these transcription factors and signaling pathways are well established and in this study they have been used as developmental cues with which to study the ability of adult human Müller stem cells to function like retinal progenitors during RGC differentiation.

One of the earliest transcription factors identified to be significant in RGC development is ATOH7 (Wang et al. 2001b). Its role in RGC development has been demonstrated by findings that Math5 null mice are completely devoid of RGC and it has been established that ATOH7 is necessary to provide retinal progenitors with the competence to form differentiated RGC (Yang et al. 2003c). The present results showed that Müller stem cells *in vitro* are able to express this transcription factor even under baseline culture conditions i.e. without the addition of matrices or growth factors, suggesting that human Müller stem cells *in vitro* possess a level of RGC competence or that a small population of these cells have the competence to form RGC given the right conditions.

BRN3B is expressed downstream of ATOH7 and plays a role in differentiation of retinal progenitors that have committed to the RGC fate and have exit the cell cycle (Xiang 1998c). In Müller stem cells, expression of BRN3B was found to be at levels higher than that of ATOH7 under baseline culture conditions. These findings suggest that developmentally the Müller stem cell population contains cells that may have begun further differentiation towards the RGC fate and are perhaps not limited to the stage of RGC competence.

ISL1 is another marker of committed RGC precursors, expressed at the same stage as BRN3B during development (Pan et al. 2008b). Interestingly expression of mRNA coding for this gene was also detected in the human Müller stem cells *in vitro*. Finally HUD, which is expressed by terminally differentiating RGC was only minimally expressed in Müller stem cells cultured under baseline conditions. HUD expression was slightly- up regulated with ECM proteins and FGF2.

It must be pointed out that while tissue sections from adult rat and human retinae were used as positive controls for the immunostaining experiments involving the BRN3B, ISL1 and HUD antibodies, no negative controls (apart from a secondary antibody only control) were used to rule out spurious staining by these antibodies. The fact that retinal structures (for example photoreceptors in retinal sections) did not stain for these markers was considered to be an endogenous negative control. Cell lines known to express these markers would have constituted ideal negative controls. These experiments would lend support to the conclusion that the proteins in question were in fact being expressed by the Müller stem cells.

Thy1 has been and continues to be a popular marker for RGC identification but was not used in these studies to identify RGC precursors. Preliminary experiments with the gene revealed that there was a considerable level of Thy1 mRNA expression in these cells under baseline conditions. Further immunostaining with the antibody to Thy1 also demonstrated a robust and uniform cytoplasmic staining pattern in almost all the cells prepared. However from the expression pattern of other differentiated RGC markers in the Müller stem cells, it was obvious that very few of these cells were actually differentiated RGC. It was concluded that there was either considerable non specific immunostaining to the antibody or that the Müller stem cells *in vitro* were aberrantly capable of producing Thy1 without possessing other features of differentiated RGC. There is also recent evidence that suggests the expression of Thy1 may not be directly related to the number of surviving RGC in an early apoptotic environment (Huang, Fileta, Guo & Grosskreutz 2006). On the basis of this literature and our own results Thy1 was not used as one of the markers identifying RGC precursors in the Müller stem cell population despite previous precedence.

Previous studies have shown that a population of Müller stem cells derived from the adult human post mortem eyes have the ability to function as retinal progenitors

given that they express retinal progenitor markers like Pax6, Chx10 and Sox2 (Lawrence, Singhal, Bhatia, Keegan, Reh, Luthert, Khaw, & Limb 2007d). From the present observations, it is possible to suggest that Müller stem cells also possess a level of RGC competence as well as commitment. These results indicate that these cells may have some potential to function as a source of RGC. Culture of human Müller stem cells in the presence of ECM proteins and the addition of growth factors like FGF2 appear to be reliable methods to achieve up regulation of the expression of these markers, particularly BRN3B, ISL1 and HUD.

These results also further indicated the heterogeneous nature of the Müller stem cell population. When immunostained it was seen that even under conditions that supported expression of the differentiated RGC markers, not all cells showed expression of the antibody in question. This phenomenon has been reported in the past with varying proportions of Müller stem cells staining for markers of retinal progenicity as well as other retinal neuronal precursor markers (Lawrence, Singhal, Bhatia, Keegan, Reh, Luthert, Khaw, & Limb 2007). It is therefore thought that the cultures derived from Müller glia are heterogenous and consist of cells at various stages of development and progenicity i.e early and late retinal progenitors at various stages of cell fate commitment and differentiation.

Other sources of stem cells like embryonic, neural and bone marrow stromal cells have all been studied for their ability to function as retinal progenitors and form differentiated retinal neurons. In most cases extensive manipulation is necessary to induce expression of progenitor markers Pax6, Chx10, Sox2 etc in these cells (Gong et al. 2008a). The neural and bone marrow stromal cells are tissue specific stem cells and it is likely that they are already at stages of terminal differentiation related to their tissue of origin. They would require de-differentiation to an earlier stage before being able to differentiate down an alternative cell fate. Differentiation of human Müller stem cells towards specific retinal neuronal cells and RGC in particular has not been previously attempted. The results presented here demonstrate the expression of such RGC precursor markers in the Müller stem cell population *in vitro* without any defined culture conditions. It is also encouraging that there is room to further boost RGC differentiation among these Müller stem cells and simple environmental manipulations are able to achieve this differentiation.

Chapter 3: Role of Notch signaling in retinal ganglion cell differentiation of Müller stem cells

3.1 Introduction

3.1.1 The Notch signalling pathway

The Notch signaling pathway comprises a single transmembrane heterodimeric cell surface receptor which is activated upon interaction with the extracellular domain of its ligands (delta and serrate) on the adjacent cell surface (Louvi & Artavanis-Tsakonas 2006b). Activation of the Notch receptor results in a presenilin gamma secretase complex mediated cleavage of the intracytoplasmic domain (ICD) from the transmembrane fragment (illustrated in Fig 3.1). The ICD then translocates to the nucleus where it interacts with the CBF-1, Suppressor of Hairless, Lag1 (CSL) complex. This results in the activation of Hes1 and Hes5, which are effectors of Notch signaling. Hes1 and Hes5 are transcriptional repressors and upon activation prevent the transcription of downstream pro neural genes required for neural differentiation (Das et al. 2005h). In this manner Notch1 activation prevents the differentiation of progenitor cells and keeps them in their state of self renewal without differentiation. Notch also works in association with other accessory signaling pathways which similarly influence progenitor cell proliferation and cell fate. Amongst these the relationship of the Wnt pathway with Notch is well established(Katoh & Katoh 2006). Apart from being activated by similar ligands like jagged, frizzled and delta, these 2 pathways also share common effectors like hairy/enhancer-of-split related with YRPW motif 2 (Hey2) and Transducin like enhancer of split 1 and 4 (TLE1 and 4) (Fox et al. 2008).

Notch is also believed to have a direct effect on cell proliferation due to the way it affects cell division. Ronchini and Capobianco in 2001 demonstrated a direct effect of Notch on Cyclin D1 expression and CDK2 activity using Notch activation in an estrogen receptor (ER) induced system (Ronchini & Capobianco 2001). They were able to show that Notch activation in neuroepithelial cells increased mRNA

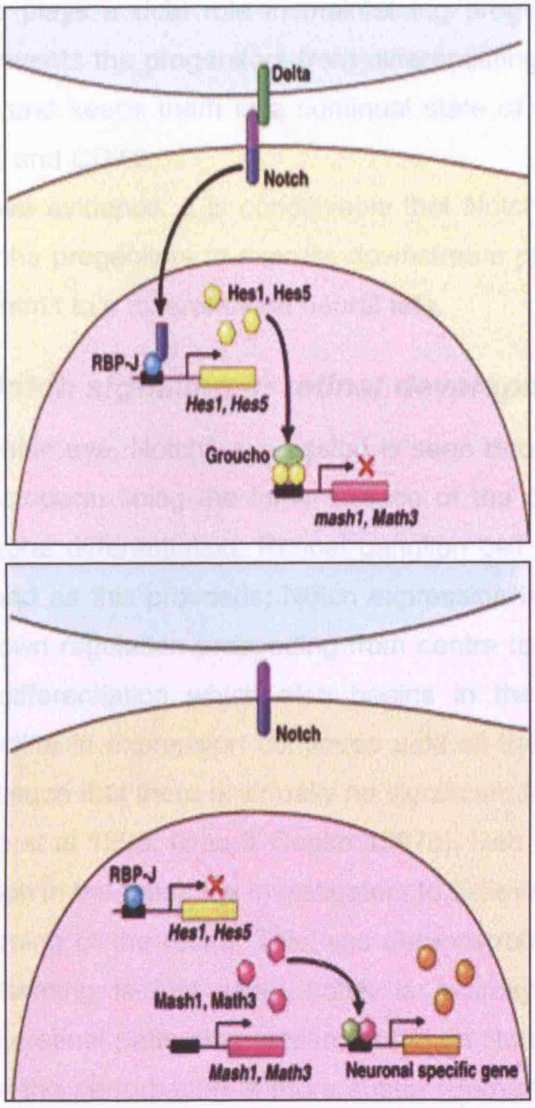

Figure 3.1: Mechanism of Notch activation

Notch is activated by binding of ligands (delta) to the transmembrane Notch receptor. Upon ligand binding, the intra cytoplasmic domain of the transmembrane receptor is cleaved by gamma secretase mediated activity and translocated to the nucleus. In the nucleus this intracytoplasmic domain mediates the activation of Hes1 and Hes5 which are transcriptional repressors. They prevent the activation of down stream neuronal specific genes thereby preventing neuronal differentiation in cells where notch is activated. (modified from Hakateyama and Kageyama, 2004)

expression of Cyclin D1 and activated CDK2 resulting in increased DNA synthesis. They also identified a CSL binding site in the promoter region of Cyclin D1 proving that cyclin D1 activation was CSL dependent and directly related to Notch. Notch signaling therefore plays a dual role in maintaining progenitor population during development. It prevents the progenitors from differentiating by inhibiting proneural gene transcription and keeps them in a continual state of proliferation through its effect on Cyclin D1 and CDK2.

In view of the above evidence, it is conceivable that Notch activity must be down regulated to allow the progenitors to express downstream proneural genes and exit the cell cycle to commit to a differentiated neural fate.

3.1.2 Role of Notch signaling in retinal development

In the early embryonic eye, Notch1 expression is seen throughout the thickness of the anterior neurectoderm lining the inner surface of the optic cup layer, prior to onset of retinal neural differentiation. Retinal ganglion cell (RGC) differentiation is the first to begin and as this proceeds, Notch expression is down regulated in the inner retina, the down regulation proceeding from centre to periphery following the pattern of RGC differentiation which also begins in the centre and proceeds outwards. This decline in expression continues until all the retinal neuronal types have differentiated such that there is virtually no significant Notch activity in the post natal retina (Cepko et al 1995, (Bao & Cepko 1997c), Reh et al 2006).This pattern of Notch1 expression in the retina led investigators to believe that Notch also played a role in the patterning of the retina. This was demonstrated by observations that normal retinal patterning is lost when notch is overexpressed (Scheer et al. 2001a).Interestingly retinal patterning is also lost when Notch is inhibited, although the exact nature of the perturbation is more subtle (Bernardos et al. 2005). In the former case it seems that Notch overexpression prevents cell differentiation and causes uncontrolled proliferation thereby causing an imbalance between the processes of progenitor production and progenitor 'utilization' for differentiation. In the latter case, inhibition of Notch activity leads to premature differentiation with too many differentiated neurons but at the wrong place at the wrong time, thereby perturbing retinal patterning. This process was further characterized by Nelson et al in 2007. They inhibited Notch activity in chick embryonic retinae at different stages

of development for different periods of time, using the gamma secretase inhibitor DAPT, and analyzed the effect of this inhibition on retinal differentiation. Their results showed that at different stages of development Notch inhibition has different effects on the retinal differentiation process. They established that transient Notch inhibition was necessary for each of the different cell types to differentiate and proposed that this transient inhibition of Notch activity synchronized the process of retinal neuronal differentiation (Nelson et al. 2007d).

3.1.3 Role of Notch signaling in retinal ganglion cell development

RGC are the first to differentiate among the retinal neurons and as already mentioned above, Notch activity is down regulated in the central inner retina, just before RGC differentiation begins at this site. This has been specifically demonstrated in the central retina of the developing chick where there is loss of Hes 1 expression before onset of Ath5 expression (Matter-Sadzinski et al. 2005b). The *Xenopus* homologue of Ath5, Xath5, also a pro neural gene regulated by Notch activity, has similar functions and can induce premature RGC differentiation when injected into cleavage stage xenopus blastomeres. This effect is prevented by the co-expression of activated Notch, establishing a direct link between the expression of this RGC competence marker and Notch activity (Schneider, Turner, & Vetter 2001). Based on these observations, it appears that retinal progenitors need to escape Notch inhibition before they can differentiate into RGC.

Various studies have shown that when Notch activity is inhibited during early retinal development, it results in premature differentiation of retinal ganglion cells. Austin et al treated embryonic chick retinae with antisense oligonucleotides to Notch and demonstrated a two fold increase in the number of ISL1 positive cells in the ganglion cell layer of the retina (Austin et al. 1995b). Silva et al studied the influence of Notch activity on retinal ganglion cell differentiation *in vitro* by culturing embryonic retinal precursors in the presence and absence of Notch antisense oligonucleotides. They found that blocking Notch activity pushes the progenitors towards premature differentiation into a ganglion cell fate. This effect was independent of an increase in cell division or cell death suggesting the effect of Notch on transcriptional repression. They also found that this effect was pronounced only in early retinal

progenitors, at a time when ganglion cells would normally develop. When the same inhibition was applied in the late retinal progenitors/ or the more mature central retina there was no significant increase in the number of differentiated ganglion cells. This suggests that Notch predominantly affects cell fate decisions in differentiating progenitors and that it does not have as significant an effect on the post mitotic differentiated cells. (Silva et al 2002).

At present it is not clear whether this effect of Notch on RGC differentiation is a result of direct inhibition of downstream proneural genes influencing RGC development. Despite the strong temporal association between Math5 and Notch expression, from data obtained in Hes1 null mice, it seems unlikely that Notch directly affects Math5. Hes1 is the principal effector gene of Notch signaling and Hes1 null mice effectively lack any Notch signaling. These mice also demonstrate premature ganglion cell differentiation but the amount of Math5 expressed in them is similar to the wild type suggesting that the premature differentiation is not as a result of Math5 up regulation (Louvi & Artavanis-Tsakonas 2006c;Takatsuka et al. 2004). Other downstream genes in the transcriptional network responsible for RGC differentiation are therefore likely to be the target and their identity is still unknown.

Recent work on the effect of chromatin remodeling might have further answers to these questions, although the work is still in its early stages. Chromatin remodeling is a tertiary level of gene regulation, and its role in development and differentiation is increasingly becoming an important subject of research in this area. Recent work on Brahma (Brm), an ATPase chromatin remodeling enzyme, suggests that this enzyme has a dual effect on RGC differentiation via its influence on Notch activity and expression of BRN3B, a marker of committed RGC precursors. Das et al have demonstrated that Brm is able to inhibit Notch activity as shown by its effect on the upregulation Hes1/5 levels in Brm null mice and a decrease in Hes1 luciferase reporter activity in cells overexpressing Brm (Das et al. 2007). At the same time, they show that Brm is able to upregulate BRN3B expression, through its effect on transcription factor Wilm's tumour 1 (Wt1) which is a known regulator of BRN3B expression. This work also suggests that Brm is able to prevent G1-S transition of retinal progenitors thereby allowing them to exit the cell cycle and proceed to terminal differentiation. While this is perhaps the first demonstration of a link between Notch activity and BRN3B expression in RGC differentiation it does not

present BRN3B as a direct target downstream of Notch1 and further work is required to delineate the relationship of these two molecules in RGC development. However the fact remains that Notch activity prevents retinal progenitors from differentiating towards an RGC fate during development and progenitors must escape this inhibition in order to be able to differentiate down the RGC lineage.

3.1.4 Role of Notch signaling in gliogenesis

Contrary to its restrictive role in ganglion cell development Notch signaling seems to support and possibly have an instructive role in gliogenesis. It has been shown to limit neurogenesis and promote gliogenesis from a variety of neural progenitor cell types including radial glia from cortical stem cells (Gaiano, Nye, & Fishell 2000), astroglia from adult hippocampal derived mutltipotent progenitors (Tanigaki et al. 2001) and Müller glia from retinal progenitors (Furukawa et al. 2000d). The effect of Notch on Müller glial differentiation was first demonstrated by Dorsky et al in 1995 when they showed that the last cells expressing Notch in the frog retina eventually became Müller glia. They also found that activated Notch actually prevented these cells from terminally differentiating into glia and that instead they seemed to acquire a neuroepithelial fate in the presence of activated Notch. They concluded that while Notch was instructive in gliogenesis, its downregulation was essential before terminal glial differentiation could take place (Dorsky, Rapaport, & Harris 1995). The same was found to be true in rat retina. Cells expressing activated Notch in this species were found to be proliferatively active, possess morphology similar to that of Müller glia and express characteristic markers of these cells (Bao & Cepko 1997b). In the zebrafish larvae expression of activated Notch results specifically in an increase in gliogenesis 6 days post fertilization despite the apparent perturbation of the remaining retinal neuronal cell types (Scheer et al. 2001b).

This evidence suggests that Notch has an instructive role in gliogenesis despite its inhibitory role in neurogenesis. As a result of this work, a novel concept regarding the relationship of this gliogenic role with its role in maintenance of retinal progenitors is being postulated (Furukawa et al. 2000c). It has been mentioned already that while Notch promotes glial cell fate, it must be down regulated before terminal glial differentiation can be achieved. Work with Hes1 null mice shows that while Müller glial numbers are reduced in the absence of Hes1, at this stage in

development most of the Hes1 expressing cells are negative for Müller glial markers such as glutamine synthase. Cells that express Notch and possess Müller glial morphology, but have not terminally differentiated, have been found to express nestin (Furukawa et al. 2000b). Furukawa et al suggest that these cells may constitute a late retinal progenitor population which will eventually gain a glial fate in the absence of other signals. It is likely that this is the population of cells that has been identified as Müller stem cells in the adult human retina (Lawrence, Singhal, Bhatia, Keegan, Reh, Luthert, Khaw, & Limb 2007d).

3.2 Objectives and experimental outline

Based on this evidence suggesting the importance of Notch signalling in RGC differentiation during development, this chapter aimed to examine the role of Notch signalling in the regulation of human Müller stem cell maintenance and differentiation *in vitro*. Notch signalling is crucial to RGC differentiation during development. The objectives were:

1. To examine the presence and levels of Notch activity in the Müller stem cells and the effect of differentiation on Notch activity in these cells.
2. Since Notch activity prevents RGC differentiation during retinal development, to also examine the effects of inhibiting Notch activity in the Müller stem cells on their differentiation towards RGC fate.
3. To specifically identify and study the committed RGC precursor population from among the human Müller stem cell population using a BRN3B reporter. The aim of using the reporter was to assess, more accurately, the effects of the various treatments on the size of the committed RGC precursor population being generated within the human Müller stem cells.

The overall aim of this chapter was to examine the possibility of enhancing the RGC differentiation potential of the Müller stem cells by altering the Notch signalling pathway in them.

The experiments were performed as follows-

1. Müller stem cells were cultured under baseline conditions for 7 days and examined for their protein and mRNA expression of Notch pathway

components including Notch1, Hes 1 and Hes5 mRNA as well as cleaved Notch protein.

2. Müller stem cells were then cultured with FGF and RA for 7 days and the effect of these treatments on Notch activity was examined.
3. Gamma secretase inhibitor DAPT (N-[N-(3,5-Difluorophenacetyl)-L-alanyl]-S-phenylglycine t-butyl ester) was used to inhibit Notch activity in Müller stem cells *in vitro*. The dose and duration of DAPT exposure to achieve Notch inhibition in Müller stem cells was optimised.
4. The Müller stem cells were cultured with the optimised DAPT dose and the effect of this treatment on the expression of RGC differentiation markers by the cells was examined. These experiments were performed in 4 different Müller stem cell lines to ensure that any effect seen was true of the different cell lines and not characteristic of one particular cell line alone.
5. A GFP BRN3B transcriptional reporter was designed to identify Müller stem cells which expressed BRN3B and were therefore committed to the RGC fate.
6. Müller stem cells were transfected with the BRN3B reporter and the number of cells committed to the RGC fate were analysed under baseline culture conditions. The cells were analysed using fluorescent cell sorting (FCS) to count the number of GFP positive cells and the results were compared with the number of committed RGC precursors (BRN3B positive cells) counted when Müller stem cells were cultured with matrices and FGF or RA.
7. To characterise the RGC committed precursor population, BRN3B reporter positive Müller stem cells were analysed for their ability to divide and express differentiated RGC markers, and the expression compared with BRN3B reporter negative cells.
8. Finally the BRN3B reporter was used to study the effect of DAPT on the number of Müller stem cells committed to the RGC fate. Reporter transfected Müller stem cells were treated with DAPT, FCS analysed and the results compared with those of cells cultured without DAPT.

To inhibit Notch activity in Müller stem cells *in vitro* a gamma secretase inhibitor (GSI) called DAPT (N-[N-(3,5-Difluorophenacetyl)-L-alanyl]-S-phenylglycine t-butyl ester) was used. DAPT has previously been shown to inhibit Notch activity and is

known to be able to inhibit the Notch effectors Hes1 and Hes5 in a manner similar to that seen with Notch conditional knock outs, as well as Hes1 and Hes5 nulls (Nelson et al. 2007c). DAPT mediated inhibition is accepted as being phenotypically similar to *in vivo* inactive Notch. This chemical was therefore used in these studies to inhibit Notch activity *in vitro* in Müller stem cells.

DAPT (D5942, Sigma-aldrich, UK) obtained in powder form was resuspended in DMSO to obtain a stock solution of 50mM/ml. This was diluted according to the desired final concentration and added to the culture media at the time of plating the cells.

3.3 Results

3.3.1 Baseline Notch activity in Müller stem cells

The results showed that Müller stem cells expess mRNA for Notch1 as well as its immediate effectors Hes1 and Hes5 in these culture conditions (Fig 3.2 A). Using the same amount of starting material as used to analyse the expression of ATOH7, BRN3B, ISL1 and HUD (1µg of starting RNA) Notch1 mRNA was found to be expressed at relatively higher levels using a 34 cycle PCR compared to the other RGC markers. The levels of Hes1 mRNA were also relatively high. However Hes5 was expressed in smaller amounts compared to Notch1 and Hes1 mRNA (Fig 3.2A). mRNA expression of Hey2 which is another accessory effector of the Notch signaling pathway was also investigated. Small levels of this transcript were found to be expressed by Müller stem cells. Transducin like enhancer of split 1 and 4 (TLE1 and 4) are effectors of the Wnt signalling pathway and transcripts of these genes were also detected in small amounts in Müller stem cells. These observations suggest that other pathways known to work in tandem with the Notch signaling pathway were also active in Müller stem cells *in vitro*. (Fig 3.2A)

To assess the level of Notch activity in Müller stem cells, the levels of total and cleaved intracytoplasmic domain (ICD) of Notch were analysed using western blotting. Notch is activated by gamma secretase mediated cleavage which results in the production of the ICD and a measure of the ICD provides a reliable estimate of the level of notch activity. Total protein isolated from Müller stem cells cultured for 7

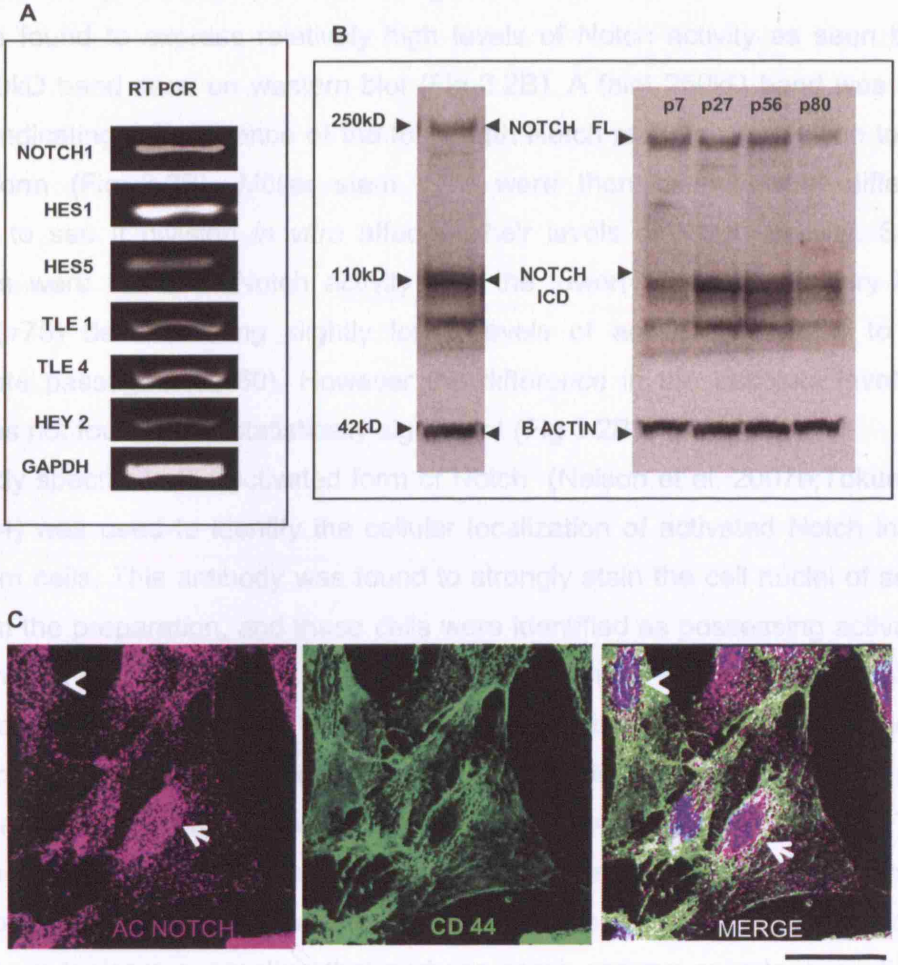

Figure 3.2: Notch activity in Müller stem cells. (A) RT PCR showing expression of genes involved in the Notch pathway namely Notch1, its effectors Hes1 and Hes5 and accessory genes Hey2, Tle1 and Tle4 in the Müller stem cells. (B) Assessment of Notch activity in Müller stem cells using western blotting shows a 110kD band corresponding to the intra-cytoplasmic domain of this molecule suggesting active Notch signalling. The levels of the ICD vary slightly with the passage time of cells in culture. Also detected on the western blot is the full length notch protein band of about 250kD (C) Immunostaining of Müller stem cells with activated notch (AC NOTCH) antibody which stains the ICD. Nuclear localisation of the antibody was seen in some Müller stem cells. White arrow highlights a cell with positive staining in the nucleus. Compare with cell highlighted by white arrow head which is negative for nuclear activated notch. CD44 was used to outline the cellular architecture of Müller stem cells and confirm that the activated Notch antibody staining was predominantly nuclear when present. Scale bar=10μm

days was run on 3-8% tris-acetate gels to resolve both the full length (250kD) and the cleaved ICD (100-110kD) bands. Using similar culture conditions Müller stem cells were found to express relatively high levels of Notch activity as seen by a strong 110kD band seen on western blot (Fig 3.2B). A faint 250kD band was also detected indicating the presence of the full length Notch receptor in addition to the cleaved form (Fig 3.2B). Müller stem cells were then examined at different passages to see if division *in vitro* affected their levels of Notch activity. Small differences were found in Notch activity with the lower(<10) and the very high passages(>75) demonstrating slightly lower levels of activity compared to the intermediate passages (20-60). However the difference in the absolute levels of activity was not found to be statistically significant (Fig 3.2B).

An antibody specific to the activated form of Notch (Nelson et al. 2007b;Tokunaga et al. 2004) was used to identify the cellular localization of activated Notch in the Müller stem cells. This antibody was found to strongly stain the cell nuclei of some cells within the preparation, and these cells were identified as possessing activated Notch signaling (Fig 3.2C). About 60% percent of the cells were found to be positive for the activated Notch under baseline culture conditions. Examples of Notch positive and negative cells are shown in figure 3.2C. Cells were counter stained with anti human CD44 which specifically binds to the cell membrane of Müller cells. This allowed the identification of the cellular architecture clearly. In cells lacking nuclear staining for activated Notch, occasional granular staining of the antibody could be seen in the cytoplasm suggesting that perhaps some gamma secretase mediated cleavage was occurring in these cells, but that it was not sufficient to generate enough ICD to cause nuclear translocation and activation of the subsequent cascade of transcriptional repression.

3.3.2 Effect of growth factors on Notch activity in Müller stem cells

As described in the previous chapter treatment of Müller stem cells with FGF2 for 7 days results in upregulation of BRN3B and HUD expression as examined by western blotting of cell lysates. Examination of Notch activity levels in similar

samples revealed considerable down regulation of this activity when the cells were cultured with RA (Fig 3.3A). Although FGF2 also caused a decrease in the levels of Notch activity, this decline was smaller than that seen with RA and not statistically significant. When the results of several repeats of this experiment were put together, the same pattern of Notch activity was observed, and while the difference in the levels of Notch activity amongst the three samples (control, RA and FGF2) were not statistically significant, the results consistently showed that RA downregulated Notch to a greater extent than FGF2. At the same time, expression of RGC differentiation markers was consistently higher in FGF2 treated cells (Fig 3.3B). These experiments were repeated with special focus on the Notch activity and BRN3B expression of FGF2 treated cells compared to control cells and revealed that Notch activity was consistently down regulated whilst BRN3B was consistently up regulated (Fig 3.3C).

3.3.3 DAPT mediated inhibition of Notch activity in Müller stem cells

A dose response to assess the dose of DAPT required to effectively inhibit Notch activity in Müller stem cells *in vitro* was first performed. Using 10μM/ml final concentration as a guideline used by others (Nelson et al. 2007e), significant inhibition of Notch activity was achieved in the Müller stem cells with a final concentration of 50μM/ml. This dose was decided upon, in light of the good inhibition of Notch activity achieved without adverse effects on cell viability. (Fig 3.4A) Western blot analysis showed a dose response related decrease in Notch activity with increasing doses of DAPT. While 50μM/ml caused a considerable decline in activity, it did not completely abolish Notch activity and it was decided to use this dose for future experiments, as higher doses were found to adversely affect cell survival (data not shown).

Further experiments were performed to investigate the time needed to achieve the best inhibition when cells were cultured with 50 μM/ ml DAPT. Cells were plated on matrigel with 50μM DAPT and 20ng/ml of FGF2 on day 1 and at different time points, the DAPT containing media was removed, cells washed and fresh media

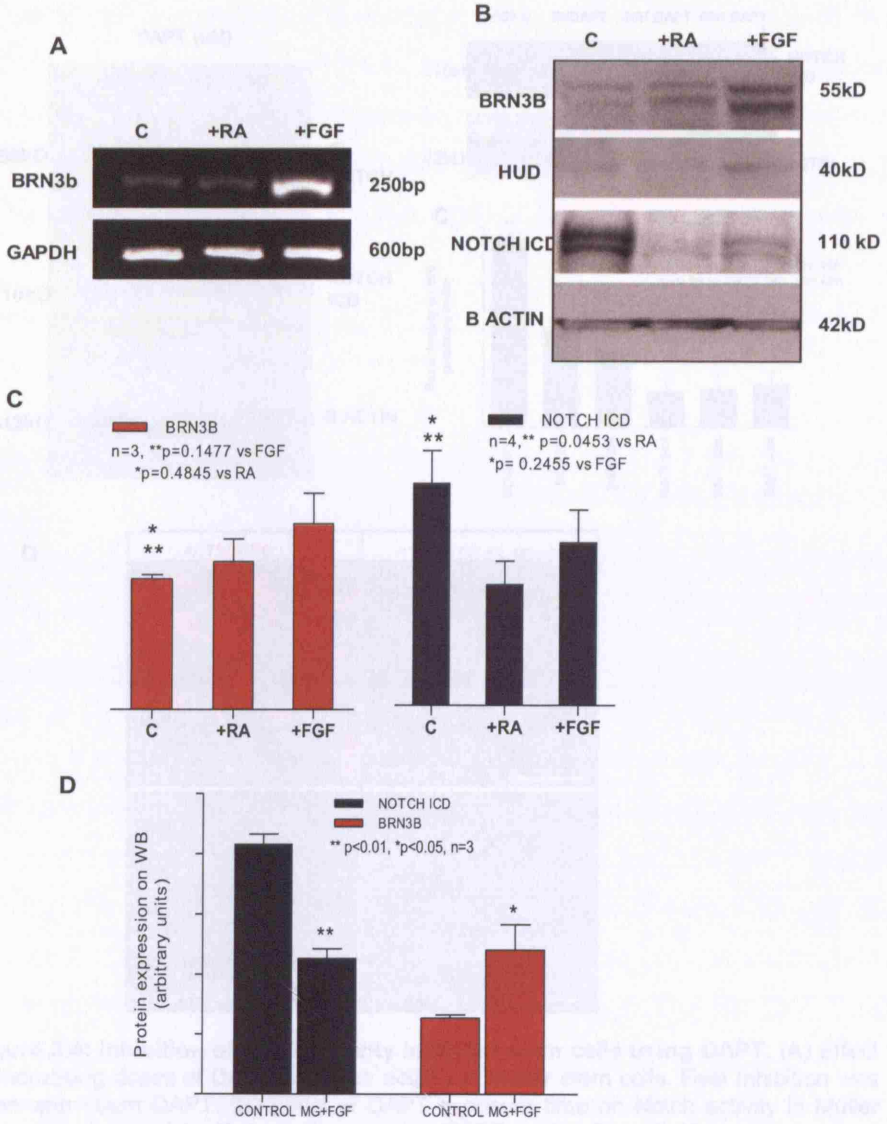

Figure 3.3: Effect of differentiation on Notch activity of Müller stem cells. (A) RT PCR showing up regulation of BRN3B gene in Müller stem cells with FGF.(B) Western blot showing up regulation of BRN3B protein expression in Müller stem cells cultured with FGF. In the same samples Notch activity as seen by the ICD band on western blots is down regulated with FGF. (C) Histograms depicting relative expression of Brn3b protein and Notch activity with RA and FGF. Brn3b expression is slightly up regulated by both FGF and RA, although not significantly ($p=0.4845$ vs RA and $p=0.1477$ vs FGF2). Conversely Notch activity is significantly down regulated by RA ($p<0.05$) but not FGF2 ($P>0.05$)(D) Histograms depicting relative Brn3b protein expression and Notch activity when cells are grown in the presence of matrigel and FGF. Notch activity was significantly down regulated in cells treated with matrigel and FGF2 when compared to control, whilst Brn3b expression was significantly upregulated. Despite the down regulation considerably level of Notch activity still persists. In each case 'n' refers to the number of independent measurements.

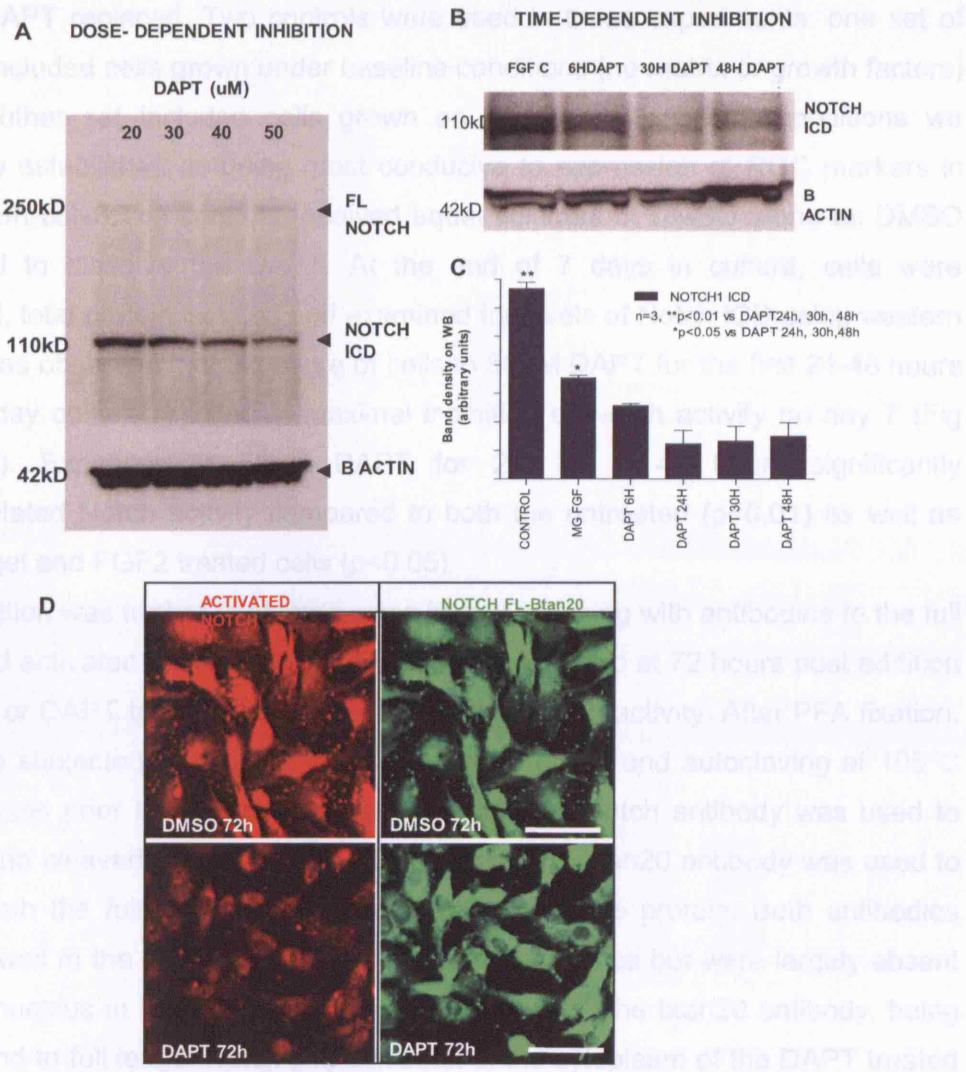

Figure 3.4: Inhibition of Notch activity in Müller stem cells using DAPT. (A) Effect of increasing doses of DAPT on Notch activity in Müller stem cells. Best inhibition was seen with 50µm DAPT. (B) Effect of DAPT exposure time on Notch activity in Müller stem cells cultured for 7 days. Exposure to DAPT for the first 30-48 hours of culture resulted in the lowest level of Notch activity at day 7. (C) Histogram showing decline in Notch activity with increasing exposure time to DAPT in Müller stem cells cultured on matrigel and FGF. Compared to the control cells and those not exposed to DAPT Notch activity in DAPT exposed cells declined steadily and was lowest in cells treated with 24-48 hours of DAPT. 'n' refers to the number of independent measurements. (D) Immunostaining of Müller stem cells, cultured with DAPT or its carrier DMSO for 72 hours, with antibodies to the activated form of Notch (Ac Notch) and the full length (FL) Notch (bTan20). Ac Notch characteristically shows nuclear staining in cells with Notch activity. bTan20 antibody characteristically stains the cytoplasm but is also present in the nucleus when cells have active Notch signalling. In these micrographs it is seen that DAPT causes decrease in the nuclear staining as observed with both antibodies at 72 hours. The full length antibody is still seen to be staining the cytoplasm of treated cells, while the activated Notch antibody stains the treated cells minimally. Scale bars=20µm

without DAPT replaced. Two controls were used in these experiments: one set of controls included cells grown under baseline conditions (no matrix or growth factors) and the other set included cells grown on matrigel with FGF2 (conditions we previously established as being most conducive to expression of RGC markers in Müller stem cells).The controls received equal volumes of DMSO alone as DMSO was used to dissolve the DAPT. At the end of 7 days in culture, cells were harvested, total protein isolated and examined for levels of Notch ICD using western blots. It was observed that exposure of cells to 50μM DAPT for the first 24-48 hours of the 7 day culture resulted in maximal inhibition of Notch activity on day 7 (Fig 3.4B &C). Exposure to 50μM DAPT for 24, 30 & 48 hours significantly downregulated Notch activity compared to both the untreated ($p<0.01$) as well as the matrigel and FGF2 treated cells ($p<0.05$).

This inhibition was further confirmed using immunostaining with antibodies to the full length and activated forms of Notch. Cells were harvested at 72 hours post addition of DMSO or DAPT to examine differences in their Notch activity. After PFA fixation, cells were subjected to antigen retrieval in citrate buffer and autoclaving at 105°C for 5 minutes prior to immunostaining. The activated Notch antibody was used to indentify the cleaved intracytoplasmic domain and the btan20 antibody was used to identify both the full length and the cleaved form of the protein. Both antibodies localized well to the nucleus in the DMSO treated samples but were largely absent from the nucleus in the DAPT treated cells (Fig 3.4D). The btan20 antibody, being able to bind to full length Notch was still seen in the cytoplasm of the DAPT treated cells but the activated Notch antibody stained the treated cells minimally.

The mRNA expression of Hes1 which is the immediate effector of Notch1 was examined by performing real time quantitative PCR on total RNA isolated from DAPT treated cells. The results were able to demonstrate a significant down regulation ($p<0.0001$) in the levels of Hes1 transcripts in treated cells compared to the control cells (Fig 3.5A)

The cells were also stained for the proliferation marker Ki67 which identifies actively dividing cells in all stages of cell division. It was found that the rate of proliferation in the DAPT treated sample was significantly higher than that in the DMSO control sample, although both had been treated with FGF2 (Fig 3.5B).

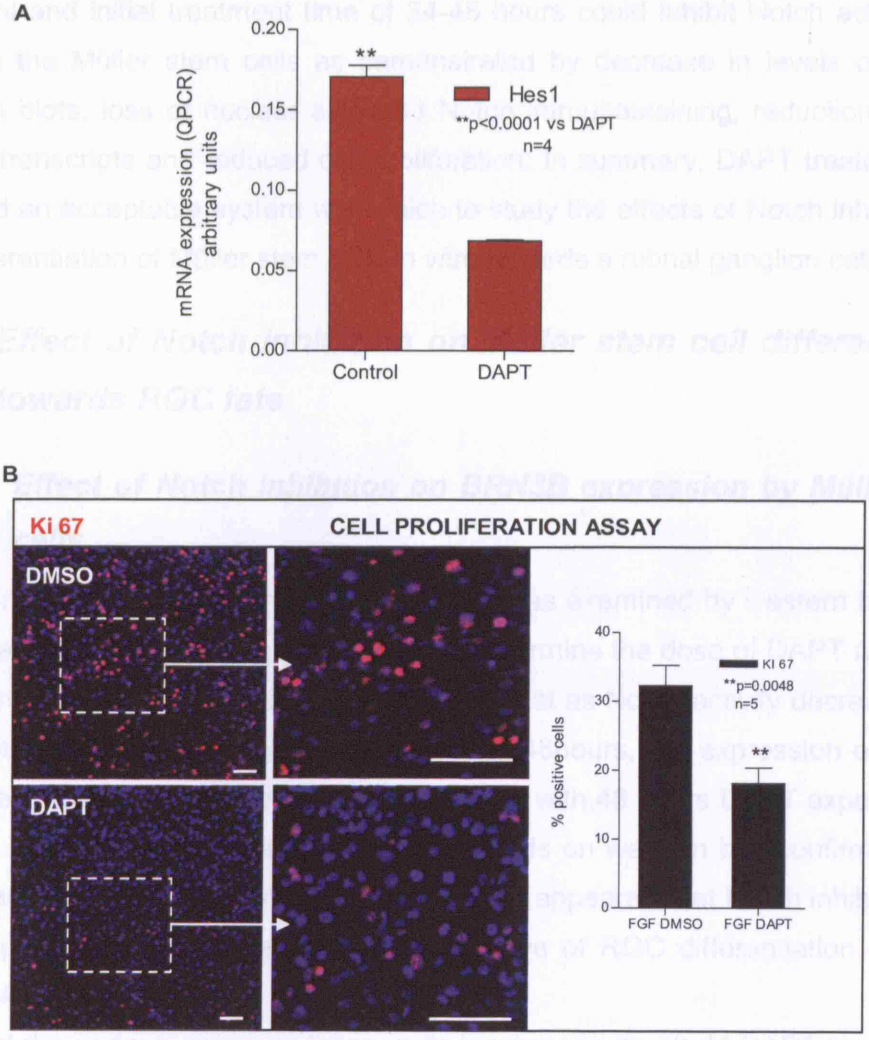

Figure 3.5: Effect of DAPT on Müller stem cell expression of Hes1 expression and their rate of proliferation. (A) Expression of Notch effector Hes1 in the Müller stem cells under control conditions and after treatment with DAPT, as seen on quantitative real time PCR. Treatment with DAPT causes a significant decline in the levels of Hes1 expression in the Müller stem cells ($p<0.0001$), n=4 (B) Immunostaining of Müller stem cells with proliferation marker ki67 with or without DAPT treatment showing a significant decrease in the number of ki67 positive cells in the the DAPT treated sample. The micrographs on the right are maganifications of inset marked with the dotted square on the left. The histogram depicts this quantitatively showing a reduction in proliferation rate from 32% to 18% with DAPT treatment. Scale bar=20µm. In each case 'n' refers to the number of independent measurements

Based on the above results, it was possible to establish that DAPT at a dose of 50μM/ml and initial treatment time of 24-48 hours could inhibit Notch activity at 7 days in the Müller stem cells as demonstrated by decrease in levels of ICD on western blots, loss of nuclear activated Notch immunostaining, reduction in Hes1 mRNA transcripts and reduced cell proliferation. In summary, DAPT treatment was deemed an acceptable system with which to study the effects of Notch inhibition on the differentiation of Müller stem cells *in vitro* towards a retinal ganglion cell fate.

3.3.4 Effect of Notch inhibition on Müller stem cell differentiation towards RGC fate

3.3.4.1 Effect of Notch inhibition on BRN3B expression by Müller stem cells

In the first instance the expression of BRN3B was examined by western blot in the same samples that were previously used to determine the dose of DAPT necessary to achieve good Notch inhibition. It was found that as Notch activity decreased at 7 days with initial DAPT exposure for 6, 30 and 48hours, the expression of BRN3B increased, and the highest expression was seen with 48 hours DAPT exposure (Fig 3.6A). Quantification of the density of the bands on western blot confirmed these trends across different experiments (Fig 3.6B). It appeared that Notch inhibition was indeed promoting BRN3B expression suggestive of RGC differentiation of Müller stem cells.

Amongst the various exposure times, cells incubated with 50μM DAPT for 48 hours produced the highest levels of BRN3B expression. On this basis, this experiment was repeated with control cells, cells treated with matrigel and FGF2 and cells treated with matrigel, FGF2 and DAPT. Apart from the MIO M1 cell line, 3 other Müller stem cell lines, previously characterized and shown to be similar to the M1 cell line, were also tested. The cells were harvested after 7 days in culture for BRN3B protein analysis by western blot. This experiment was repeated at least 3 times with each of 4 different Müller stem cell lines tested. This was to rule out the possibility that this effect might have been confined to a particular cell line alone. In all cases it was found that DAPT had the same effect: Matrigel and FGF2 increased BRN3B expression compared to control cells whilst DAPT treatment further

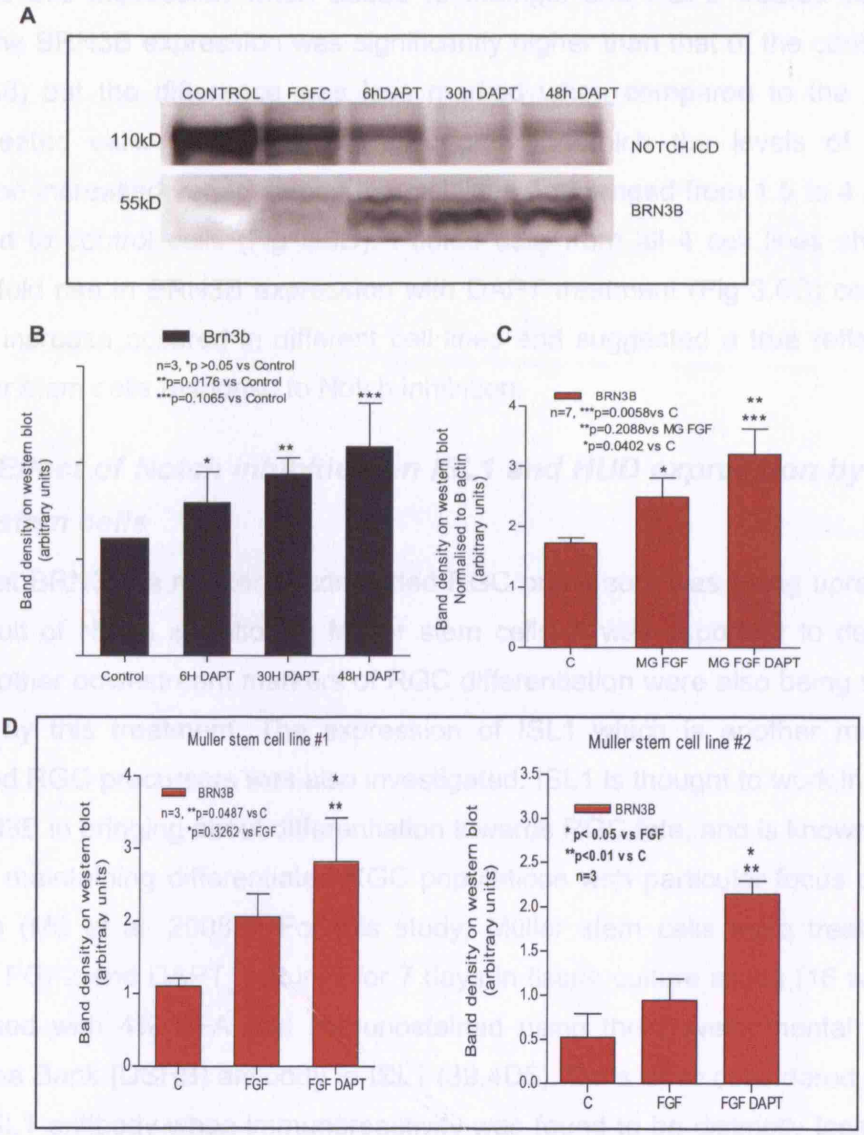

Figure 3.6: Effect of Notch inhibition on Brn3b expression by Müller stem cells (A) Western blot for Notch ICD and BRN3B showing proportional increase in BRN3B expression accompanying DAPT mediated decline in Notch activity. (B) Histogram of BRN3B expression by cells cultured for 7 days with matrigel, FGF2 and increasing duration of exposure to DAPT for upto 48 hours of the initial culture period. Increasing BRN3B expression was observed as the time of exposure to DAPT was increased. (C) Histogram comparing BRN3B expression of Müller stem cells cultured with matrigel and FGF2 vs those cultured with matrigel, FGF2 and DAPT. DAPT causes a further increase in Brn3b expression when compared to the matrigel and FGF2 treated cells ($p < 0.01$vs Control and P=0.2088 vs MG FGF2). This histogram depicts data obtained from 7 different experiments from 4 different cells lines. (D) Histograms showing the effect of DAPT treatment on Brn3b expression within 2 different Müller stem cell lines. In each case the DAPT treated cells show the highest degree of Brn3b expression. In each case 'n' refers to the number of independent measurements

increased this expression when added to matrigel and FGF2 treated cells (Fig 3.6C). The BRN3B expression was significantly higher than that of the control cells (p=0.0058) but the difference was less marked when compared to the matrigel FGF2 treated cells (p=0.2088). The degree to which the levels of BRN3B expression increased varied across the cell lines and ranged from 1.5 to 4 fold rise compared to control cells (Fig 3.6D). Pooled data from all 4 cell lines showed a mean 2 fold rise in BRN3B expression with DAPT treatment (Fig 3.6C) confirming that this increase occured in different cell lines and suggested a true reflection of the Müller stem cells response to Notch inhibition.

3.3.4.2 Effect of Notch inhibition on ISL1 and HUD expression by Müller stem cells

Given that BRN3B, a marker of committed RGC precursors was being upregulated as a result of Notch inhibition in Müller stem cells, it was important to determine whether other downstream markers of RGC differentiation were also being similarly affected by this treatment. The expression of ISL1 which is another marker of committed RGC precursors was also investigated. ISL1 is thought to work in parallel with BRN3B in bringing about differentiation towards RGC fate, and is known to play a role in maintaining differentiated RGC populations with particular focus on axon formation (Mu et al. 2008c). For this study, Müller stem cells were treated with matrigel, FGF2 and DAPT, cultured for 7 days in tissue culture slides (16 wells per slide), fixed with 4% PFA and immunostained using the Developmental Studies Hybridoma Bank (DSHB) antibody to ISL1 (39.4D5). Cells were considered positive for the ISL1 antibody when immunoreactivity was found to be distinctly localized to the nucleus. Nuclear staining by the ISL1 antibody is the characteristic staining pattern seen *in vivo* (Fig 2.3A&B). Cells with cytoplasmic staining without nuclear staining were considered negative. It was found that treatment with matrigel and FGF2 alone resulted in some expression of ISL1 in the cytoplasm, but very few cells showed localization of the antibody to the nucleus (Fig 3.7A). Addition of DAPT was however extremely effective in eliciting nuclear expression of ISL1 in Müller stem cells, causing an increase in the number of nuclear positive ISL1 cells from about 32% in the controls to over 70% in the DAPT treated cells (Fig 3.7A). These results further suggest that Notch inhibition causes an increase in the actual number of

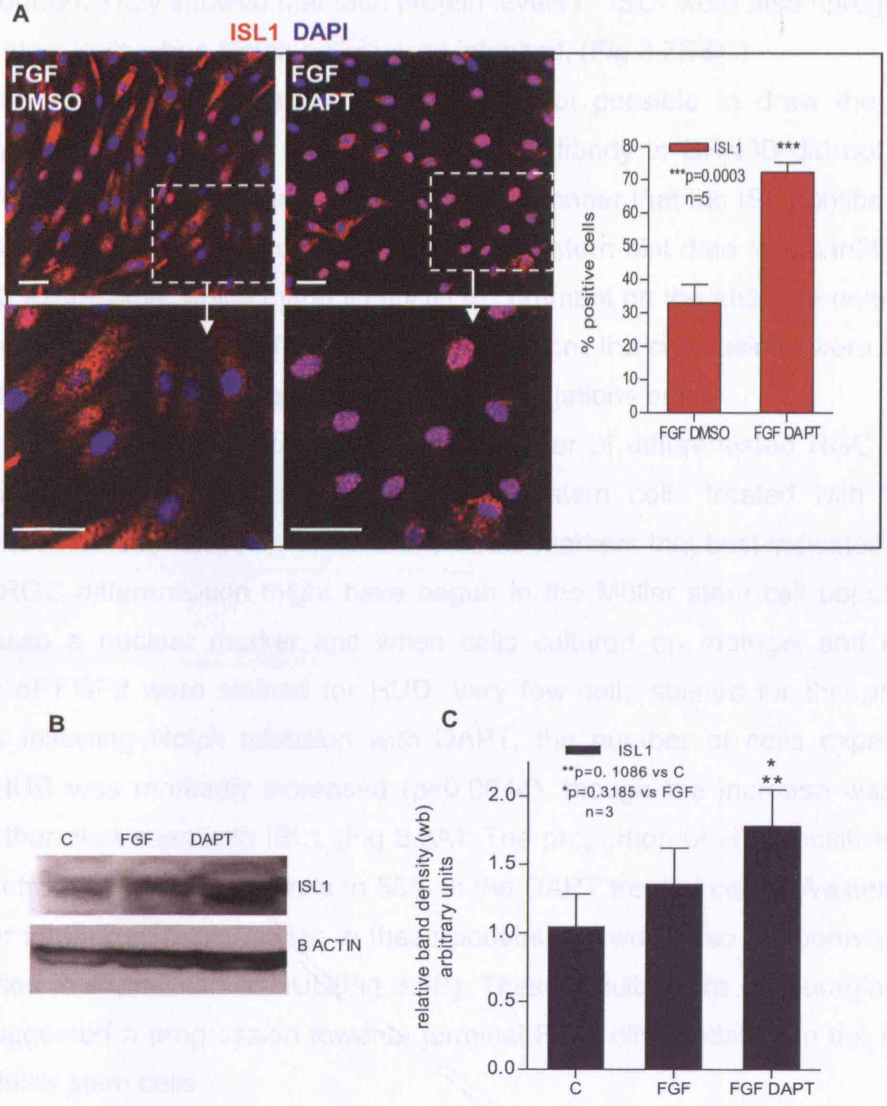

Figure 3.7: Effect of DAPT on ISL1 expression by Müller stem cells (A) Immunostaining of Müller stem cells cultured on matrigel with FGF alone or with matrigel, FGF and DAPT showing increased nuclear staining with the ISL1 39.4D5 antibody in cells treated with DAPT. Inset as marked by the dotted white line is magnified beneath each image. Scale bar=10μm. Histogram shows that the percentage of ISL1 positive cells (cells with nuclear immunostaining for the antibody) increases from just above 30% to over 70% with DAPT treatment. (B) Western blot using the same ISL1 antibody showing a similar increase in ISL1 protein expression with 48hours DAPT treatment as seen on day 7. (C) Histogram shows the results of western blot with ISL1 on the FGF and FGF DAPT treated Müller stem cells. Data from 3 experiments shows that there is a small increase (although not significant) in ISL1 total protein expression with DAPT treatment compared to control (p=0.1086) and FGF treated cells (p=0.3185). In each case 'n' refers to the number of independent measurements

cells committing to the RGC fate. Western blots for ISL1 in DAPT treated cells were also performed. They showed that total protein levels of ISL1 were also upregulated in Müller stem cells when Notch activity was inhibited. (Fig 3.7B&C)

It is worth mentioning at this point that it was not possible to draw the same conclusions from the BRN3B work because the antibody to BRN3B did not show specific reactivity to give a definite read out in the manner that the ISL1 antibody did (Fig 2.2B). It was therefore necessary to rely on western blot data for quantification of BRN3B expression, which made it difficult to comment on the absolute number of cells expressing this marker of commitment. Therefore the conclusions were based on the total protein being expressed by the cell populations only.

The expression of HUD or ELAVL4, another marker of differentiated RGC in the post natal retina was also examined in Müller stem cells treated with DAPT (Ekstrom & Johansson 2003b). HUD is one of the markers that best indicates if any terminal RGC differentiation might have begun in the Müller stem cell population. HUD is also a nuclear marker and when cells cultured on matrigel and in the presence of FGF2 were stained for HUD, very few cells stained for this protein. However, following Notch inhibition with DAPT, the number of cells expressing nuclear HUD was markedly increased ($p=0.0044$), though the increase was less dramatic than that seen with ISL1 (Fig 3.8A). The proportion of HUD positive cells increased from 30% in the controls to 53% in the DAPT treated cells. Western blot results for total protein expression in these populations were also supportive of an upregulation in expression of HUD(Fig 3.8B). These results were encouraging and further suggested a progression towards terminal RGC differentiation in the DAPT treated Müller stem cells.

3.3.4.3 Effect of Notch inhibition on Müller stem cell morphology

In addition to differences in the expression of markers for committed and differentiating RGC precursors amongst Müller stem cells after Notch inhibition, it was noticed that the morphology of these cells also changed in response to DAPT treatment. Müller stem cells under baseline culture conditions possessed a fibroblast-like morphology. When they were treated with FGF2, this morphology changed slightly with the most noticeable difference being that the soma became phase bright and the cytoplasmic processes became narrower. When these cells

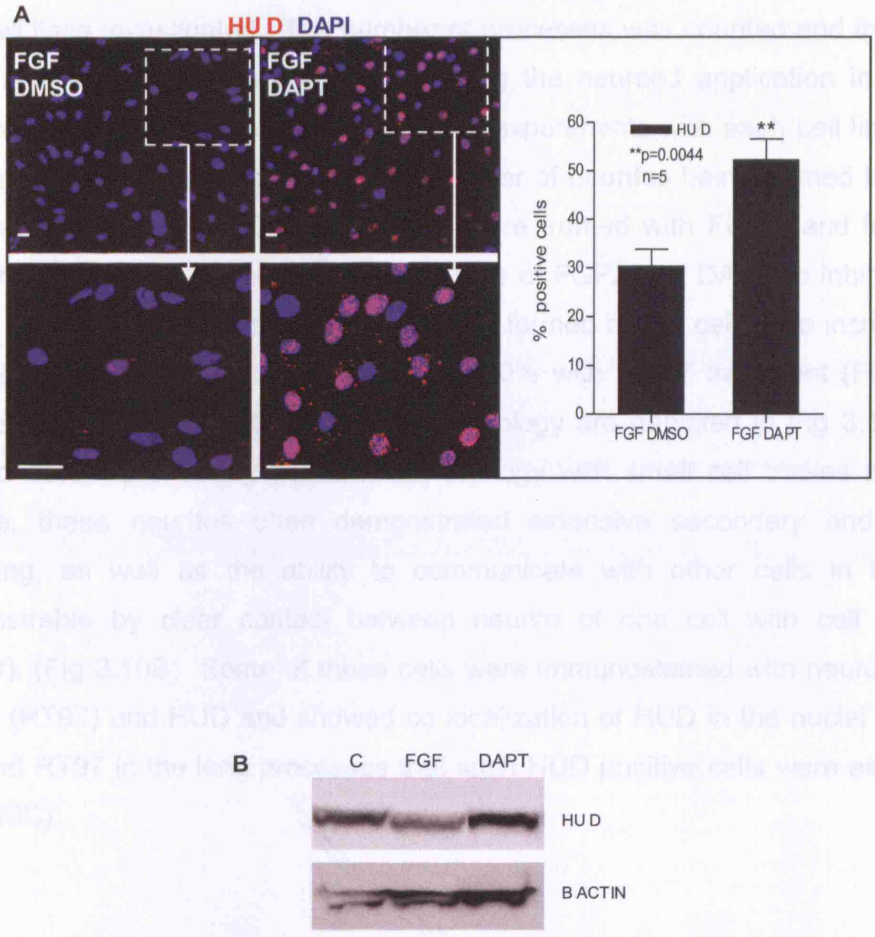

Figure 3.8: Effect of DAPT on HUD expression by Müller stem cells (A) Immunostaining of Müller stem cells cultured on matrigel with FGF alone or in the presence of matrigel, FGF and DAPT. Increased nuclear staining of the HUD antibody in cells treated with DAPT was observed. The insets marked with dotted lines are magnified in the micrographs below as indicated by the white arrows, to better demonstrate the nuclear staining of the antibody. The histogram shows that the percentage of ISL1 positive cells increases from 30% to over 50% with DAPT treatment. These results are the mean of 5 different experiments and the difference in expression was found to be statistically significant (p=0.0044) (B) Western blot of proteins isolated from cells cultured with FGF or FGF and DAPT, with the same HUD antibody, also shows a similar increase in ISL1 protein expression with DAPT treatment. In each case 'n' refers to the number of independent measurements

were further treated with DAPT however, the morphology became dramatically neuronal in some cells with very small phase bright cell bodies extending long neurites which occasionally branched out to give secondary and tertiary neurites (Fig 3.9A). Similar morphological differentiation was observed with 4 different Müller stem cell lines investigated. The number of processes was counted and the length of the neurites per cell was measured using the neuronJ application in ImageJ software. Using data pooled from 3 different experiments with each cell line and 4 different cell lines, it was found that the number of neurites being formed by Müller stem cells increased by 30 % when cells were treated with FGF2, and further to 50% when they were cultured in the presence of FGF2 and DAPT to inhibit Notch activity (Fig 3.9B). The length of the neurites formed by the cells also increased to about 28% with FGF2 alone and to nearly 50% with DAPT treatment (Fig 3.9C). Some examples of dramatic neuronal morphology are depicted in Fig 3.10A. Not only did cells have strong neuronal morphology with small cell bodies and long neurites, these neurites often demonstrated extensive secondary and tertiary branching, as well as the ability to communicate with other cells in the field (demonstrable by clear contact between neurite of one cell with cell body of another). (Fig 3.10B) Some of these cells were immunostained with neurofilament marker (RT97) and HUD and showed co localization of HUD in the nuclei of these cells and RT97 in the long processes that such HUD positive cells were extending. (Fig 3.10C)

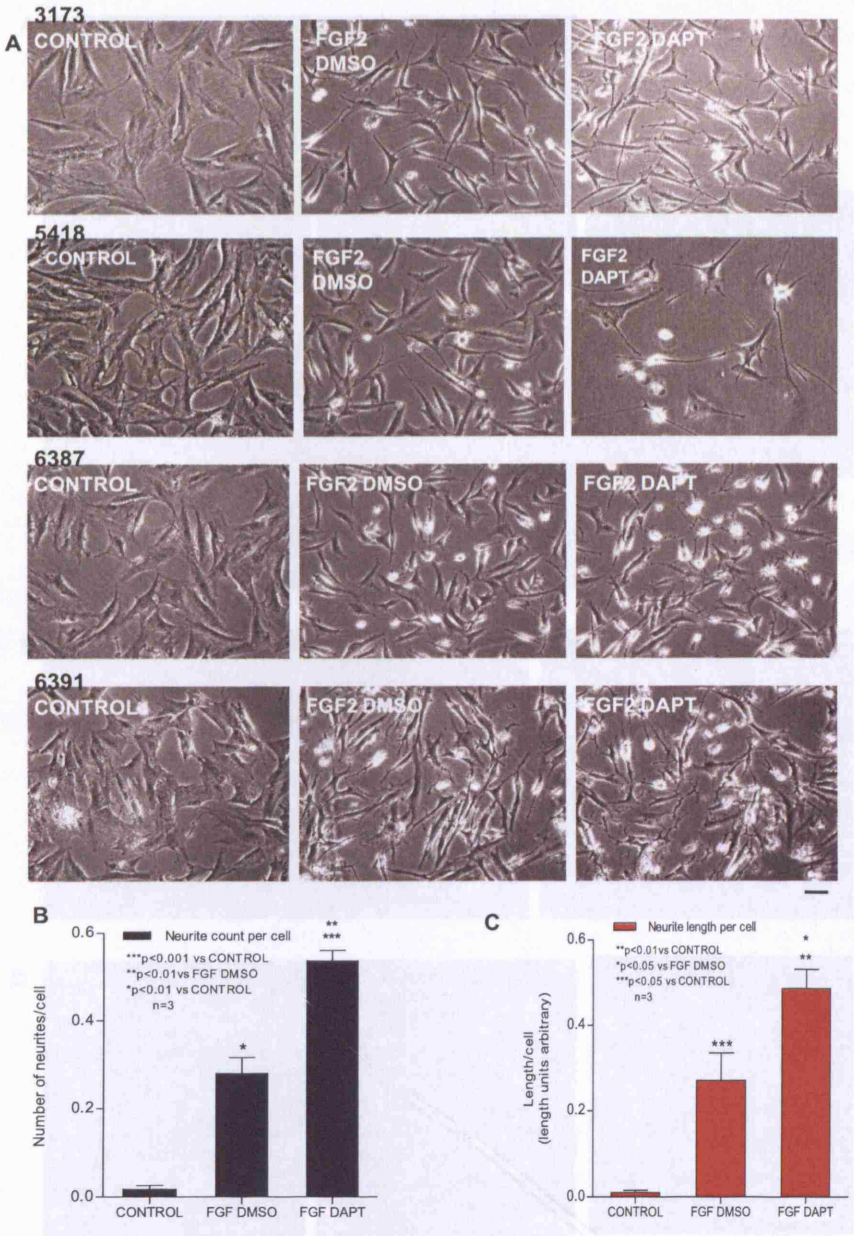

Figure 3.9: Effect of DAPT on morphology of Müller stem cells (A) Phase contrast images of 4 different Müller stem cell lines cultured under baseline conditions, with FGF alone or with FGF and DAPT. In each cell line FGF induces change in morphology with phase bright cell bodies and a few neurites. Addition of DAPT further alters this morphology particularly inducing more and longer neurites in each cell. Scale bar=10μm (B) Histogram showing the quantification of neurite numbers per cell in the three different culture conditions (cumulative results from 3 different cell lines). DAPT causes significant increase in number of neurites per cell. (C) Histogram showing the quantification of neurite length per cell in the three different culture conditions (cumulative results from 3 different cell lines). DAPT also causes significant increase in length of neurites per cell. In each case 'n' refers to the number of independent measurements

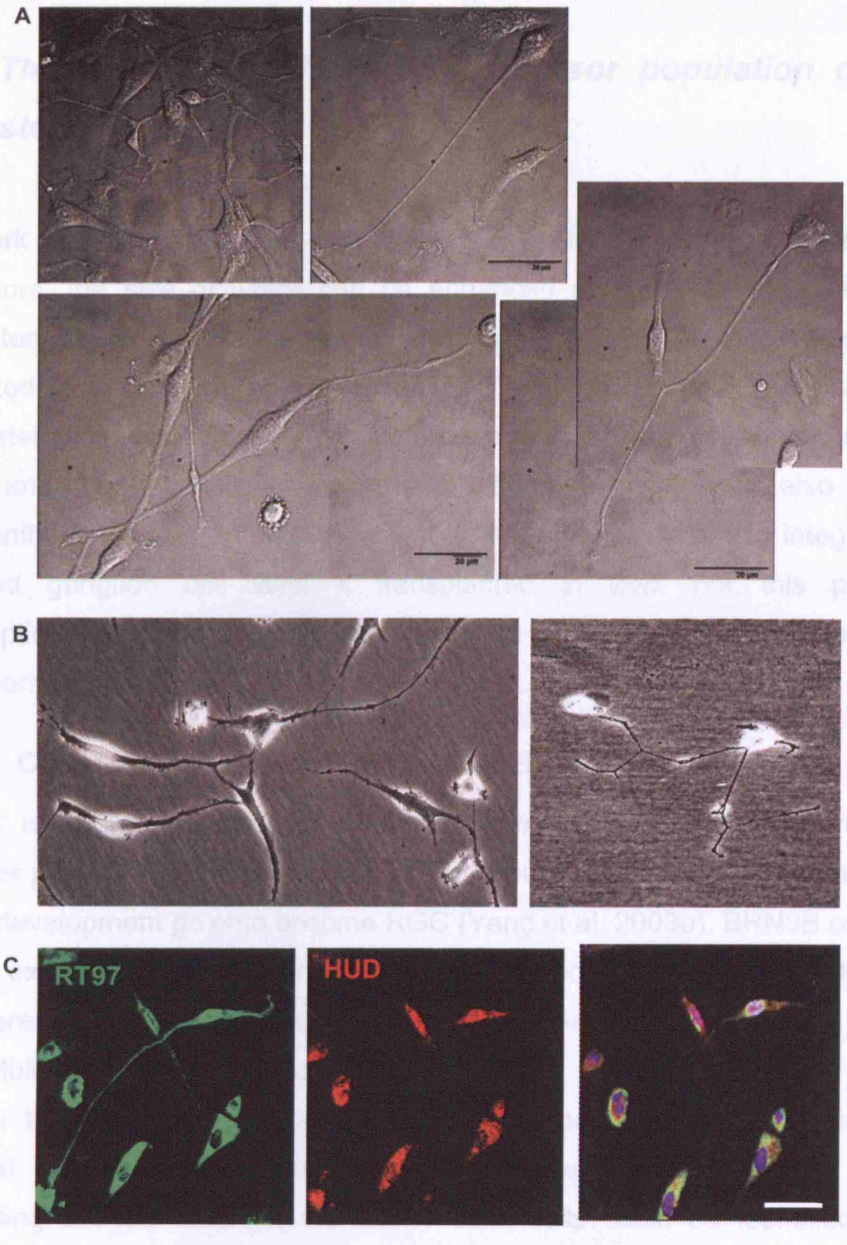

Figure 3.10: Induction of neural morphology in Müller stem cells with FGF2 and DAPT treatment (A and B) Phase contrast images of Müller stem cell lines showing details of extensive branching and long neurite formation induced by DAPT treatment. (C) Immunostaining of Müller stem cells treated with DAPT for neurofilament marker RT 97 and retinal ganglion cell marker HUD showing cells with long RT97 positive neurites and HuD positive nuclei. Co-localisation with DAPI in the image on the extreme right showing nuclear HUD in the same cell which possesses long RT97 positive neurites. Scale bar= 20µm

3.3.5 The BRN3B positive RGC precursor population of Müller stem cells.

The work so far demonstrates that Müller stem cells contain a population of RGC precursors, the size of which can be enhanced *in vitro* with the use of matrix substrates, growth factors as well as inhibition of Notch signaling. It was therefore attempted to isolate this population of RGC precursors from the heterogeneous Müller stem cell population, as it would allow a more accurate study of the effects of growth and differentiation factors on RGC differentiation. It would also provide an opportunity to study the selective ability of this sub population to integrate into a diseased ganglion cell layer if transplanted *in vivo*. For this purpose, a transcriptional reporter to BRN3B was designed in order to identify committed RGC precursors within the Müller stem cell population.

3.3.5.1 Construction of a transcriptional BRN3B reporter

BRN3B is a well established marker of committed RGC precursors. ATOH7 identifies progenitors competent to form RGC but not all cells that express ATOH7 during development go onto become RGC (Yang et al. 2003b). BRN3B on the other hand is expressed in more than 70% of differentiated RGC (Gan et al. 1999a) and it was therefore decided to use this gene as a marker of committed RGC precursors in the Müller stem cell population.

As with transcriptional reporters used in developmental mouse studies, it was intended to generate a reporter for BRN3B expression such that only cells expressing BRN3B amongst the Müller stem cells could be identified. For this purpose a promoterless GFP (p-egfp-clonetech) vector with a Kanamycin resistance cassette was used as a backbone into which the putative promoter region of the human BRN3B gene was inserted. When this reporter was transfected into cells, GFP expression would be driven by the BRN3B promoter (Fig 3.11A). Activation of the promoter in cells expressing BRN3B would also cause GFP expression, thereby eliciting green fluorescence in BRN3B expressing cells. Since this was a

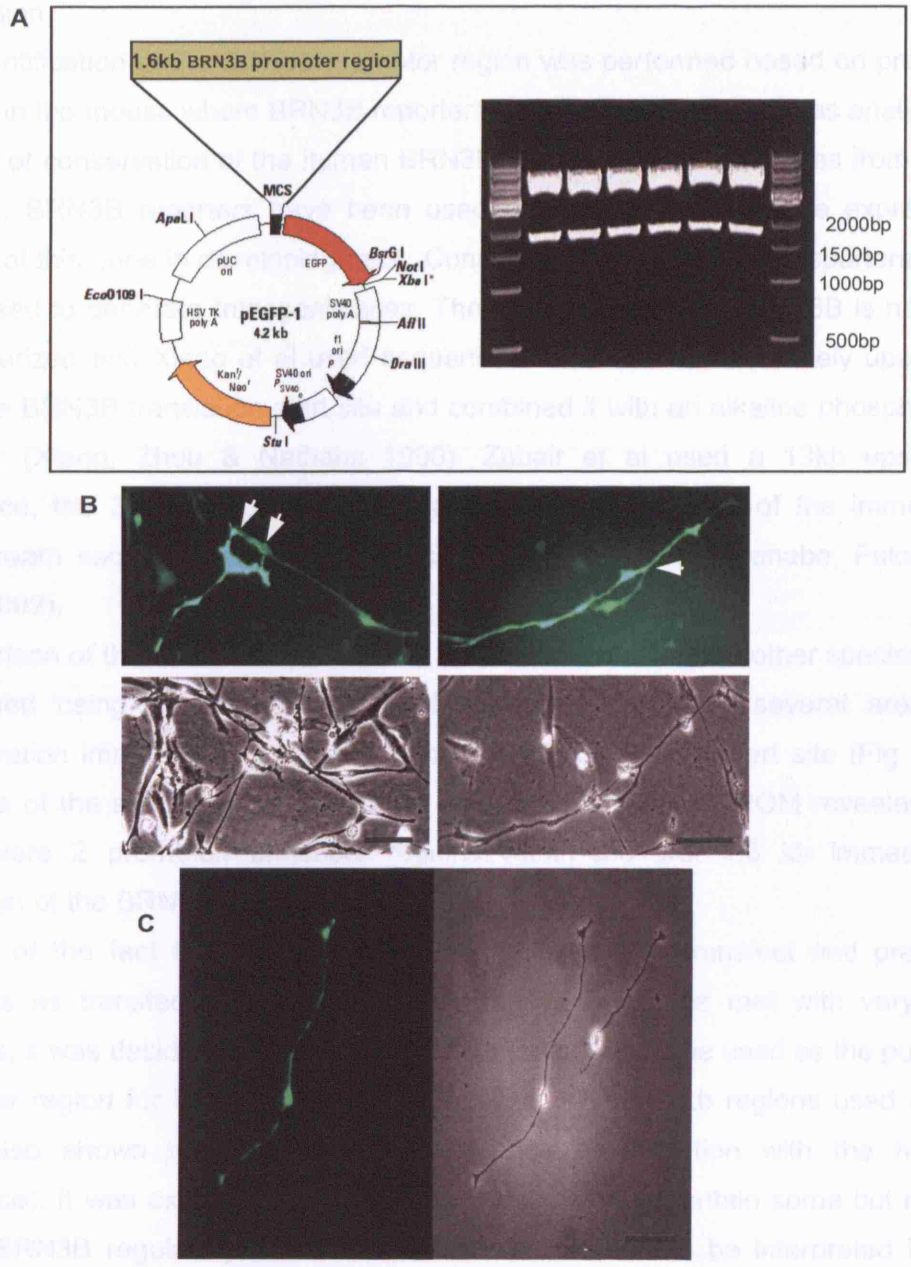

Figure 3.11: Generation of human BRN3B GFP reporter (A) Vector map of pEGFP-1 promoterless GFP vector showing site of insertion of the 1.6kb human BRN3B putative promoter region. The gel image shows results of digestion post ligation to confirm presence of the 1.6kb insert in six clones generated. (B and C) Müller stem cells transfected with the GFP BRN3B trancriptional reporter and cultured on matrigel with FGF2. Green cells of neural morphology within the Müller stem cell population exhibit green fluorescence upon transfection with the reporter. The green cells possess long neurites which also form connections with other cells as shown by the white arrows in B. Scale bar= 20μm

transcriptional reporter it would be able to detect the native levels of BRN3B expression.

The identification of the BRN3B promoter region was performed based on previous studies in the mouse where BRN3B reporters have been used as well as analysis of regions of conservation of the human BRN3B sequence with sequences from other species. BRN3B reporters have been used in the past to study the expression pattern of this gene in developing mice. Consequently most of these reporters have been used to generate transgenic lines. The promoter region of BRN3B is not well characterized and Xiang et al used sequences 4.6 to 13kb immediately upstream from the BRN3B translation start site and combined it with an alkaline phosphatase reporter (Xiang, Zhou & Nathans 1996). Zubair et al used a 13kb upstream sequence, the 3kb intron exon sequence of BRN3B and 3kb of the immediate downstream sequence along with a lacZ reporter (Zubair, Watanabe, Fukada & Noda 2002).

Comparison of the human sequence with those of the mouse and other species was performed using the UCSC genome browser and revealed several areas of conservation immediately upstream of the BRN3B translation start site (Fig 3.12). Analysis of the sequence with promoter prediction software FPROM revealed that there were 2 promoter/ enhancer regions within the first 1.6 kb immediately upstream of the BRN3B translation start site.

In light of the fact that Müller stem cells are difficult to transfect and previous attempts as transfecting plasmids greater than 7kb in size met with very little success, it was decided that this smaller 1.6kb region would be used as the putative promoter region for BRN3B instead of the larger 4.6 or 13kb regions used in the past (also shown to have areas of sequence conservation with the human sequence). It was expected that the 1.6kb sequence may contain some but not all of the BRN3B regulatory elements and the results were to be interpreted in the context of this limitation. Detailed methodology of the construction of the reporter can be found in the materials and methods section (chapter 9).

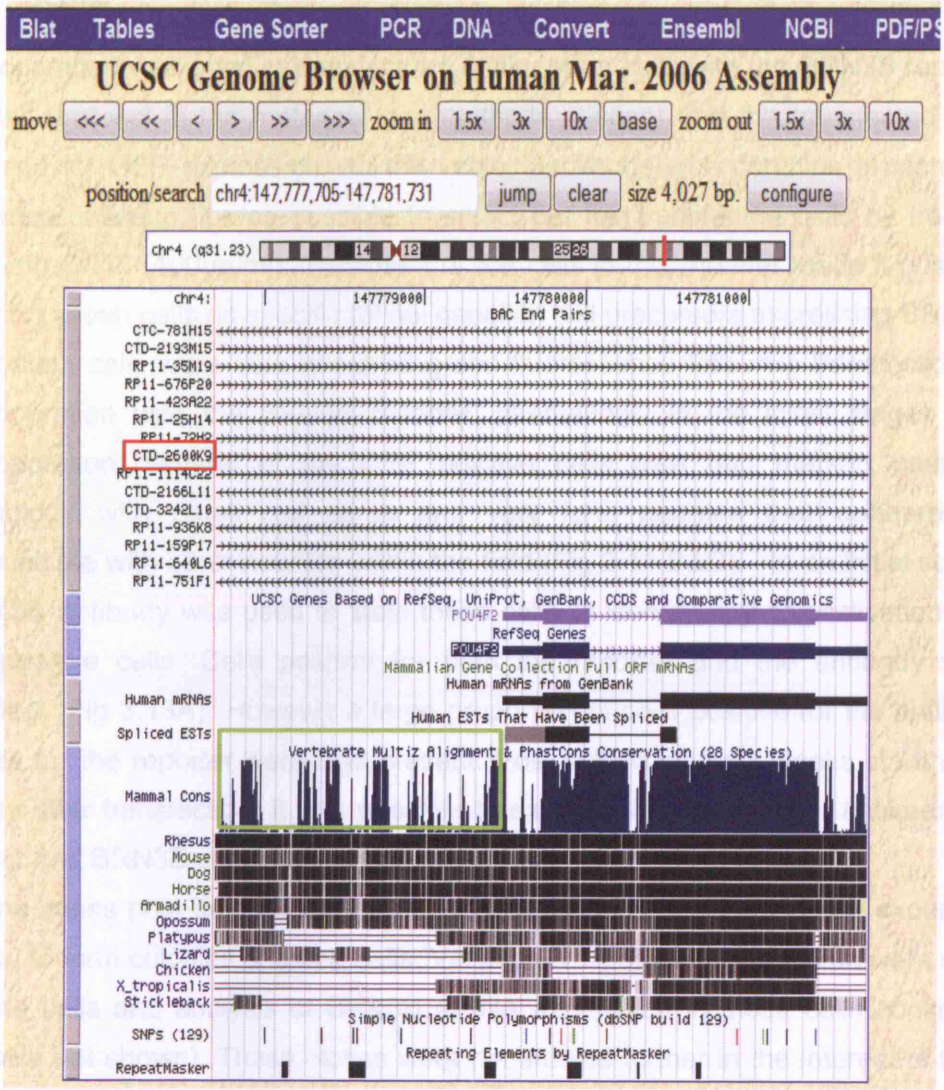

Figure 3.12: Identification of the human BRN3B promoter region The UCSC genome browser was used to identify the areas of sequence conservation upstream of the Brn3b coding sequence that were likely to contain the promoter regions. In the above image of the web interface, the coding sequence of the BRN3B gene is seen in light blue labelled POU4F2 (the alternative name) RefSeq Genes. The area highlighted by the light green box represents the region just upstream of the coding region. The blue spikes within the box show areas of sequence conservation of the human sequence across various species listed beneath. 1.6kb of this region (nearly all of the area highlighted) was used as the promoter sequence based on the above conservation pattern. The red box highlights the BAC clone containing this sequence which was used as template to amplify the promoter region.

3.3.5.2 Transfection and validation of BRN3B reporter in Müller stem cells

Electroporation was used to transfect the Müller stem cells with the BRN3B reporter (detailed protocol in the materials and methods section) and the transfected cells examined for GFP expression. As the vector backbone also contains a neomycin resistance cassette, it was possible to select out the transfected cells by treating them with G418 (400µg/ml). Treatment of the cells in this manner made it possible to identify green cells as specific retinal ganglion cell precursors expressing BRN3B. Müller stem cells were able to exhibit green fluorescence following transfection by electroporation with the BRN3B reporter. Interestingly in the initial stages post electroporation, several of the GFP positive cells also had marked neuronal morphology with small cell soma and very long neurites that appeared to communicate with other neurites within the field (Fig 3.11 B&C). In an initial screen a BRN3B antibody was used to stain these cells to identify any colocalisation with GFP positive cells. Cells positive for both the reporter and the antibody were identified. (Fig 3.13A) However a large proportion of cells positive for the antibody and not for the reporter were also present. Post selection (for 3 weeks starting on the day after transfection) it was possible to examine the relationship between the reporter and BRN3B expression more accurately.

In some cases post selection, it was seen that an occasional green cell expanded clonally to form colonies of green cells. Varying levels of GFP expression were seen in these cells and analysis of BRN3B mRNA expression in these cells confirmed this (data not shown). These clones were not studied further in the interest of time. All the work described below was performed on mixed transfected populations which were selected to allow only the transfected cells (green and non green to survive).

To validate the correlation of green fluorescence by the reporter and BRN3B expression by the cells, the selected population was cultured on matrigel and in the presence of FGF2 and subsequently sorted into green and non green cells using fluorescence assisted cell sorting (FACS). RNA was then isolated from the 2 populations and examined for their respective expression of BRN3B. This experiment was performed on 4 different sets of cells that had been transfected and

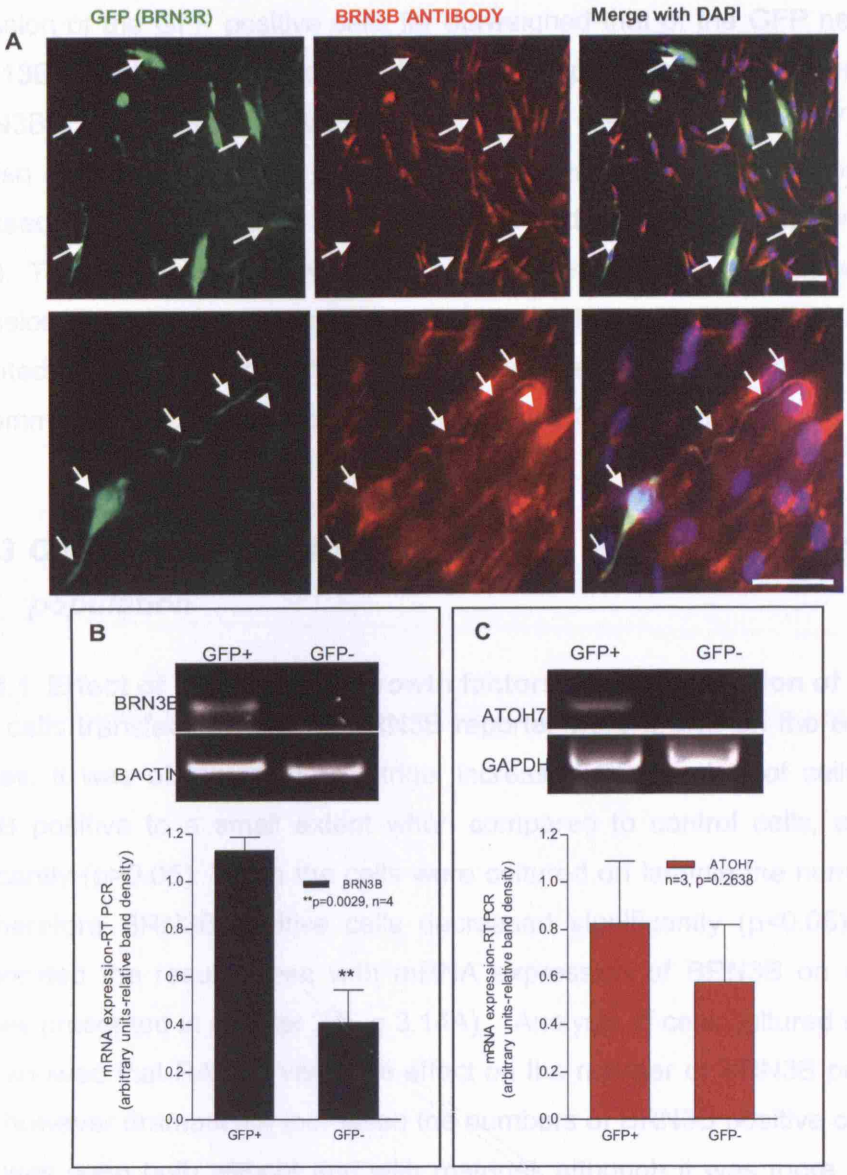

Figure 3.13: Validation of the human BRN3B GFP reporter (A) BRN3B immunostaining of Müller stem cells transfected with the GFP BRN3B reporter showing co localisation of the GFP (green) with the BRN3B (red) in some cells, highlighted by white arrows. Most GFP+ cells were positive for the anti Brn3b antibody. Since the population was unselected there were also several non green cells positive for antibody which were in all likelihood non-transfected. Scale bar= 20µm (B) RT PCR comparing expression of BRN3B mRNA in GFP+ cells (BRN3B reporter positive) and GFP- cells (Brn3b reporter negative) FACS sorted from a BRN3B reporter transfected and selected Müller stem cell population. The GFP+ cells show significantly higher levels (p=0.0029) of BRN3B mRNA expression compared to GFP- cells. Results from 4 different experiments were put together to generate the accompanying histogram. (C) RT PCR for ATOH7 also showed that GFP+ cells express higher levels of ATOH7 mRNA than the GFP- cells, though not significantly so (p=0.2638), as seen in the accompanying histogram generated from the results of 3 different experiments. In each case 'n' refers to the number of independent measurements.

selected as described above. In each instance it was seen that the BRN3B mRNA expression of the GFP positive cells far outweighed that of the GFP negative cells (Fig 3.13B). Analysis of pooled data from the 4 experiments showed the difference in BRN3B expression to be statistically significant ($p=0.0029$). ATOH7 expression was also analysed in the two populations and it was found that GFP positive cells expressed higher amounts of this gene compared to the GFP negative cells (Fig 3.13C). The difference however was not as marked as that seen with BRN3B expression ($p=0.2638$). Nevertheless this data shows that the BRN3B reporter generated could reliably identify cells that were expressing this marker of competent and committed RGC precursors (Gan et al. 1999c;Xiang 1998b).

3.3.5.3 Characterization of RGC precursors within the Müller stem cell population

3.3.5.3.1 Effect of matrices and growth factors on differentiation of RGC

When cells transfected with the BRN3B reporter were grown on the extra cellular matrices, it was observed that matrigel increased the number of cells that were BRN3B positive to a small extent when compared to control cells, although not significantly ($p>0.05$). When the cells were cultured on laminin the number of GFP and therefore BRN3B positive cells decreased significantly ($p<0.05$). This data corroborated the results seen with mRNA expression of BRN3B on extracellular matrices presented in chapter 2 (Fig 3.14A). Analysis of cells cultured with RA and FGF2 showed that RA had very little effect on the number of BRN3B positive cells. FGF2 however dramatically increased the numbers of BRN3B positive cells and this effect was seen both without and with matrigel, although it was more pronounced when the cells were cultured on matrigel (Fig 3.14B).

3.3.5.3.2 BRN3B positive Müller stem cells are post mitotic

Müller stem cells transfected with the BRN3B reporter and selected for the reporter containing cells were fixed after 7 days in culture and immunostained for proliferation marker Ki67. The proportion of GFP positive cells expressing Ki67 (and therefore dividing) was compared with those of GFP negative cells. Data from 4

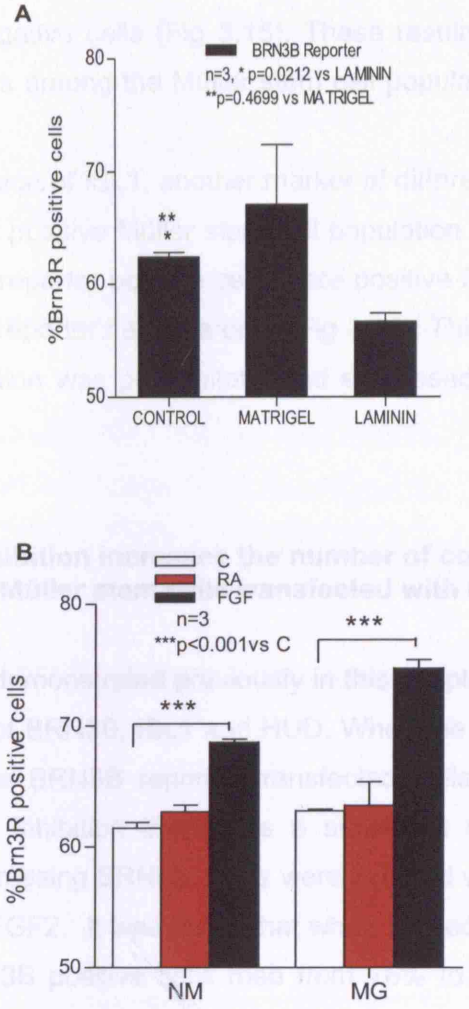

Figure 3.14: Effect of matrices and growth factors on the committed BRN3B positive RGC precursor population in Müller stem cells (A) Histogram showing results of FACS analysis on Müller stem cells transfected with the Brn3b reporter and cultured on matrigel or laminin. Matrigel causes a small but not significant increase in the number of BRN3B positive cells (p=0.4699) while laminin causes a considerable decline (p=0.0212). (B) Histogram showing results of FACS analysis on Müller stem cells transfected with the BRN3B reporter and cultured with FGF or RA. When cultured without any additional matrices (NM) FGF causes a significant increase in cells expressing the BRN3B reporter (p<0.001 vs C). The same effect is seen when the cells are cultured on matrigel but the absolute percentage of BRN3B positive cells is higher. RA does not significantly affect the number of cells expressing BRN3B when the cells are cultured without matrix or with matrigel. In each case 'n' refers to the number of independent measurements.

different repeats of the experiment were pooled and revealed that less than 10% of the BRN3B reporter positive cells were dividing in comparison to almost 50% of the BRN3B reporter negative cells (Fig 3.15). These results therefore suggested that BRN3B positive cells among the Müller stem cell population *in vitro* were also post mitotic.

The relative expression of ISL1, another marker of differentiating RGC precursors in the BRN3B reporter positive Müller stem cell population was also analyzed. Almost 70% of the BRN3B reporter positive cells were positive for ISL1 compared to about 35% of the BRN3B reporter negative cells (Fig 3.16). This indicates that the BRN3B positive cell population was post mitotic and expressed other markers of specific RGC differentiation.

3.3.5.3.3 Notch inhibition increases the number of committed RGC precursors amongst Müller stem cells transfected with the BRN3B reporter

Notch inhibition as demonstrated previously in this chapter is able to upregulate the protein expression of BRN3B, ISL1 and HUD. When the same treatment conditions were applied to the BRN3B reporter transfected cells it was found that in the presence of Notch inhibition there was a small but significant increase in the number of cells expressing BRN3B. Cells were cultured with or without matrigel and in the presence of FGF2. It was found that when treated in addition with DAPT the percentage of BRN3B positive cells rose from 76% to 81% without matrigel and from 77% to 84% with matrigel (Fig 3.17A). Representative FACS scatter plots showing this difference are depicted in Fig 3.18. The same effect was also observed when the cells were cultured with RA although the difference was only significant when the cells were cultured in the absence of matrix with the addition of RA (Fig 3.17B). It appeared therefore that treatment of the Müller stem cells with matrigel, FGF2 and DAPT increased the actual number of cells committed to the RGC fate.

In summary, the BRN3B reporter allowed confirmation of what was seen in the previous chapters with respect to the effect of extracellular matrices and growth factors on RGC differentiation *in vitro.* It was also able to establish the post mitotic RGC precursor nature of this population of cells.

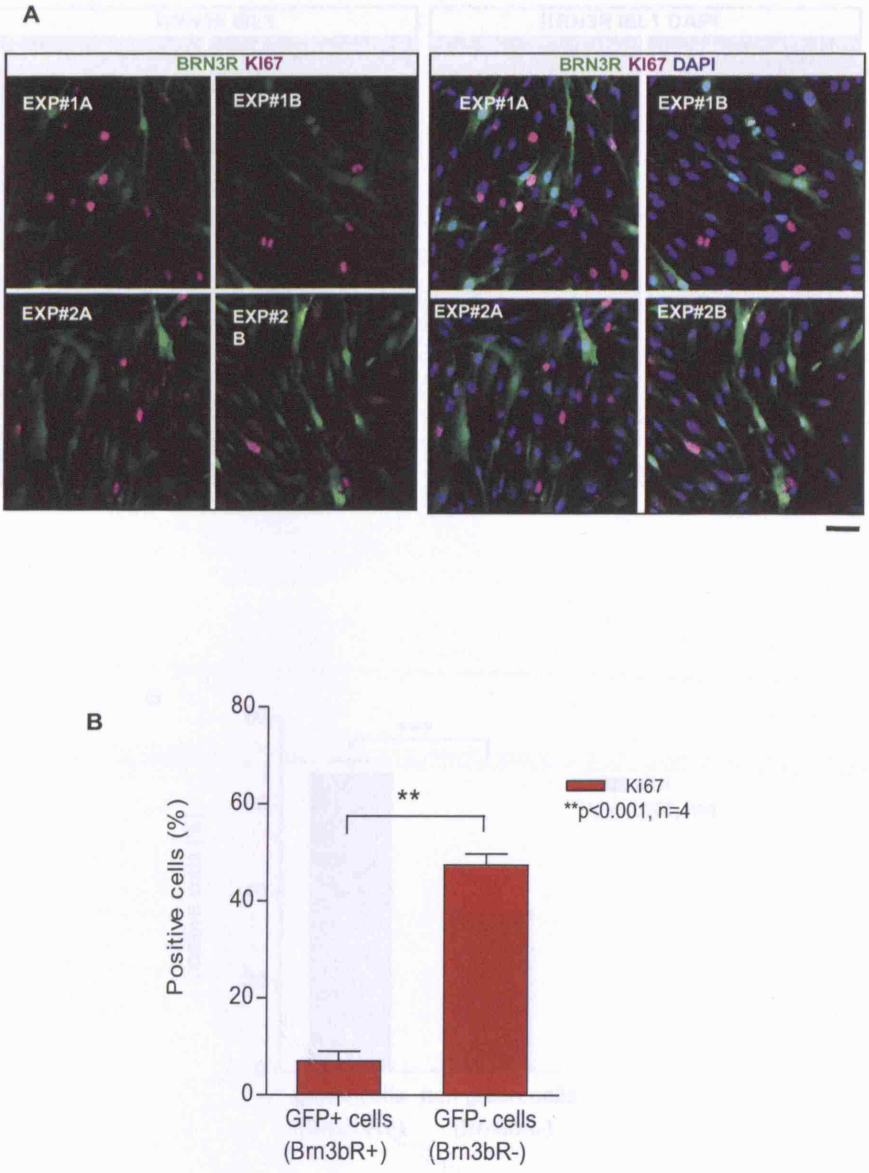

Figure 3.15: Proliferation in the committed BRN3B positive RGC precursor population of Müller stem cells (A) Ki67 immunostaining of Müller stem cells transfected with the GFP BRN3B reporter showing that most of the BRN3B positive cells are non dividing and do not express ki67. Two representative images are shown from each of 2 different experiments. The first set of micrographs show GFP in green and Ki67 in magenta. The second set of micrographs show the same fields but with DAPI in blue in addition to the GFP (green), Ki67(magenta), to outline the nuclei. Scale bar= 20µm (B) Histogram quantifying the percentage of dividing cells among the GFP- compared to the GFP + cells. Less than 10% of the GFP+ cells are actively dividing while over 40% of the GFP- cells are in a state of active division. 'n' refers to the number of independent measurements

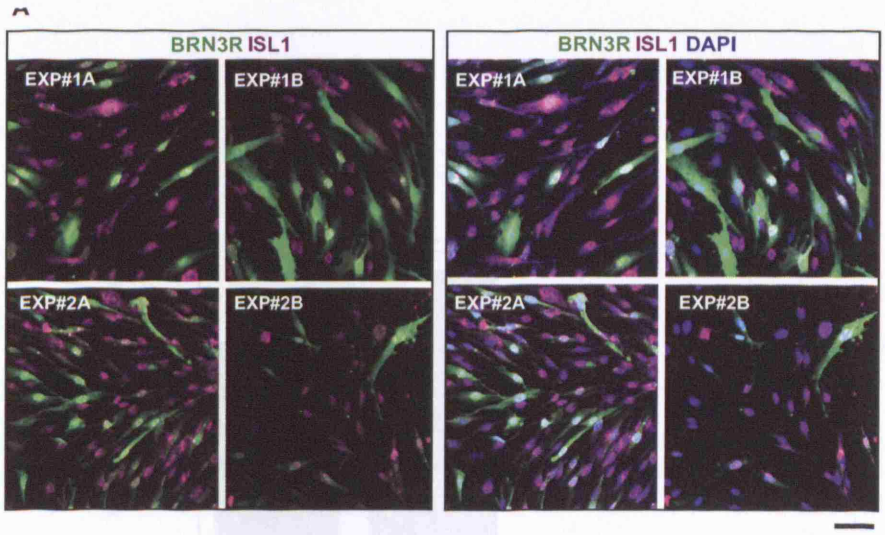

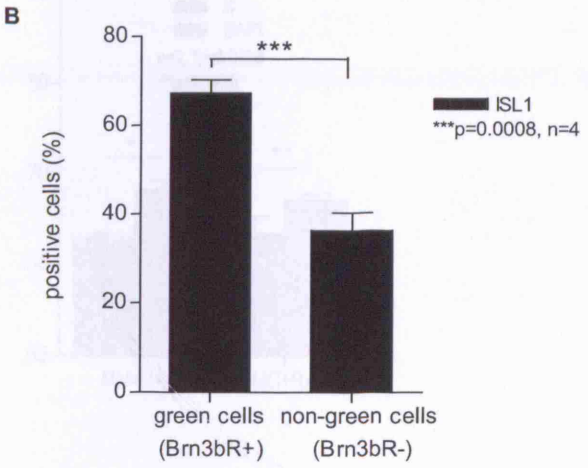

Figure 3.16: ISL1 expression in the committed BRN3B positive RGC precursor population of Müller stem cells (A) ISL1 immunostaining of Müller stem cells transfected with the GFP BRN3B reporter showing multiple ISL1(magenta) positive green cells. Two representative images are shown from 2 different experiments. The first set of images shows GFP in green with ISL1 in magenta. The second set of micrographs show the same fields but with additional DAPI staining to delineate the nuclei clearly. Scale bar= 20µm (B) Histogram quantifying the percentage of ISL1 positive cells among the GFP- cells compared to the GFP+ cell population. Over 60% of the GFP positive (BRN3B reporter positive) cells were also positive for ISL1 while less than 40 % of the GFP- cells were positive for ISL1. 'n' refers to the number of independent measurements

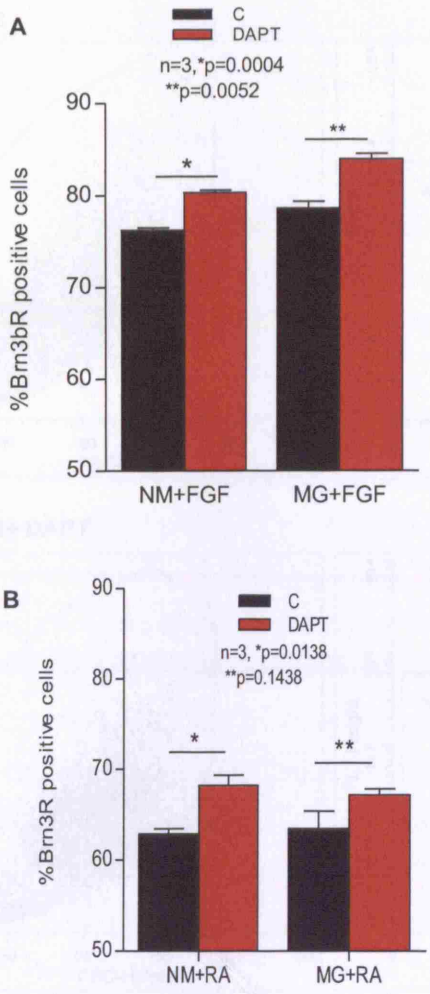

Figure 3.17: Effect of DAPT on the committed BRN3B positive RGC precursor population of Müller stem cells (A) Histogram shows results of FACS analysis on BRN3B reporter transfected Müller stem cells cultured with FGF alone or with FGF and DAPT. DAPT caused a significant increase in the number of BRN3B positive committed RGC precursors compared to control when cultured without matrices ($p<0.001$) and when cultured on matrigel ($p<0.01$). (B) Histogram shows results of FACS analysis on BRN3B reporter transfected Müller stem cells cultured with RA alone or with DAPT. Although there was a significant increase in the BRN3B reporter positive cells when cultured with RA and DAPT without matrices ($p<0.05$), the effect of DAPT on BRN3B positive committed RGC precursor population was not as pronounced with RA as it was with FGF. Small increase in level of expression of BRN3B was seen but dis not rise to above 70% compared to nearly 85% seen with matrigel and FGF in (A). In each case 'n' refers to the number of independent measurements

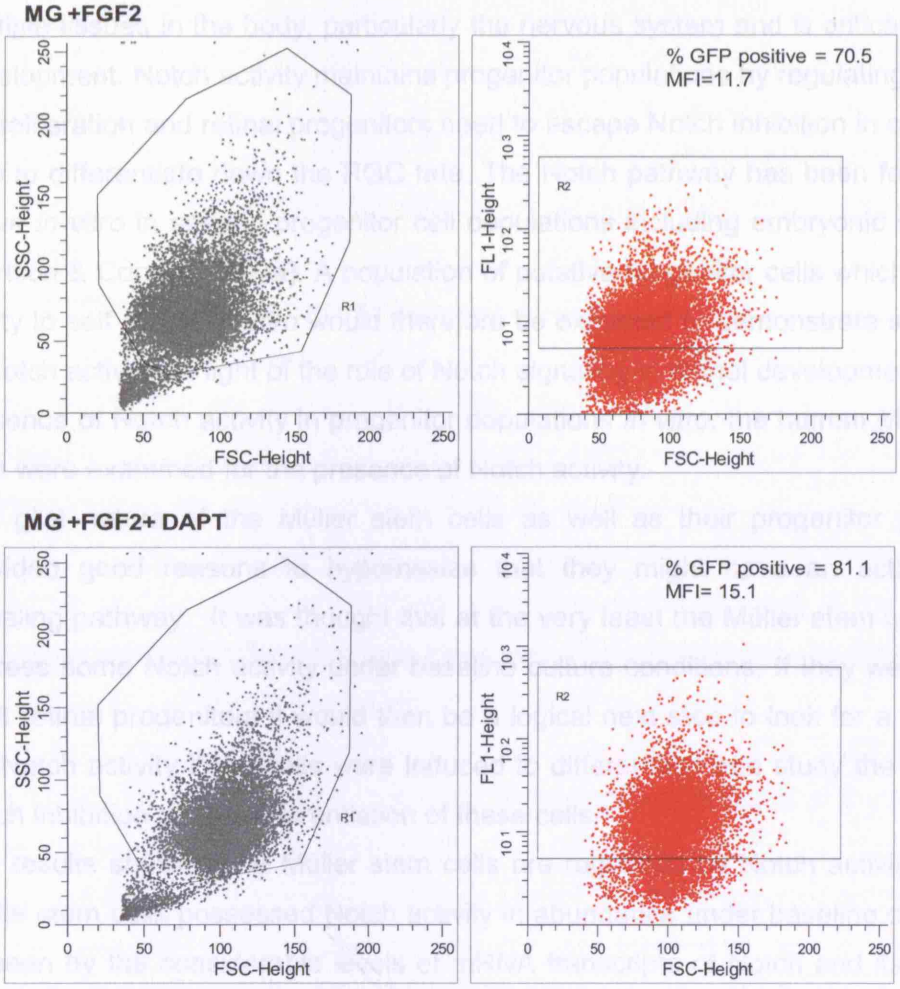

Figure 3.18: Fluorescent activated cell sorting (FACS) of Brn3b reporter transfected Müller stem cells The images show representative scatter plots of Müller stem cells transfected with Brn3b reporter, cultured with matrigel and FGF2 or matrigel, FGF2 and DAPT for 7 days and subjected to fluorescent cell sorting. The plots in grey depict the cell scatter based on cell viability in each case and the plots in red depict the scatter based on fluorescence intensity. The gate (black box in the red scatter plots) shows the cells designated as positive for GFP. Cells falling within this box are counted as positive for the Brn3b reporter. In each red scatter plot the percentage of cells positive for GFP and the Mean Fluorescence Intensity (MFI) of the green cells is depicted on the top right of the graph. Here the Matrigel (MG) and FGF2 treated sample shows 70.5% green cells while the MG, FGF and DAPT treated sample shows 81.1% green cells suggesting that DAPT treatment is increasing the proportion of Brn3b expressing reporter transfected Müller stem cells.

3.4 Discussion

Notch activity is a key regulator of progenitor proliferation and differentiation in multiple tissues in the body, particularly the nervous system and is critical to retinal development. Notch activity maintains progenitor populations by regulating their rate of proliferation and retinal progenitors need to escape Notch inhibition in order to be able to differentiate down the RGC fate. The Notch pathway has been found to be active *in vitro* in several progenitor cell populations including embryonic stem cells (Carlson & Conboy 2007a). A population of putative progenitor cells which have the ability to self renew *in vitro* would therefore be expected to demonstrate some level of Notch activity. In light of the role of Notch signaling in retinal development and the presence of Notch activity in progenitor populations *in vitro*, the human Müller stem cells were examined for the presence of Notch activity.

The glial nature of the Müller stem cells as well as their progenitor properties provided good reasons to hypothesize that they might have an active Notch signaling pathway. It was thought that at the very least the Müller stem cells would express some Notch activity under baseline culture conditions. If they were indeed adult retinal progenitors it would then be a logical next step to look for a decline in the Notch activity if the cells were induced to differentiate and study the effects of Notch inhibition on the differentiation of these cells.

The results showed that Müller stem cells are regulated by Notch activity *in vitro*. Müller stem cells possessed Notch activity in abundance under baseline conditions, as seen by the considerable levels of mRNA transcripts of Notch and its effectors Hes1 and Hes5, the detection of ICD on western blot, and positive nuclear staining for the activated Notch antibody in these cells. In light of published literature in the field, it was thought that this information added to the hypothesis that Müller stem cells are retinal glial cells with stem cell properties. Notch was also found to regulate their rate of proliferation and when Müller stem cells were put into differentiating conditions; Notch activity was down regulated in a similar manner to embryonic retinal progenitors. The results also indicated that like other progenitor populations, Müller stem cells too were under the regulation of the Notch signaling pathway.

When Müller stem cells were cultured with FGF2 while there was a considerable increase in the expression of RGC markers, the down regulation of Notch activity

was not very marked. It has been previously described that FGF can increase the levels of Notch activity in neuroepithelial cells (Faux et al. 2001) and if this was to apply to Müller stem cells, it could be expected that the Notch activity would be higher in FGF2 treated cells as compared with the controls, which was not the case in our studies. In addition Faux et al also described an inhibitory effect of FGF on neural differentiation in the neuroepithelial cells. These observations are also not in agreement with the present results which suggest that FGF2 increases the expression of RGC markers in Müller stem cells. It is possible therefore that the effect of FGF2 on these cells differs from that on neuroepithelial cells. The glial nature of these cells may play a role in this difference. Additionally in view of the above results it was thought that FGF2 itself might be able to induce cell proliferation in the Müller stem cells thereby being associated with high Notch activity. Overall the results from analysis of Notch activity of Müller stem cells cultured with FGF2 suggested that FGF2 promotes neural differentiation of Müller stem cells and that Notch activity was down regulated as a result of this effect. Of note was the fact that this down regulation was not complete and much smaller than that compared to the significant down regulation seen with RA.

These experiments led to a situation where cells treated with FGF2 expressed higher levels of RGC markers compared to the control cells, yet at the same time demonstrated considerable levels (more than 50% of the control) of Notch activity. The role of Notch activity in preventing progenitor differentiation into retinal neurons and the necessity for its down regulation for retinal differentiation to proceed has been discussed above. With the addition of ECM proteins (matrigel as discussed in the previous chapter) and FGF2 it has already been shown that the Müller stem cells could be made to up regulate expression of RGC markers. These results lead to the postulate that inhibition of Notch activity in the matrix and FGF2 treated cells might further up regulate the expression of these RGC markers and drive these cells even closer towards a retinal ganglion cell fate.

The effect of Notch inhibition on the Müller stem cells in differentiating conditions was analyzed using DAPT, a gamma secretase inhibitor, which has previously been used previously to cause chemical inhibition of Notch activity *in vitro* (Nelson et al. 2007g). The present results showed that DAPT was equally effective in inhibiting

the Notch activity of Müller stem cells, causing a drop in proliferation and expression of Notch effectors such as Hes1.

More crucially, Notch inhibition in the Müller stem cells upregulated expression of BRN3B and other downstream RGC markers such as ISL1 and HUD. It also had a significant impact on the morphology of these cells, making them much more neuronal, with smaller cell soma and longer and more numerous neurites. Neural morphology of the cells in response to DAPT treatment was studied using neurite length per cell and neurite count per cell statistics. This method of analysis was chosen over measurement of the percentage of cells with neurites to eliminate any bias that might arise during the counting of such cells, given the subjective nature of making such identification. It was also attempted to only use fields with similar cell density while making these measurements to avoid confounding factors that arise in cell morphology with density. It was frequently seen that the more sparsely distributed cells were able to put out longer processes and such fields were not used for the measurements since they would naturally have fewer cells and longer processes thereby skewing the measurements. However such fields often gave the best indication of the potential of this treatment to give rise to RGC precursors. These neurites were positive for neurofilament markers and cells expressing these neurites also expressed HUD in their nuclei, characteristic of RGC. These results confirmed that Notch inhibition by DAPT could drive the Müller stem cells towards a retinal ganglion cell fate when used in conjunction with extracellular matrix proteins like matrigel and growth factors like FGF2. The treatment promoted the differentiation of these cells into committed RGC precursors as demonstrated by its effect on BRN3B and ISL1 expression. In some cases, the treatment appeared to induce cells to terminally differentiate into RGC as determined by their characteristic neuronal morphology and HUD expression. Inhibition of Notch activity in these cells may be a key switch to bring about this differentiation.

Closer examination of cells that were committed to the RGC fate within the Müller stem cell population was made possible by the use of a BRN3B reporter designed for the study. Since BRN3B marks committed RGC precursors, using this BRN3B promoter driven GFP construct, it was possible to mark BRN3B positive cells within the Müller stem cell population. The study so far had focused on data obtained by pooling the results from a heterogenous population of Müller stem cells. While they

indicate relative levels of expression, it was not possible to determine if the selective treatments merely increased BRN3B expression in cells already expressing it, or actually induced more cells to begin expressing it. This was also compounded by the lack of a reliable BRN3B antibody. With the reporter it was possible to overcome this problem, thus facilitating the analysis of the effect of various matrices and growth factors on the actual number of BRN3B positive committed RGC precursors. Committed RGC precursors during retinal development are post mitotic. BRN3B expression has been shown to be present almost exclusively in cells that have exit the cell cycle (Xiang 1998d). For this reason it was investigated whether the committed RGC precursor population in the Müller stem cells was also post mitotic. Examination of the BRN3B reporter positive cells in culture confirmed that these cells were indeed committed RGC precursors: they were post mitotic and expressed BRN3B and ISL1. This data is in agreement with *in vivo* work presented by others (Xiang 1998a) on differentiating retinal progenitors and adds further support to the suggestion that differentiation in the Müller stem cells *in vitro* follows some of the same intrinsic programming observed in the retinal progenitors *in vivo* during development.

Using the reporter it was also possible to establish that apart from levels of mRNA expression, extra cellular matrices and growth factors increased the actual number of cells committing to the RGC fate within the Müller stem cell population. Finally Notch inhibition by DAPT also showed that the committed RGC precursor population was amplified by this treatment.

However the limitations of the reporter were taken into account at this point. As discussed in the section on the construction of the reporter (p96), the promoter region used was likely to contain only some of the BRN3B regulatory elements and therefore the information this reporter gives us was likely to be incomplete. The specificity of the reporter was also considered. The validation performed here included co immunostaining with an antibody and comparison of BRN3B gene expression between cells positive and negative for the reporter. There was however some cross talk with small amounts of the reporter negative cells showing some BRN3B expression. It was also of note that while most of the reporter positive cells were post mitotic (as seen *in vivo*), there was a small percentage (~10%) which were still dividing further suggesting the leaky nature of the reporter. Testing the

expression of this reporter in retinal ganglion cell lines (as a positive control) and non neural/non RGC cell lines (as negative controls) would be a useful way of further establishing the reliability of this reporter.

As a source of stem cells to replace damaged retinal neurons, Müller stem cells are ideal in that they are derived from retinal tissue, already express retinal progenitor markers and can be induced to express RGC precursor markers. This work indicates that further differentiation can be achieved by the simple process of inhibiting Notch activity in these cells. This inhibition as shown here can be easily achieved by adding a chemical to the culture media making a significant difference to the commitment of these cells towards an RGC fate. It is therefore proposed that Müller stem cells treated with matrigel, FGF2 and Notch inhibition are a good source of RGC precursors and could have significant potential for use in RGC replacement therapy.

Chapter 4: *In* vitro neural function of Müller stem cells differentiated towards RGC fate

4.1 Introduction

In order to be able to designate Müller stem cells differentiated with growth factors and DAPT treatment as retinal ganglion cell precursors it is also necessary to establish if they are able to acquire neuronal function, particularly in their ability to respond to various neurotransmitters that retinal ganglion cells characteristically respond to. However emerging research has revealed that the response to neurotransmitters is not restricted to neurons. A large body of work in the last few years has shown that other cells express some of these receptors and in a few instances they also have the ability to respond to them. These cells fall into two broad categories namely the neural stem or progenitor cells and the glial cells.

Neural progenitors of the central nervous system have been shown to express receptors to various neurotransmitters (Cai et al. 2004;Schipke et al. 2001a). While the expression of these receptors does not equate to the receptors being functional, response to any one of these can no longer be interpreted as evidence of terminal neuronal differentiation. However while there are a number of neurotransmitters and their receptors which have been identified in neural progenitors, there are still those that are exclusively expressed in differentiated neural cells (Das et al. 2005f). The last are potential candidates that may be used to delineate differentiated neurons from undifferentiated neuronal progenitors.

The fact that Müller stem cells are glial in nature adds another facet to this investigation. Glial cells are also able to respond to various neurotransmitters and it is believed that this ability is crucial to the supportive and facilitating functions they perform in their interaction with neurons (Das et al. 2005e;Lopez, Lopez-Colome, & Ortega 1997;Puro, Yuan, & Sucher 1996). This presents the added complication of distinguishing Müller stem cell response to neurotransmitters because of their glial nature as opposed to their neuronal nature. This part of the research therefore focuses on what is currently known about glial cell, particularly Müller glial cell response to neurotransmitters and how they might be differentiated from a neuronal response.

Calcium imaging techniques were used to study neurotransmitter response in the human Müller stem cells. The ability of a cell to respond to neurotransmitters by

changing its membrane potential is characteristic of a neuron (Wong 1998). However, not all neuronal activity is associated with changing membrane potential and examination of the rise in cytosolic calcium levels (with or without associated membrane current studies) has progressively been accepted as a method of detecting neuronal activity in a cell. Changes in intracellular calcium in response to neurotransmitter ligands suggest the presence of functional receptors to these neurotransmitters and are a useful tool in assessing neural functionality (Wong 1995;Wong 1998).

4.1.1 Neurotransmitter expression and function in retinal progenitors

Retinal progenitors in the ventricular zone starting at the stage of optic cup formation express receptors to multiple neurotransmitters, including members of the muscarinic, purinergic, GABA and glutamatergic systems (Das et al. 2005d). These receptors are thought to play a role in the proliferation and differentiation of retinal progenitors (Martins & Pearson 2008a) and their expression and function can be used as indicators of the state of differentiation of retinal neurons. Three of these receptor ligand systems- the glutamatergic, the muscarinic and the nicotinic are of particular interest to this work because of the significant role they play in retinal ganglion cell function. They are known to be highly functional in differentiated RGCs and constitute ideal candidates for identification of RGC precursors derived from the Müller stem cells. However some of these receptors are also known to be expressed by retinal progenitors and in the Müller glia and therefore precise knowledge of their expression and function is necessary to be able to draw any conclusions from analysis of Müller stem cell response to them.

4.1.1.1 The Glutamatergic system

The glutamatergic system consists of glutamate, the principal excitatory neurotransmitter in the CNS, and two types of receptors - the ionotropic and the metabotropic. The metabotropic channels are G-protein coupled receptors that work via intracellular second messengers. The ionotropic channels are glutamate gated cationic channels and include those that respond to α-amino-3-hydroxy-5-methyl-4-isoxazolepropionic acid or AMPA or kainate (KA), and the highly calcium permeable

ones that respond to N-methyl D-aspartate (NMDA) (Verkhratsky & Kirchhoff 2007). The retinal ganglion cells possess NMDA receptors in abundance and are sensitive to NMDA which is known to be specifically toxic to RGC when introduced into the retina (Shen, Liu, & Yang 2006a).

In retinal progenitors glutamate receptor expression has been documented early during development, including AMPA/KA and NMDA receptors. It has been shown that glutamate stimulation of progenitor cells affects their rate of proliferation and that glutamatergic influence causes the progenitors to exit cell cycle and proceed towards differentiation (Martins, Linden, & Dyer 2006). Investigation of the type and levels of glutamate receptor expression in retinal progenitors have revealed that the metabotropic receptors and the AMPA receptors are the ones expressed in early retinal progenitors (E14), but that NMDA expression only establishes itself significantly in later and more differentiated retinal progenitors (E18) (Das et al. 2005c). This was shown by microarray studies in retinal progenitors isolated at different stages of rat retinal development and was subsequently confirmed by other groups in various species (Grunder et al. 2000).

Sugioka et al examined the embryonic chick retina and found that the earlier retina responded well to AMPA/KA but not to NMDA up to E9. From E9-13 the AMPA/KA response fell and NMDA response increased suggesting that NMDA was more characteristic of retinal progenitors at a more advanced stage of differentiation (Sugioka, Fukuda, & Yamashita 1998). Compelling evidence for the difference in response of retinal progenitors to NMDA also comes from work in the developing rabbit retina. An immunological study established that glutamate expression in the RGCs appeared at around E20 and became prominent by E25 but that the strong glutamate responsiveness only developed around P10 (Pow, Crook, & Wong 1994). This was followed by other studies which showed that retinal progenitors in the ventricular zone (almost exclusively retinal neuronal precursors) did not respond to NMDA. Cells present in the inner retinal margin at E20 (containing early differentiated retinal ganglion cells) only responded to non-NMDA receptors at this stage and only a few days later at E24 did these cells acquire the ability to respond to NMDA. This response was measured as a change in intra-cellular calcium level, suggesting that only advanced differentiating RGC were responsive to NMDA (Wong 1995). The same study also showed that it was largely the ganglion cells

and not the amacrine cell precursors that responded to NMDA during development. These studies demonstrated the selectivity of the NMDA receptor response of RGC precursors in the developing retina. Other studies in mice added to this knowledge by showing the spatiotemporal appearance of NMDA expression in differentiating retinal neurons. Acosta et al used the X chromosome inactivation mouse model where as a result of the lacZ gene on one X chromosome and X chromosome inactivation, cells originating from a single beta- galactosidase positive cell can be followed in columns. Using this model they showed that only cells that had moved away from their site of origin (i.e. away from the columns) to their final destination in the developing retina, demonstrated NMDA expression (Acosta et al. 2007). These observations added further support to the suggestion that NMDA receptors were expressed and functional only in terminally differentiating RGC during retinal development.

While retinal progenitors express glutamate receptors with the ability to respond to some of the neurotransmitters in the glutamate system, it appears that they do not contain functional NMDA receptors and that this property may be restricted to terminally differentiating retinal ganglion cells. Based on the current evidence, it was decided that NMDA be used as one of the ligands that could help identify differentiating retinal ganglion cell precursors amongst the Müller stem cell population. However the use of NMDA as a single functional assay in the Müller stem cells was not thought to be optimum, since Müller glia, given their glial nature are known to be responsive to glutamate and NMDA themselves. It was decided that a better approach in this regard would be a combined one where the response of Müller stem cells to NMDA was studied in conjunction with their response to other neurotransmitters known to be characteristic of retinal ganglion cells. Towards this end cholinergic receptor systems were explored as candidate neurotransmitters to use in these experiments.

4.1.1.2 The Cholinergic system

The acetylcholine neurotransmitter system is another important neurotransmitter involved in retinal ganglion cell signalling. Two receptor types within this system, the muscarinic and the nicotinic receptors, play a role in RGC function, although nicotinic stimulation may be more crucial for RGC function. The expression of both

muscarinic and nicotinic acetylcholine receptors has been demonstrated in embryonic retinal progenitors, and the role of muscarinic receptors is better established. The muscarinic receptors are expressed at low levels in the early (E14) retinal progenitors with increasing levels in the later retinal progenitors (E18) (Das et al. 2005b). As with the glutamatergic receptors, muscarinic receptors have been shown to influence cell proliferation rates in retinal progenitors. All these receptors have been shown to be present and functional in early undifferentiated retinal progenitors of the ventricular zone. Functionality of these receptors is well documented with calcium imaging studies confirming that early embryonic retinal progenitors can respond to muscarinic receptors (Pearson et al. 2002d;Sakaki, Fukuda, & Yamashita 1996).

The expression and function of nicotinic receptors in retinal progenitors is not as widespread as that of muscarinic receptors. Levels of nicotinic receptor expression are minimal in the early retinal progenitors (E14), differentiated and undifferentiated, and are only significantly upregulated in the late differentiated retinal progenitors at E18 (Das et al. 2005a). Fetal neural stem cells derived from the rat caudal neural tube segment of rats have been studied for their response to muscarine and nicotine and showed the earliest documented response of neural progenitors to nicotine at E10.5. The response was found to be small in about 20% of the cells as demonstrated by patch clamp techniques (Cai, Cheng, Luo, Lu, Mattson, Rao, & Furukawa 2004). In the retina, data on undifferentiated retinal progenitor response to nicotinic agonists is sparse. The same study that defined the response of retinal progenitors in the ventricular zone to muscarinic agonists also showed that response of these cells to nicotine was negligible (less than 10% of cells responding to nicotine compared to nearly 90% responders to muscarine) (Pearson et al. 2002c).

Work at the transcriptional level suggests that the β3 promoter of the nicotinic receptor is activated early, just before retinal progenitors commit to the RGC fate. This has lead to the proposal that nicotinic receptor expression occurs in the retinal progenitors at the point of neural fate determination (Matter, Matter-Sadzinski, & Ballivet 1995b). In agreement with this suggestion, when presumptive RGCs in the developing chick retina were studied by patch clamping on retinal explants at different stages of development, 21% of the presumptive RGCs responded to

nicotine stimulation with a change in membrane potential at E12. The response rose to 57% at E15 and reached a near maximum of about 100% at E18 (Lecchi et al. 2005). These results indicate that nicotinic receptors are not expressed by early undifferentiated retinal progenitors, but that they make their first appearance when neural cell fate, particularly RGC fate, is determined. The level of expression then appears to increase with progressive RGC differentiation.

4.1.2 Neurotransmitter expression and function in Müller glia

4.1.2.1 Glutamatergic responses of Müller glia

The glial origin of the Müller stem cells poses the added complication of taking into account the response of these cells to various neurotransmitters by virtue of not just their progenitor nature, but their glial nature as well.

In the work first defining the isolation and characterisation of Müller stem cell line MIO-M1, their depolarising response to glutamate was described, consistent with what was known about Müller glial response to glutamate (Limb et al. 2002c). Cortical astrocytes are known to express mRNA specific to the various NMDA receptor subunits (NR1 and NR2) (Schipke et al. 2001b). They are also known to respond to NMDA stimulation with change in membrane currents and increase in cytosolic calcium indicating that NMDA receptors in this cell type are functional. Similar data has also been acquired from other specialised glial cells including Bergmann glia and the Müller glial cells of the retina (Lopez, Lopez-Colome, & Ortega 1997). Activation of NMDA receptors in retinal glia also have a mitogenic effect on these cells, and this is thought to be one of the mechanisms by which Müller glia are able to proliferate in response to various retinal pathologies (Uchihhori & Puro 1993). In human Müller glia in particular, NMDA receptor expression has also been demonstrated using western blot and immunohistochemistry (Puro, Yuan, & Sucher 1996). This study also showed that NMDA elicits neural currents and associated changes in cytosolic calcium in the human Müller glia in culture, a response that is blocked by specific NMDA antagonists. These results establish categorically the NMDA response of Müller glia and the likelihood of the Müller stem cells responding positively with a change in intracellular calcium when exposed to NMDA, by virtue of their glial nature.

4.1.2.2 Cholinergic responses of Müller glia

In contrast to extensive literature on Müller glial response to glutamate, very little is known about the response of these cells to cholinergic stimulation. In fact very little is known about the response of any glial cell type to cholinergic stimulation. Despite the significant interaction between neurons and glia, most work with glia focuses on the production or uptake of these neurotransmitters by these cells rather than their ability to respond to them with changes in membrane potential and levels of cytosolic calcium. It has however been identified that astrocytes possess muscarinic receptors (both M1 an M2 subtypes) (Murphy, Pearce, & Morrow 1986;Van Der Zee et al. 1993). There is also one report on the expression of nicotinic receptor alpha 7 in microglia and its role in regulation of the microglial inflammatory response, but it contains no reference to the response of these cells to nicotinic stimulation (Carnevale, DeSimone, & Minghetti 2007). In Müller glial cells, apart from the glutamate receptor function outlined above, the only other neurotransmitter function well established is the GABAergic one (Newman & Reichenbach 1996). Following this line of research, Wakakura et al studied the effect of acetylcholine on changes in cytosolic calcium levels in Müller glial cells, and compared their responses to those of retinal neurons. Amongst other findings and of particular interest to this work was the observation that Müller glial cells were able to respond to muscarinic agonists.Through antagonist studies, they identified that their response was mainly M1 and only partially M2 mediated. This group also established that the response of Müller cells to muscarinic agonists was about 10 times less sensitive than that of neurons. Significantly, no response could be elicited from the Müller glia when stimulated with acetylcholine or nicotine (Wakakura, Utsunomiya-Kawasaki, & Ishikawa 1998a).This is the best evidence available to us of the nature of Müller glial response to cholinergic agonists. Recently this work has been confirmed independently by another group who have also demonstrated the presence of the β2 nicotinic receptor sub unit protein in chicken Müller cells although there is no evidence of a functional response to this receptor (Kubrusly et al. 2005).

4.1.3 Analysis of neural function by calcium imaging

The neural nature of a cell can be identified by changes in membrane potential characteristic of a neuronal action potential. This is traditionally detected by patch clamping. A quicker and simpler way of examining these changes is to study the rise in intra cellular calcium levels that are associated with depolarization of a neuron. With the advent of calcium indicator dyes this technique has gained immense popularity as a quick way of assessing response of cells to various neurotransmitters, particularly in cells where neuronal activity may not necessarily associate with changes in membrane potential (Wong 1998).

The technique requires cells to be loaded with a calcium indicator dye which is a fluorophore linked to a calcium chelator 1,2 bis (2 aminophenoxy) ethane-N N N' N' Tetraacetic acid. The dye is usually in the form of a lipophilic membrane permeable ester soluble in DMSO. It is dissolved in media and the cells to be analysed are incubated with it. The membrane permeable ester enters the cell during incubation and is subsequently broken down by the intracellular esterases which result in the active form of the dye being released into the cell. The incubation is often carried out at around 37°C to promote the activity of the esterases. Upon calcium binding, the tetracarboxylate moiety of the dye is altered, resulting in changes in the spectral property of the fluorophore linked to it. This change can either be in the intensity or the spectrum of emission of the fluorophore and when quantified and plotted against time, gives an indication of the levels of intracellular calcium as well as the kinetics of any change in them (Wong 1998). In this manner calcium imaging provides a useful and practical tool with which to study neural cell function *in vitro*.

4.2 Objectives and experimental outline

Previous results showing that extracellular matrices and growth factors in combination with Notch inhibition caused Müller stem cells to differentiate towards an RGC phenotype, could not be considered absolute proof of the presence of differentiated RGC amongst the Müller stem cell population. Further studies analyzing the ability of these cells to function as neurons were needed to validate this data. On this basis the objectives of this work were -

1. To establish the baseline responses of Müller stem cells to NMDA, muscarinic and nicotinic agonists using calcium imaging techniques.
2. To identify changes (as seen by calcium imaging) in the responses of the Müller stem cells to NMDA, muscarinic and nicotinic agonists following treatment with FGF2 and DAPT to promote RGC differentiation.

The experiments performed were as follows-

1. Müller stem cells were cultured on coverslips for 7 days under control conditions, with matrigel and FGF2 or with matrigel, FGF2 and DAPT.
2. The cells were then loaded with calcium dye Fura Red and under live imaging exposed to NMDA, muscarinic or nicotinic agonists.
3. The response to each of these neurotransmitters by cells in the three different culture conditions was compared.

In these studies the long single wavelength dye Fura Red was used. This dye as the name suggests works in the long wavelength (visible) spectrum, exciting at around 470-480nm and emitting around 640-660nm (Poenie 2006). In response to calcium binding, there is a drop in the intensity of the fluorescence which can be directly quantified. Fura Red among the other long wavelength dyes (most of which emit in the green spectrum-fluo3, fluo-4, Calcium green, Oregon green etc) is the only one which has a decrease in fluorescence upon calcium binding and is usually used in combination with Fluo-3 for a ratiometric analysis (Segal & Auerbach 1995). Here it was used in a non-ratiometric manner, using the change in intensity of fluorescence as a direct (albeit relative) measure of intra cellular calcium levels.

All cells were cultured on the coverslip chamberwell slides before being subjected to calcium imaging studies. The cells response under the 3 different treatment conditions to a particular ligand were studied together thereby allowing comparison between them without additional inter experimental variation. In each case at least 4 different experiments were performed for each treatment condition and the results pooled for the final analysis. For each condition, the response of at least 50 cells or more was taken into account for the final analysis.

4.3 Results

4.3.1 Standardization of calcium imaging in Müller stem cells

Fura Red was dissolved in DMSO and then diluted in serum free medium (1 in 1000) before addition to the cells which were incubated with it at 37°C for 30 minutes. Initial standardization revealed that this combination of incubation time and temperature was superior to incubation at 15°C for 60 mins (Fig 4.1A). Post incubation, the dye was washed off with PBS and the cells were allowed to recover in serum containing media for 30 minutes at 37°C. Experiments performed without recovery showed that the response of Müller stem cells to NMDA was dramatically diminished suggesting the onset of stress in the absence of serum (Fig 4.1B). In light of this and because all of the previous data on gene and protein expression of these cells was studied in serum containing conditions, the calcium imaging experiments were all performed with 30 minutes recovery time in serum containing media. Following recovery, the cells were washed with PBS twice before addition of optically clear L-15 medium and transfer to the microscope. All imaging was carried out on a heating stage at 37°C.

To estimate the dose of each neurotransmitter to be added to the cells, a titration of the dose response was carried out. The lowest doses that were able to elicit a reliable response for each ligand were chosen and these doses were then used across the samples to look for a difference in the response. Based on the titration (Fig 4.1C) a final dose of 2mM was chosen for all three ligands- NMDA, Muscarine (M1 agonist McN-A-343) and Nicotine. Accordingly a stock solution of 10mM was prepared for each ligand and when stimulating the cells, 50ul of it was added to 200ul of media in each well to achieve the final concentration of 2mM.

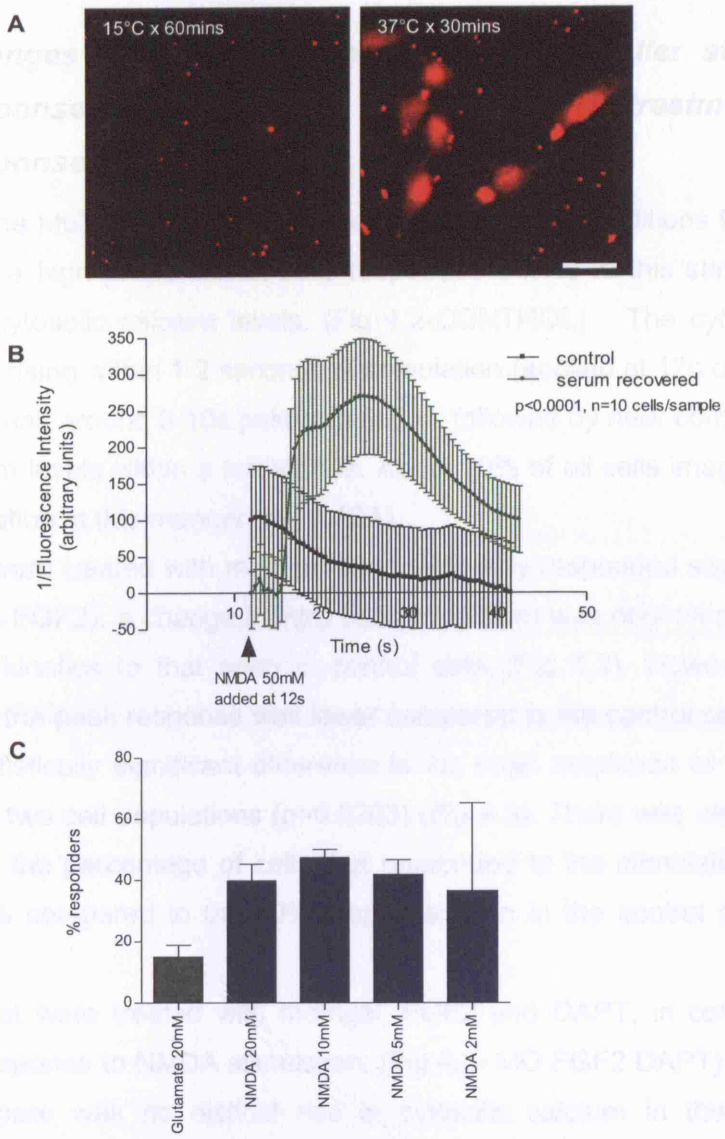

Figure 4.1: Standardization of calcium imaging in Müller stem cells. (A) Micrographs showing the uptake of Fura Red dye by the Müller stem cells at 2 different loading conditions. Incubation with the dye at 37°C for 30mins showed better uptake of the dye than when the cells were incubated at 15°C for 60mins. Scale bar=10µm (B) Graph comparing the response of Müller stem cells to 50mM NMDA without and with serum recovery. In the absence of serum, the cells do not respond to the NMDA as seen by the flat response line. When incubated with 10% serum for 30 mins, the cells respond better to NMDA with rise in cytosolic calcium. Fura red intensity declines with rise in cytosolic calcium and therefore the Y axis depicts 1/fluoresecence intensity to generate a characteristic response curve.(C) Histogram depicting the response of Müller stem cells to glutamate and different doses of NMDA. Müller stem cells were more responsive to NMDA than to glutamate at the same dose of 20mM. Müller stem cells were able to respond to NMDA doses of as low as 2mM and this dose was used for these studies.

4.3.2 Müller stem cell response to neurotransmitters

4.3.2.1 Changes in cytosolic calcium levels of Müller stem cells in response to NMDA and effect of DAPT treatment on this response

Analysis of the Müller stem cell response under baseline conditions to 2mM NMDA showed that a high proportion of cells responded briskly to this stimulation by an increase in cytosolic calcium levels. (Fig 4.2-CONTROL) The cytosolic calcium levels began rising within 1-2 seconds of stimulation (applied at 12s of imaging) and reached its peak around 8-10s post stimulation, followed by near complete recovery of the calcium levels within a further 10s. About 70% of all cells imaged responded to the stimulation in this manner (Fig 4.10A).

When cells were treated with matrigel and FGF2 they responded slightly differently (Fig 4.2- MG FGF2): a change in intra cellular calcium was observed in some cells with similar kinetics to that seen in control cells (Fig 4.3). However, the mean amplitude of the peak response was lower compared to the control cells. There was in fact a statistically significant difference in the peak amplitude of the responses between the two cell populations ($p=0.0203$) (Fig 4.3). There was also a significant difference in the percentage of cells that responded to the stimulation, which was less than 5% compared to the 70% response seen in the control population (Fig 4.10B).

The cells that were treated with matrigel, FGF2 and DAPT, in contrast, showed almost no response to NMDA stimulation. (Fig 4.2- MG FGF2 DAPT) Barring minor fluctuation there was no distinct rise in cytosolic calcium in these cells upon treatment with 2mM NMDA and the cumulative curve was almost a flat line (Fig 4.3). Less than 2% cells showed a small response (Fig 4.10).

In summary, the majority of control cells had a brisk definitive rise in intracellular calcium upon stimulation with 2mM NMDA, a response which diminished in amplitude and percentage of responders with matrigel and FGF2 treatment and was almost completely eliminated with further addition of DAPT to the culture conditions (Fig 4.2 and Fig 4.3).

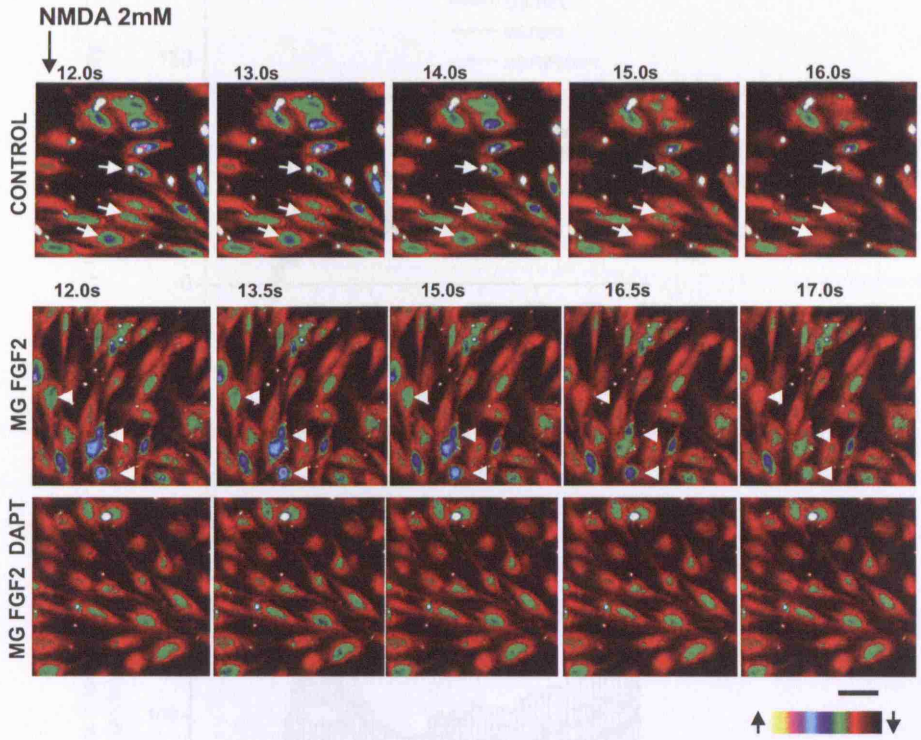

Figure 4.2: Changes in cytosolic calcium levels of Müller stem cells in response to NMDA and effect of DAPT treatment on this response.

Heat map images of Müller stem cells cultured under baseline conditions and loaded with fura red. The colour bar describes the intensity colour relationship with yellow being brightest and black being the dimmest. Fura red intensity declines with increase in cytosolic calcium and a shift from yellow towards black is indicative of rising cytosolic calcium in these micrographs. The ligand in each case was added at 12s of imaging, with the images prior to ligand addition being used to establish baseline fluorescence. Control cells show rapid decrease in cytosolic calcium in response to NMDA exposure, within 2-3 seconds of ligand exposure. Example of some such cells are marked with white arrows . Cells cultured with matrigel and FGF2 also show some response but in fewer numbers and the response was slower than that seen in the control cells. Examples are highlighted with white arrows. Cells cultured with matrigel and DAPT showed a negligible response. Scale bar=10μm

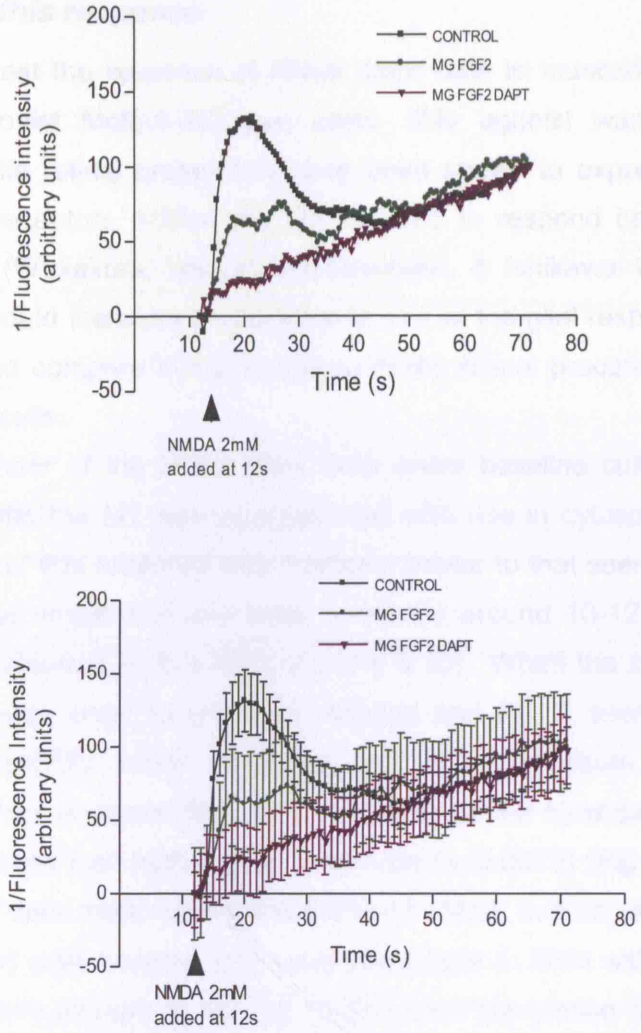

Figure 4.3: Changes in cytosolic calcium levels of Müller stem cells in response to NMDA and effect of DAPT treatment on this response.

Graphs comparing the characteristic curve generated by changing cytosolic calcium in response to NMDA in Müller stem cells. Control cells demonstrate a brisk rise in cytosolic calcium (represented in the graph by an inverse change in fluorescence intensity) followed by a slower decline. Cells treated with matrigel and FGF2 also show increase in cytosolic calcium but to a lesser degree and more slowly. Cells cultured with matrigel, FGF2 and DAPT do not show any change in cytosolic calcium levels. The graphs represent cumulative data from over 40 cells per sample. The graph on top is depicted without error bars to allow visualisation of the curves clearly. The graph below shows the same data with error bars (SEM). Response of the control cells is significantly different from that of the other 2 cell types particularly at peak amplitude ($p=0.0203$ Control vs MG FGF2, $p<0.0001$Control vs MG FGF2 DAPT).

4.3.2.2 Changes in cytosolic calcium levels of Müller stem cells in response to muscarinic agonists and effect of DAPT treatment on this response

In order to test the response of Müller stem cells to muscarinic receptors the M1 receptor agonist McN-A-343 was used. This agonist was specifically chosen because while retinal progenitors have been shown to express both M1 and M2 muscarinic receptors, Müller glia are believed to respond better to M1 receptors than to M2 (Wakakura, Utsunomiya-Kawasaki, & Ishikawa 1998b). By using M1 agonists it would therefore be possible to look at the glial response to muscarine in particular and compare it with response of the retinal precursors derived from the Müller stem cells.

A small number of the Müller stem cells under baseline culture conditions when stimulated with the M1 agonist responded with rise in cytosolic calcium (Fig 4.4). The kinetics of this response was relatively similar to that seen with NMDA but with much smaller amplitudes and peak amplitude around 10-12s. About 30% of the control cells showed such a response (Fig 4.10). When the same concentration of McN-A-343 was used to stimulate matrigel and FGF2 treated cells however, a larger and slightly earlier response with peak amplitude around 8-10s post stimulation was observed (Fig 4.4). Following similar kinetics as the control cells, these responses had higher peak amplitude ($p=0.0079$) (Fig 4.5). About 50% of this group of cells responded in this fashion to McN. In contrast, matrigel FGF2 and DAPT treated cells showed very small responses to McN with a barely detectable rise in cytosolic calcium at around 10-12 s post stimulation (Fig 4.5). Only 8-10% cells imaged responded (Fig 4.10). Interestingly the morphology of the cells that responded to muscarine in all 3 samples was glial and not neuronal (Fig 4.4 and compare with morphology of cells in Fig 4.8). There was also a decline in the change in cytosolic calcium of matrigel, FGF2 and DAPT treated cells compared to the controls ($p=0.037$). Glial cells and retinal progenitors are known to respond to muscarinic agonists and the results of these experiments consistent with this. However this data did not conclusively demonstrate a difference in the muscarinic response of RGC precursors from that of undifferentiated retinal progenitors.

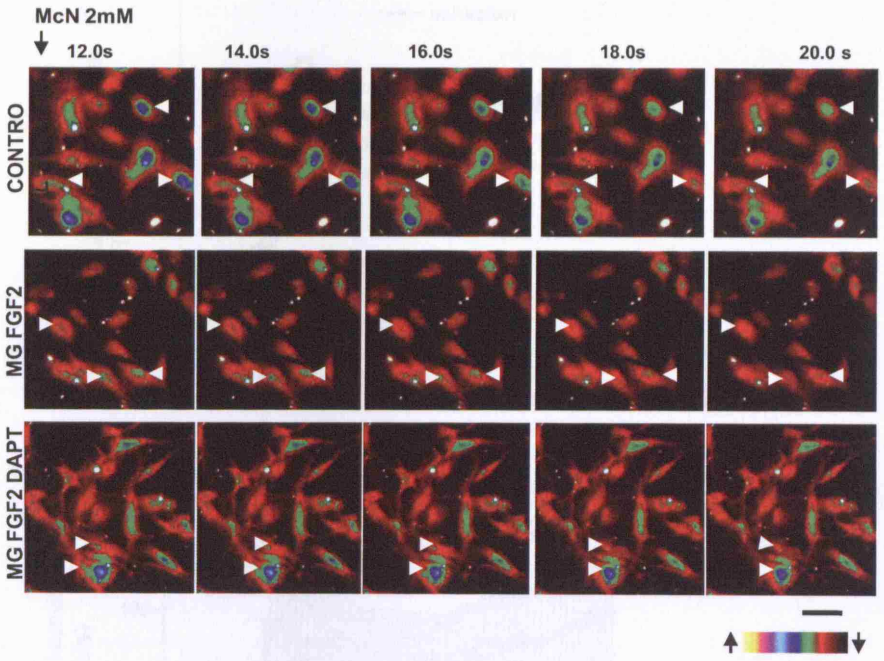

Figure 4.4: Changes in cytosolic calcium levels of Müller stem cells in response to Muscarinic agonists and effect of DAPT treatment on this response.

Heat map images of Müller stem cells cultured under baseline conditions and loaded with fura red. The colour bar describes the intensity colour relationship with yellow being brightest and black being the dimmest. Fura red intensity declines with increase in cytosolic calcium and a shift from yellow towards black is indicative of rising cytosolic calcium in these micrographs. The ligand in each case was added at 12s of imaging, with the images prior to ligand addition being used to establish baseline fluorescence. In response to M1 agonist McN-A343 control cells show occasional slow decrease in fluorescence intensity. Examples of some such cells marked with white arrows. Cells cultured with matrigel and FGF2 (MG FGF2) alone or with DAPT (MG FGF2 DAPT)also show similar responses. Examples highlighted with white arrows. Scale bar=10μm

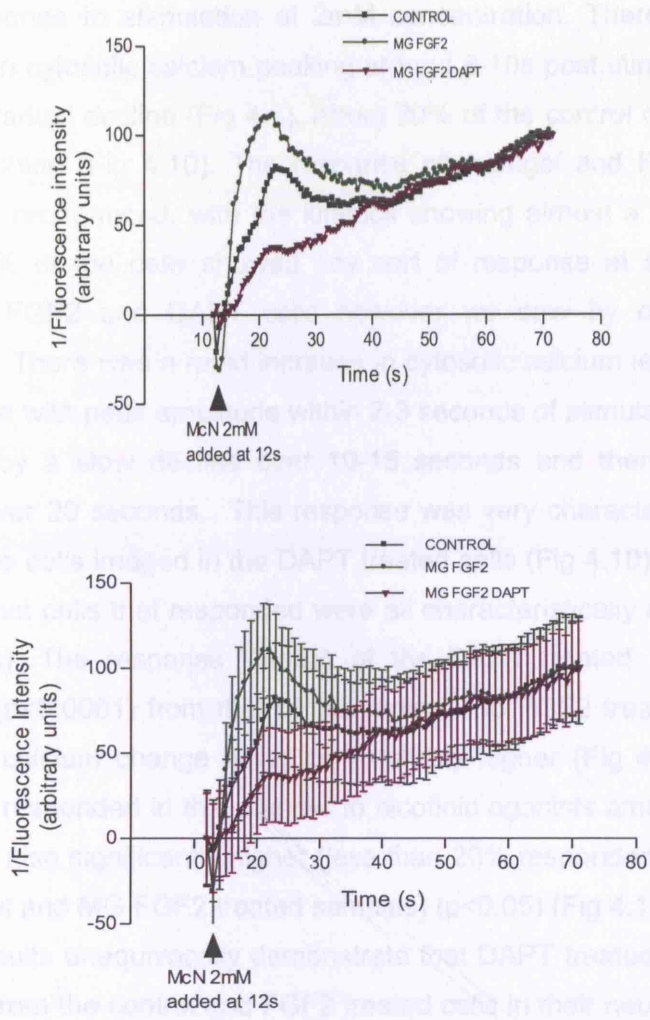

Figure 4.5: Changes in cytosolic calcium levels of Müller stem cells in response to Muscarinic agonists and effect of DAPT treatment on this response.

Graphs comparing the calcium response curve to McN-A343 of Müller stem cells under the different culture conditions. All three samples show similar response curves with slightly varying amplitudes of response. The graphs represent cumulative data from over 40 cells per sample. The graph on the top is depicted without error bars to allow visualisation of the curves clearly. The graph at the bottom shows the same data with error bars (SEM). The response pattern between the three cell types was similar and the difference in response amplitudes was small. Control vs MG FGF2-p=0.0079, control vs MG FGF2 DAPT-p=0.037

4.3.2.3 Changes in cytosolic calcium levels of Müller stem cells in response to nicotinic agonists and effect of DAPT treatment on this response

With nicotine a small number of Müller stem cells under control conditions showed a slow response to stimulation at 2mM concentration. There was a gradual small increase in cytosolic calcium peaking around 8-10s post stimulation, followed by an equally gradual decline (Fig 4.6). About 20% of the control cells imaged responded in this fashion (Fig 4.10). The response of matrigel and FGF2 treated cells was even less pronounced, with the kinetics showing almost a flat line (Fig 4.7). Only about 20% of the cells showed any sort of response at all (Fig 4.10). With the matrigel, FGF2 and DAPT cells however we saw by comparison a dramatic response. There was a rapid increase in cytosolic calcium levels within a second of stimulation with peak amplitude within 2-3 seconds of stimulation (Fig 4.8). This was followed by a slow decline over 10-15 seconds and then a slightly more rapid decline over 20 seconds. This response was very characteristic and seen in over 95% of the cells imaged in the DAPT treated cells (Fig 4.10). Of particular note was the fact that cells that responded were all characteristically neuronal in morphology (Fig 4.8B). The response kinetics of the DAPT treated cells were significantly different ($p<0.0001$) from that of the control and FGF2 treated cells with the peak cytosolic calcium change being considerably higher (Fig 4.9). The percentage of cells that responded in this manner to nicotinic agonists amongst the DAPT treated cells was also significantly higher (less than 20% responded to nicotinic agonists in the control and MG FGF2 treated samples) ($p<0.05$) (Fig 4.10).

These results unequivocally demonstrate that DAPT treated cells were functionally different from the control and FGF2 treated cells in their neurotransmitter response. Nicotine, as established from published literature, is not functional in Müller glia or undifferentiated retinal progenitors. In the retina its earliest functionality is seen in early differentiated retinal ganglion cells and this progresses as development of these RGC advances. In this study it was observed that control cells which have both Müller glial and undifferentiated retinal progenitor properties are unable to respond to nicotine, and this is in agreement with previous work by others. The results also showed that treatment with matrigel and FGF2 is not sufficient to elicit

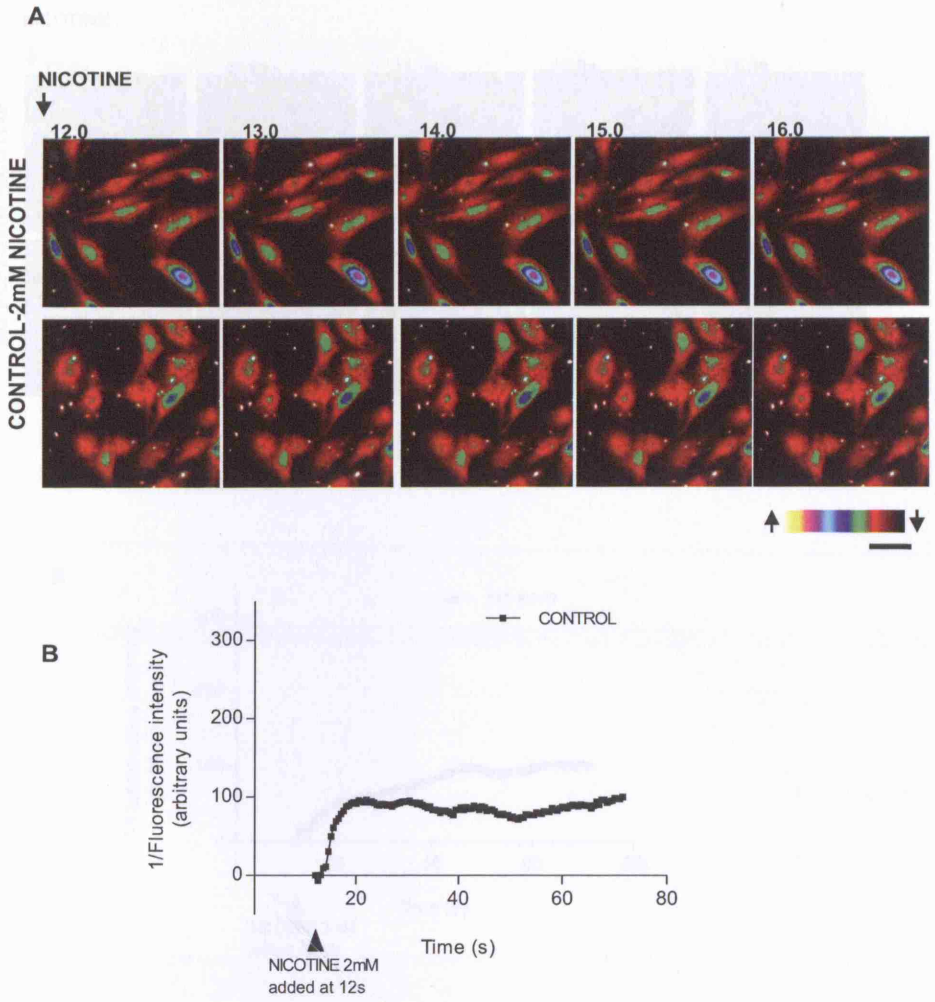

Figure 4.6: Changes in cytosolic calcium levels of control Müller stem cells in response to Nicotinic agonists. Heat map images of Müller stem cells cultured under baseline conditions and loaded with fura red. The colour bar describes the intensity colour relationship with yellow being brightest and black being the dimmest. Fura red intensity declines with increase in cytosolic calcium and a shift from yellow towards black is indicative of rising cytosolic calcium in these micrographs. The ligand in each case was added after 12s of baseline imaging. (A) In response to nicotinic stimulation, control Müller stem cells show no change in their cytosolic calcium levels. 2 different experiments for each cell type are shown. (B) Graph representing the kinetics of change in fura red intensity in the control Müller stem cells when exposed to nicotinic agonists. Cumulative results from 50 cells show no significant response and the curve is largely a flat line. Scale bar=10μm

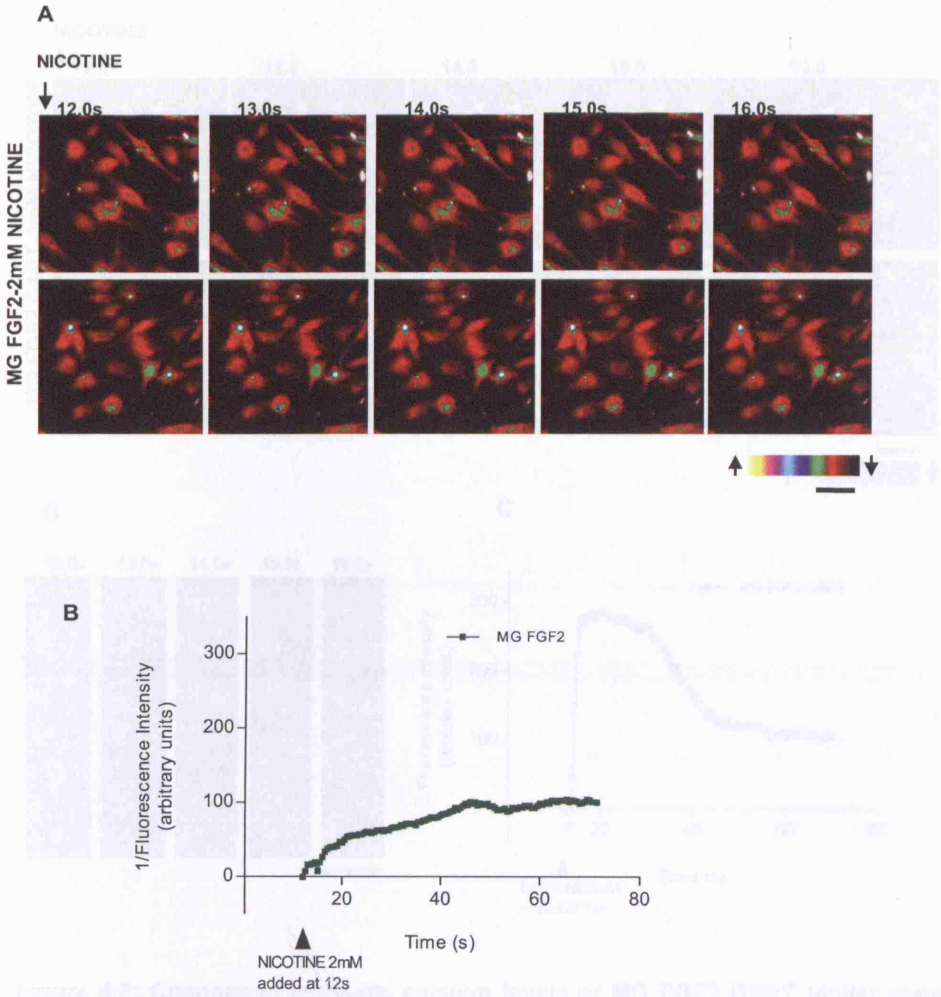

Figure 4.7: Changes in cytosolic calcium levels of MG FGF2 treated Müller stem cells in response to Nicotinic agonists. Heat map images of Müller stem cells cultured under baseline conditions and loaded with fura red. The colour bar describes the intensity colour relationship with yellow being brightest and black being the dimmest. Fura red intensity declines with increase in cytosolic calcium and a shift from yellow towards black is indicative of rising cytosolic calcium in these micrographs. The ligand in each case was added after 12s of baseline imaging. (A) In response to nicotinic stimulation, Müller stem cells treated with matrigel and FGF2 (MG FGF2) show no change in their cytosolic calcium levels. 2 separate experiments are shown. Scale bar=10μm (B) Graph representing the kinetics of change in fura red intensity in the MG FGF2 treated Müller stem cells when exposed to nicotinic agonists. Cumulative results from 47 cells show no significant response and the curve is largely a flat line.

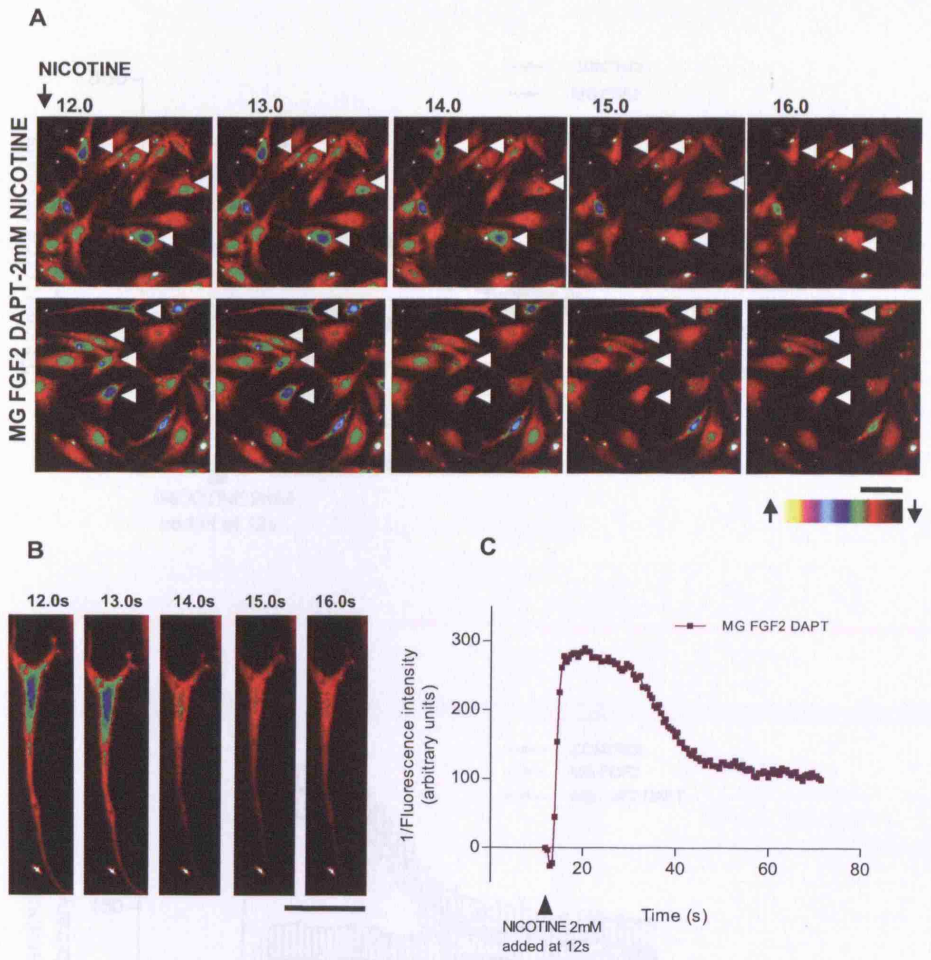

Figure 4.8: Changes in cytosolic calcium levels of MG FGF2 DAPT Müller stem cells in response to Nicotinic agonists.

Heat map images of Müller stem cells cultured under baseline conditions and loaded with fura red. The colour bar describes the intensity colour relationship with yellow being brightest and black being the dimmest. Fura red intensity declines with increase in cytosolic calcium and a shift from yellow towards black is indicative of rising cytosolic calcium in these micrographs. The ligand in each case was added after 12s of baseline imaging. (A) In response to nicotinic stimulation, Müller stem cells treated with matrigel, FGF2 and DAPT (MG FGF2 DAPT) show a brisk decline in fluorescence intensity occurring within 2 seconds of exposure and present in almost every cell in the field. 2 different fields are shown and some examples of responding cells are highlighted with white arrows. (B) Magnified images of one MG FGF2 DAPT treated cell with neural morphology showing rapid change in cytosolic calcium in response to nicotinic stimulation. Scale bar=10μm (C) Graph representing the kinetics of change in fura red intensity in the MG FGF2 DAPT treated Müller stem cells when exposed to nicotinic agonists. Cumulative results from 50 cells show dramatic rise in cytosolic calcium (depicted by 1/fluorescence intensity of fura red) within 2 seconds of exposure, followed by an initial slow and subsequent rapid recovery.

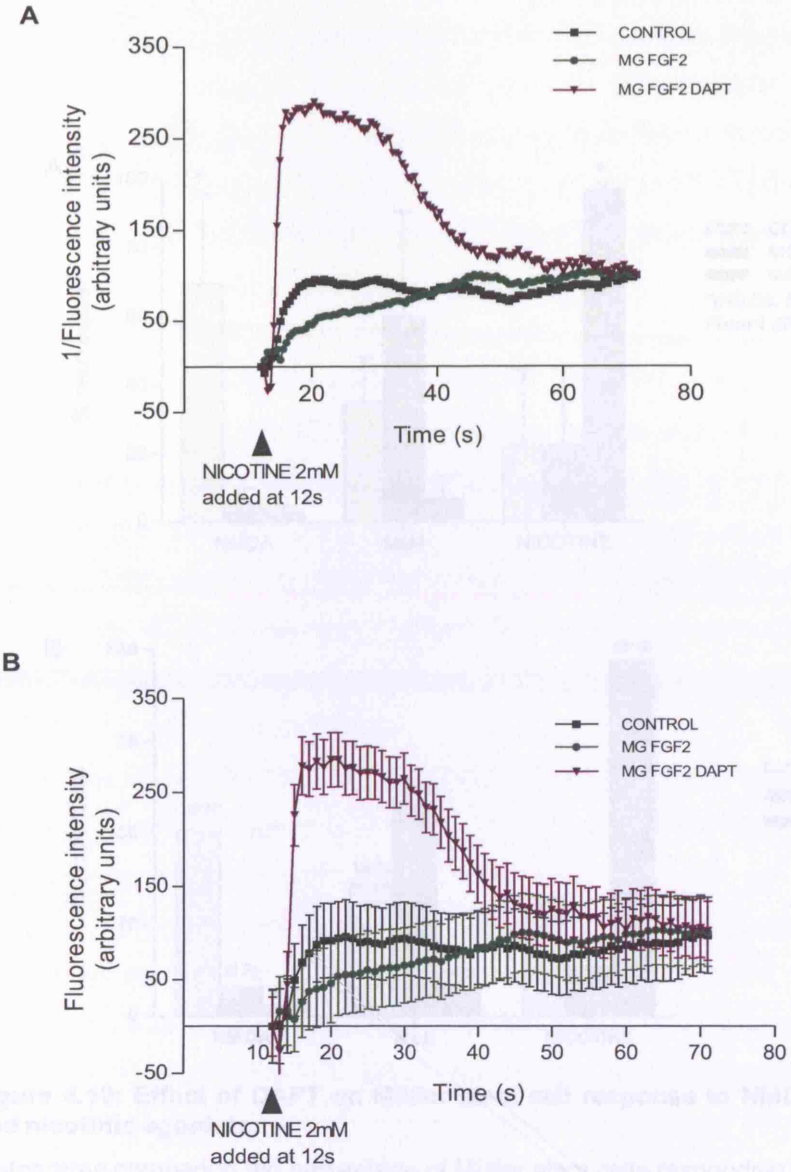

Figure 4.9: Changes in cytosolic calcium levels of Müller stem cells in response to Nicotinic agonists and effect of DAPT treatment on this response

(A) Graph comparing the calcium response curve to Nicotine of Müller stem cells under the different culture conditions. Cells cultured under control conditions or with matrigel and FGF2 do not show any response. Müller stem cells cultured with matrigel, FGF2 and DAPT however respond briskly by increasing cytosolic calcium levels (within 2 seconds) which then decline more slowly over 20-25 seconds. The graphs represent cumulative data from over 40 cells per sample. This graph is depicted without error bars to allow visualisation of the curves clearly. Graph (B) shows the same data with error bars (SEM). There is a significant difference in the response of DAPT treated cells to nicotine compared to the other 2 treatment conditions ($p<0.0001$ vs control and vs MG FGF2 treated cells).

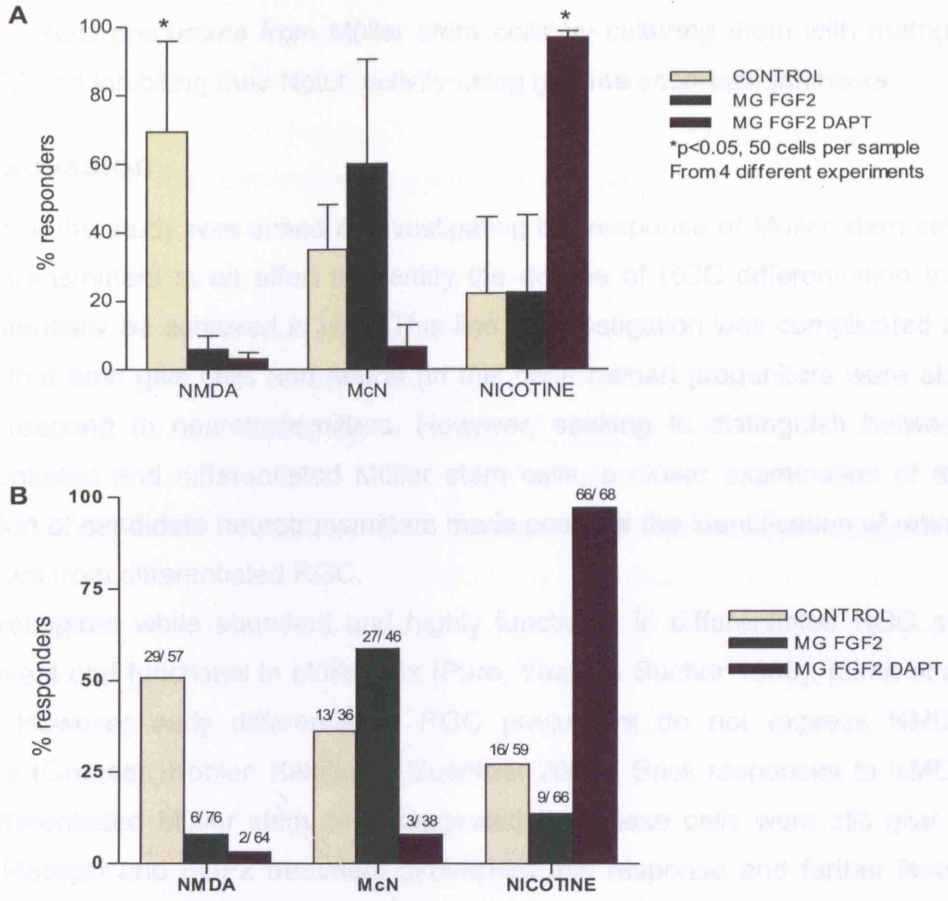

Figure 4.10: Effect of DAPT on Müller stem cell response to NMDA, Muscarinic and nicotinic agonists.

Histograms comparing the percentage of Müller stem cells responding to the 3 ligands when cultured under the 3 different conditions. Graph (A) shows the mean percentage response and was generated using individual percentage responses from 4 different experiments. Graph (B) depicts percentage response based on actual numbers of cells that responded to the stimuli and was generated by counting the number of cells that responded in each experiment. The numbers on each histogram show the total number of responsive cells over total number of cells examined.

In response to NMDA the control cells respond in significantly larger numbers compared to the matrigel and FGF2 alone or DAPT treated cells. In response to the muscarinic agonists the matrigel FGF2 treated cells respond best although not significantly differently from the control cells and the DAPT treated cells have a much smaller response. The DAPT treated cells however respond best to the nicotinic agonists with almost 100% of them responding, while cells in the other culture conditions have a significantly smaller response.

this response in these cells and it is the Notch inhibition by gamma secretase inhibitor DAPT that pushes these cells to a stage of differentiation where they are able to express functional nicotinic receptors and respond to nicotine stimulation by a rise in cytosolic calcium. Since this response is characteristic of differentiating RGC precursors, the present results strongly suggest that it is possible to achieve functional RGC precursors from Müller stem cells by culturing them with matrigel and FGF2 and inhibiting their Notch activity using gamma secretase inhibitors.

4.4 Discussion

This part of the study was aimed at investigating the response of Müller stem cells to neurotransmitters in an effort to identify the degree of RGC differentiation that could potentially be achieved *in vitro*. This line of investigation was complicated by the fact that both glial cells and neural (in this case retinal) progenitors were also able to respond to neurotransmitters. However, seeking to distinguish between undifferentiated and differentiated Müller stem cells, a closer examination of the expression of candidate neurotransmitters made possible the identification of retinal progenitors from differentiated RGC.

NMDA receptors while abundant and highly functional in differentiated RGC are also present and functional in Müller glia (Puro, Yuan, & Sucher 1996), (Limb et al. 2002b). However early differentiating RGC precursors do not express NMDA receptors (Grunder, Kohler, Kaletta, & Guenther 2000). Brisk responses to NMDA by undifferentiated Müller stem cells suggested that these cells were still glial in nature. Matrigel and FGF2 treatment diminished this response and further Notch inhbibition completely erased it. This suggests that with this treatment Müller stem cells lose their glial properties and are induced to undergo neuronal differentiation.

Muscarinic receptors are present in abundance in undifferentiated retinal progenitors and are believed to play a role in their proliferation (Martins & Pearson 2008b;Pearson et al. 2002b). The Müller glial cells also possess muscarinic receptors, particularly the M1 receptors and can respond to their stimulation with rising cytosolic calcium. The response of differentiating RGC to muscarinic receptors has not been previously compared with that of undifferentiated retinal precursors and in this study no significant difference was found between the

differentiated and undifferentiated Müller stem cells in their response to muscarinic agonists.

Nicotinic response on the other hand is characteristic of differentiated retinal ganglion cells and neither undifferentiated retinal progenitors nor Müller glial cells have been found to be able to the respond to nicotinic stimulation (Matter, Matter-Sadzinski, & Ballivet 1995a;Pearson et al. 2002a;Wakakura, Utsunomiya-Kawasaki, & Ishikawa 1998c).The earliest response to nicotine during development is restricted to the early differentiating RGCs (Das et al. 2005g). This study showed that Müller stem cells were largely unresponsive to nicotinic stimulation until they were subjected to Notch inhibition. These results indicate that this treatment caused a significant change in the nicotinic receptor properties of Müller stem cells, rendering them swiftly responsive to nicotinic stimulation, in a manner similar to that seen in differentiating RGC precursors. It is therefore possible to conclude that treatment with gamma secretase inhibitors to down regulate Notch activity is able to direct Müller stem cells towards a retinal ganglion cell fate. It is of note that even under baseline conditions a small percentage of cells were able to respond to nicotinic stimulation and this may be explained by the heterogenous nature of the Müller stem cells whereby not all cells in a given population are at the same stage of differentiation.

In these studies the calcium dye Fura Red was used to analyse the responses of cells to the various neurotransmitters. Changes in the fluorescence intensity of Fura Red are however not strictly linear and in order to be able to quantify the changes in calcium levels, Fura Red is usually used along with a second dye so as to be able to perform a ratiometric analysis. This was not done in these experiments and this must be kept in mind when interpreting the response kinetics, since in the absence of the ratiometric analysis it is difficult to establish accurately the magnitude of the changes observed.

While Notch inhibition might be inducing a population of Müller stem cells to differentiate into RGC precursors, it is not possible to suggest the presence of terminally differentiated RGC in this population. The nicotinic response though highly suggestive of their RGC precursor nature is not characteristic of that seen in terminally differentiated RGC. This characterisation would require further phenotypic and functional examination of these cells. Mouse cortical stem cells were found to

respond to nicotinic agonists in a similar manner to that seen here with the Müller stem cells, with a rapid rise and slow recovery. There was however a difference in the kinetics of the response of these cells depending upon their stage of differentiation. Both early and late cortical stem cells demonstrated swift rise in cytosolic calcium when stimulated with nicotinic agonists. In the late cortical stem cells, the recovery of cytosolic calcium to baseline levels was much faster than that seen with the early cortical stem cells (Atluri et al. 2001). The response kinetics of the differentiated Müller stem cells to nicotinic stimulation were similar to that seen with early cortical stem cells and suggests that these cells still require further differentiation before they function fully as RGC. The use of retinal ganglion cell lines as a positive control when performing these calcium imaging experiments would have been useful to establish definite RGC specific control data against which the responses of differentiated Müller stem cells could have been compared. It would also be of interest to examine expression patterns of the glutamatergic, muscarinic and nicotinic receptors under control conditions in the Müller stem cells and the effect of Notch inhibition on this expression.

From the present observations however it is possible to conclude that with these treatments it has been possible to establish a population of differentiating RGC precursors with some of the functionality seen in terminally differentiated RGC. However the results are not sufficient to support the conclusion that these cells are terminally differentiated RGC and more work is required to identify the signals that might induce them to terminally differentiate.

Chapter 5: Barriers to Müller stem cell transplantation in vivo

5.1 Introduction

5.1.1 Stem cell transplantation into the diseased retina

In retinal diseases where there is irreversible damage to the retinal neurons, stem cell therapy remains the only hope for visual restoration (Ali & Sowden 2003). However transplantation of stem cells into the retina to restore vision has largely been unsuccessful so far. Attempts have been made with several different cell types transplanted into several different models of retinal disease (Chacko et al. 2003b;Lund et al. 2003). In most instances, the success of these transplants is severely impaired by poor transplant cell migration, differentiation or integration into the host retina.

A good model of retinal disease is the Royal College of Surgeons (RCS) model of retinal degeneration. Photoreceptor degeneration in the RCS rat retina begins at around 4 weeks of age as a result of a MERTK defect (which prevents outer segment phagocytosis by RPE thereby causing accumulation of these outer segments and eventual degeneration) and resembles the retinitis pigmentosa (RP) phenotype.(D'Cruz et al. 2000;Gal et al. 2000) Others have successfully transplanted potential stem/ progenitor cells from various sources (including hippocampal progenitors, other brain derived stem cells and retinal progenitors) into the RCS retina and achieved good migration but a closer look at these studies revealed that successful migration was almost always from an allogenic graft (Canola et al. 2007;Qiu et al. 2005;Takahashi et al. 1998a;Wojciechowski et al. 2002a;Young et al. 2000b). All previous attempts at xenograft transplantation into RCS rats (Mizumoto, Mizumoto, Whiteley, Shatos, Klassen, & Young 2001) or even normal adult rats (Banin et al. 2006a;Dong et al. 2003) have resulted in limited migration. Recently Gamm et al transplanted human neural progenitor cells into the sub retinal space (SRS) of RCS rats and were able to demonstrate a certain degree of migration into the inner retina, although majority of the grafted cells still remained confined to the SRS (Gamm et al. 2007). There have also been a considerable number of sub retinal xenograft RPE cell transplants in the RCS model showing preservation of function (Little et al. 1996b;Lund et al. 2001c;Lund et al. 2007b). In

these cases however the transplanted cells are not required to migrate away from the SRS which is their intended final destination. To our knowledge there are no reports of successful stem cell migration into the inner retina following xenograft transplantation into the SRS of adult degenerating RCS retina.

When transplanted into the sub retinal space (SRS) of neonatal Lister-hooded rats human Müller stem cells successfully migrate into the inner retinal layers and express markers of differentiated retinal neurons, substantiating their retinal stem cell nature *in vivo* (Lawrence et al. 2007b;Limb et al. 2002a). The neonatal retina however is known to provide an amenable environment for cell transplantation given the immature state of development of the retina and often initial studies on the *in vivo* properties of potential stem cells are carried out on neonatal retinae for this reason (Sakaguchi, Van Hoffelen, & Young 2003a).

The potential application of the Müller stem cells in the future is likely to be in conditions like macular degeneration, retinitis pigmentosa, glaucoma etc where there is characteristically a considerable degree of chronic degeneration and inflammation in the retina (Chen, Yang, & Kijlstra 2002;Rodrigues 2007). The retinal environment into which the Müller stem cells will need to be effective is therefore likely to be very different from that of a pliable neonatal retina and more akin to the degenerating RCS retina. It is therefore essential to study the behaviour of Müller stem cells in a diseased retinal environment like the RCS retina in order to assess more accurately the potential of these cells to repair such a retina.

5.1.2 Microglia and Chondroitin sulphate proteoglycans in degenerated retina and implications for retinal transplantation

When Müller stem cells were transplanted *in vivo* into the retina (Lawrence, Singhal, Bhatia, Keegan, Reh, Luthert, Khaw, & Limb 2007d) it was found that the transplanted cells were associated with some macrophage and microglial reactivity. Microglia in the retina can adopt many forms-in the undamaged retina the cells have small nuclei and are multiprocessed, whereas, when activated by injury or disease they become round and are larger, becoming more like macrophages in appearance. Microglia are normally present in several inner retinal layers but

migrate to the outer layers when photoreceptors are damaged (Sauvé et al., 2001; Thanos and Richter, 1993). In the presence of degeneration, the retina is associated with robust microglial activity (Ng & Streilein 2001;Thanos & Richter 1993c). Microglia are known to migrate and proliferate within the degenerating retina of the RCS rat (de Kozak et al. 1997b;Roque, Imperial, & Caldwell 1996b;Thanos & Richter 1993b) Presence of such microglial activity in the host retina at the time of transplantation could potentially affect the survival of any transplanted cells.

Apart from the underlying presence of activated microglia in a diseased retina, injury caused by the transplantation procedure itself is also likely to induce some microglial activity. Not only may peripheral macrophages be recruited when the blood-retina barrier is disturbed at the time of surgery, resident microglia also respond rapidly to injury (Kreutzberg, 1996). These responding microglia perform several functions (Chen et al., 2002) which can either be neuroprotective (Harada et al. 2002c) or neurotoxic depending on the local environment (Schwartz, 2003). They phagocytose potentially toxic debris and release growth factors which may act on neurons directly or indirectly (through Müller glial cells) (Harada et al., 2002) and they can also release pro-inflammatory cytokines such IL-1β, TNF-α and IL-6 that have been shown to inhibit neurogenesis in the brain (Ekdahl et al., 2003; Monje et al., 2003). Activated macrophages and microglia may also release TGFβ and EGF which have been implicated as regulators of CSPG production by astrocytes after CNS injury (Smith and Strunz, 2005). Based on these observations, it is evident that microglial activity is likely to be associated with most retinal stem cell transplantations, particularly when the transplantation is being performed into a diseased retina. Furthermore work from these publications suggests that activated microglial cells are likely to produce other factors that would further prevent the migration and differentiation of transplanted cells *in vivo*.

Amongst other factors that microglia produce, of particular significance are the Chondroitins sulphate proteoglycans (CSPG). The CSPG are extracellular matrix proteins found in the central and peripheral nervous system and are believed to be crucial neuronal support and guidance proteins. Microglia have been shown to produce CSPGs *in vitro* (Uhlin-Hansen & Kolset 1988c) and *in vivo* upon spinal cord injury (Jones et al. 2002a;Jones & Tuszynski 2002c). Of interest to this work is the

fact that sulphated proteoglycans (such as neurocan) act as barriers in the developing CNS and are associated with the guiding of axonal pathways (Margolis and Margolis, 1997). They have been implicated in the inhibition of neurite extension in the damaged central nervous system (Davies et al., 1994; Jones et al., 2002; Lemons et al., 1999) and it has been well documented that CSPGs are up regulated at sites of injury and prevent migration of transplanted cells through lesions in the brain and spinal cord (Jones, Margolis, & Tuszynski 2003;Jones, Sajed, & Tuszynski 2003b;Morgenstern, Asher, & Fawcett 2002).

In the eye CSPG expression is found in the normal rodent retina, although the expression decreases with age (Inatani and Tanihara, 2002; Popp et al., 2004) CSPG expression is up-regulated in lesions of the optic nerve (Selles-Navarro et al. 2001a), in retinal ischemia (Inatani et al. 2000) and during photoreceptor degeneration (Landers et al. 1994). Importantly CSPGs and neurocans are expressed extensively in the dystrophic RCS rat retina (Chu et al., 1992; Zhang et al., 2003) and are known to prevent migration of retinal neurons *in vitro* (Inatani et al. 2001b).

5.2 Objectives and experimental design

The above review outlined the current challenge of achieving successful transplant cell survival and migration into a model of diseased retina like the RCS rat retina. A diseased retina is likely to be inflamed and therefore possess high levels of microglial activity. Microglia also produce several factors that adversely affect transplant cell survival including chemokines which cause further inflammation as well as extracellular matrix proteins like chondroitin sulphate proteoglycans (CSPGs), the deposition of which could potentially prevent transplant cell migration and integration. In accordance with the above evidence, microglial activity and CSPG deposition were thought to be likely candidiates preventing survival and migration of transplanted stem cells within a diseased retina. On this basis the objectives of this work were to:

1. Transplant Müller stem cells into the SRS of RCS rat eyes and compare the migration and integration seen in this model with that seen in the neonatal lister hooded rat eyes.

2. To compare the microglial activity and CSPG deposition in these 2 models, under control, sham injection and transplant conditions.
3. To analyse to effects of immunosuppression (to reduce microglial activity) and enzymatic digestion with Chondroitinase ABC (to break down the CSPG deposits) on transplant cell survival and migration.

The experiments performed were as follows-

1. Non-transplanted neonatal LH retina and adult RCS rat retinal sections were examined for microglial activity (CD68 expression) and the expression of chondroitin sulphate proteoglycans.
2. Müller stem cells were transplanted into neonatal Lister hooded and adult RCS rat retina and their migration assessed.
3. Transplanted retinae from neonate LH and adult RGC rats were investigated for the presence of microglia and deposition of chondroitin sulphate proteoglycans and these features compared with that seen in non-transpanted eyes.
4. Transplants were then repeated in the adult RCS rats which received systemic immunosuppression together with Chondroitinase ABC treatment and the migration and integration of the transplanted cells was assessed compared with that seen in untreated rats.

5.3 Results

5.3.1 Comparison of Müller stem cell migration in the neonate LH and adult RCS rat sub retinal space

Two weeks after transplantation of Müller stem cells into the sub retinal space of neonate (2 days old) Lister Hooded (LH) rats, migration of cells into the inner and outer retinal cell layers was observed. However, relatively few cells migrated and this migration only occurred into the area adjacent to the transplantation site (Fig 5.1A). In contrast, two weeks after transplantation of these cells into the sub retinal space of 4-5 week old dystrophic Royal College of Surgeons (RCS) rats, (4-5 weeks is the age at which the photoreceptor cell layer has been reduced to about half of its normal thickness) cells accumulated at the interface between the outer segment debris zone (DZ) and the retinal pigment epithelium (RPE) and (Fig 5.1B). Cells

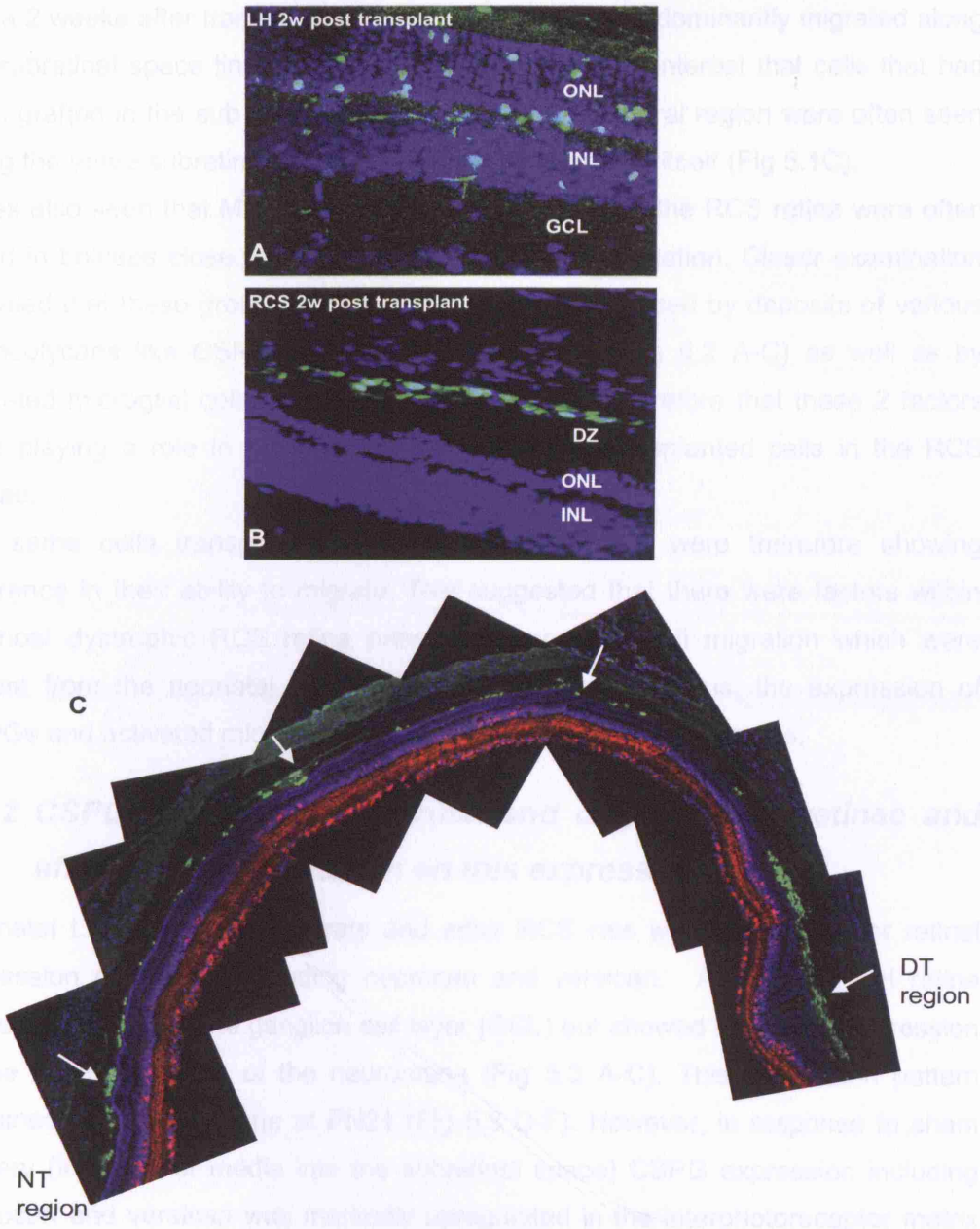

Figure 5.1: Migration of Müller stem cells from the subretinal space of neonatal lister-hooded and dystrophic RCS rats after transplantation.
(A) Migration of Müller stem cells (GFP labelled) into the inner and outer nuclear cell layers (INL and ONL) 2 weeks after transplantation into a 2 day old LH rat. (B) Müller stem cells (GFP labelled) remained in the subretinal space 2 weeks after transplantation into a 5 week old RCS rat. (C) Montage of whole retina to show widespread GFP labelled Müller stem cell migration along the subretinal space 5 weeks after subretinal injection into a 5 week old RCS rat. Red staining indicates reactivity to an antibody against the neural marker HuD. Cell nuclei were stained with DAPI (blue).

rarely migrated into the retina of these animals. Examination of the whole RCS retina 2 weeks after transplantation showed that cells predominantly migrated along the subretinal space lining the DZ (Fig 5.1C). It was of interest that cells that had been grafted in the sub retinal space of the dorso temporal region were often seen along the entire subretinal space, but not within the retina itself (Fig 5.1C).

It was also seen that Müller stem cells transplanted into the RCS retina were often found in boluses close to the site of the initial transplantation. Closer examination revealed that these groups of cells were frequently encased by deposits of various proteoglycans like CSPGs, neurocan and versican (Fig 5.2 A-C) as well as by activated microglial cells (Fig 5.2 D-F). It appeared therefore that these 2 factors were playing a role in preventing migration of the transplanted cells in the RCS retinae.

The same cells transplanted into 2 different models were therefore showing difference in their ability to migrate. This suggested that there were factors within the host dystrophic RCS retina preventing transplant cell migration which were absent from the neonatal lister hooded retina. On this basis, the expression of CSPGs and activated microglia was investigated in these two models.

5.3.2 CSPG expression in normal and degenerating retinae and effect of transplantation on this expression

Neonatal Lister hooded (LH) rats and adult RCS rats were examined for retinal expression of CSPGs including neurocan and versican. At PN2 the LH retina expressed CSPG in the ganglion cell layer (GCL) but showed little to no expression at the ventricular side of the neuroretina (Fig 5.3 A-C). This expression pattern remained almost the same at PN21 (Fig 5.3 D-F). However, in response to sham surgery (injection of media into the subretinal space) CSPG expression including neurocan and versican was markedly upregulated in the interphotoreceptor matrix (IPM) around the outer segements (OS) (Fig 5.3 G-I).

By contrast the 4 week old RCS retina showed strong immunoreactivity to CSPGs including neurocan and versican in the IPM around the OS, even in an unoperated eye. (Fig 5.4 A-C) This expression was similar to the expression seen in the sham

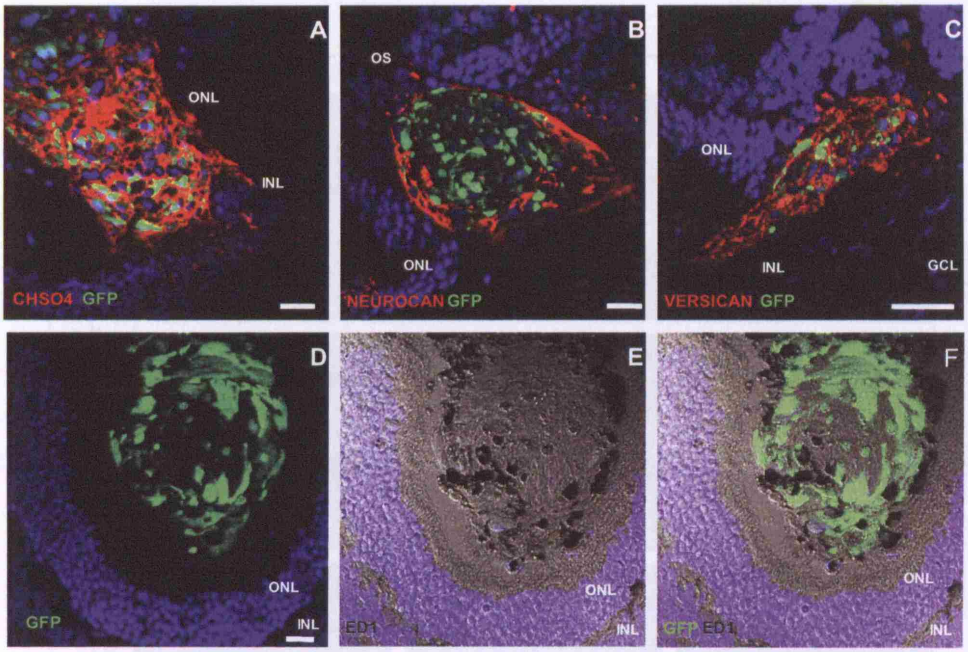

Figure 5.2: Association of transplanted cells with CSPG and microglia in the RCS retina

GFP labelled Müller stem cells transplanted into the 5 week old degenerating RCS retina were often seen in the form of cell boluses as depicted in these micrographs. Immunostaining (seen as red) with antibodies to CSPG n-terminal ($CHSO_4$) (A), neurocan (B), and versican (C) revealed that the green cells were surrounded closely by these matrix proteins. Immunostaining with microglial antibody ED1 revealed that the cell boluses were also encircled by ED1 positive activated microglia seen in black (E,F). D shows the cell bolus in the subretinal space and E&F show the same field with nomarski illumination to highlight the peroxidase staining of ED1 in black. Cell nuclei were stained with DAPI (blue). Scale bar=20µm.

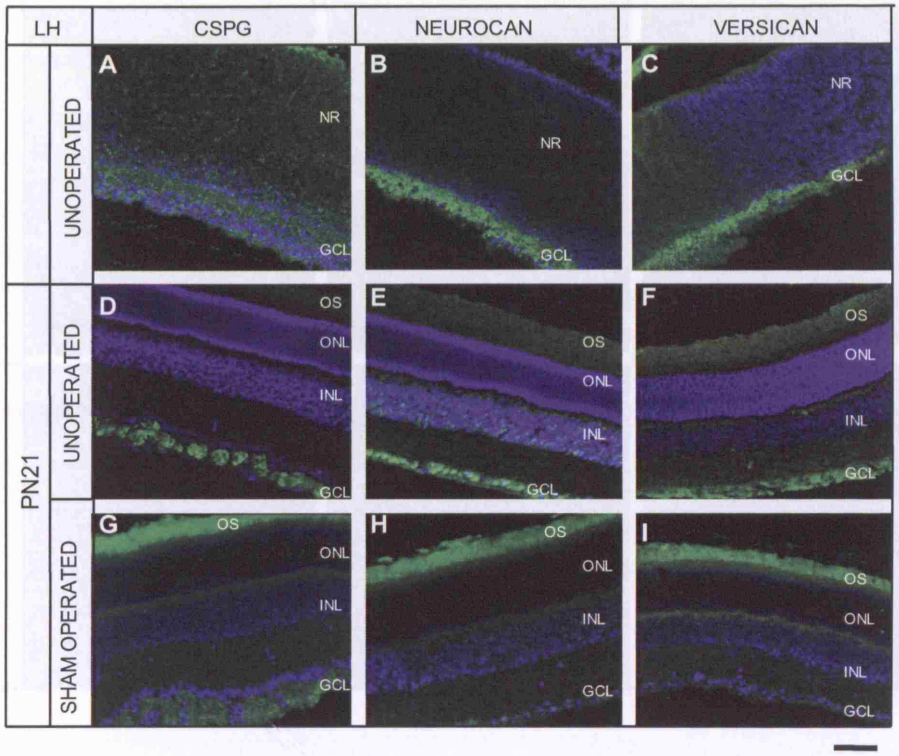

Figure 5.3: CSPG expression in the normal Lister Hooded rat retina
Immunostaining of the neonatal PN2 and adult PN21 Lister Hooded rat retina with antibodies to the CSPGs is demonstrated in these micrographs. In all images the CSPG proteins are identifiable by the green staining. (A-C) The unoperated neonatal PN2 LH retina expresses CSPG, neurocan and versican exclusively in the ganglion cell layer. (D-F) The unoperated adult PN21 LH retina also expresses CSPG, neurocan and versican primarily in the ganglion cells layer, with very low levels of expression in the outer segment (OS) region. (G-I) When the adult LH retina is sham operated, the trauma from the surgery appears to upregulate the expression of CSPG, neurocan and versican in the OS region compared to that seen in the un operated retinae. The cell nuclei are counter stained with DAPI. Scale bar=40μm.

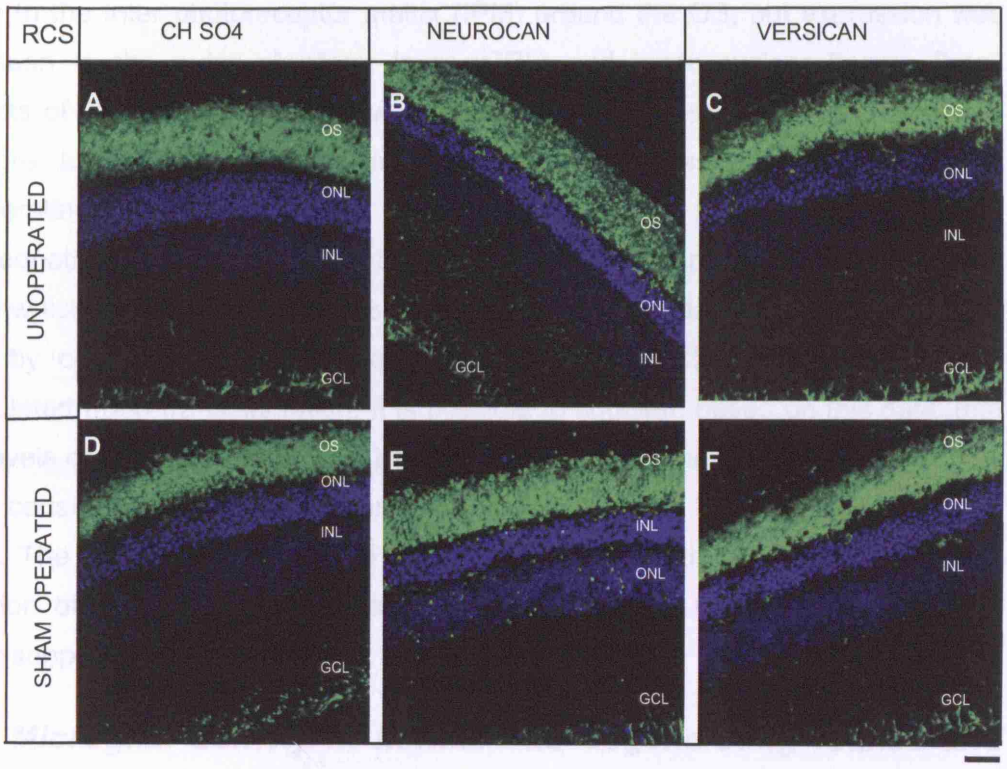

Figure 5.4: CSPG expression in the degenerating RCS retina.
Immunostaining of the 5week old RCS rat retina with antibodies to the CSPGs is demonstrated in these micrographs. In all images the CSPG proteins are identifiable by the green staining. (A-C) The unoperated adult RCS retina shows strong expression of CSPG, neurocan and versican at the region of the outer segments (OS). Some expression of neurocan and versican is also seen in the ganglion cell layer (D-F) The sham operated adult RCS retina also shows similar immunoreactivity for CSPG, neurocan and versican in the outer segment (OS) region with some additional expression in the ganglion cell layer. The cell nuclei are counter stained with DAPI. Scale bar=20μm.

operated eyes 2 weeks post surgery (Fig 5.4 D-F), suggesting that the production of these ECM proteins is already enhanced at the time of surgery.

Upon transplantation of Müller stem cells into the 2 rat models and comparison of CSPG production at 2 weeks post surgery it was found that the dystrophic RCS retinae expressed higher amounts of neurocan and versican than the healthy LH retinae (Fig 5.5). Most of the CSPG expression in the RCS retina was confined as before to the inter photoreceptor matrix (IPM) around the OS, but expression was also seen in the outer plexiform layer (OPL) and inner nuclear layers. Small amounts of CSPG and neurocan were also detected in the GCL. There appeared therefore to be a generalised increase in the expression of CSPG in the degenerating RCS retina.

The neonatal lister hooded retina therefore appears to express very low levels of CSPG which are upregulated to a small extent upon transplantation. The adult RCS retina by contrast appears to express high levels of CSPG which are further upregulated upon transplantation. It is possible to suggest, based on this data, that high levels of CSPG expression in the RCS retina at the time of transplantation may be the cause of the limited migration and bolus formation of transplanted cells in this model. The fact that neonatal and adult Lister hooded retinae, which allow better migration of the Müller stem cells, have lower levels of CSPG production adds further support to this suggestion.

5.3.3 Microglial activity in normal and degenerating retinae and effect of transplantation on this activity

Microglial activity in the normal lister hooded (LH) and degenerating RCS retinae was examined using immunostaining for the CD68 (ED1 antibody), a characteristic marker of rat microglial cells. The results showed a significant difference in ED1 expression of these 2 retinal models. The RCS retina showed high levels of ED1 expression, primarily in the region of the OS even in the un-operated 5 week old RCS retina (Fig 5.6A). Further the ED1 expression in the unoperated RCS retinae was comparable to that seen in the sham operated retinae (Fig 5.6C) The un operated LH retina in comparison showed almost no ED1 expression in the OS at

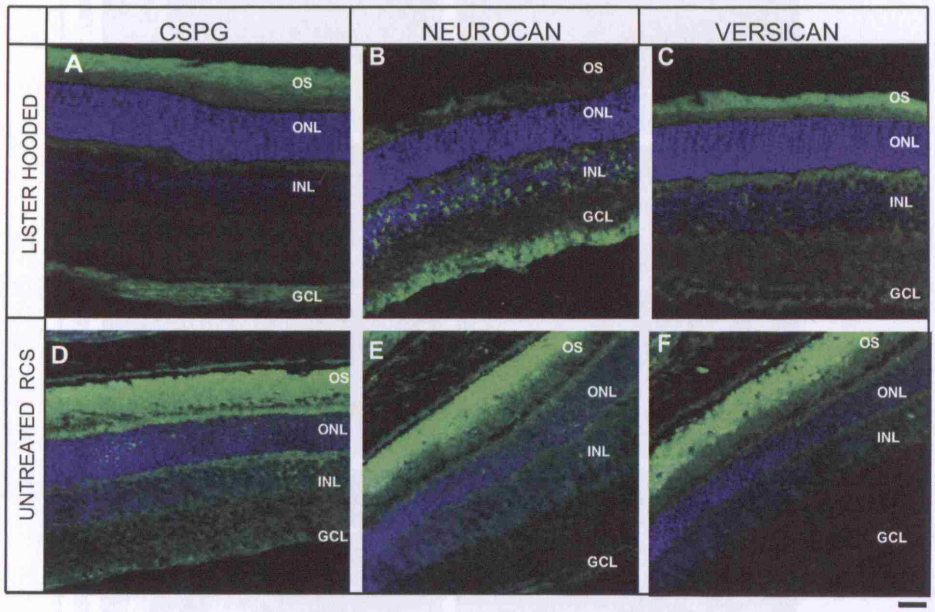

Figure 5.5: CSPG expression in the normal LH and degenerating RCS retina post transplantation.

Immunostaining of the Lister Hooded and RCS rat retina at 2 weeks post transplantation with antibodies to the CSPGs is demonstrated in these micrographs. In all images the CSPG proteins are identifiable by the green staining and the cell nuclei are counter stained with DAPI.

(A-C) The post transplant LH retina expresses CSPG, neurocan and versican in high amounts in the region of the outer segments (OS). The expression of CSPG and neurocan in the ganglion cell layer also appears to be upregulated compared to the untransplanted retinae shown in Fig 4.2. (D-F) The post transplant RCS retina expresses CSPG, neurocan and versican in the outer segment (OS) region, at higher levels than that seen in the untransplanted RCS retina. There also appears to be a generalised increase in the expression of the three matrix proteins through the whole width of the retina as well. Scale bar=20μm.

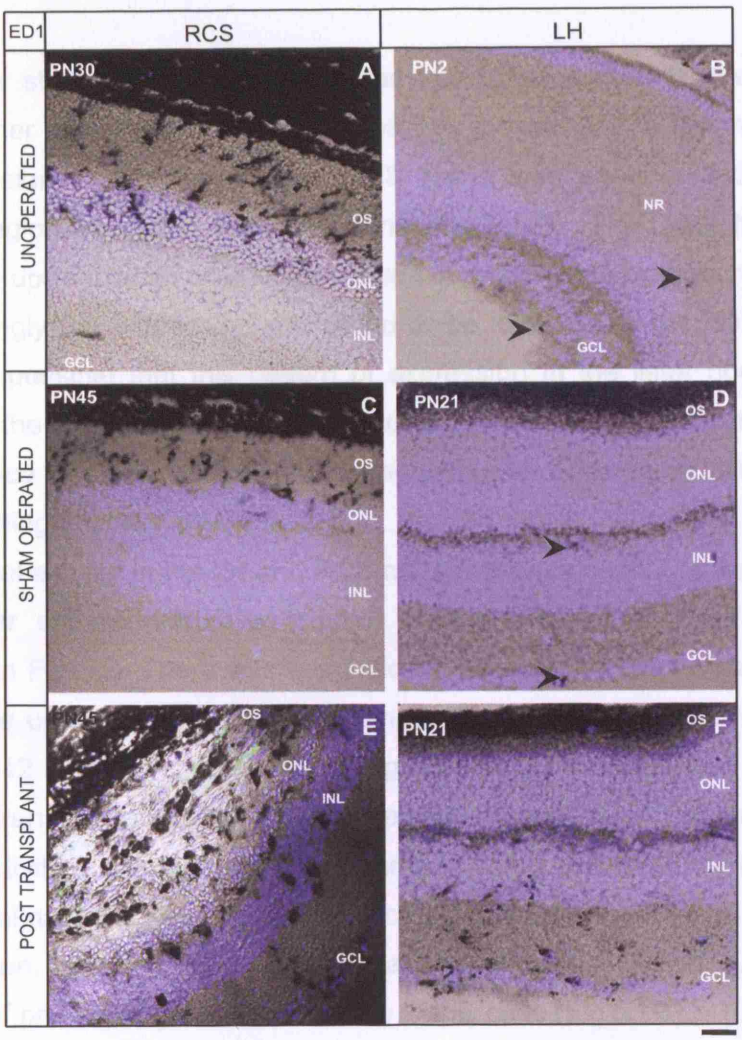

Figure 5.6: Microglial activity in the normal LH and degenerating RCS retina and the effect of transplantation on this activity.
Immunostaining of the Lister Hooded and RCS rat retinae before and after transplantation with antibodies to the microglial marker CD68/ED1 is demonstrated in these micrographs. In all images the microglial activity is identifiable by the peroxidase staining for ED1 in black and the cell nuclei are counter stained with DAPI. All images are under nomarski illumination to enable visualisation of the ED1 staining in black.
(A) The un operated RCS retina shows considerable microglial activity in the region of the outer segments. (B) In contrast the unoperated neonatal LH retina shows only 1-2 ED1 positive cells in the entire field. (C) Following sham surgery the ED1 activity in the OS region of the RCS retina remained comparable to that seen in the unoperated retina. (D) In the LH retina, post sham surgery there was no significant change in micrgolial activity, with only an occasional ED1 positive cells seen. (E) Post transplantation, the RCS retina showed dramatic up regulation of ED1 expression and the microglia were seen throughout the thickness of the retina. (F) Post transplantation in the LH retina ED1 activity is upregulated and seen in the inner plexiform and ganglion cell layers, although not as marked as that seen in the LH rat retina. Scale bar=20µm.

PN2 (Fig 5.6B)and only the occasional ED1 positive cell post sham surgery at PN21 (Fig 5.6D).

When Müller stem cells were transplanted into these 2 models, the RCS retina showed further upregulation of ED1 expression. In response to the transplantation ED1 expression in the transplanted RCS retina was seen in and around the transplant region as well in the inner retina (Fig 5.6E). The Lister hooded retina also showed up regulation of ED1 expression in response to cellular transplantation but interestingly the expression was found to be localised to the inner retina (Fig 5.6F). It is possible that this pattern of expression in the lister hooded rat is a reflection of the distance the transplanted cells are able to migrate within the retina in the absence of pre existing CSPG upregulation and microglial activation before eventually being attacked by them.

The microglial activity in the LH and RCS rat retinae was quantified as a function of microglia per square millimetre (sqmm) of the retina. These are depicted as histograms in Fig 5.7. There was a significant difference in the levels of microglial activity in the un-operated LH retinae compared to the RCS retinae with the latter showing 10-12 fold higher levels of microglial activity by comparison ($p<0.01$) (Fig 5.7A). Post transplantation, there was a dramatic (nearly 20 fold rise) in the levels of microglial activity in the LH retinae compared to the unoperated retinae (Fig 5.7B). The RCS retinae also showed a significant increase in microglial activity post transplantation, although not as dramatic as that seen with the LH eyes, given the high levels of pre existing microglial activity in this case (Fig 5.7C).

5.3.4 Association of microglia with CSPGs in the transplanted retina

Transplanted cells in the RCS retina were found to have a very close spatial relationship with both microglia and CSPGs. Müller stem cells which had failed to migrate away from the SRS post transplantation were found to lie in close proximity with the CD68 positive cells and had a characteristic round morphology (Fig 5.8).

When the transplanted cells which were found in boluses were co stained for microglial and CSPG markers, it was found that there was a close spatial relationship in the expression of these markers in association with the transplanted

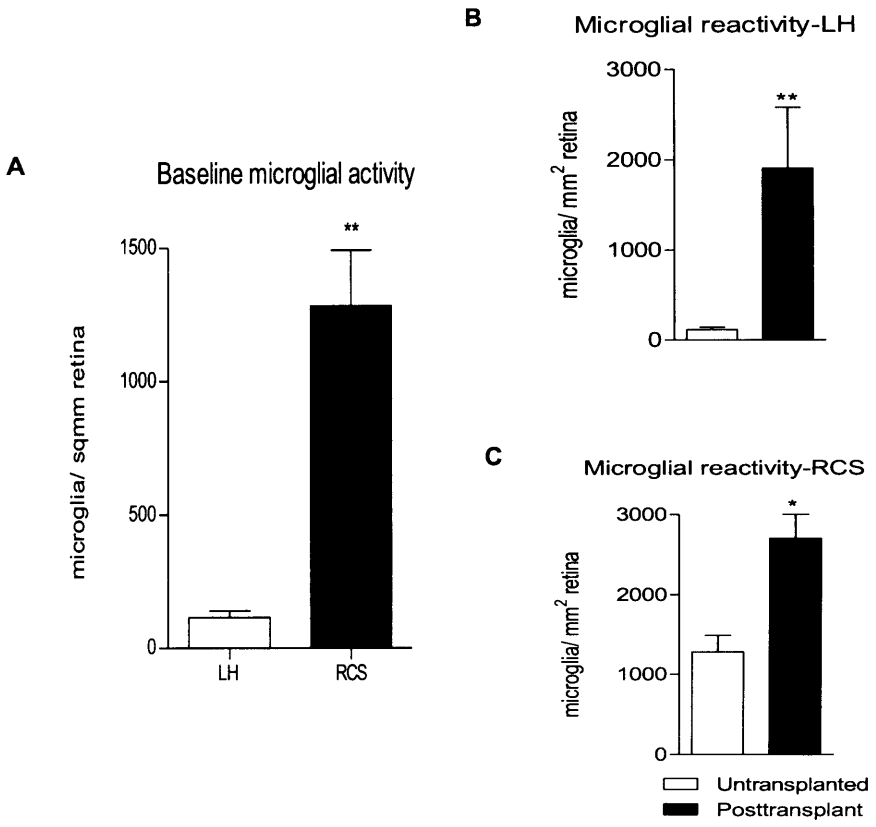

Figure 5.7: Microglial activity in the normal LH and degenerating RCS retina and the effect of transplantation on this activity.
Histograms depicting the relative microglial activity of LH and RCS retinae and the effect of transplantation on this activity. (A) The unoperated neonatal LH retina has almost no microglial activity while the unoperated adult RCS retina has high levels of microglial activity, significantly higher than that seen with the LH retina ($p<0.01$). (B) In the LH retina, post transplantation, there is a significant increase in levels of microglial activity ($p<0.01$) (C) In the RCS retina too, there is a significant increase in microglial activity post transplantation, but the increase is smaller than that seen with the LH retina, given the high levels of pre-existing activity ($p<0.05$).

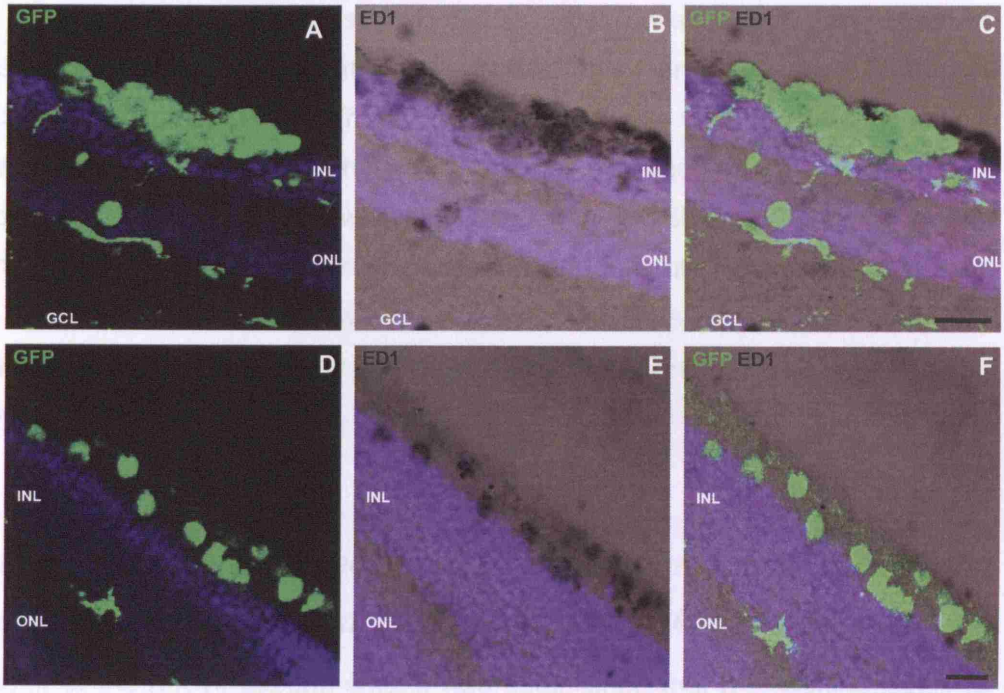

Figure 5.8: Colocalization of microglia with transplanted Müller stem cells in the RCS retina.

Micrographs depicting 2 different transplant fields within an adult RCS retina. Müller stem cells are labelled with GFP and microglia are stained in black with ED1 (A,D) 2 different examples of Müller stem cells in the subretinal space of adult RCS retina. The green GFP labelled Müller stem cells are seen along the subretinal space and have characteristic round morphology. (B,E) The same fields as A and D but without the GFP and with the ED1 labelling in black in the subretinal space. (C,F) Colocalisation of GFP and ED1 staining in the 2 fields, showing the close relationship between the transplanted cells and microglial activity. Scale bar=20µm.

cells (Fig 5.9). Transplanted Müller stem cells which failed to migrate and were confined to the SRS in a cell bolus were frequently found to be surrounded by cells which were positive for CD68 as well as for proteoglycan markers including CSPG (Fig 5.9A), neurocan (Fig 5.9B) and versican (Fig 5.9C). Given that microglia have been shown to produce CSPGs *in vitro* (Uhlin-Hansen & Kolset 1988b) and *in vivo* (Jones et al. 2002b;Jones & Tuszynski 2002b), it is possible that this pattern of expression was as a result of microglial production of proteoglycans. To further corroborate this, retinal sections from 5 week old RCS rats were immunostained for CSPGs and CD68 (Fig 5.10). These preparations showed that microglial activity was mainly localized at the sites where accumulation of CSPGs could be observed. Furthermore microglia observed outside the DZ and infiltrating the ONL co-stained for the N-terminal of CSPGs as well as neurocan and versican, adding strength to the suggestion that microglia may constitute a source of CSPGs in the degenerating RCS rat retina.

5.3.5 Effect of combined CSPG digestion and microglial suppression on the migration of grafted Müller stem cells

As a result of the above experiments, it was established that pre existing levels of high microglial activity and proteoglycan deposits in the degenerating RCS retina were likely to be contributing to the poor survival and migration of the transplanted Müller stem cells in this model. To further characterise the contribution of these 2 factors to inhibition of graft cell migration and integration, the next set of experiments examined the effect of their removal on transplant outcome. Chondroitinase ABC (ChABC) is a bacterial enzyme which digests the proteoglycan moiety of the CSPG and has previously been used to facilitate migration of transplanted cells through the glial scar in the spinal cord. (Massey et al. 2006b). Müller stem cells were transplanted into 5 week old RCS rats together with ChABC to promote degradation of the CSPG matrix. In addition, an enhanced microglial suppression regime was used in these animals, combining oral cyclosporine A, azathioprine and prednisolone with daily intraperitoneal injections of indomethacin for the duration of the experiment. The aim of the experiment was to remove the

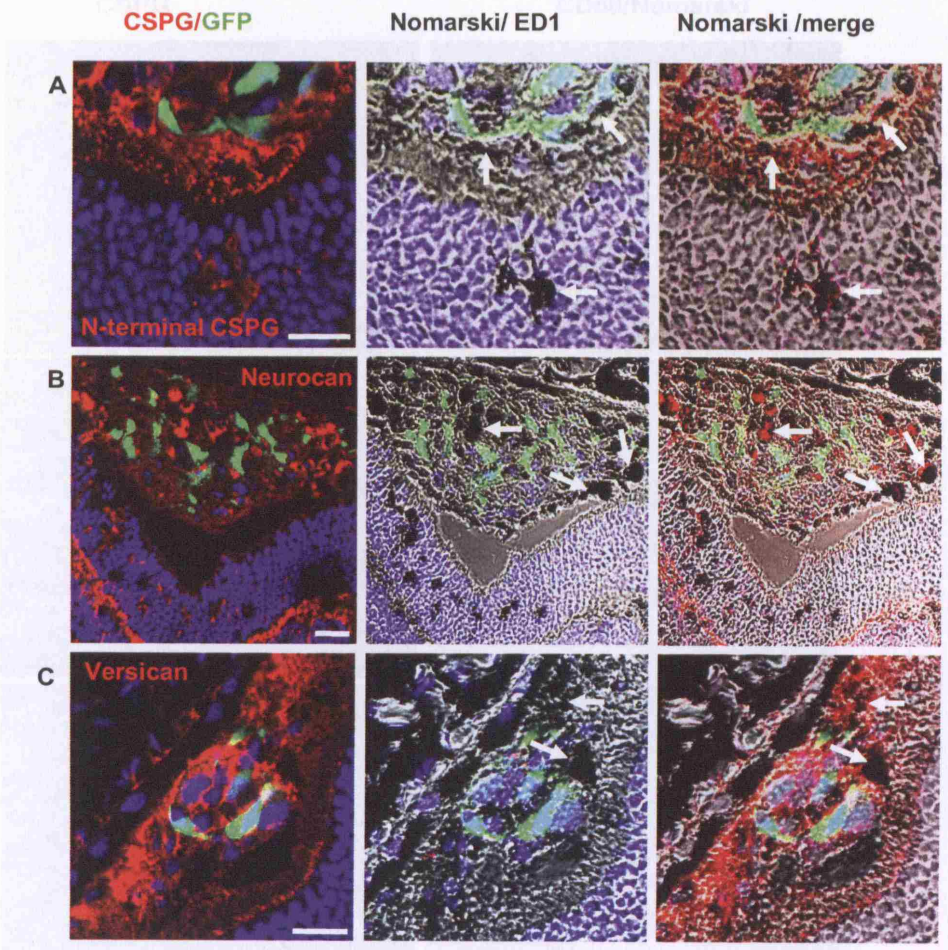

Figure 5.9: Colocalization of microglia and CSPG with transplanted Müller stem cells in the RCS retina.
Micrographs depicting different transplant fields within an adult RCS retina and their close association with CSPG proteins as well as activated microglia. Müller stem cells are labelled with GFP (green), the matrix proteins are labelled in red and microglia are stained in black with ED1. White arrows highlight cells which are positive for both ED1 and the CSPG matrix protein. (A) Micrographs showing CSPG expression around GFP cells, colocalisation of CSPG with ED1 and a merged image with GFP, ED1 and CSPG staining. (B) Micrographs showing neurocan expression around GFP cells, colocalisation of neurocan with ED1 and a merged image with GFP, ED1 and neurocan staining. (C) Micrographs showing versican expression around GFP cells, colocalisation of versican with ED1 and a merged image with GFP, ED1 and versican staining. Scale bar=20µm.

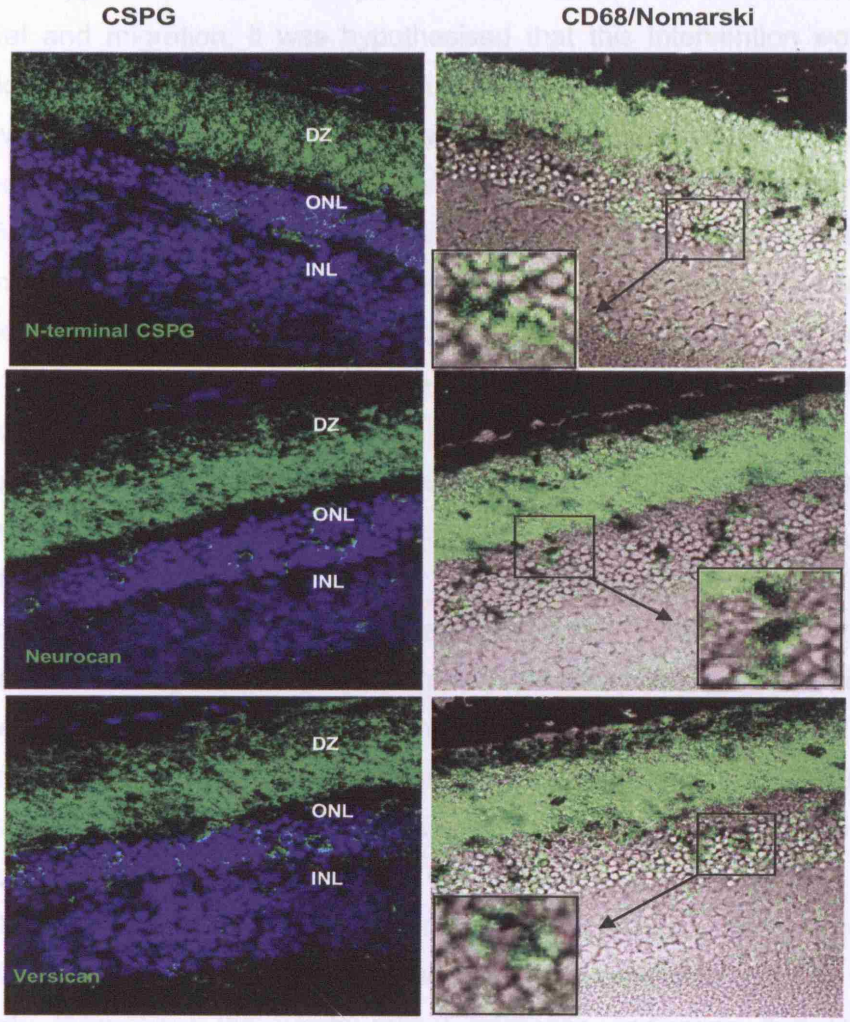

Figure 5.10: Colocalization of microglia and CSPG in the RCS retina.
Micrographs depicting microglial activity in the adult RCS retina and its close association with CSPG proteins The CSPG matrix proteins are labelled in green and microglia are stained in black with ED1. Cell nuclei are counterstained with DAPI in blue.
The images on the left show CSPG, neurocan and versican staining in the adult RCS retina with predominant green staining in the debris zone (DZ) of the outer segments and some staining in the ONL. The images on the right show the same fields but with nomarski illumination to visualise the black staining of ED1. Inset are magnified regions from within the field which show in greater detail the co localisation of ED1 staining in black with the green staining of the various CSPG proteins.

negative influences of microglial activity and CSPG deposition with the use of the immunosuppression and the enzyme. If these factors were crucial to transplant cell survival and migration, it was hypothesised that this intervention would cause a significant improvement in transplant outcome in these two respects.

Two weeks post transplantation we saw a dramatic improvement in the migration of grafted cells through the entire thickness of the retina in eyes treated with ChABC (Fig 5.11A). Many of the migrating cells interestingly bore characteristic neuronal morphology. We quantified this change in migration by counting the total number of grafted cells detected in the retina and classifying them based on their localisation to the subretinal space (SRS) or to the inner retinal layers beyond the ONL. Almost 80% of the cells were found to have migrated into the inner retinal layers when transplanted in conjunction with ChABC. This was in contrast to the control animals where almost all of the cells remained in the subretinal space (t test, n=4, p=0.0011). (Fig 5.12B)

Reduction in CSPG expression in eyes treated with ChABC was confirmed by a decreased staining for CSPG N-terminal, neurocan and versican in the outer segment DZ (Fig 5.11B) when compared with untreated retinae. In addition, to confirm that reduction in CSPG expression was indeed a result of ChABC digestion, we stained untreated and ChABC treated retinal sections with the chondroitin sulphate stub (CS stub) IB5 antibody which detects CS stub epitopes exposed on CSPG molecules by ChABC enzymatic digestion. As seen in (Fig 5.11C) (+ChABC), the ChABC treated retinae showed widespread staining for the stub antibody throughout the whole retinal thickness, indicating that CSPGs were reduced as a result of ChABC digestion. Interestingly, untreated retinae also showed a localized staining for the CS stub epitopes in the outer segment DZ suggesting that some degree of CSPG digestion also occurs during photoreceptor degeneration. Despite the ChABC enzymatic activity, the retinal architecture of treated animals appeared to be well preserved. Further confirmation that absence of CSPGs facilitates migration of the transplanted cells was shown by observations that areas of cell migration did not stain for CSPGs in retina treated with ChABC at the time of transplantation (Fig 5.13).

With the use of enhanced microglial suppression in the ChABC treated animals, in addition to improved migration of grafted cells, we also saw a decrease in the

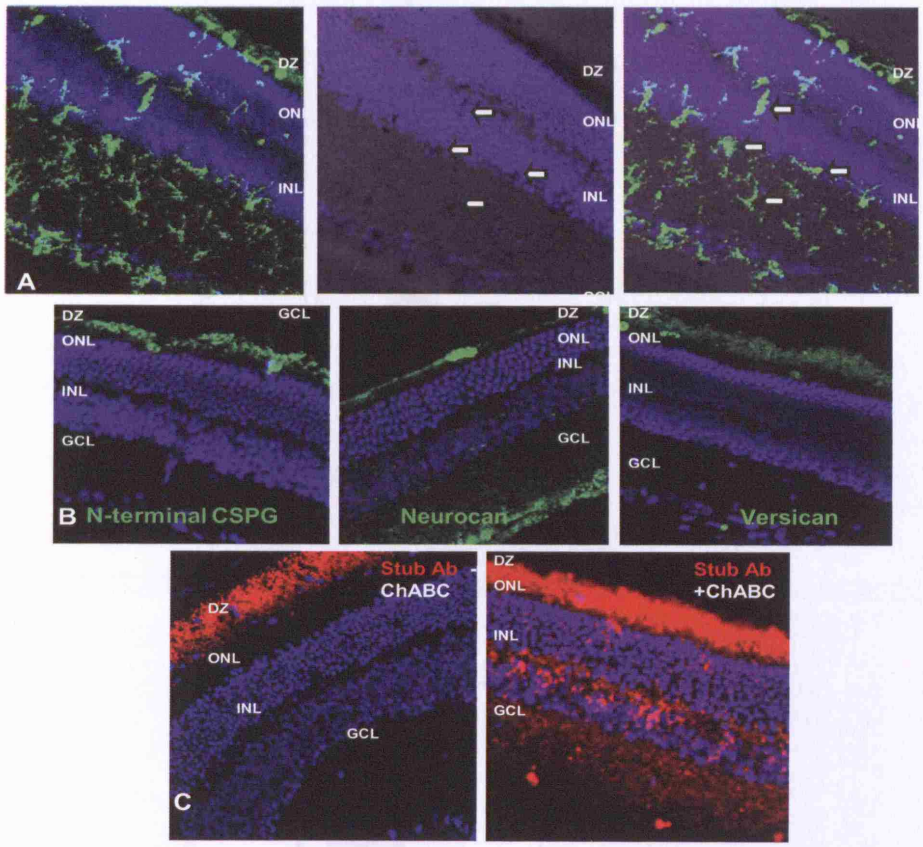

Figure 5.11: Digestion of CSPGs and enhanced microglial suppression facilitates migration of grafted Müller stem cells (A) Micrograph on the left shows a confocal image of a retinal section from a 7 week old RCS rat 2 weeks after Müller stem cell transplantation in the presence of ChABC and enhanced immune suppression for the duration of the experiment. Transplanted cells (GFP labelled) are observed throughout the whole width of the retina. Middle image shows the same retinal section under Nomarski illumination to illustrate retinal infiltration by CD68 positive cells (black) (arrows). Right image shows the same section under Nomarski illumination to illustrate the colocalization of CD68 positive microglia with the migrated cells (GFP labelled) (arrows). (B) Confocal images from retinal sections of a 7 week old RCS rat 2 weeks after injection of ChABC. Sections stained for CSPGs showed a marked reduction in the expression of the N-terminal region of CSPGs, neurocan and versican (green fluorescence). (C) Image on the left shows a retinal section of a 5 week old non transplanted RCS rat staining for the stub epitope. Spontaneous degradation of CSPGs is shown by the red staining. Image on the right shows a retinal section of a 7 week old rat following 2 weeks after subretinal injection of ChABC. Red staining indicates the exposure of the stub epitope upon degradation of CSPGs by this matrix degrading enzyme.

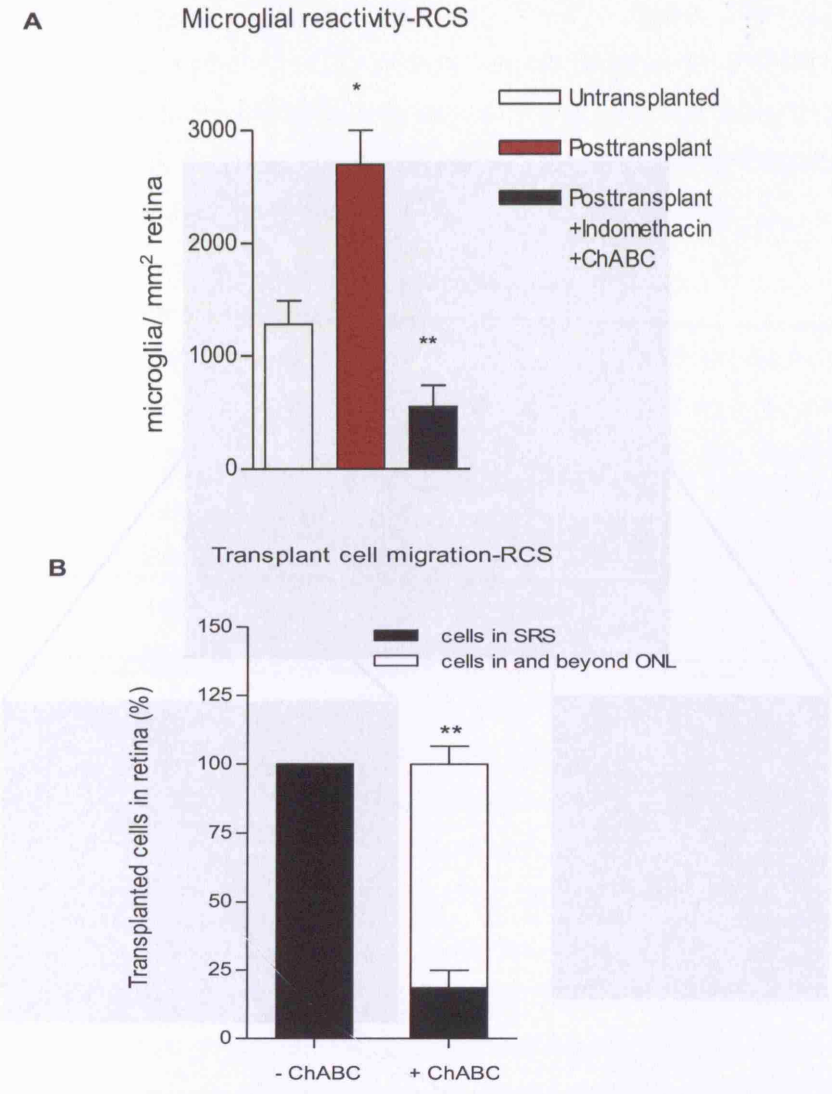

Figure 5.12: Effect of additional immunosuppression and chondroitinase ABC on Müller stem cell migration. (A) Histogram showing marked increase in the number of infiltrating microglia as a result of subretinal injection of Müller stem cells into RCS rats (*p< 0.05v. non-transplanted animals). Enhanced immune suppression induces a significant reduction in the number of infiltrating retinal microglia (**p<0.001v.transplanted animals). (B) Histogram depicting increased migration of Müller stem cells into the inner retinal layers when transplanted with ChABC. No cells were detected beyond the ONL in the control animals (-ChABC) while nearly 80% of cells migrated beyond the INL into the inner retinal layers with ChABC (*p=0.001). Results are the mean ± SE of the mean of four different experiments.

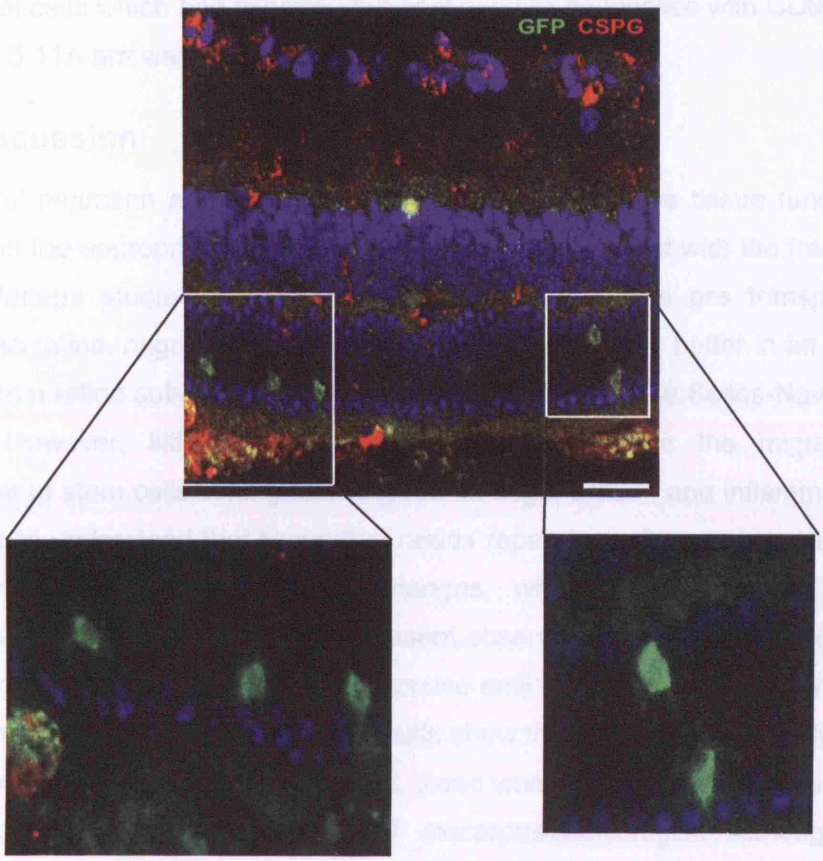

Figure 5.13: Chondroitinase ABC prevents accumulation of CSPGs around transplanted cells. Confocal image of a 7 week old RCS rat retina 2 weeks after transplantation in the presence of ChABC. Staining for the N- terminal of CSPGs (red) shows that cells that had migrated (GFP) were not surrounded by these extracellular matrix proteins. Migratory cells are shown within white squares and magnified. Scale bar=20μm

amount of microglial accumulation (Fig 5.12A). Quantitative analysis showed that the number of microglia within the retina of animals treated with ChABC and enhanced immune suppression, was significantly lower than in animals transplanted without additional immune suppression (Bonferroni $p<0.001$). Despite the reduction in microglial infiltration, however, it was still possible to identify the occasional cells which had migrated but continued to co localise with CD68 positive cells (Fig 5.11A arrows).

5.4 Discussion

Successful migration and integration of stem cells to restore tissue function may depend on the appropriate interaction of the host environment with the transplanted cells. Various studies have shown that when stem cells are transplanted to regenerate retina, migration and integration of grafted cells is better in an immature retina or in a retina subject to acute injury (Chacko et al. 2003a;Selles-Navarro et al. 2001b). However, little consideration has been given to the migration and integration of stem cells in long standing retinal degeneration and inflammation. It is important to understand that tissue that needs repair has often undergone a series of inflammatory and degenerative changes, which may limit the functional integration of grafted stem cells. The present observations confirm previous reports that the neonatal retina provides a permissive environment in which stem cells can migrate and integrate. However, our results show that although grafted Müller stem cells migrated into the neonate LH retina, these were often found in association with cells expressing CD68, a marker of macrophage/microglia. Although recent evidence suggests that microglia not only promote neurotoxicity, but that also have a neuroprotective role and enhance nerve repair (Harada et al. 2002b), it might be possible to speculate that they closely associate with the transplanted cells to promote their migration and survival. However, the present observations that extensive microglial activation was frequently associated with poor migration and survival of Müller stem cells, strongly suggest that microglia may have been responsible for inhibiting cell graft migration and integration.

In accordance with previous studies, considerable microglial activation was seen in the degenerating retina of the dystrophic RCS rat prior to transplantation (de Kozak et al. 1997a;Roque, Imperial, & Caldwell 1996a;Thanos & Richter 1993a). It is

therefore likely that pre-existing activated microglia may constitute a first line of response to retinal stem cell transplantation, as they may be ready to exert their cytotoxic and phagocytic functions(Harada et al. 2002a). Stem cell clusters were often seen in the subretinal space of the RCS rat, densely surrounded by microglia and resembling granuloma-like structures. These clusters were not observed in the neonate LH rat retina, indicating that in the absence of microglia the grafted cells were able to migrate into the retina. It is possible that the xenograft nature of the transplant (human cells to rat retina) further enhanced the microglia response, but allogeneic transplantation of Müller stem cells in the RCS rat retina resulted in similar microglia reactivity. Müller stem cells derived from RCS rat retinae were transfected with GFP and transplanted into adult dystrophic RCS rat retinae sub retinally. It was found that the green cells continued to remain in a bolus at the transplant site and were associated with extensive microglial activation comparable to that seen with human cell transplantation. (Lawrence JM, preliminary unpublished data).

CSPGs are produced during glial scarring in the central nervous system (Morgenstern, Asher, & Fawcett 2002), and their role as inhibitory axon guidance molecules (Inatani et al. 2001a;Jones, Sajed, & Tuszynski 2003a) is well documented. We observed in accordance with other studies that the retina of the dystrophic RCS rat shows heavy accumulation of the N-terminal of chondroitin sulfate proteoglycans (Porrello & LaVail 1986), neurocan (Zhang, Rauch, & Perez 2003) and versican. Our results further demonstrated that microglia, which are known to produce CSPGs *in vitro* (Uhlin-Hansen & Kolset 1988a) and *in vivo* upon spinal cord injury (Jones et al. 2002c;Jones & Tuszynski 2002a), also express the N-terminal fraction of CSPGs, as well as neurocan and versican in the degenerating RCS rat retina. Significantly, co-staining of retinal sections from transplanted RCS rat retinae for CSPGs and CD68 expression, showed that microglia surrounding the grafted cells stained for CSPGs. These observations suggest that one of the mechanisms by which microglia might be inhibiting stem cell migration and integration into the damaged retina is by releasing CSPGs.

Since stem cell migration from the subretinal space into the damaged or injured retina is crucial to retinal repair, we aimed to facilitate cell migration by inhibiting the microglial response in RCS rats using intra-peritoneal indomethacin and a

combination of oral prednisolone, cyclosporine and azathioprine (Lawrence et al. 2007a). Despite a reduction in microglial accumulation in the vicinity of the transplants as a result of this treatment, residual microglial reactivity was still observed in association with the grafted cells. Microglia remained in the DZ, where CSPGs accumulation was observed in the degenerating retina, indicating that microglial suppression alone is not sufficient to promote migration of the grafted cells. The effect of this extensive immunosuppressive regime on the transplanted cells must also be considered. Steroids and anti inflammatory reagents such as those used here are likely to affect signalling not just of the host tissue, but also of the transplanted cells and the exact effect they might have on these cells is unkown. It would be of interest to culture these cells in the presence of the immunosuppressive drugs to better understand the effect of these drugs on Müller cell behaviour and differentiation *in vivo*.

Degradation of CSPGs by chondroitinase has been shown to promote migration of transplanted cells and regenerating axons through glial scars, particularly in the spinal cord (Bradbury et al. 2002;Huang et al. 2006;Kim et al. 2006), and in the retina it has been used to improve lentiviral vector mediated transduction of photoreceptors (Gruter et al. 2005a). Extensive work on the role of CSPG in neuronal plasticity has also revealed that the deposition of this ECM protein is inhibitory to the formation of new neuronal synaptic connections and is a mechanism by which the mature mammalian nervous system protects itself from the formation of aberrant neuronal synapses when injured (Rhodes & Fawcett 2004). In addition, ChABC has been shown to restore synaptic plasticity by breaking down the CSPG-rich perineural nets in the visual cortex of mature rats (Berardi, Pizzorusso, & Maffei 2004b;Pizzorusso et al. 2002a), and more recent research showed that this enzyme caused improved synapse formation of transplanted photoreceptor precursors with host neurones (Suzuki, Akimoto, & Imai 2007). On this basis, the role of ChABC might extend beyond its effect on cell migration by facilitating neurite extension of the transplanted cells, as suggested by the observation that Müller stem cells also adopted a neuronal morphology when grafted in the presence of this enzyme.

The present observations that ChABC in conjunction with oral azathioprine/cyclosporine and intraperitoneal indomethacin, were able to

dramatically improve migration of transplanted Müller stem cells into the retina, strongly indicate that abnormal deposition of extracellular matrix and activation of the innate inflammatory responses constitute major barriers to retinal stem cell transplantation. Development and refinement of approaches to simultaneously modify the extracellular matrix and suppress microglia reactivity may therefore help to overcome the present limitations to achieve integration of stem cells into degenerated retina.

Chapter 6: Development of an *in vivo* model of Retinal Ganglion Cell depletion

6.1 Introduction

6.1.1 Rat glaucoma models

There are several *in vivo* models of glaucoma/ RGC damage being developed and most of the high end glaucoma models aim to increase the intra ocular pressure thereby resulting in ganglion cell death in a manner seen in the patients with glaucoma, the idea being to mimic the pathophysiology of the condition as faithfully as possible. These techniques include the transient ischemia reperfusion injury models (Adachi et al. 1996a;Selles-Navarro et al. 1996c), sclerosis of episcleral veins using hypertonic saline preventing aqueous outflow (Morrison et al. 1997c) and diode laser treatment which works through a dual mechanism causing aqueous outflow obstruction through damage to the episcleral veins as well as scarring of the trabecular meshwork (Levkovitch-Verbin et al. 2002c).

While it would be ideal to use a model of glaucoma that was similar in pathophysiology to the original condition (and it is intended that these models will be used for future work), in order to be able to assess the initial ability of the Müller stem cells to integrate *in vivo* a model that was simply able to provide an environment devoid of RGC was considered sufficient. Further, the development of all of these techniques and the characterisation of the models thereafter can take several months. Given the time constraints of the project, it was essential that a model of RGC depleted retina be developed over a short period of time. On this basis, an NMDA model of RGC death was developed in order to test the biological activity of Müller stem cells differentiated into a RGC phenotype.

6.1.2 NMDA induction of RGC damage

N-methyl D-Aspartate or NMDA is a chemical agonist of NMDA receptors of the glutamate system. The NMDA receptors when stimulated by glutamate are highly calcium permeable and excessive stimulation of these receptors is therefore capable of causing excitotoxic damage in cells that possess these receptors. In the retina, retinal ganglion cells (as discussed in Chapter 3) possess these receptors in

abundance and are particularly vulnerable to NMDA mediated excitotoxic damage (Sucher, Lipton, & Dreyer 1997). Indeed it has now been shown that high intraocular pressure related RGC death is also mediated through the glutamate related excitation, particularly the NMDA receptors (Nucci et al. 2005). Considerable work is currently underway to devise means of protecting the ganglion cells from such damage and form the basis of a large proportion of work in prevention of glaucoma through neuroprotection.

Of greater interest to this work, however, NMDA has been used in the study of glutamate mediated excitoxicity in RGC in various *in vitro* (Calzada et al. 2002) and *in vivo* models. In particular the effect of intravitreal injections in rat eyes has shown that NMDA does causes apoptotic death of cells in the RGC layer as well as of some cells in the inner nuclear layer in a dose dependent manner, an effect that is blocked by NMDA specific antagonists (Lam et al. 1999b). The results from this study also show that such damage can be seen within 7 days of treatment with NMDA and is fairly reproducible. To identify the ability of the grafted cells to repair the damaged RGC, it is also necessary that the damage is largely confined to the RGC as the presence of additional photoreceptor damage would complicate any functional analysis of the transplanted cells. That NMDA causes specific RGC death has however been shown by mRNA studies looking at the expression of Thy1, Neurofilament -light chain (NF-L) and rhodopsin expression in NMDA treated eyes (Chidlow & Osborne 2003). Thy1 and NF-L mark RGC and this work showed that their levels of expression fall dramatically when the eyes are treated with NMDA. The difference in RGC depletion 8 days post NMDA treatment was in fact greater than that seen with the ischemia reperfusion injury model which the authors analysed in parallel. The expression of rhodopsin on the other hand remained almost completely unchanged in all of the groups studied suggesting that NMDA mediated damage was confined to the RGC and did not compromise photoreceptor integrity.

In terms of the mechanism of action, the time required for the induction of RGC death and the actual nature of RGC damage NMDA treatment suited the needs of this work for an *in vivo* model to study the ability of Müller stem cells to replace RGC.

6.1.3 Triamcinolone as an intravitreal anti-inflammatory drug

The ischemia, hypertonic saline injections and the lasers used to generate the chronic hypertension model of glaucoma, also induce considerable microglial activation within the retina in association with the RGC death (Naskar, Wissing, & Thanos 2002a). The role of microglia in preventing transplant cell migration *in vivo* has already been discussed. If an RGC damage model is associated with high microglial activity, it would be a poor model in which to study the potential of stem cell replacement. Any cells transplanted would fail to migrate and integrate. It is therefore essential to identify a means of controlling the microglial activation associated with RGC death in these models. This is important not only for transplant studies but also for clinical translation of this research. Control of microglia is likely to be extremely significant to the outcome when the cells are transplanted into a patient with long standing glaucoma, who is also likely to have extensive microglial activation. To this end the use of anti- inflammatory drugs as an adjuvant therapy to promote cell grafting of transplanted cells needs to be addressed.

Triamcinolone is a synthetic corticosteroid drug that is FDA approved and widely used for various anti inflammatory applications throughout the body. It is used topically for various allergic conditions, for hay fever, intra articularly to reduce inflammation and when inhaled has also been found to have its uses in reducing inflammation in chronic obstructive pulmonary disease (The Lung Health Study Research Group 2000).

In the eye, Triamcinolone has been used intra-vitreally for the treatment of diabetic macular oedema and is found to reduce the oedema and improve vision for short periods of time (Cunningham, Edelman, & Kaushal 2008;Jonas et al. 2004;Jonas, Harder, & Kamppeter 2004). The effect of Triamcinolone on reducing inflammation within the retina is also well documented. In the human eye, it has been found to reduce post operative inflammation after surgeries like pars plana vitrectomy which are characteristically associated with inflammation (Mankowska et al. 2008).

In animal models and particularly in rat models, Triamcinolone has been used for various studies. It has been shown to reduce choroidal neovascularisation in laser treated rat retinae (Ciulla et al. 2001), reduce development of diabetic macular oedema through stabilization of the blood brain barrier (via its effect on

VEGF)(Zhang et al. 2008) and reduce inflammation caused by streptozotocin toxicity when the drug is used to induce diabetes (Kim et al. 2007b). In addition, Triamcinolone has also been found to reduce expression of pro inflammatory genes in the oxygen induced rat retinopathy model (Kim et al. 2007c). In all of the above studies Triamcinolone was used intravitreally.

Based on the extensive evidence in support of Triamcinolone's ability to suppress intra retinal inflammation, it was thought to be a good candidate to attempt control of microglial activation in the RGC damage model. However it is also known that Triamcinolone has the ability to be cytotoxic itself. Retinal cells (RPE and RGC cultures) were found to be dramatically affected by direct contact with Triamcinolone resulting in high levels of cell death (Szurman et al. 2007). The same effect was not seen *in vivo* at similar doses and it is believed that the inner limiting membrane and the vitreous offer some kind of protection from Triamcinolone mediated cytotoxicity of retinal neurons. Others have compared the effects of preservative containing and preservative free formulations to determine if the cause of the cytotoxicity lies in the preservative and have found that even the preservative free formulations retain some degree of cytotoxicity *in vivo* (Shaikh et al. 2006). Recently the effect of Triamcinolone crystals on retinal explants *in vitro* was also studied and doses higher than 1mg/ml affected the a and b waves of the electroretinogram elicited from these explants in a dose dependent manner (Luke et al. 2008). These ERG changes became irreversible at a dose of 20mg/ml at which point ganglion cell death was also detectable.

In contrast when Triamcinolone is used in patients, the short term complications are minimal. About 21% are found to develop transient ocular hypertension and less that 1% develop ocular inflammation (Roth et al. 2008). Therefore while the drug itself seems to be cytotoxic *in vitro*, it appears that its effect *in vivo* is less damaging and has benefits.

In order to use Triamcinolone as an anti inflammatory agent to control microglial activation in the NMDA model of RGC death, it would have to be administered intravitreally together with NMDA into the LH rat eye. While there are several instances of the use of NMDA or Triamcinolone intravitreally in rat eyes individually, there is very little previous work on the use of the two together. Barring a reference to the use of NMDA blockers in studying the effect of triamcinolone mediated

hormone secretion (Brann & Mahesh 1991), literature searches were unable to locate any other previous work where the two chemicals had been injected together into the eye or used in conjunction anywhere else in the body. Based on this knowledge it was therefore important to investigate the use of NMDA and Triamcinolone together, to establish their potential to create a model in which the functional ability of stem cells could be investigated.

6.2 Objectives and experimental plan

While there are several different pre existing models of RGC damage, in this work it was necessary to use a model that could be developed in a short period of time, could reliably deplete RGC from the host retina, and was not associated with extensive microglial activation. The aim of this work was therefore-

1. To investigate the use of NMDA as a reliable means of inducing RGC death in the eyes of 3-4 week old Lister Hooded rats.
2. To study the microglial response associated with NMDA treatment of the LH eyes.
3. To investigate the potential of Triamcinolone acetate (TA) as an intra vitreal anti inflammatory agent to be used in concert with NMDA to produce RGC death without associated microglial activation.

The experiments performed to achieve this were as follows-

1. 3-4 week old Lister hooded rat eyes were treated to intravitreal NMDA and analysed for RGC death and associated retinal microglial activation for up to 2 weeks post treatment.
2. This was followed by treatment of 3-4 week lister hooded rat retina with NMDA and TA. The retinal sections from these eyes were also assessed for RGC death and microglial activity and compared with that of NMDA treatment alone.

Intra vitreal injections of NMDA were used in 3-4 week old wild type lister-hooded rat eyes. Based on the doses used by Lam et al in their 1999 paper (Lam et al. 1999a), 2µl of 40mM NMDA diluted in serum free DMEM was injected intravitreally in each eye. The total dose each eye received therefore was 80nmoles. Detailed methodology of the intravitreal injections can be found in the materials and methods

section. Post injection, the animals were allowed to recover and sacrificed at 1 week for analysis of the level of RGC death we were achieving. The eyes were perfused, fixed in 4% paraformaldehyde (PFA), embedded in OCT medium and cryosectioned for tissue analysis.

In order to administer NMDA and triamcinolone together, both the chemicals were prepared separately and then mixed together (1µl of each) just prior to the intravitreal injection.

NMDA as described before was injected at a dose of 80nmoles per eye in 2 µl of serum free media. To keep constant the total volume of injection, the NMDA was prepared at twice the concentration originally used so as to be able to inject half the volume and achieve the same effect. Therefore 1 µl of 80 µM solution was used per eye.

The Triamcinolone formulation used was the same one used clinically in patients – Triamcinolone Acetonide (TA) (Kenalog) 40mg/ml. However given the toxic nature of the carrier solution, the TA was treated to remove the carrier solution from the final formulation. In order to do this the TA solution was centrifuged to allow the Triamcinolone particles to settle at the bottom of the tube. This allowed for the removal of the carrier containing supernatant. The TA particles were then resuspended and washed thoroughly in 2 changes of sterile saline for injection before being resuspended in the same to achieve a solution 80mg/ml in concentration. 1ul of this solution therefore contained 80ug of TA and given the presumptive rat vitreal volume of about 55-60 µl, the estimated final concentration of TA in the eye is about 1.33mg/ ml similar to the concentration of 1mg/ml usually used in patients clinically (Gao et al. 2004b). 1 µl of this solution was mixed with 1 µl of the 80 µM NMDA and injected as outlined before into the intravitreal space of 3-4wk old lister hooded rat retinae. The animals were followed up at 1 and 2 weeks with tissue histology to assess the level of RGC damage and inflammation being caused by this dual treatment. Four days after injection of the NMDA TA combination, the levels of RGC damage and microglial activity were examined and compared with that seen with NMDA alone.

6.3 Results

6.3.1 Effect of NMDA on the lister-hooded rat retina

Haematoxylin and eosin staining revealed that NMDA treatment resulted in a reduction of the number of cell soma in the ganglion cell layer (GCL) of the retina (Fig 6.1) & (Fig 6.2). Compared to the controls which had 3-4 layers of cells in the GCL, all the treated eyes had a severe reduction of RGC. In some cases there was just a single layer of RGCs and in others even this was incomplete. Immuno-staining of retinal sections for HUD and neurofilament (NFL) proteins showed a similar pattern of RGC depletion (Fig 6.3). There was a dramatic reduction in the number of HUD and NFL positive cells in the GCL layer of the treated retinae at 1wk post treatment. This was clearly observed in flat mounts of control and NMDA treated retinae immunostained with antibody to neurofilament to identify the axons (Fig 6.4). It was seen that the density, thickness and direction of axons was severely affected by NMDA treatment. Compared to the control eyes, there was a dramatic reduction in the thickness and number of axons seen per field in the NMDA treated eyes. It also appeared that with NMDA treatment the orientation of the axons was lost (Fig 6.4). We surmised that NMDA treatment in the lister hooded rat, mimicked results seen previously in rat eyes, and could cause effective RGC death.

6.3.2 Extensive inflammation of the rat retina with NMDA treatment

LH retinae were examined post NMDA treatment for signs of inflammation. Most other glaucoma models are known to be associated with microglial activation in response to the ganglion cell death (Naskar, Wissing, & Thanos 2002b) and it was likely that NMDA would cause a similar reaction in the LH retina. Immunostaining with ED1 and HUD revealed that there was intensive microglial activation present in regions of severe RGC death as well as in those regions where some RGC still persisted (Fig 6.5A &B). Other signs of inflammation were also seen with NMDA treatment. In response to the cell death there appeared to be upregulation of nestin and expression of proliferation marker Ki67 (Fig 6.5C) in the retina. Montages of

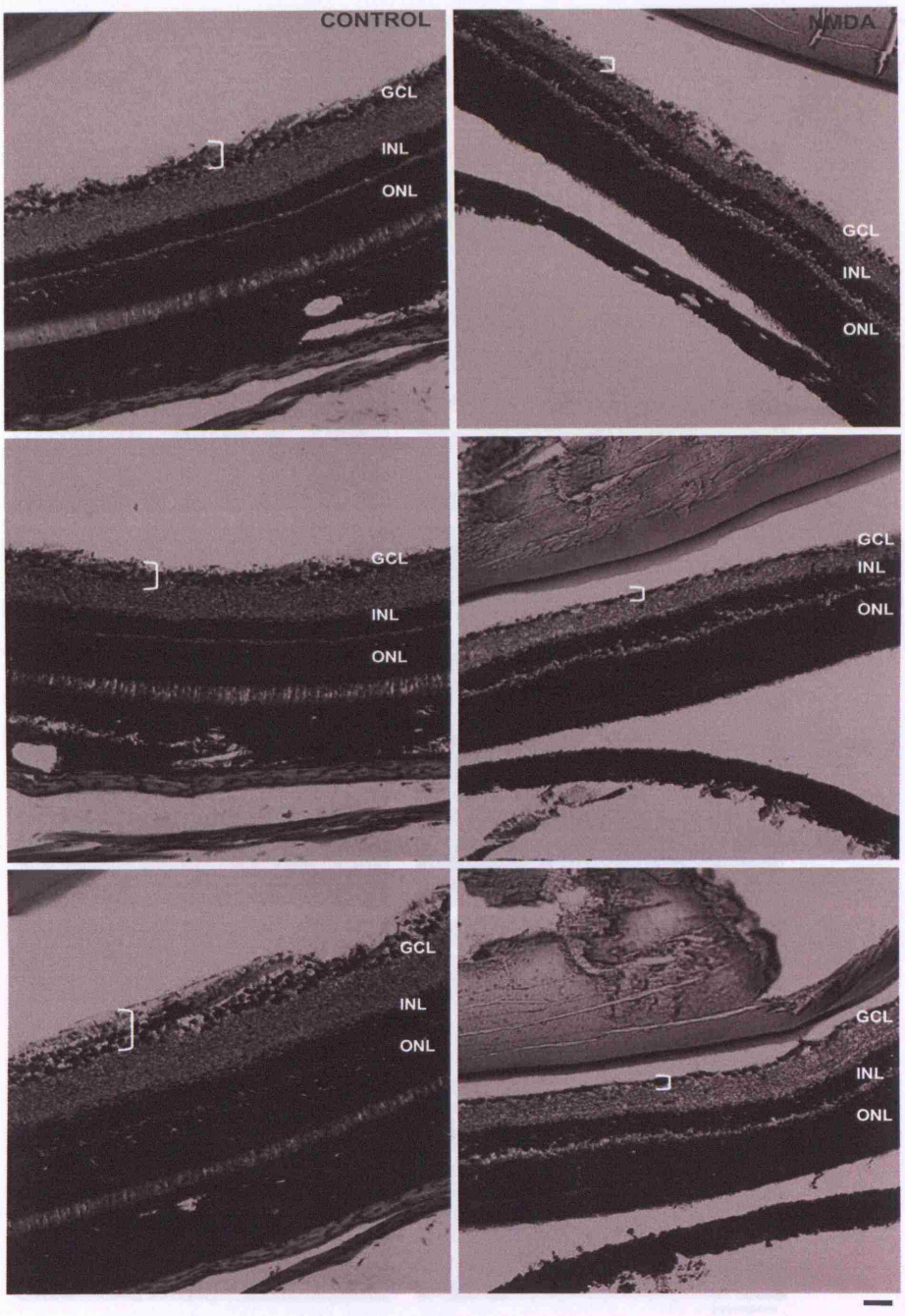

Figure 6.1: Effect of NMDA on the retinal ganglion cell layer of the lister hooded rat retina (A) Comparison of haematoxylin and eosin stained sections of normal lister hooded rat retinae with those treated with NMDA (1 week post treatment). The images show marked reduction in the number of nuclei in the retinal ganglion cell layer of the NMDA treated retinae compared to the control retinae. Examples from three different fields in each case. Scale bar=25μm

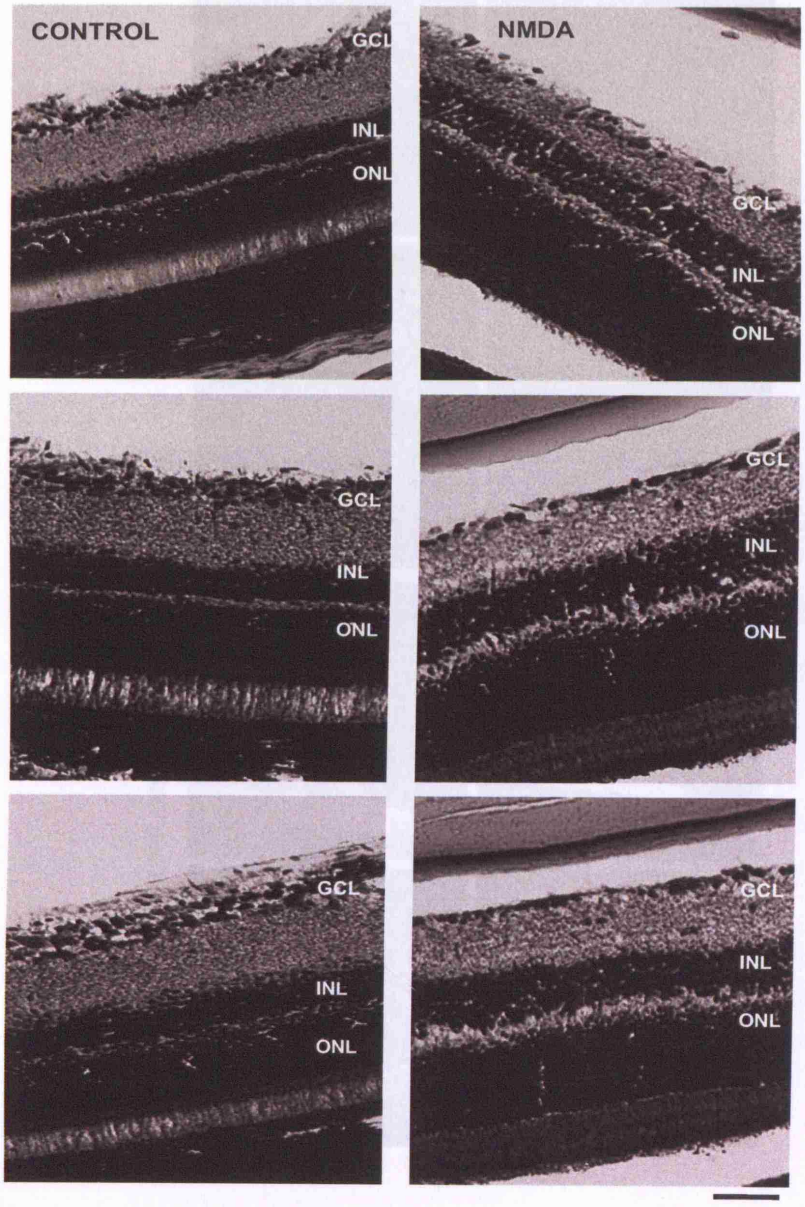

Figure 6.2: Effect of NMDA on the retinal ganglion cell layer of the lister hooded rat retina (A) Images from Figure 5.1 at higher magnification showing in more detail the loss of nuclei in the retinal ganglion cell layer with NMDA treatment. Scale bar=25µm

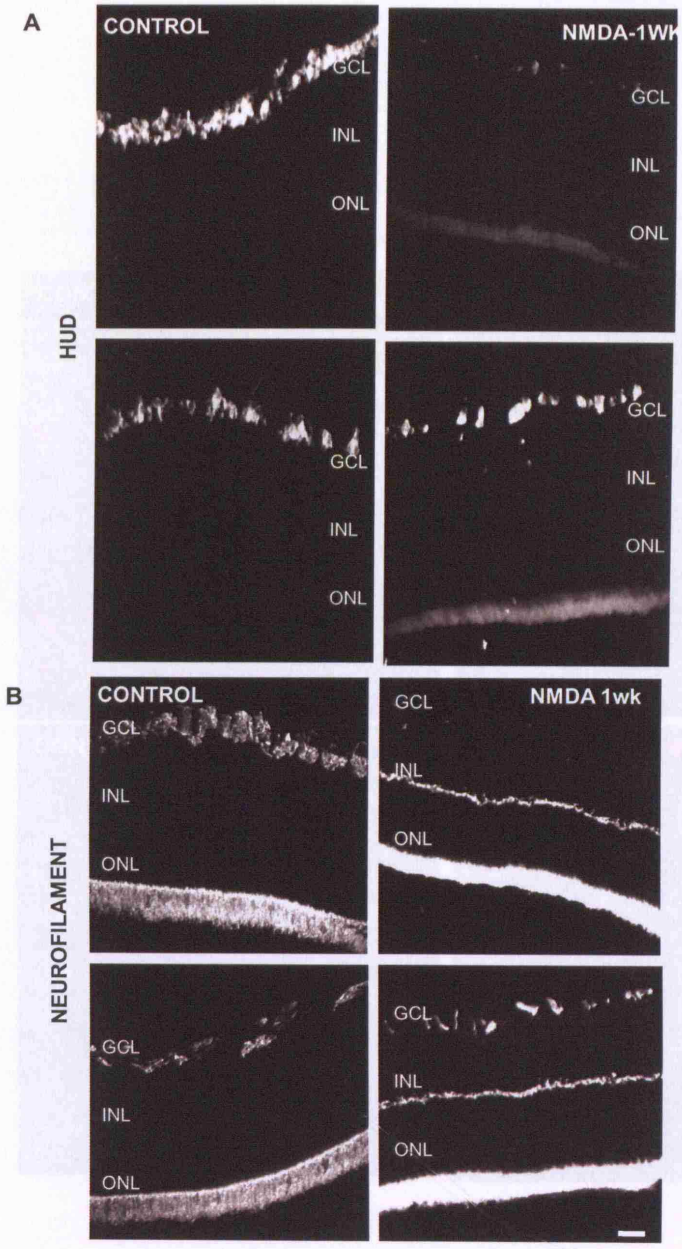

Figure 6.3: Effect of NMDA on the HuD and neurofilament expression in the lister hooded rat retina (A) Comparison of HuD immunostaining of normal and NMDA treated lister hooded rat retinal sections. 2 examples of each are depicted and show that control eyes have significantly higher levels of HuD protein expression in the RGC layer compared to the NMDA treated eyes. (B) Comparison of neurofilament (RT97) immunostaining of normal and NMDA treated lister hooded rat retinal sections. 2 examples of each are depicted and show that neurofilament staining in the nerve fibre layer of the NMDA treated retinae is significantly lower than that seen in the control eyes. Scale bar=20µm

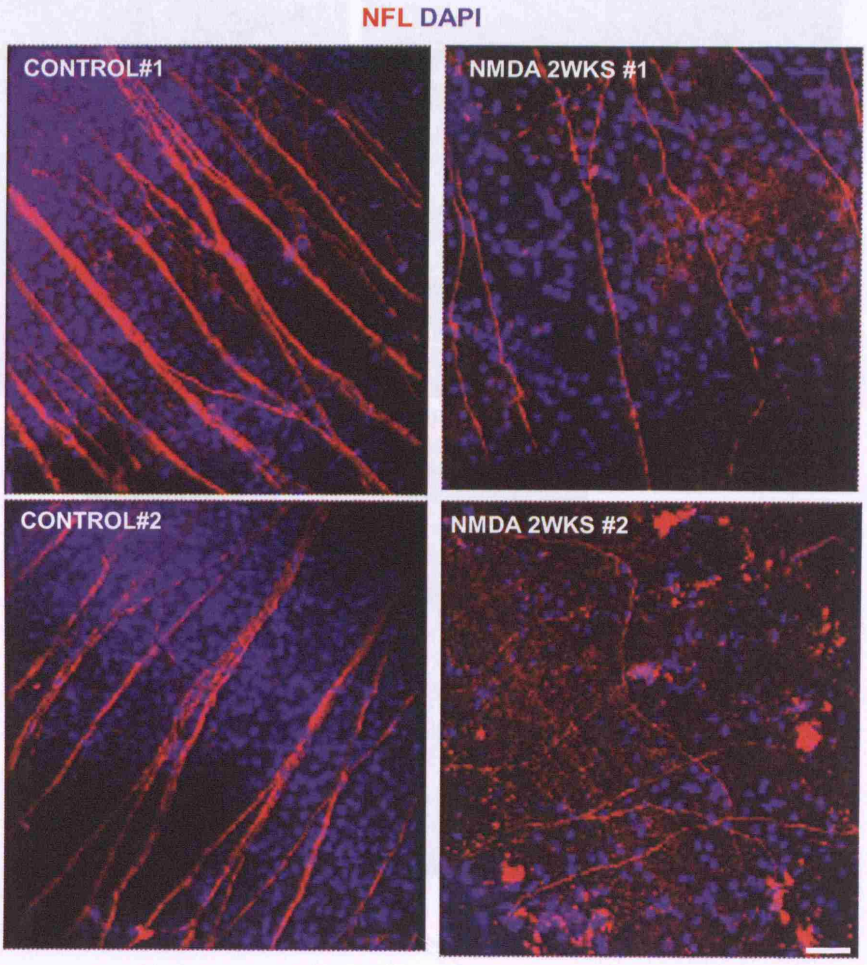

Figure 6.4: Effect of NMDA on the RGC axons in the lister hooded rat retina
Micrographs showing immunostaining of flat mounts of normal control and NMDA treated lister hooded rat retinae 2 weeks after treatment. The retinae are immunostained with neurofilament marker RT97 (NFL) in red and the nuclei are counterstained with DAPI in blue. Control eyes show thick axons staining for NFL lying parallel to each other extending in the same direction. NMDA treated retinae show thin axons staining weakly for NFL. The NMDA treated retinae have fewer thinner axons compared to the control eyes and appear to have lost their orientation. Scale bar=20µm

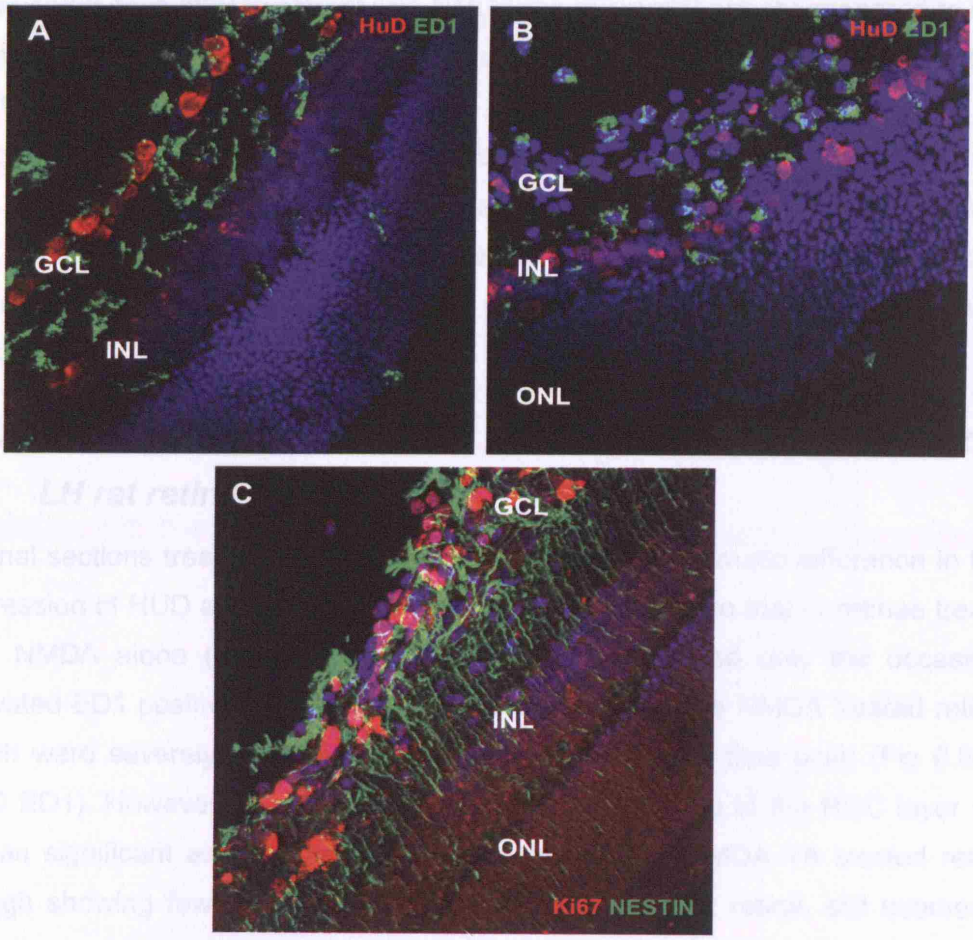

Figure 6.5: NMDA induces microglial activity and inflammation in the LH rat retina
(A,B) Micrographs showing sections of Lister hooded rat retina treated with NMDA and immunostained with HuD (magenta) and ED1 (green) 4 days after treatment. Site of maximal ganglion cell loss with near complete loss of HuD immunostaining in the ganglion cell layer is shown in A.This region shows extensive ED1 stainings as well. B shows a field with some surviving RGC seen staining HuD in red. This field also appears to be extensively invaded with microglia. (C) Evidence of cell proliferation in the NMDA treated retina as seen by staining for Ki67 (Red) along with nestin (green) which is a reactive molecule upregulated during gliosis. Nuclei are counterstained with DAPI. Scale bar=20µm

whole retinae treated with NMDA revealed that there was microglial activation throughout the retina and not just at the site of the injection where maximal RGC depletion was observed (Fig 6.6). This extensive microglial invasion of the entire retina was seen as early as 4 days after NMDA treatment. When the eyes were examined 9 days after treatment with NMDA the microglial activity appeared to have subsided with time. However microglial activity still persisted 9 days after NMDA treatment (Fig 6.7).

It appeared therefore that while NMDA treatment resulted in selective RGC loss, like in other glaucoma models, the cell death itself was causing microglial invasion and thereby rendering the host environment unsuitable for transplantation. Although the microglial activity subsided with time post NMDA treatment, it was still present after 9 days.

6.3.3 Effect of combined NMDA and Triamcinolone treatment on LH rat retina

Retinal sections treated with NMDA and TA revealed a dramatic difference in their expression of HUD and ED1 on immunostaining compared to that of retinae treated with NMDA alone (Fig 6.8). The NMDA TA eyes showed only the occasional activated ED1 positive microglia in the field compared to the NMDA treated retinae which were severely infiltrated with microglia at the same time point (Fig 6.8 D4 HUD ED1). However it was also observed that the damage to the RGC layer was not as significant as that seen with NMDA alone. The NMDA TA treated retina, though showing fewer HUD positive cells than the control retina, still seemed to have a considerable number of them in the GCL. The NMDA only treated eyes at the same time point had lost almost all of their HUD positive cells in GCL. These results led to the speculation that microglia may be enhancing NMDA induced RGC damage and their inhibition may therefore prevent or slow down the RGC death (Baptiste et al. 2005;Roque et al. 1999b).

To further investigate this, an apoptosis assay was employed. The TUNEL assay (**T**erminal deoxynucleotidyl Transferase Biotin-d**U**TP **N**ick **E**nd **L**abeling) was used to identify if there were any apoptotic cells in the NMDA TA eyes. TUNEL is specifically used to identify cells in the early stages of apoptosis, cells that are dying

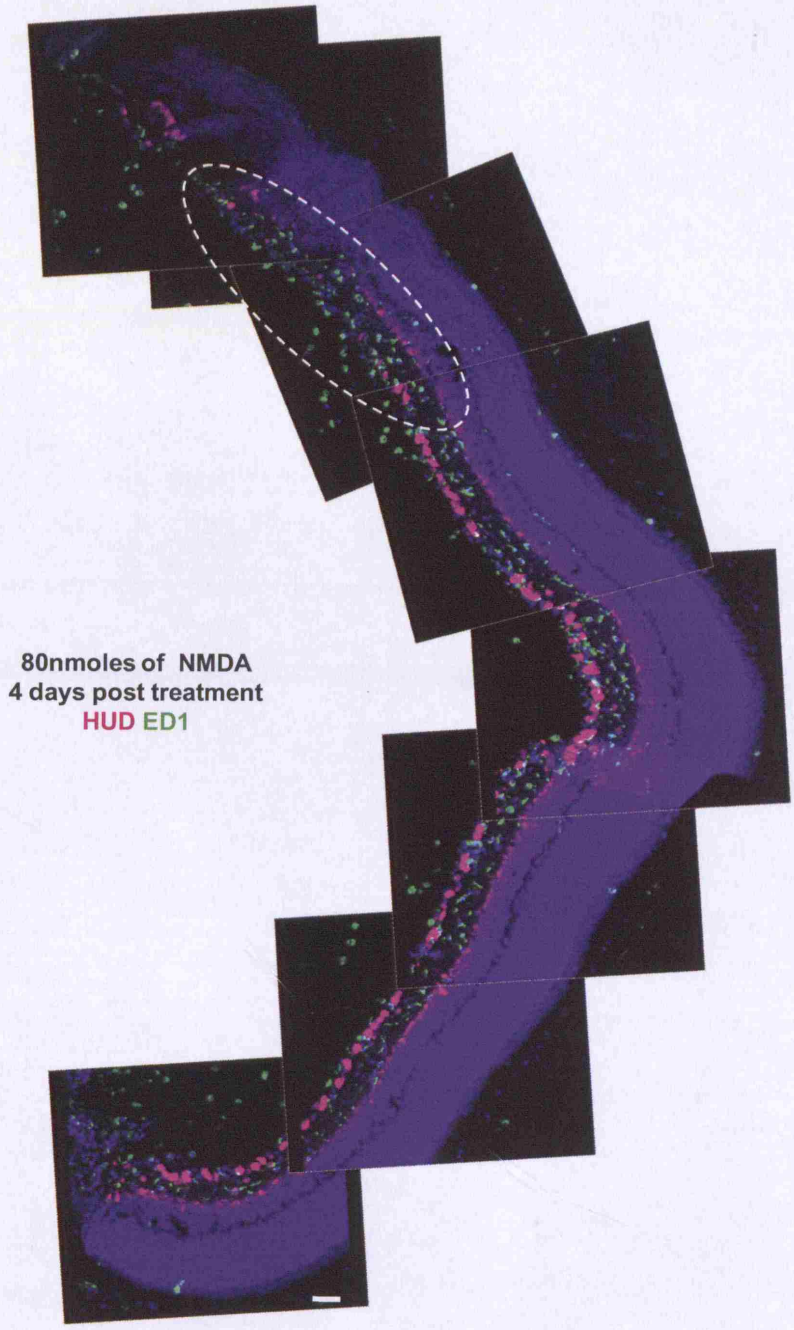

Figure 6.6: NMDA induces microglial activity in the LH rat retina (A) Montage of lister hooded rat retina treated with NMDA. Immunostaining with HuD (magenta) and ED1 (green) 4 days after treatment. Area circled in white shows site of maximal ganglion cell loss as evidenced by near complete loss of HuD immunostaining in the ganglion cell layer. However the ganglion cell layer and inner plexiform layer of the retina through its entire length is infiltrated with ED1 positive microglia. Scale bar=20μm

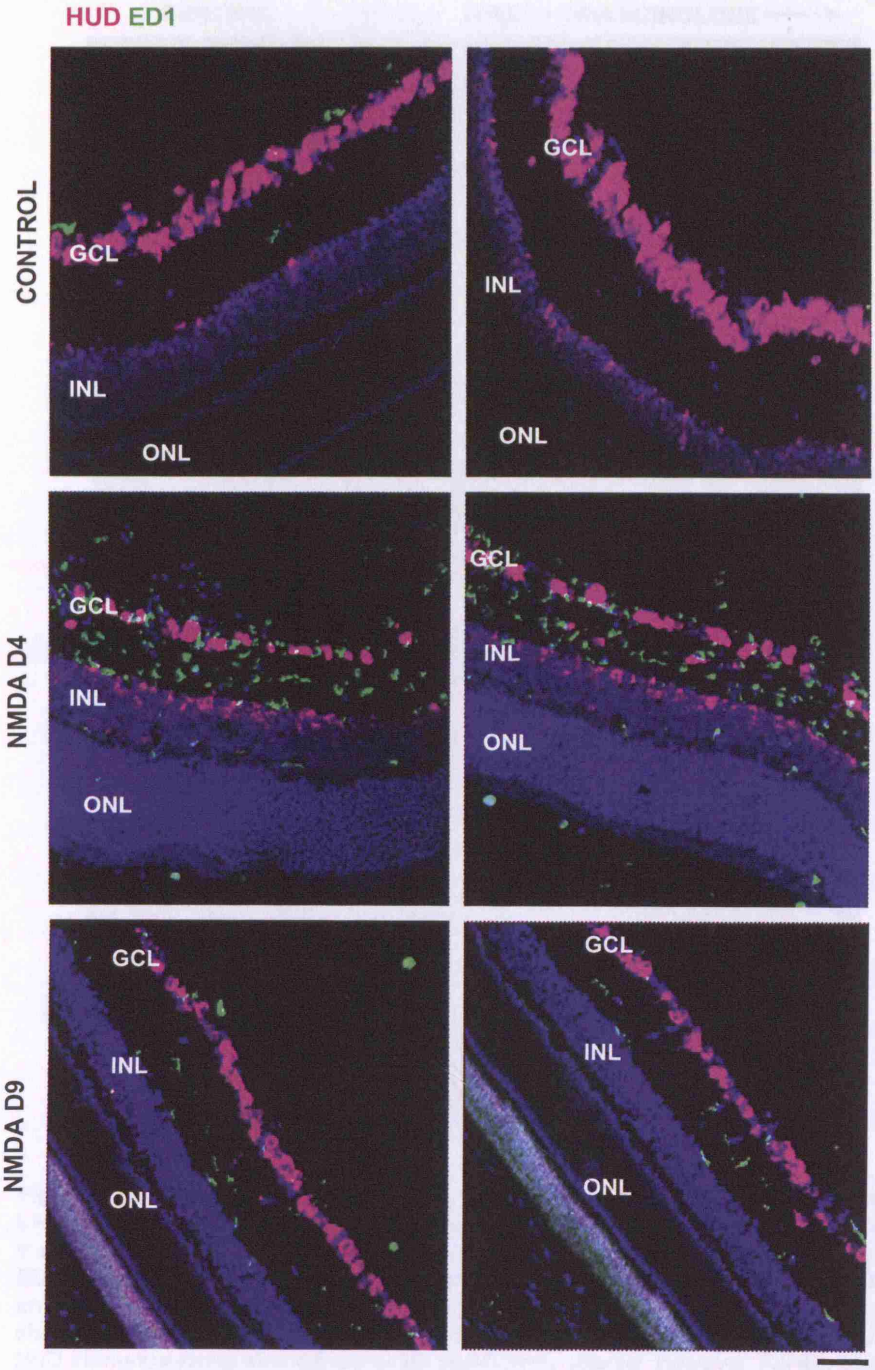

Figure 6.7: NMDA induces microglial activity in the LH rat retina. Lister hooded rat retina treated with NMDA immunostained with HuD(magenta) and ED1 (green) 4 and 9 days after NMDA treatment and compared with normal untreated lister hooded rat retina at the same age. Confocal micrographs show robust HuD staining and no ED1 staining in the control eyes. The NMDA treated eyes 4 days post treatment have high levels of ED1 immunostaining and 9 days post treatment, while the ED1 staining declines compared to the 4 day time point, it still persists. Note that at D4 there is some residual HuD immunostaining in the INL but this is no longer present by D9. Scale bar=20µm

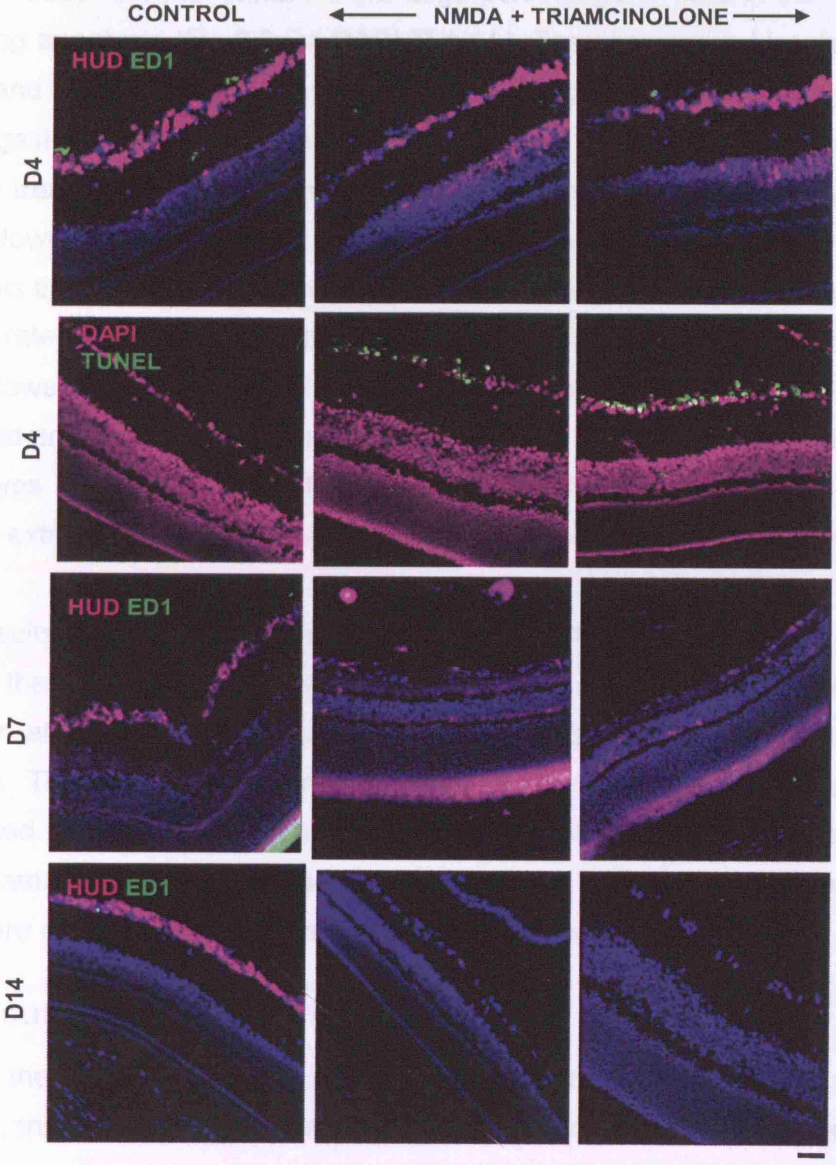

Figure 6.8: Triamcinolone can prevent NMDA induced microglial activity in the LH rat retina Lister hooded rat retinae were given intra vitreal triamcinolone (TA) at the same time as the NMDA injection and immunostained with HuD(magenta) and ED1 (green) 4 and 7 and 14 days after NMDA treatment and compared with normal untreated lister hooded rat retina at the same age. At day 4 the NMDA TA treated eyes showed very little ED1 reactivity (no significant difference compared to control) but the HuD immunostaining also did not seem significantly altered. However TUNEL staining revealed presence of apoptotic cells exclusively in the ganglion cell layer of the NMDA TA treated eyes. At day 7 the HuD staining in the NMDA TA treated eyes had diminished significantly compared to the control, without any significant increase in ED1 reactivity. By day 14 almost no HuD positivity was seen in the ganglion cell layer and ED1 expression continued to be negligible. Scale bar=20μm

but not dead yet. Retinal sections immunostained with the TUNEL kit showed that 4 days after treatment with NMDA TA, a large percentage of cells in the GCL were undergoing apoptosis (Fig 6.8 D4 DAPI TUNEL). The staining was localised to the nucleus and suggested that the apoptosis was occurring specifically in the RGC. This suggested that NMDA was still able to cause RGC death in these eyes. It appeared that TA was not preventing NMDA mediated RGC death but slowing the process down. RGC death had already occurred in the eyes treated with NMDA only by this time point and this fact agreed with the suggestion that with the addition of TA the rate of RGC death brought about by the NMDA was being delayed.

By 1wk however the RGC loss in the NMDA TA treated eyes was found to have progressed and reached levels that were comparable to that seen in the NMDA only treated eyes (Fig 6.8 D7). The levels of microglial activity on the other hand still remained extremely low. The same was also seen 2 weeks post treatment (Fig 6.8 D14).

These results showed that Triamcinolone was able to suppress the inflammatory response that was being generated by NMDA yet at the same time allowing RGC death, for at least 2 weeks post treatment, this being the longest time point examined. This meant that during the time frame when the cells were to be transplanted into the NMDA treated eyes, TA was able to keep under control the retinal inflammatory response, and would perhaps be able to offer the transplanted cells a more conducive environment to migrate and integrate in.

6.4 Discussion

Amongst the several different rodent models currently used in the study of glaucoma, this work chose to look at the usefulness of NMDA as one such model. Most glaucoma models use generation of chronic hypertension as a means of developing glaucoma (Adachi et al. 1996b;Levkovitch-Verbin et al. 2002b;Morrison et al. 1997b;Selles-Navarro et al. 1996b). These models are pathophysiologically close to glaucoma but although the rise in pressure in some of them can occur as early as 1-2 weeks after treatment, when establishing the model afresh standardisation and validation can take several weeks to a few months. They are also associated with considerable microglial activity as a result of the ganglion cell death (Naskar, Wissing, & Thanos 2002c).

In this work, NMDA was used to cause rapid onset of RGC death in 3-4 week old lister hooded rat eyes. It was found that NMDA could be used to induce RGC death in LH eyes within 1 week of treatment and Müller stem cells could subsequently be transplanted into these at this time point and analysed for their ability to replace the damaged RGC thereafter. While effective RGC death was achieved by 1 week, this was also associated with extensive microglial infiltration which lasted even longer as seen with the other RGC models. Considering that the cells were to be transplanted into the eyes 7 days after NMDA treatment, it was likely that transplantation at this stage would mean that the cells were being placed in an environment already primed with microglial activity and therefore hostile for cell migration and integration. It was also crucial that any residual NMDA activity in the eye did not adversely affect the transplanted Müller stem cells. While no direct studies were performed to analyse the effect of NMDA on Müller stem cells in culture, preliminary work showed that Müller stem cell survival 1-2 weeks *in vivo* was comparable to that seen in eyes untreated with NMDA. A more detailed study of the effect of NMDA on the transplanted cells will be essential in the future to ensure that NMDA does not have an effect on transplanted Müller cell survival and differentiation.

Triamcinolone has been used in the past as an intravitreal anti inflammatory agent for various clinical applications (Kim et al. 2007a;Mankowska, Rejdak, Oleszczuk, Kiczynska, Lekawa, Choragiewicz, & Zagorski 2008). In this case it was necessary to use an intra vitreal anti inflammatory agent that could work in co ordination with NMDA to cause retinal ganglion cell death and at the same time control the microglial activation caused by the RGC death. Independently it is known that NMDA can cause selective retinal damage and Triamcinolone suppresses retinal immunity, but it was also important to consider that Triamcinolone alone could cause a rise in the intraocular pressure (Jaissle, Szurman, & Bartz-Schmidt 2004;Konstantopoulos et al. 2006). It was possible therefore that the use of Triamcinolone and NMDA together could result in retinal morbidity more advanced than that achieved with NMDA alone. On the other hand it was also possible that Triamcinolone's anti inflammatory properties could interfere with NMDA mediated RGC death. There is some previous evidence to suggest that steroids might have a protective effect on neurons. Corticosterone (and not triamcinolone specifically) was found to have the ability to inhibit NMDA receptor currents in adult cultured

hippocampal neurons (Liu et al. 2007) and it was possible that Triamcinolone could exert the same protective effect on the RGC *in vivo*. The levels of corticosterone used in the study however were stress levels and much lower than the dose that would be used in this study. In addition the protective effect demonstrated by Liu et al was directed at existing NMDA activity in the hippocampal neurons. At the toxic doses of NMDA being used in the experiments in this study, it was unlikely that the protective effect would be sufficient to prevent RGC damage. It was therefore with limited previous work to use as guidelines, that NMDA and Triamcinolone were applied together in the lister hooded rat eyes to see if it was possible to achieve RGC death without excessive microglial activation.

When NMDA was injected with Triamcinolone into the eye intravitreally, there was a dramatic reduction in the microglial activity seen in the retina compared to that seen with NMDA treatment alone. The suppression of microglial activity was long lasting and was seen to be effective up to 2 weeks post injection. Triamcinolone was found to interfere with NMDA mediated cell death of RGC in the initial stages of the treatment. It is well established that microglial activity is able to produce factors and chemokines that induce retinal neuronal death (Roque et al. 1999a;Srinivasan et al. 2004;Zeng et al. 2005). It has also been shown before that control of microglial activation can offer some degree of neuroprotection to the RGC in the axotomised retina (Baptiste, Powell, Jollimore, Hamilton, Levatte, Archibald, Chauhan, Robertson, & Kelly 2005). It is therefore possible that the delay in NMDA induced RGC death when used in conjunction with TA was a function of some neuroprotection offered by TA mediatetd inhibition of the microglia. However, by one week post injection the level of RGC death caused by NMDA without and with Triamcinolone was comparable.

These results suggest that NMDA along with Triamcinolone may be used to cause rapid retinal ganglion cell death in rodent eyes without the associated microglial activity normally seen with cell death in the retina.This offers a valuable model for transplant studies whereby the transplanted cells may be placed in an environment devoid of RGC and yet at the same time conducive to transplant cell migration and integration. Remarkably it appears that TA is able to achieve this level of microglial suppression without the help of any additional systemic immunosuppression. If therefore used in conjunction with some systemic immunosuppression, it is likely

that the retinal immune response could be effectively controlled, thereby giving the transplanted cells a good chance of survival and integration *in vivo.*Triamcinolone is already a drug approved for use clinically and for intra vitreal injections. It may therefore by extremely useful for application in the future when retinal stem cell transplantation therapy reaches the stage where it is ready to be taken to the clinic.

Chapter 7: Histological and functional assessment of differentiated Müller stem cell transplantation into an experimental model of retinal ganglion cell depletion

7.1 Introduction

7.1.1 Stem cell therapy in Glaucoma

The current mainstay of glaucoma treatment is ocular hypotensive therapy, although neuroprotection has more recently gained popularity as a possible therapeutic option. Replacement therapy for RGC disease has largely been considered a secondary and rather unlikely modality of treatment (Lebrun-Juleien & DiPolo 2008). The limited research in this field is a result of the considerable challenge presented by the task of achieving formation of extensive synaptic connections between the transplanted cells and the host retina and brain necessary to restore lost RGC function (Bull & Martin 2007a). However attempts have been made to use stem cells to replace dead or damaged RGC and these have produced mixed results (Quigley & Iglesia 2003).

Neural stem cells injected into mouse eyes depleted of RGC have shown that damage to the RGC layer promotes integration of transplanted neural stem cells into the ganglion cell layer but does not promote differentiation of these cells towards an RGC fate (Mellough et al. 2004). Embryonic stem cells differentiated into eye-like structures have also been transplanted into NMDA treated eyes (Aoki et al. 2008b), and results from this study showed structural integration of transplanted cells into the RGC layer with expression of RGC specific markers by the integrated cells. However no functional restoration could be demonstrated in these experiments. Adult hippocampal progenitors co-cultured with embryonic retinal explants (to promote retinal neuronal differentiation) and transplanted into RGC depleted retina were shown to integrate into the ganglion cell layer and express RGC marker to greater degree compared to cells which had not been co-cultured with retinal explants (Mellough, Cui, & Harvey 2007). However, no functional studies were performed in this model.

Human umbilical cord blood mesenchymal stem cells transplanted into rat retina depleted of RGC with optic nerve transection showed very little migration or integration into the host retina (Hill et al. 2008b). While human cells were able to survive in the rat retina for up to 3 weeks, they failed to differentiate *in vivo* into

retinal ganglion cells. Human Müller stem cells have also been previously transplanted into a rat models of RGC disease in which damage to these cells was caused by increase in intra-ocular pressure as a result of laser damage to the trabecular meshwork (Bull, Limb, & Martin 2008a). Using this model, transplanted cells survived for 2-3 weeks *in vivo* but their integration was precluded by severe microglial activation. These transplants were performed under conditions of host immunosuppression and suggest that xenograft survival is possible with immunosuppression.

The stage of differentiation of the transplanted cells has been shown to influence the functional success of transplantation (MacLaren et al. 2006a). This suggests that in order to achieve functional integration *in vivo*, it might be necessary to differentiate stem cells *in vitro* into specified neural types prior to transplantation.

It was hoped therefore that using human Müller stem cells differentiated towards an RGC precursor fate, it might be possible to achieve considerable integration and consequently functional restoration in an RGC depleted retina. The human Müller stem cells despite being xenografts, would meet the requirement of being differentiated *in vitro* prior to the transplantation. In addition the use of oral immunosuppression and intravitreal Triamcinolone would be expected to overcome any immune and inflammatory reaction that might be detrimental to the transplant.

7.1.2 Assessment of RGC function by electroretinograms

In developing cell based therapies, achieving successful migration and integration of transplanted cells should be accompanied by restoration of neural function. Restoration of lost RGC function would be the crucial evidence representing success of stem cell transplantation.

In the retina, visual function can be assessed in many ways. In patients this usually involves measurements of visual acuity which are highly reliable. In animal models, particularly in rodents, measurement of visual acuity is less accurate but still a good tool when such visual outcome is being investigated. However in assessing RGC disease, the functional outcome cannot be measured accurately by visual acuity because it does not specifically represent RGC function. In patients this is examined by visual field assessment when visual acuity is intact but electrophysiological means are necessary when visual acuity is poor. In rodents measurement of retinal

ganglion cell function is even more challenging. Only in the last 3-4 years has the use of electrophysiology to study RGC function come into prominence and some of this work is outlined below.

When the retina is stimulated with light, there occurs a mass change in its electrical potential as a result of the stimulation of the photoreceptors and the consequent transmission of neural electrical signals through the retinal neurons. This change in retinal electrical potential in response to light stimulation can be measured using a corneal electrode and plotted as a change in voltage with time. This is referred to as an electroretinogram (ERG) and is used as a reliable measure of retinal function. Since the change in potential is a mass phenomenon, in order to study the function of specific retinal neurons, their individual contributions to the ERG need to be delineated (*http://webvision.med.utah.edu/ClinicalERG.html*).

While extensive research into this field has revealed the specific contributions of some retinal neurons to the ERG, the exact role of others still remains elusive. For example, it is well known that the photoreceptors contribute to the 'a' wave (Robson et al. 2003) and that the 'b' wave arises from retinal neurons post synaptic to the photoreceptors, including bipolar and Müller cells (Stockton & Slaughter 1989;Tian & Slaughter 1995;Wurziger, Lichtenberger, & Hanitzsch 2001). However, the contribution of the retinal ganglion cells to the ERG is less well- defined. A recent study outlined the role of retinal ganglion cells in a rat electroretinogram and indicates that the scotopic threshold response (STR) is almost exclusively a result of intact retinal ganglion cell function (Bui & Fortune 2004d). The scotopic threshold response is a small slow negative potential that materializes in response to very weak light stimuli in a dark adapted eye (Saszik, Robson, & Frishman 2002). This negative potential (nSTR) saturates rapidly with increasing light intensity. It can be preceded by a small slow positive potential (pSTR) which also saturates rapidly with increasing light and is replaced by the b wave as the stimulating light gets brighter.

Since the initial work by Bui & Fortune in 2004, others have used STR to analyse RGC function in various models. Selective loss of the pSTR has been demonstrated in the chronic hypertension model of glaucoma, where the episcleral veins were injected with hypertonic saline to cause them to sclerose (Fortune et al. 2004). The authors of this study showed that 4 out of 5 eyes treated in this fashion had their pSTR amplitude reduced by over 50% thereby establishing that their glaucoma

model was causing selective ganglion cell loss. Bui et al extended their work by studying the sensitivity of the STR to various degrees of acute elevation of intra ocular pressure. They showed that the nSTR was most sensitive to acute rise in IOP (change seen at 50mmHg) and that pSTRs had intermediate sensitivity (changing at 60mmHg) (Bui et al. 2005). pSTR has also been used to demonstrate loss of inner retinal function in rat models of streptozotocin induced diabetic eyes suggesting that other retinal pathologies leading to ganglion cell death may also be studied using STRs (Kohzaki, Vingrys, & Bui 2008).

Elimination of STRs in response to intravitreal aspartate has been demonstrated in the past, although this was done in cat and monkey eyes (Wakabayashi, Gieser, & Sieving 1988). In this case the authors were using the aspartate treatment to determine the difference between the nSTR and the 'a' wave contributions by the retinal neurons and showed that aspartate eliminated the nSTR but did not affect the 'a' wave. Also in the cat, kainic acid and NMDA have been shown to eliminate STRs and affect components of the pattern ERGs arising from the RGC (Vaegan & Millar 1994). In rat eyes however, very few studies have specifically studied the effect of NMDA treatment on STRs. The effect of NMDA on the ERG of RCS rat eyes has been investigated (Ohzeki et al. 2007) but it is difficult to extrapolate the results of this study or even to use them as a guideline when studying the effect of NMDA on normal rat eyes.

7.2 Objectives and experimental design

Having established the NMDA model of RGC depletion and the benefits of Triamcinolone in maintaining microglial suppression, this work was aimed at assessing the ability of Müller stem cells differentiated towards an RGC phenotype to migrate and integrate and restore function in this model. The objectives were:

1. To examine the immuno-histological features of rat retina depleted of RGC by NMDA following transplantation of DAPT treated Müller stem cells, with particular focus on the survival and migration of the transplanted cell.
2. To investigate the effect of local Triamcinolone acetate mediated microglial suppression on migration and expression of RGC markers by the DAPT treated Müller stem cells in retinae depleted of RGC by NMDA.

3. To determine the STR response of retinae depleted of RGC by NMDA and to compare this response with that of normal retina and RGC depleted retinae transplanted with DAPT treated Müller stem cells.

To assess the effect of transplantation in the restoration of RGC function lost by NMDA treatment, the following protocol was used: Müller stem cells were induced to differentiate into RGC by treatment with DAPT (see chapter 3). Cell preparations thus enriched in cells expressing RGC markers were transplanted into 3-4 week old Lister hooded rat eyes depleted of RGC by NMDA in the presence of triamcinolone (TA) to control microglial reactivity. 2-4 weeks after transplantation, the eyes were analysed for RGC function using ERGs to assess the STR response of the transplanted retina. For this purpose, STRs were examined in rat eyes treated with NMDA and triamcinolone alone and compared with the STR responses of rat eyes transplanted with DAPT treated cells following RGC depletion by NMDA. The transplanted retinae were then analysed for the survival, migration and integration of grafted cells into the retina using immunohistochemical techniques and confocal microscopy.

7.2.1 Transplant protocol

GFP transfected Müller stem cells were cultured with matrigel, FGF2 and DAPT for 7 days. They were then harvested by trypsinisation, tested for their viability, washed free of any serum and resuspended in serum free media at a concentration of $4X10^4$ cells per µl. One µl of this cell suspension was mixed with 1µl of 10U/ml Chondroitinase ABC just prior to transplantation and injected into the intravitreal space using a 30G metal needle attached to a glass Hamilton syringe. The injection was performed under direct fundal visualisation and attempts were made to place the cells over the regions of the retina that appeared to have lost their nerve fibre organisation. This loss of nerve fibre layer organisation is evident as a mottled appearance in the retina 1wk post NMDA treatment. Care was taken to avoid perforating the large rat lens during the process of injection by changing the direction of the needle from inwards to downwards as soon as the tip was visible through the retina in the intravitreal space, before proceeding with advancement of the needle and subsequent injection (Fig 7.1). The bevel of the needle was

maintained upward as the needle was advanced into the vitreal space but rotated to face downward before the cells were injected.

Only one eye of each animal was treated with NMDA and triamcinolone, and subsequently transplanted with cells. The other eye was used as an internal control. Post injection the animals were followed for 2-4 weeks, subjected to electroretinograms and then sacrificed for tissue analysis. The electroretinograms were used to delineate the scotopic threshold responses (STR) in these eyes. The responses from the transplanted eyes were compared with those from NMDA treated eyes as well as control contralateral eyes. The 'a' and 'b' waves of these eyes were also analysed to ensure that photoreceptor function was unaffected by the treatment.

Immunocytochemistry was then used to correlate the functional results with the migration and integration of cells *in vivo*. Eyes were processed as previously outlined and cryostat sections (20µm thickness) were prepared for histological analysis. These were examined for integration of the transplanted cells into the host retina, as well as for the expression of RGC markers (HUD and Isl-1) by grafted cells. In addition, retinal sections were investigated for the presence of proliferating cells within the grafted population by immunostaining for the proliferating antigen Ki67. Presence of microglia in the transplanted retina was examined by immunostaining with anti-CD68 (ED1) antibodies. Sections were analysed by confocal microscopy.

7.2.2 Examination of STR function using ERG

In order to detect any improvement in RGC function following transplantation of differentiated Müller stem cells, the transplanted animals were subjected to electroretinogram (ERG) recordings. Detailed methodology of the ERG set up and

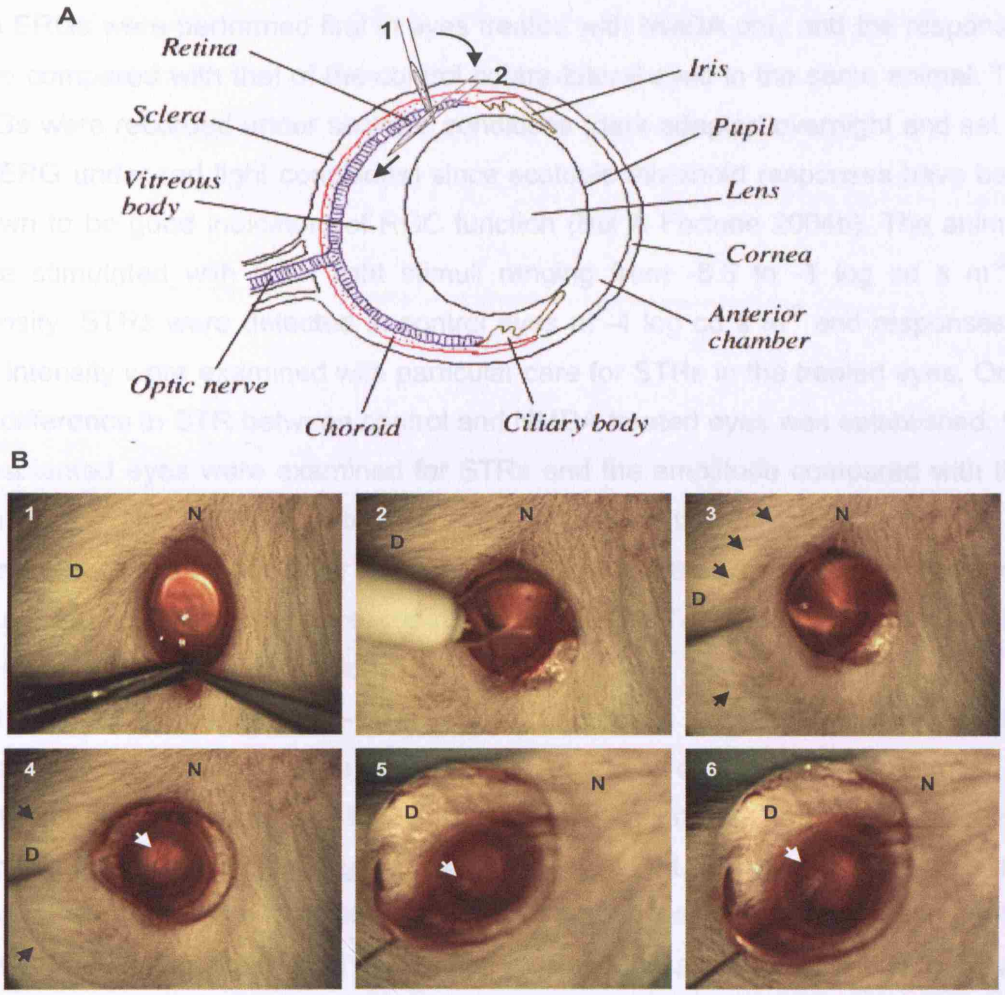

Figure 7.1: Intravitreal transplantation into rat retina
(A) Schematic diagram showing cross section of the rat eye with its large lens and small vitreous space. The bevel of the needle is positioned directly perpendicular to the sclera to begin the injection (1). Once the tip of the needle is visible through the retina, the needle is rotated so that it points backwards and nearly parallel to the inner surface of the retina (2). The cells are then injected towards the posterior retina in the direction shown by the straight arrow. Image modified from www.ratbehaviour.org/Eyes.html
(B) Photomicrographs showing the sequence of events during intravitreal transplantation. 1-Incision in the conjunctiva with a fine forceps and scissors in the dorsotemporal quadrant. 2- Application of viscotears over the cornea 3-Placement of coverslip over the viscotears on the cornea (edge of coverslip outlined by the black arrows) 4- Placement of coverslip (edge of the coverslip marked by the black arrows) allows visualisation of the fundus. The white arrow marks visible fundal vasculature. 5-30G metal needle is inserted into the retina through the sclera dorsotemporally till the tip of the needle is just visible through the retina in the intravitreal space (white arrow) 6-The metal needle is then extended under direct fundal visualisation deeper into the intra vitreal space (white arrow) before the cells are transplanted. N=nasal, D=dorsal

placement of the electrodes is presented in the section on materials and methods (chapter 8). The brief principles of the examination protocol are outlined here.

The ERGs were performed first in eyes treated with NMDA only and the responses were compared with that of the control contra-lateral eyes in the same animal. The ERGs were recorded under scotopic conditions (dark adapted overnight and set up for ERG under red light conditions) since scotopic threshold responses have been shown to be good indicators of RGC function (Bui & Fortune 2004b). The animals were stimulated with flash light stimuli ranging from -6.5 to -1 log cd s m^{-2} in intensity. STRs were detected in control eyes at -4 log cd s m^{-2} and responses to this intensity were examined with particular care for STRs in the treated eyes. Once the difference in STR between control and NMDA treated eyes was established, the transplanted eyes were examined for STRs and the amplitude compared with that seen in the NMDA TA only treated eyes as well as the control eyes to look for improvement in function over the NMDA TA only treated eyes if any. The three groups studied were therefore control eyes, NMDA TA treated eyes and NMDA treated eyes with transplantation.

At the higher intensities (-2& -1 log cd s m^{-2}), the eyes were also examined for the 'a' and 'b' waves to gain an estimate of the effect of the NMDA treatment on photoreceptor as well as third order retinal neuronal function respectively (*http://webvision.med.utah.edu/ClinicalERG.html*). Light flashes at -1 log cd s m^{-2} were shown to be able to elicit the normal 'a' and 'b' wave responses in the control eyes and this intensity of light stimulation was used to assess the 'a' and 'b' waves in the treated eyes as well.

Responses in each of the three groups for the light intensity of interest were grouped and analysed using the graph pad prism statistical software for significant differences.

7.3 Results

7.3.1 Migration and survival of DAPT treated Müller stem cells transplanted into RGC depleted retina without microglial suppression

Two weeks after transplantation of RGC rich preparations into NMDA treated retinae without microglial suppression, good transplant cell survival was observed. The transplanted cells retained their GFP expression and were detectable in all 12 eyes transplanted. The cells maintained the neuronal morphology they possessed *in vitro* and were also found to express long processes *in vivo* (Fig 7.2).

There was some evidence of cell migration in these eyes. Small groups of cells were observed migrating into the retina and aligning onto the GCL. However, not all the cells aligned on the GCL and in several instances transplanted cells were observed clustered in the vitreous, rather than dispersing generally into the retina (Fig 7.2). Staining of retinal sections with the antibodies to RGC markers HUD and ISL1 showed that some of the GFP transplanted cells co expressed these markers. However the number of cells expressing these markers was quite small and most of the retinae continued to be devoid of RGC with gaps of HUD expression in the GCL (Fig 7.3). Retinal sections stained for the proliferation marker Ki67 showed that the transplanted Müller stem cells not only survived *in vivo*, but were also able to proliferate (Fig 7.4). While these results were encouraging in that Müller stem cells were able to express RGC markers *in vivo*, the number of such cells was very small. Staining of retinal sections with the microglial marker ED1 revealed that there was still considerable microglial activation in these retinae (Fig 7.5) and it was likely that this was the cause of restricted migration of the transplanted Müller stem cells.

From the above results it was possible to conclude that Müller stem cells when differentiated into RGC precursors have the ability to differentiate into RGC *in vivo* as seen by their neural morphology and expression of RGC markers in the host retina. It was also concluded that NMDA treatment caused significant levels of microglial activation and this would need to be controlled for successful migration of

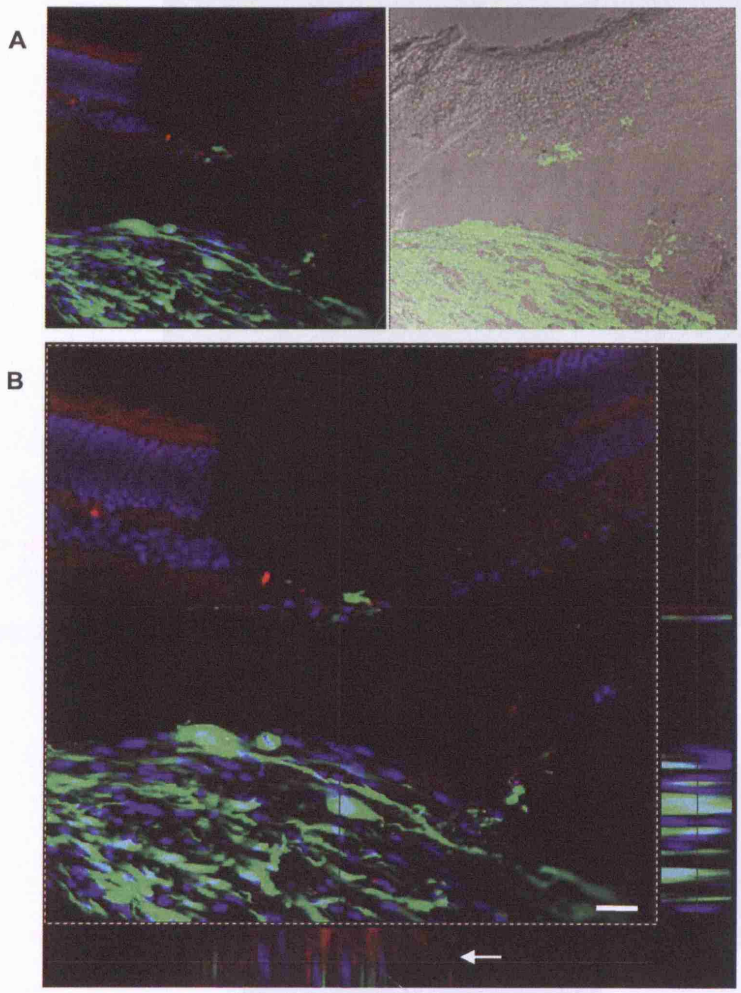

Figure 7.2: Transplanted DAPT treated Müller stem cells show neural morphology and localise to the ganglion cell layer when injected into NMDA treated LH rat retina (A) Müller stem cells treated with DAPT were transplanted into NMDA treated LH rat eyes intravitreally. Confocal micrographs show bolus of GFP DAPT treated cells in the vitreal space and a few cells in the ganglion cell layer. Phase contrast image on the right merged with the GFP image provides additional information on the placement of the Müller stem cells within the eye after transplantation. (B) 3D projection of z stac of images obtained on the confocal showing that the green cells are present in the same plane as the nuclei of the ganglion cell layer (white arrow). The red stain is Brn3b. Scale bar=20µm.

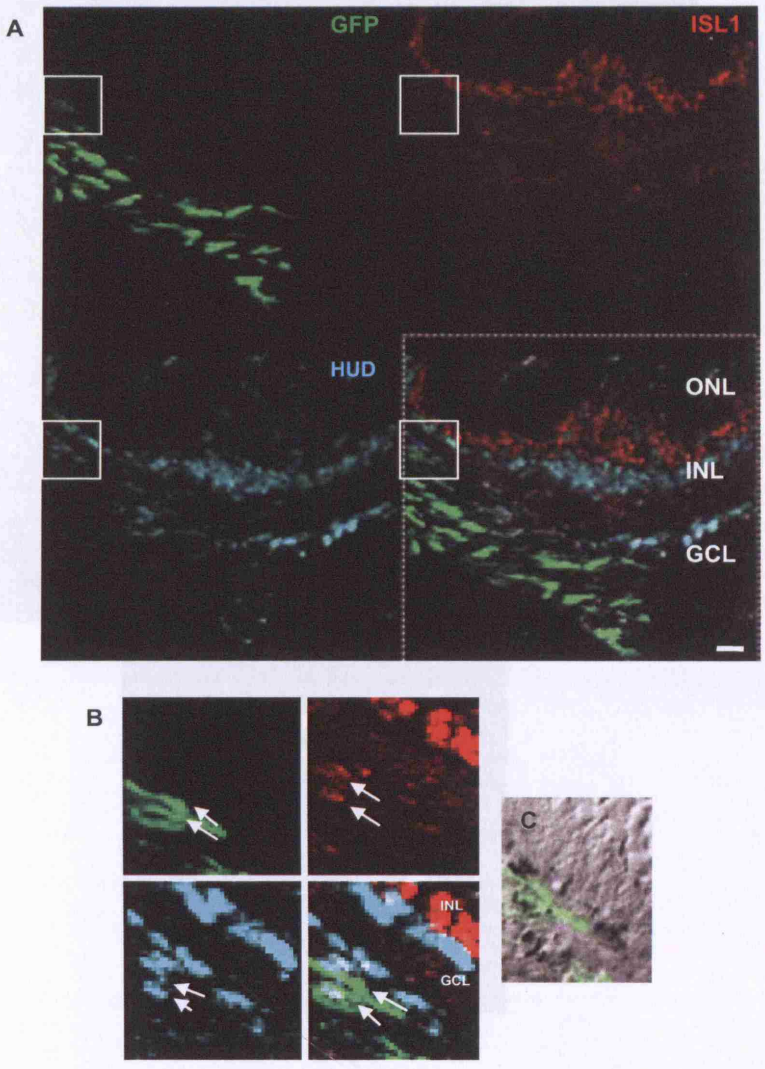

Figure 7.3: DAPT treated Müller stem cells express RGC markers following transplantation into NMDA treated LH rat retina (A) Confocal micrograph of lister hooded rat retina treated with NMDA without microglial suppression and transplanted with DAPT treated Müller stem cells at 2 weeks post transplantation. Immunostaining with HuD (cyan) and Isl1 (red) outlines the ganglion cell and inner nuclear layers. The GFP labelled Müller stem cells are aligned next to the ganglion cell layer but are not seen to be expressing either Isl1 or HuD in abundance. (B) Magnifications of areas marked in (A) (white boxes) showing GFP labelled cells colocalising with Isl1 and HuD immunostaining. (C) Phase contrast micrograph of region in (B) merged with GFP showing some microglial reactivity (ED1 in black) around the GFP cells. Scale bar=20μm.

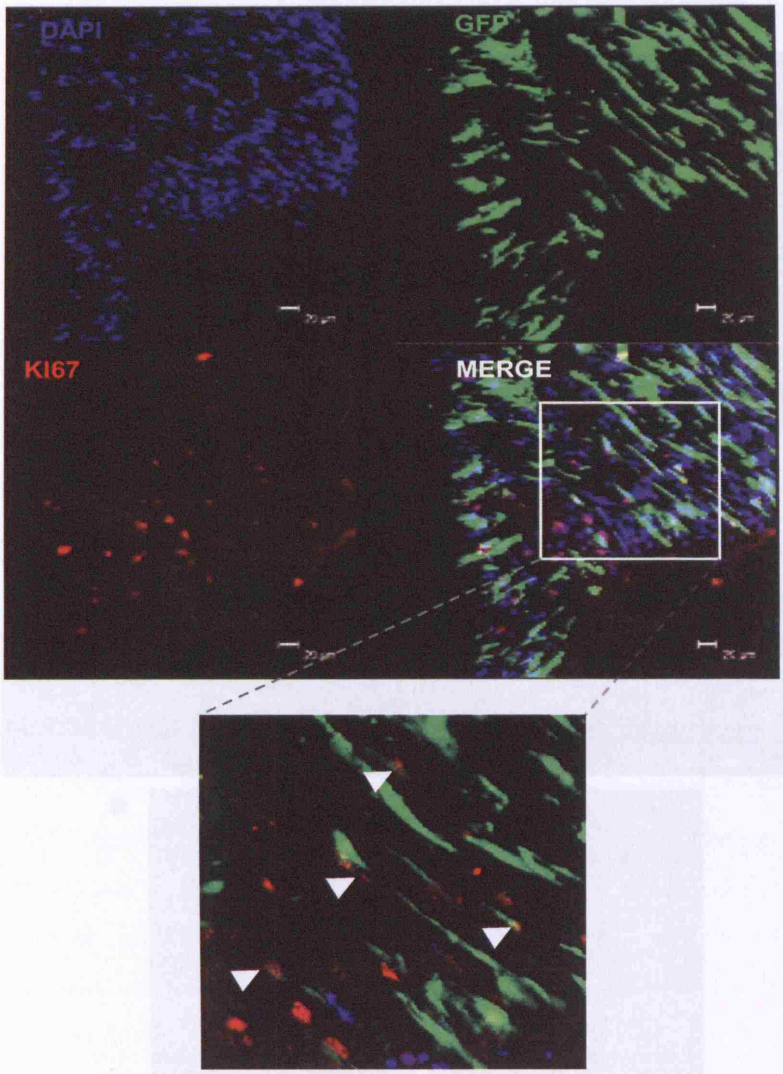

Figure 7.4: Transplanted Müller stem cells show active division *in vivo* Confocal micrograph of lister hooded rat retina treated with NMDA but without additional microglial suppression and transplanted with DAPT treated Müller stem cells (GFP+) at 2 weeks post transplantation. Immunostaining with ki67 (red) shows that some of the GFP+ cells are also positive for Ki67 (red) in red suggesting that the cells are proliferating *in vivo*. A section of the merged image is magnified in the micrograph at the bottom, and the white arrows indicate GFP labelled transplanted Müller stem cells expressing Ki67. Cell nuclei are counterstained with DAPI.

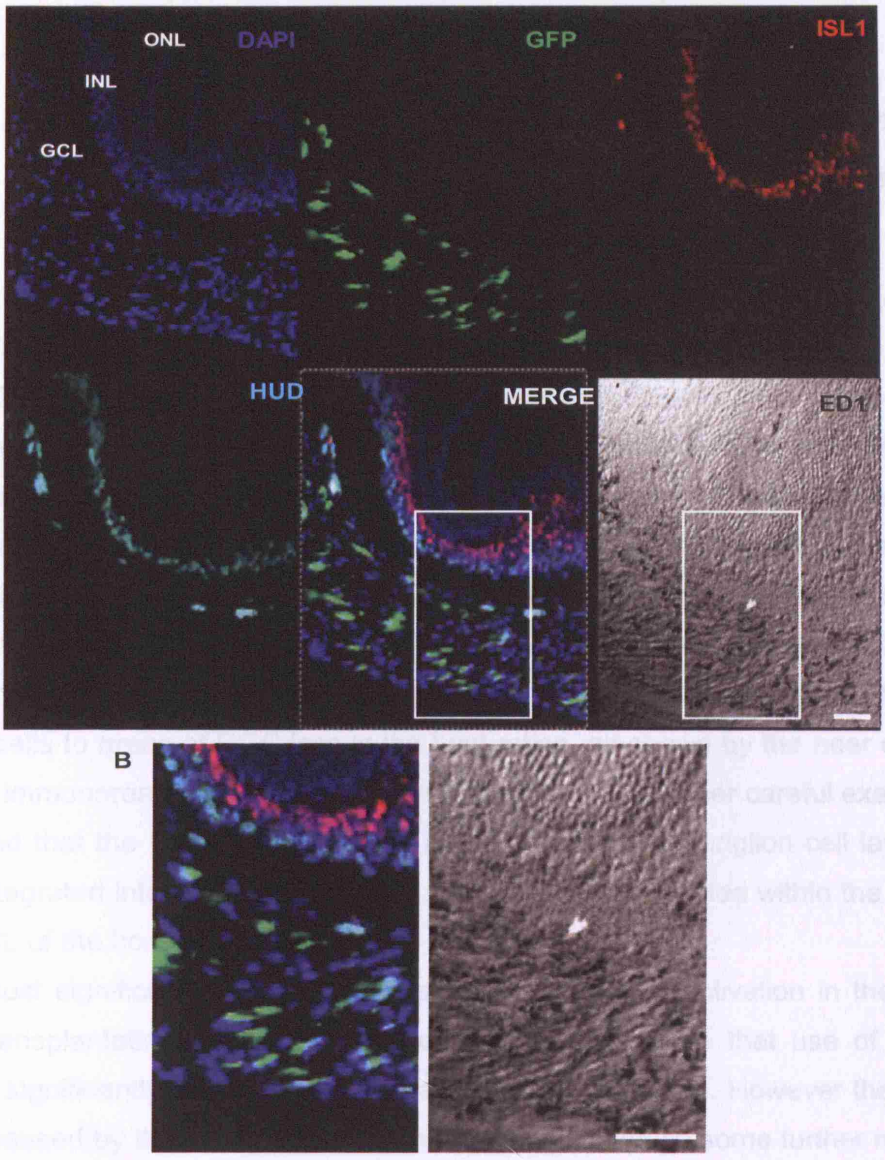

Figure 7.5: Microglial reactivity associated with transplanted DAPT treated Müller stem cells in NMDA treated LH rat retina (A) Confocal micrograph of lister hooded rat retina treated with NMDA but without microglial suppression and transplanted with DAPT treated Müller stem cells at 2 weeks post transplantation. Immunostaining with HuD (cyan) and Isl1 (red) outlines the ganglion cell and inner nuclear layer. Although the GFP labelled Müller stem cells are aligned next to the ganglion cell layer they are associated with microglia (peroxidase staining in black) as seen in the phase contrast micrograph on the bottom right. (B) Magnified areas from the white boxes in (A) showing in greater detail association of extensive microglial activity with the GFP labelled cells. Scale bar=20µm.

the transplanted Müller stem cells. However despite NMDA mediated microglial activation, the transplanted cells were able to survive for up to 2 weeks *in vivo.*

7.3.2 Migration and survival of DAPT treated Müller stem cells transplanted into RGC depleted retina in the presence of microglial suppression

This study showed that when injected intra vitreally into NMDA TA treated eyes, DAPT treated Müller stem cells were able to migrate, survive and express markers of RGC *in vivo* for the 4 week duration of the experiments. Five out of 6 eyes examined between 3-4 weeks post transplant were found to have surviving GFP+ transplanted cells. Several GFP+ cells were identified in the intravitreal space of the transplanted eyes and a large proportion of these cells were found to have aligned in close proximity to the ganglion cell layer (Fig 7.6). Attempts had been made during transplantation to place the donor cells over areas of visible nerve fibre layer loss and examination of these eyes post mortem confirmed the proximity of the donor cells to areas of RGC loss in the host retina, as shown by the near complete loss of immunoreactivity to HUD in this region (Fig 7.6). Further careful examination revealed that the GFP+ cells not only aligned next to the ganglion cell layer, they also integrated into it. GFP+ cells were seen to be disseminated within the nuclei in the GCL of the host retina (Fig 7.6).

Of utmost significance was the assessment of microglial activation in these eyes post transplantation. In the previous chapter it was shown that use of TA with NMDA significantly diminishes microglial activity in the retina. However the second injury caused by the cell transplantation was likely to induce some further microglial activation. It was important therefore to examine the microglial activity in these eyes and determine whether TA continued to be effective enough to control microglial activation caused by the transplant injury as well. Immunostaining of the sections with ED1 revealed that there was some residual level of microglial activity persisting in the retina despite the TA treatment (Fig 7.7). This was seen in association with some GFP+ cells in the intravitreal space and in the inner plexiform layer (Fig 7.7). However most of the GFP+ cells were free of any microglial activity and did not

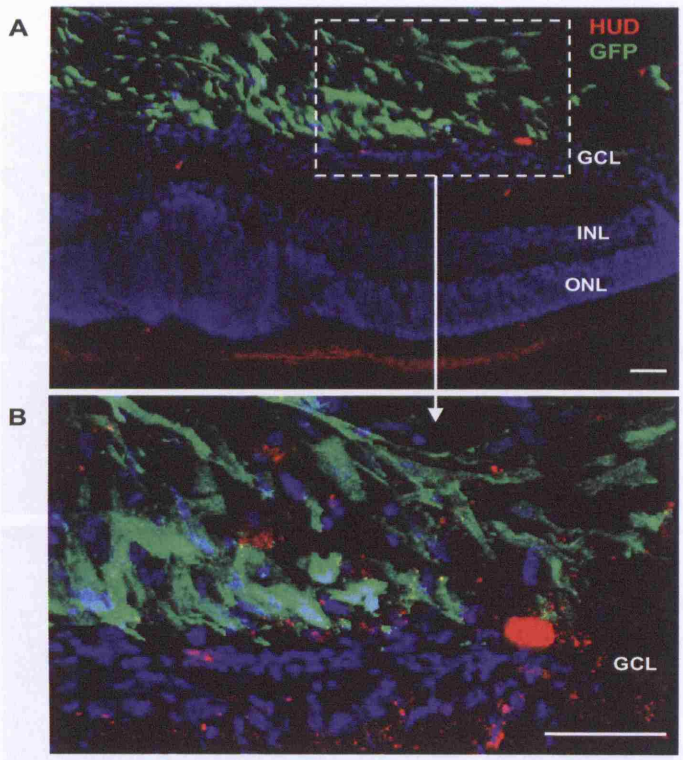

Figure 7.6: Survival and migration of transplanted DAPT treated Müller stem cells in NMDA/ TA treated LH rat retina (A) Confocal micrograph of lister hooded rat retina treated with NMDA/ TA and transplanted with DAPT treated Müller stem cells, examined at 3 weeks post transplantation. Immunostaining was performed with HuD (red), GFP (green) and DAPI (blue) to delineate the cell nuclei. The micrograph on top shows numerous GFP+ cells aligned next to the ganglion cell layer. (B) Magnification of dotted area in (A) showing in greater detail, the close proximity and integration of GFP+ cells into the GCL of the host retina. Very little HuD immunostaining was seen in the host GCL or in the GFP + cells. Scale bar=20μm

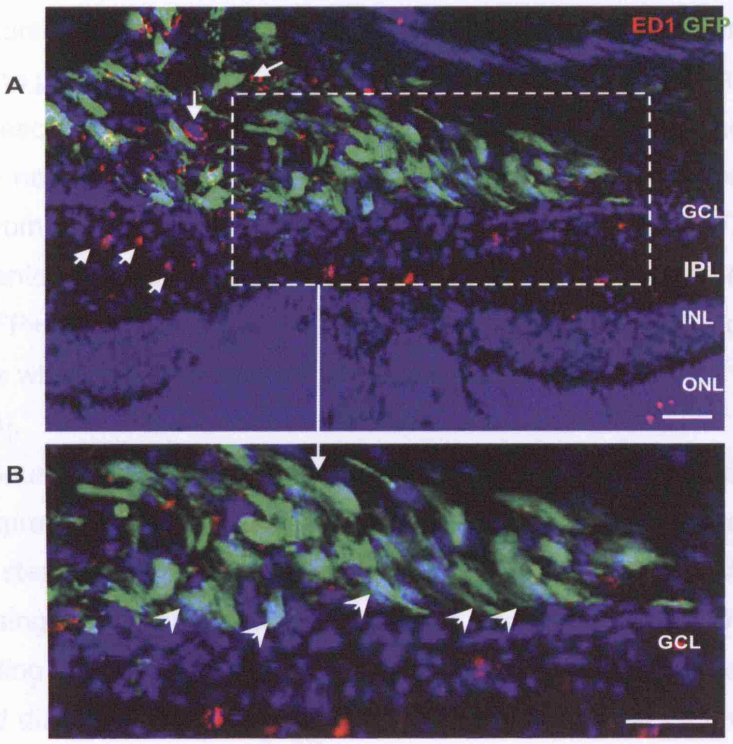

Figure 7.7: Microglial suppression facilitates migration and integration of DAPT treated Müller stem cells transplanted into NMDA/ TA treated LH rat retina (A) Confocal micrograph of a lister hooded rat retina treated with NMDA /TA and transplanted with DAPT treated Müller stem cells, examined at 3 weeks post transplantation. Immunostaining was performed with microglial marker ED1(red), GFP (green) and DAPI (blue) to delineate the cell nuclei. The upper micrograph shows numerous GFP+ cells aligned next to the ganglion cell layer. Some ED1 staining is seen in the intravitreal space, interspersed with the GFP+ cells away from the GCL and in the IPL (white arrows). (B) Magnification of the area in the dotted box showing that GFP+ cells that are aligned and integrating into the GCL are free of ED1 immunoreactivity (white arrow heads). Scale bar=20µm

colocalize with cells immunostaining for ED1. Importantly the cells aligning next to the GCL and interspersed with the GCL nuclei were also negative for ED1 as was most of the host GCL (Fig 7.8). This suggested that transplanted Müller stem cells were able to survive and integrate into the host GCL without being hindered by microglial activity. It also suggested that TA was able to exert considerable control over microglial activation in the retina up to 5 weeks post injection, despite the added injury caused by the transplantation.

Transplanted GFP+ cells also demonstrated characteristic neuronal morphology in the retina post transplantation. In the experiments performed on NMDA only treated eyes, described in the section above, the transplanted Müller stem cells were found to have neural morphology but most of the cells with such morphology were seen away from the GCL in the intra vitreal space. In the NMDA TA treated eyes, the transplanted cells displayed neural morphology as they interspersed with the GCL. The GFP+ cells in the GCL demonstrated large round cell bodies with thin long neurites which were seen to be extending both into the GCL as well as away from it (Fig 7.8).

In previous transplant experiments, it had been difficult to detect any transplanted cells expressing differentiated markers of RGC. In these transplants of differentiated Müller stem cells in to the NMDA TA treated rat retina however, several cells expressing RGC marker were observed. In addition, multiple GFP+ cells were seen integrating into the GCL, IPL and INL of the host retina and several of these cells showed distinct colocalisation with HUD (Fig 7.9). These GFP+ cells were present in line with nuclei present in the inner nuclear and ganglion cell layers, extended processes into the IPL and INL and stained for HUD in their nuclei (Fig 7.9 -arrow heads) and cell processes (Fig 7.9-arrows).

In summary the transplant histology of these experiments showed that differentiated Müller stem cells could migrate and integrate into the ganglion cell layer of Lister hooded rat eyes treated with NMDA TA. The transplanted GFP+ cells were free of microglial activity, expressed characteristic neural morphology and extended processes into the GCL, IPL and INL. Most importantly some of the transplanted cells demonstrated the ability to express markers of differentiated RGC as they integrated into the GCL suggesting that perhaps the DAPT treated Müller stem cells

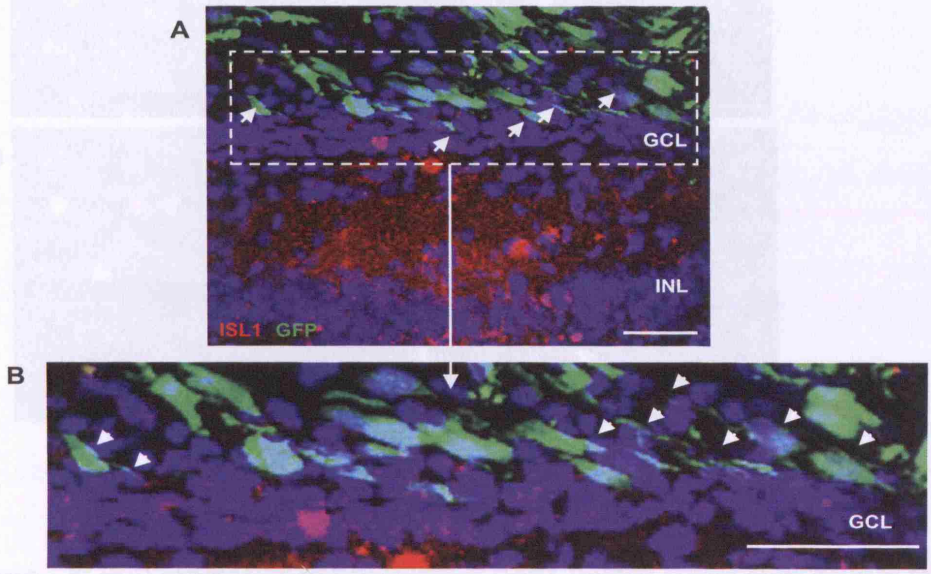

Figure 7.8: Neuronal morphology of transplanted DAPT treated Müller stem cells in NMDA/ TA treated LH rat retina (A) Confocal micrograph of lister hooded rat retina treated with NMDA TA and transplanted with DAPT treated Müller stem cells, examined at 3 weeks post transplantation. Immunostaining was performed for the ganglion cell marker Isl1(red), GFP (green) and DAPI (blue) to delineate the cell nuclei. The upper micrograph shows numerous GFP+ cells aligned next to the ganglion cell layer and extending neural processes (white arrows). The area in the dotted box is magnified underneath and shows in greater detail the neural morphology of the integrating GFP+ cells. Several cells show large cell bodies and extend neural processes into and away from the GCL (white arrowheads). Scale bar=20μm

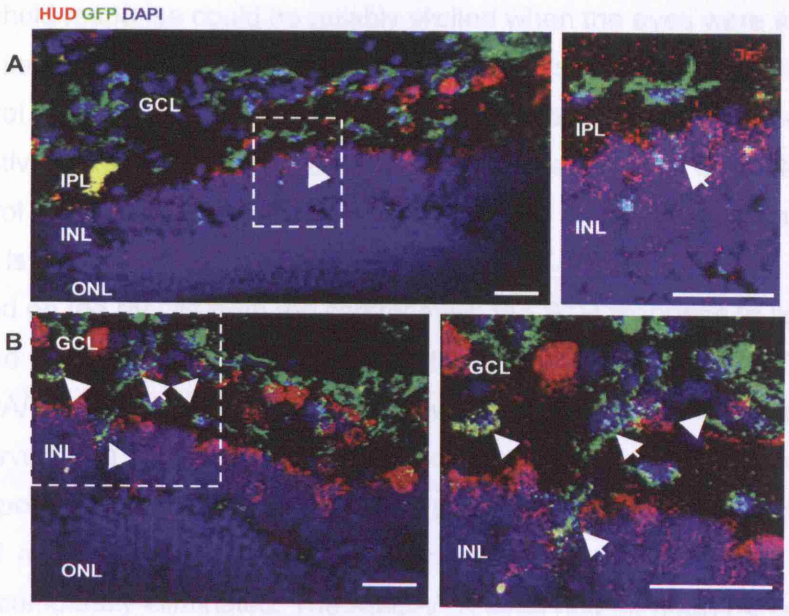

Figure 7.9: HuD expression of transplanted DAPT treated Müller stem cells in to NMDA TA treated LH rat retina (A) Confocal micrograph of lister hooded rat retina treated with NMDA TA and transplanted with DAPT treated Müller stem cells, examined at 3 weeks post transplantation. Immunostaining was performed for the ganglion cell marker HuD (red), GFP (green) and DAPI (blue) to delineate the cell nuclei.

A and B are two different areas of a NMDA/TA treated retina transplanted with DAPT treated Müller stem cells showing migration and integration of GFP+ cells into the GCL, IPL and INL. In (A) GFP+ cells are seen aligning with the GCL, interspersed in the IPL and occasionally integrated in the INL (dotted box). The area in the dotted box of A is magnified on the right to show in detail the presence of GFP+ cells in the IPL and a single GFP and HuD positive cells integrated in the inner layers of the INL (white arrow)

In (B) GFP+ cells are seen integrating into the GCL and INL, extending processes into the IPL and expressing HuD. The dotted area is magnified on the right and shows in detail the processes extended by the GFP+ cells integrating into the GCL and INL (white arrows). It also shows distinct coexpression of HuD with a GFP+ cell in the IPL (white arrowhead)

Scale bar=20μm

we

re capable of forming differentiated RGC *in vivo* when transplanted into the NMDA TA treated retina depleted of RGC.

7.3.3 Partial restoration of RGC function following transplantation of DAPT treated Müller stem cells into NMDA TA treated eyes

Electroretinograms performed on untreated control eyes showed that the scotopic threshold response could be reliably elicited when the eyes were stimulated with the light flashes of - 4 log cd s m^{-2} intensity. At this threshold light intensity all of the control eyes tested showed an STR with a small positive component and a larger negative component (Fig 7.10). The response pattern was consistent in each of the control eyes tested and a cumulative curve of the STR response derived from 5 eyes is depicted in Fig 7.10.

Based on the results from the control eyes, the STR response to light intensity of - 4 log cd s m^{-2} was then examined in the eyes treated with NMDA/TA alone and NMDA/TA treated eyes transplanted with DAPT treated Müller stem cells. It was observed that NMDA/TA treatment alone caused a dramatic decline in the STR. The positive component of the STR (pSTR) was significantly reduced although a small residual response was still identifiable. The negative STR (nSTR) however was completely eliminated. The NMDA/TA eyes had no negative component to their STR. The cumulative response from 4 different eyes treated with NMDA/TA alone is depicted in Fig 7.10.

The eyes which had received NMDA/TA followed by transplantation of differentiated Müller stem cells also showed a significant loss of the pSTR. The response was similar to that seen with the NMDA/TA eyes. However the eyes which had received the transplantation showed a partial recovery of the negative component of the STR. Cumulative curves from 10 animals which received cell transplantation after NMDA/TA treatment showed that there was indeed a significant recovery of the nSTR in the transplanted eyes when compared to the eyes treated with NMDA/TA only (Fig 7.10).

The amplitudes of the pSTR and nSTR in the three conditions were compared. Data from 4-10 animals in each group was plotted and showed that NMDA/TA treatment caused a significant decline in the amplitude of pSTR ($p<0.05$ vs control, Fig 7.11A)

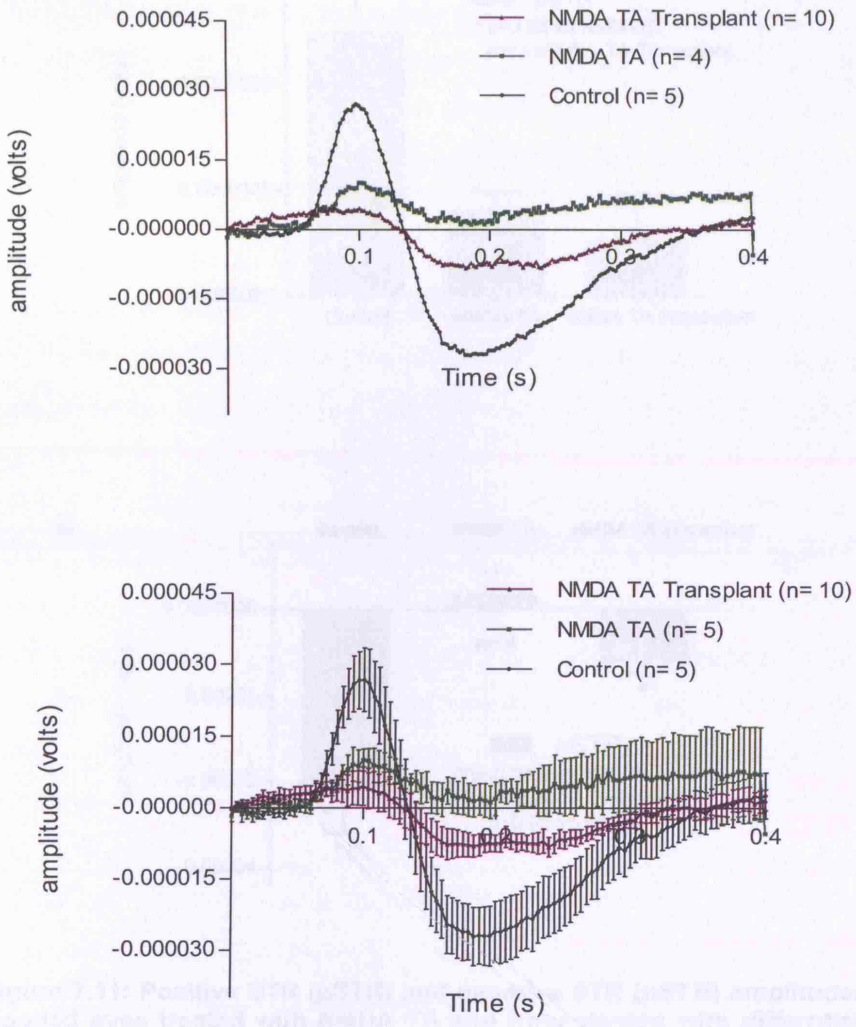

Figure 7.10: Scotopic Threshold Response (STR) in NMDA TA treated cells with differentiated Müller stem cell transplantation

Graphs showing the STR response of Lister hooded rats. The control eyes (black) show a characteristic STR curve with a positive response (pSTR) followed by a larger negative response (nSTR). The NMDA TA treated eyes (green) show a small positive response (pSTR) but do not demonstrate a negative component (nSTR). The NMDA TA eyes which have been transplanted with differentiated Müller stem cells have a small pSTR and demonstrate an nSTR as well which is significantly different from that of the NMDA TA treated eyes only. The graph on the top depicts the cumulative curves only, to allow for better visualisation of the response. The graph below shows the same curves with error bars for SEM to provide an estimate of the difference in responses in the three groups.

as

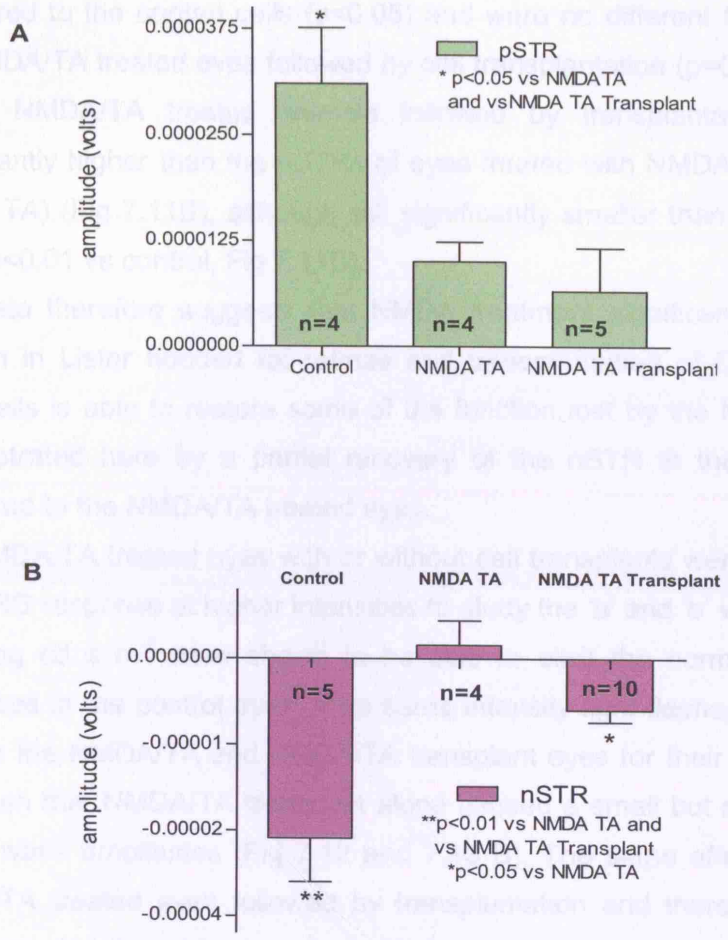

Figure 7.11: Positive STR (pSTR) and negative STR (nSTR) amplitudes in Lister Hooded eyes treated with NMDA TA and transplanted with differntiated Müller stem cells.

(A) Graph comparing the pSTR amplitudes observed in control eyes, eyes treated with NMDA TA and eyes treated with NMDA TA and transplanted with cells. The pSTR amplitude declined significantly after treatment with NMDA TA ($p<0.05$ vs C). pSTR amplitudes were also seen to be significantly lower than the controls in the NMDA TA transplant eyes. Transplantation of Müller stem cells into NMDA TA treated eyes did not result in any recovery of the pSTR ($p=0.5892$ NMDA TA vs NMDA TA transplant)
(B) Graph comparing the nSTR amplitudes of the control eye, NMDA TA treated eyes, and NMDA TA treated eyes with cell transplantation. The nSTR seen in control eyes was completely lost with NMDA TA treatment (no negative component in the response was seen). Eyes treated with NMDA TA and cell transplantation had a detectable nSTR. The amplitude of this nSTR though significantly lower than that seen in the control eyes ($p<0.01$ vs control) was significantly higher than the nSTR seen with NMDA TA alone ($p<0.05$). The number of animals studied in each condition is shown as the n number on each bar.

well as nSTR ($p<0.05$ vs control, Fig 7.11B) compared to the control eyes. The NMDA/TA transplanted eyes also showed a significant decline in amplitude of pSTR compared to the control cells ($p<0.05$) and were no different from pSTRs seen in the NMDA/TA treated eyes followed by cell transplantation ($p=0.5892$). The nSTRs in the NMDA/TA treated animals followed by transplantation were however significantly higher than the nSTRs of eyes treated with NMDA/TA only ($p<0.05$ vs NMDA TA) (Fig 7.11B), although still significantly smaller than those of the control eyes ($p<0.01$ vs control, Fig 7.11B).

This data therefore suggests that NMDA treatment significantly diminishes RGC function in Lister hooded rat retinae and transplantation of DAPT treated Müller stem cells is able to restore some of the function lost by the NMDA treatment, as demonstrated here by a partial recovery of the nSTR in the transplanted eyes compared to the NMDA/TA treated eyes.

The NMDA/TA treated eyes with or without cell transplants were also examined for their ERG response at higher intensities to study the 'a' and 'b' waves. Light flashes at -1 log cd s m^{-2} were shown to be able to elicit the normal 'a' and 'b' wave responses in the control eyes. The same intensity light flashes were then used to analyse the NMDA/TA and NMDA/TA transplant eyes for their 'a' and 'b' waves. It was seen that NMDA/TA treatment alone caused a small but significant decline in the 'b' wave amplitudes (Fig 7.12 and 7.13 B). The same effect was seen in the NMDA/TA treated eyes followed by transplantation and there was no significant difference in the 'b' wave amplitudes between the non-transplanted and transplanted NMDA/TA treated eyes (Fig 7.12 and 7.13 B). The 'a' wave amplitudes of the NMDA TA treated eyes (transplanted and non-transplanted) were also smaller than that of the control eyes. However, this difference was not significant ($p>0.05$ vs controls in both cases, Fig 7.12 and 7.13 B). One representative set of ERG recordings for each of the three treatment groups is depicted in Fig 7.14.

Both bipolar and amacrine cells have been shown to posses NMDA receptors and (Shen, Liu, & Yang 2006b) it is possible that they are also affected by the NMDA treatment. This would explain the significant decline in 'b' wave amplitudes in the NMDA treated eyes compared to the controls. It was likely however that photoreceptor function remained largely intact with the NMDA/TA treatment given

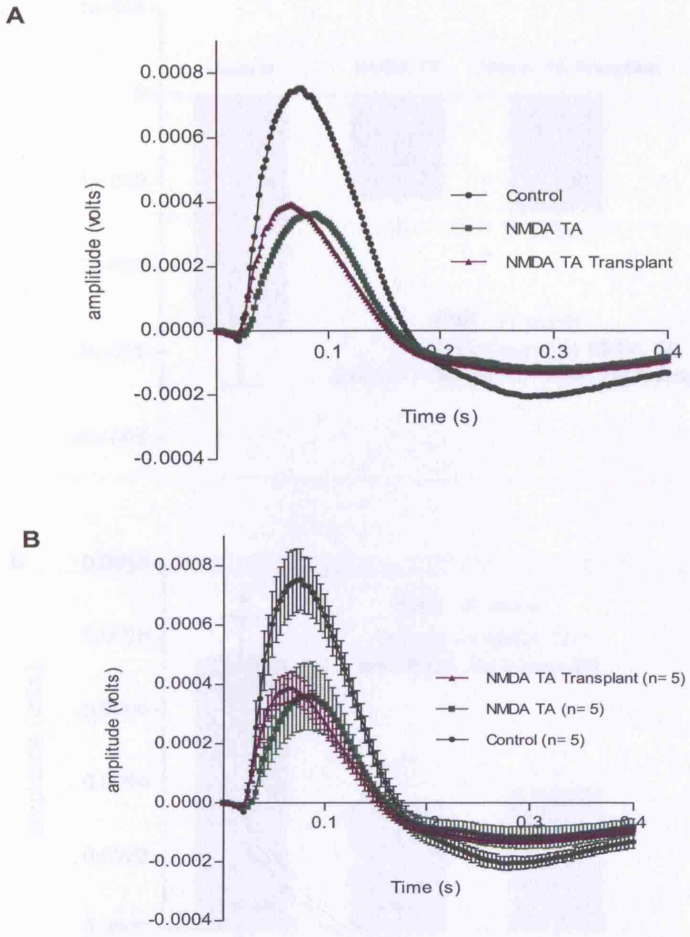

Figure 7.12: 'a' and 'b' waves in NMDA TA treated eyes transplanted with differentiated Müller stem cells

(A) Graphs showing the 'a' and 'b' wave responses of Lister hooded rats. The control eyes (black) show characteristic 'a' and 'b' wave with an initial early small negative response (a wave) followed by a large positive response (b wave). The NMDA TA treated eyes (green) and the NMDA TA treated eyes which received cell transplantation (magenta) show a significantly smaller 'b' wave compared to the control eyes. The graph on the left depicts the cumulative curves only, to allow for better visualisation of the response. The graph on the right shows the same curves with error bars for SEM to provide an estimate of the difference in responses in the three groups. (B) Graph showing in greater detail the 'a' wave in the three conditions. Control eyes (black) show a normal negative 'a' wave. The NMDA TA and NMDA TA transplanted eyes show a smaller 'a' wave compared to the control eyes.

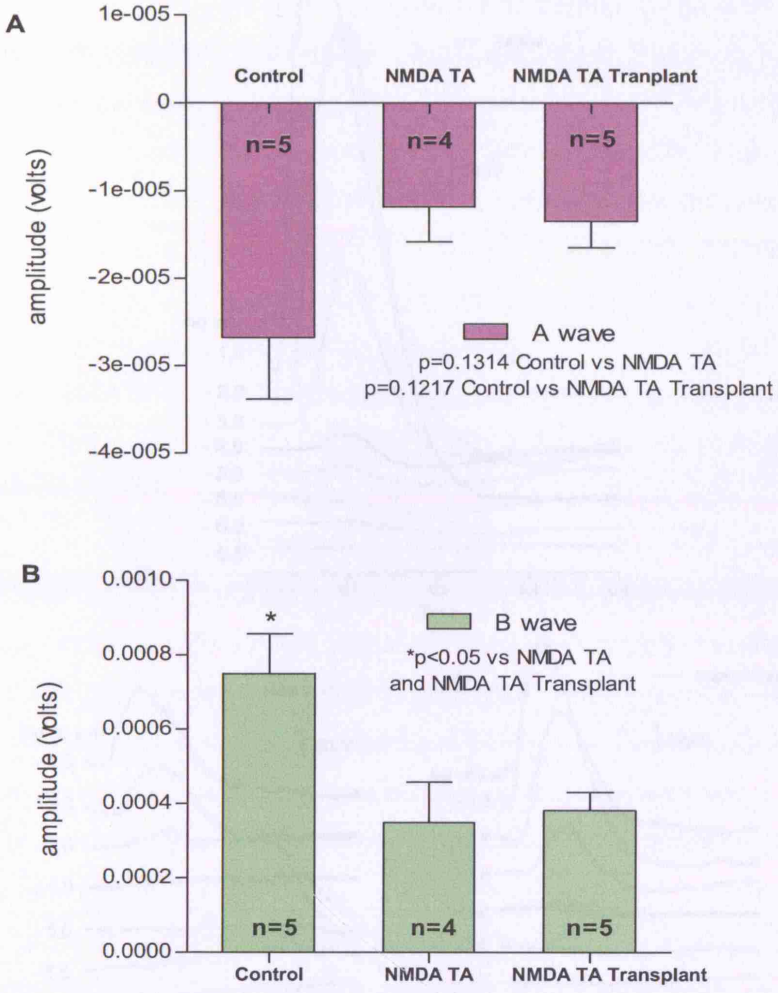

Figure 7.13: 'a' and 'b' wave amplitudes in Lister Hooded eyes treated with NMDA TA and transplanted with differentiated Müller stem cells.

(A) Graph comparing the 'a' wave amplitudes observed in control eyes, eyes treated with NMDA TA and eyes treated with NMDA TA and transplanted with cells. The 'a' wave amplitudes of the NMDA TA treated eyes and the NMDA TA treated eyes with cell transplantation were smaller than that of control eyes but the difference was not statistically significant ($p>0.05$ vs C in both samples). There was no significant difference in the 'a' wave amplitudes between the NMDA TA and NMDA TA cell transplant eyes. ($p=0.7486$ NMDA TA vs NMDA TA transplant)

(B) Graph comparing the 'b' wave amplitudes of the control eyes, NMDA TA treated eyes, and NMDA TA treated eyes with cell transplantation. The b wave amplitudes in the NMDA TA and the NMDA TA cell transplant eyes were significantly smaller than the b wave amplitudes of the control eyes ($p<0.05$). There was no significant difference in 'b' wave amplitude between the NMDA TA and the NMDA TA cell transplant eyes ($p=0.7747$ NMDA TA vs NMDA TA transplant).

The number of animals studied in each condition is shown as the n number on each bar.

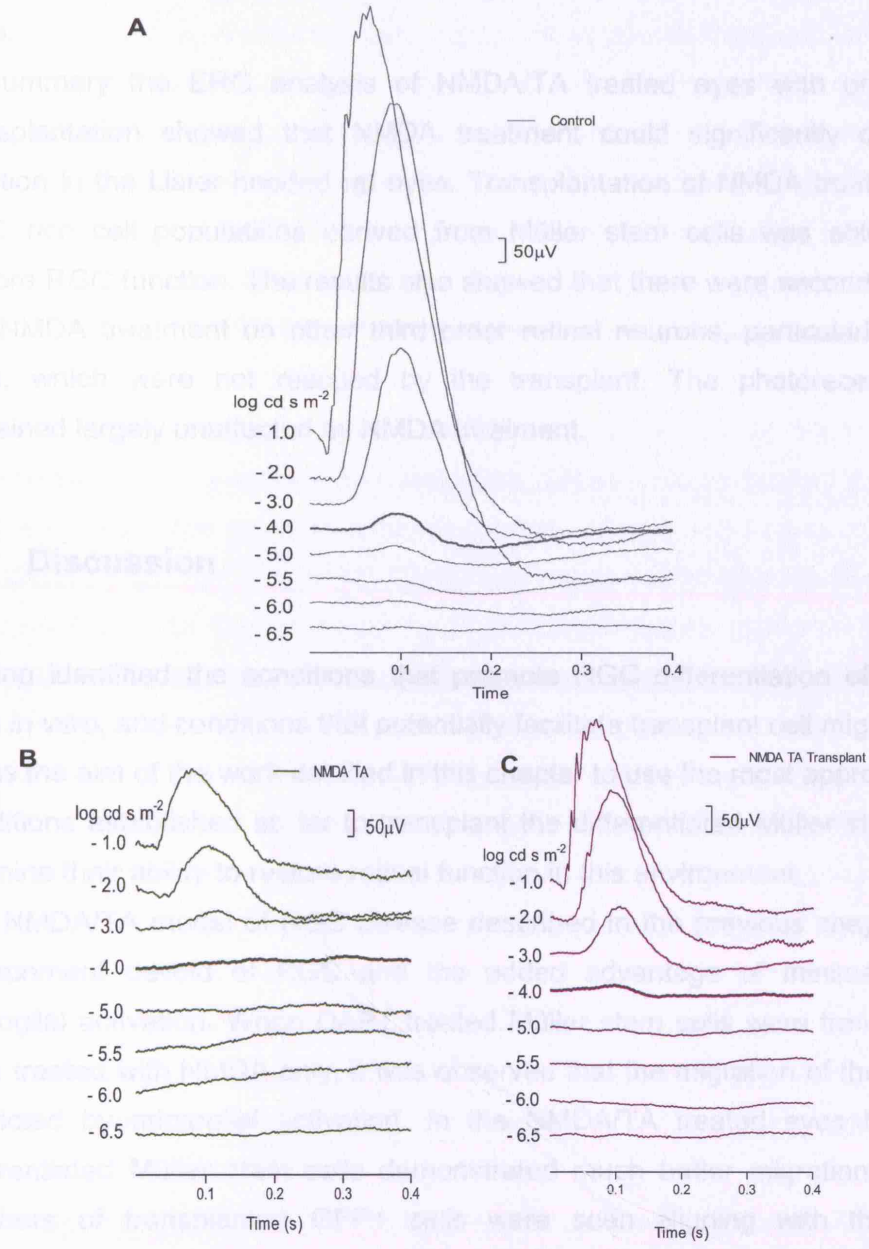

Figure 7.14: Representative ERG recordings of Lister hooded eyes under control conditions, with NMDA/TA treatment alone and following transplantation with DAPT treated Müller stem cells. Representative ERG recordings from a lister hooded control eye (A), an NMDA/ TA treated eye (B) and an eye treated with NMDA/TA followed by Müller stem cell transplantation (C). In each case the retina was stimulated under scotopic conditions with low intensity light flashes (-6 to-1 log cd s m^{-2}). The bold line in each graph represents the STR response seen in these experiments at -4 log cd s m-2. In the control eye (A) the STR has a distinct positive and negative slope. In the NMDA/TA treated eye (B), response to stimulation with light at -4 log cd s m-2 is almost a flat line. In the NMDA/TA treated and transplanted eye (C), there is a distinct negative component to the STR, not seen in the NMDA/TA treated eye.

that the 'a' wave amplitudes were not significantly different from that of the control eyes.

In summary the ERG analysis of NMDA/TA treated eyes with or without cell transplantation showed that NMDA treatment could significantly deplete RGC function in the Lister hooded rat eyes. Transplantation of NMDA treated eyes with RGC rich cell populations derived from Müller stem cells was able to partially restore RGC function. The results also showed that there were secondary effects of the NMDA treatment on other third order retinal neurons, particularly the bipolar cells, which were not rescued by the transplant. The photoreceptor function remained largely unaffected by NMDA treatment.

7.4 Discussion

.

Having identified the conditions that promote RGC differentiation of Müller stem cells *in vitro*, and conditions that potentially facilitate transplant cell migration *in vivo*, it was the aim of the work detailed in this chapter to use the most appropriate *in vivo* conditions established so far to transplant the differentiated Müller stem cells and examine their ability to restore retinal function in this environment.

The NMDA/TA model of RGC disease described in the previous chapter offers an environment devoid of RGC and the added advantage of minimal associated microglial activation. When DAPT treated Müller stem cells were transplanted into eyes treated with NMDA only, it was observed that the migration of these cells was restricted by microglial activation. In the NMDA/TA treated eyes however, the differentiated Müller stem cells demonstrated much better migration and greater numbers of transplanted GFP+ cells were seen aligning with the GCL and integrating with it. In addition, these transplanted cells were largely free of any association with microglia. This finding is extremely significant since it suggests that TA exerts a significant effect on microglial activity and is able to control their activation for long periods of time. A single intravitreal injection in these animals was shown to be able to control microglial activation for up to 5 weeks. This treatment might be of great use in controlling microglial activation in transplantation studies that can be potentially translated into human therapies. TA is already used as an

anti inflammatory agent in patients with retinal inflammatory diseases (Mankowska, Rejdak, Oleszczuk, Kiczynska, Lekawa, Choragiewicz, & Zagorski 2008) and its use as an adjuvant to stem cell transplantation could be easily implemented.

In an environment depleted of RGC but still conducive to integrate donor cells, DAPT treated cells were also able to express RGC markers *in vivo*. Cell integrating within the GCL, IPL and INL demonstrated neuronal morphology and transplanted cells that integrated into the RGC layer expressed HUD, suggesting that these cells were able to maintain some degree of terminal RGC differentiation *in vivo* after transplantation.

To validate the migration and apparent structural integration observed with the transplanted DAPT treated Müller stem cells, ERGs were performed to assess if this integration was also resulting in functional restoration of RGC function. Using STRs to delineate RGC function on the ERG, it was seen that NMDA treatment selectively destroys RGC, as demonstrated by near complete loss of the STR. The nSTR appeared to be affected more significantly than the pSTR with NMDA treatment alone and transplantation with the differentiated Müller stem cells was able to restore some of this lost nSTR. While the degree of restoration was small and still lower than the control response, it was significantly greater than that of the non-transplanted NMDA/TA treated eyes and provides crucial first evidence of functional recovery of RGC function following stem cell transplantation in a model of RGC depletion. The ERG analysis also showed that NMDA/TA treatment affected third order retinal neurons but did not significantly disrupt photoreceptor function.

This partial recovery of function could be as a result of transplanted cells forming functional synapses with the remaining viable RGC in the retina but no evidence for the same is presented here. Immunostaining for synaptic antigens is part of the future work intended to further explain this improvement in function. Alternatively the functional recovery could also be attributed to neurotrophic support offered by the Müller stem cells to the surviving RGC in the host retina. While the individual contributions of cell replacement versus neurotrophic support would be difficult to delineate, as part of future work, comparison of the effects of undifferentiated Müller stem cells with that of differentiated cells on functional recovery could be used as a screen.

This work therefore establishes that NMDA/TA treated rat eyes are a good model to study potential sources of retinal stem cells for their ability to replace damaged RGC. It demonstrates the usefulness of TA as an anti inflammatory agent in this regard. It also shows that ERG and specifically STRs can be used to study RGC function in rats and more importantly, it can be used as an objective functional outcome in transplant studies. Finally this work shows that adult human Müller stem cells that have the ability to differentiate into RGC can also align into the RGC layer *in vivo* and partially restore lost RGC function.

To our knowledge, this is the first known report of recovery of lost RGC function following stem cell transplantation. It is proposed therefore that Müller stem cells may constitute a useful source of retinal stem cells for functional restoration in retinal disease.

Chapter 8: General Discussion

Fish and amphibians are known to possess the ability to regenerate their retina throughout life and Müller glial cells have been shown to be the source of neurons for this regeneration (Raymond, Barthel, Bernardos, & Perkowski 2006). Müller glia with stem cell characteristics have also been demonstrated in the chick (Fischer & Reh 2001;Fischer & Reh 2003a) and rodent retina (Das, Mallya, Zhao, Ahmad, Bhattacharya, Thoreson, Hegde, & Ahmad 2006), and more recent studies have identified the existence of a Müller glial population in the adult human retina, which exhibit neural stem cell characteristics (Lawrence, Singhal, Bhatia, Keegan, Reh, Luthert, Khaw, & Limb 2007d). These cells can be easily isolated from postmortem retina and therefore constitute an interesting line of research for the development of cell based therapies to treat retinal degenerative conditions such as glaucoma.

Glaucoma, one of the largest causes of blindness in the world, is currently primarily treated with ocular hypotensive therapy. This treatment modality is largely preventative and advanced glaucoma is irreversible and inevitably leads to blindness. Stem cell therapy for retinal ganglion cell disease is not currently considered a viable treatment option. In addition to the challenge of finding a source of stem cells that are able to differentiate into retinal ganglion cells *in vivo*, stem cell therapy for RGC disease is also made more difficult by the extensive synaptic connections that the transplanted cells are required to form with the host retina and brain in order to restore lost retinal ganglion cell function (Bull & Martin 2007b). Despite this there have been a few attempts at RGC restoration by stem cell therapy (Aoki et al. 2008a;Bull, Limb, & Martin 2008b;Hill et al. 2008a) and while most of these studies are able to demonstrate some degree of differentiation and structural integration into the damaged host retina, none of them are able to demonstrate any functional recovery.

It was therefore the aim of this investigation to explore the potential of Müller stem cells as a source of RGC for use in stem cell therapy for glaucoma. Towards this end the abiltiy of Müller stem cells to differentiate towards RGC *in vitro* was examined. Environmental factors and developmental cues were used to promote this differentiation. The differentiated Müller stem cells were then transplanted into

models of RGC disease and the potential of these cells to migrate, integrate and restore function *in vivo* was analysed.

8.1 Müller stem cells express markers of RGC differentiation and possess active Notch signalling

Retinal ganglion cell differentiation is regulated by a complex network of transcription factors and signalling pathways which influence the competence of the retinal progenitors to form RGC and their ultimate cell fate commitment and differentiation (Mu & Klein 2004b). Specific developmental cues from this network of factors were used in this investigation to study the potential of Müller stem cells to form RGC. The expression of ATOH7, a marker of retinal ganglion cell competence(Yang et al. 2003a), BRN3B and ISL1, markers of retinal ganglion cell specification (Pan et al. 2008a), and HUD a marker of differentiated RGC (Ekstrom & Johansson 2003a) was studied in the Müller stem cells. It was found that Müller stem cells are able to express markers of retinal ganglion cell competence and specification. Very low levels of differentiated RGC marker expression was also seen the Müller stem cells. Various differentiation stimuli were then applied to these cells and the expression of these markers reanalysed. The differentiation stimuli included the use of extracellular matrix proteins such as laminin, matrigel, fibronectin and vitronectin as culture substrates and growth factors such as FGF2 and RA as additives in the culture medium. It was found that addition of matrix substrates and growth factors could upregulate the expression of these markers, in particular the RGC specification and differentiation markers. Matrigel and Fibroblast growth factor 2 (FGF2) were identified as the conditions that best supported expression of RGC specification markers in the Müller stem cells.

During development one of the most important signalling pathways that regulate retinal progenitor proliferation and differentiation is the Notch pathway. By preventing the expression of pro neural genes Notch activity allows retinal progenitors to continue to proliferate (Louvi & Artavanis-Tsakonas 2006d) and in order to differentiate into RGC, retinal progenitors need to escape this Notch mediated inhibition of neural differentiation (Matter-Sadzinski et al. 2005c). In this study, the levels of Notch activity in the Müller stem cells were investigated under

baseline culture conditions and following culture in the presence of extracellular matrix proteins and growth factors. Müller stem cells were found to have high levels of Notch activity under baseline conditions and this activity was down regulated when the cells were cultured under differentiating conditions i.e. with matrices and growth factors. These observations suggest that Müller stem cells are regulated by the Notch signalling pathway and are subject to its influence on their differentiation.

8.2 Notch inhibition promotes Müller stem cell differentiation towards the RGC fate *in vitro*

Since Notch activity is known to inhibit neuronal differentiation, it may be possible that in progenitors with high levels of Notch activity, neural differentiation is unlikely unless Notch activity is down regulated. Inhibition of Notch activity using gamma secretase inhibitor DAPT has been shown to promote RGC differentiation *in vivo* in chick embryonic retinal explants (Nelson et al. 2007a). In this study DAPT was used to inhibit Notch activity in the Müller stem cells *in vitro* and it was found that as seen in embryonic retinal progenitors, Notch inhibition in Müller stem cells too promoted their exit from the cell cycle and commitment to an RGC precursor fate. Not only did Notch inhibition in the Müller stem cells promote expression of RGC markers like BRN3B, ISL1 and HUD, it also induced these cells to adopt a neuronal morphology with extensive neurites and branching.

In order to establish whether Notch inhibition was merely causing an increase in the expression of these markers as opposed to increasing the number of cells differentiating towards an RGC fate, a BRN3B GFP reporter was designed. Müller stem cells were transfected with this reporter and every cell that expressed BRN3B was then identified using its concomitant GFP expression. The reporter studies revealed that treatment with the Notch inhibitor caused a greater number of cells to commit to an RGC fate. The committed cells were found to have exit the cell cycle and expressed high levels of the RGC differentiation markers. In brief, Notch inhibition was found to significantly promote RGC differentiation among the Müller stem cells.

8.3 Differentiated RGC precursors derived from Müller stem cells by Notch inhibition exhibit properties of functional neurons *in vitro*

To identify RGC precursors generated from the Müller stem cells through these *in vitro* treatments, in addition to the expression of selected RGC related transcription factors, functional elements which might indicate an RGC neuronal phenotype were also studied. The ability of the differentiated cells to respond to specific neurotransmitters by changes in their cytosolic calcium levels was examined by calcium imaging studies. This approach allowed assessment of the neural function of differentiated Müller stem cells with RGC phenotype. Calcium imaging techniques were employed to analyse the rise of cytosolic calcium in response to glutamate agonists like NMDA, and cholinergic agonists like muscarine and nicotine, both characteristically known to stimulate depolarising responses in the adult RGC. Response of Müller stem cells to stimulation by these neurotransmitters revealed that upon differentiation with Notch inhibitors, Müller stem cells acquire the ability to respond to nicotinic agonists as demonstrated by changes in their cytosolic calcium levels which are characteristic of neuronal responses. Retinal progenitors derived from embryonic rat retinae have been shown to demonstrate some neuronal activity in the form of action potentials when cultured *in vitro* (Chen et al. 2008). However the results shown here constitute the first known report of acquisition of neuronal function by a population of Müller stem cells derived from the adult human eye, following differentiating treatments *in vitro*.

8.4 Microglia and CSPGs prevent migration and integration of transplanted cells in the diseased retina

To study Müller stem cell behaviour *in vivo*, these cells were transplanted into various rat models of retinal degeneration. The ability of both the undifferentiated and differentiated cells to migrate and integrate *in vivo* was examined. Initially the Müller stem cells were transplanted into neonatal lister hooded rats since the neonatal retina is known to be amenable to transplantation. The fact that the neonatal retina has not fully completed the process of differentiation and is immunologically quiet made this a good model in which to begin studies on the

ability of Müller stem cells to migrate and integrate upon transplantation. This was followed by transplantation into the adult Royal College of Surgeon (RCS) rat eyes where the ability of Müller stem cell behaviour in a degenerating and inflamed retina was analysed. The MERTK defect in the RCS rat results in severe photoreceptor degeneration and this was therefore a good model to study Müller stem cell behaviour in a diseased retina.

Undifferentiated Müller stem cells were found to migrate and integrate into the neonatal lister hooded retina but the adult degenerating RCS retina proved to be hostile to the cells. The transplanted cells failed to migrate in the RCS retina. It was found that microglia and chondroitin sulphate proteoglycans were present in abundance in the RCS retina and prevented the transplanted cells from migrating. Microglia were found to engulf the transplanted cells thereby killing them. They were also found to be associated with chondroitin sulphate proteoglycans *in situ*, forming granuloma like structures that encircled the transplanted cells and prevented their migration and integration. Having identified these barriers to transplant cell migration and integration, systemic immunosuppression to control microglial activation and Chondroitinase ABC injections to break down the CSPG barrier were used in conjunction to promote transplant cell survival and migration. This combination was able to significantly improve the number of cells surviving the transplantation and the number of cells migrating into the different retinal layers following subretinal transplantation. Chondroitinase ABC has been used to overcome the glial scar and promote neural regeneration in spinal cord injury(Massey et al. 2006a). It has also been used in the retina to promote lentiviral mediated transduction of photoreceptors (Gruter et al. 2005b). The results from this investigation show that Chondroitinase ABC can be used to promote transplant cell migration in inflamed and degenerating retinal tissue. In light of increasing evidence of the role of CSPGs in plasticity (Berardi, Pizzorusso, & Maffei 2004a;Pizzorusso et al. 2002b), it is also possible that treatment with ChABC could improve the ability of the transplanted cells to form functional synapses with the host retina, a phenomenon that has already been demonstrated in the case of photoreceptor precursor transplantation into the retina (Suzuki, Akimoto, & Imai 2007).

8.5 A rat model of RGC depletion without microglial activation can be generated using intravitreal NMDA combined with Triamcinolone

To specifically study the ability of differentiated Müller stem cells to restore RGC function *in vivo* a rat model of RGC depletion was developed. Many of the chronic hypertension models of rat glaucoma (Adachi et al. 1996c;Levkovitch-Verbin et al. 2002a;Morrison et al. 1997a;Selles-Navarro et al. 1996a) result in slow onset RGC death with progressive rise in intraocular pressure and are associated with considerable microglial activation in response to cell death (Naskar, Wissing, & Thanos 2002d). In this work NMDA which causes excitotoxic damage to RGC when injected intravitreally was used to selectively damage RGC. NMDA itself causes microglial activation in the retina and intravitreal Triamcinolone acetate (TA) injections were used alongside to control retinal inflammation. Characterisation of this model showed that 1 week after injection with NMDA and TA, the adult lister hooded rat retina was markedly depleted of RGC and exhibited very little associated microglial activation. This provided a model of RGC depletion that was conducive to transplant cell survival and migration. While the pathophysiology of ganglion cell loss in the NMDA TA model is not similar to that seen in glaucoma, it nevertheless provides a good screen to study the ability of transplanted stem cells to replace lost RGC.

8.6 Transplantation of Müller stem cells differentiated into RGC phenotype using Notch inhibition partially restores RGC function *in vivo* in the NMDA TA model of RGC depletion

Müller stem cells differentiated towards the retinal ganglion cell fate *in vitro* were transplanted into the NMDA TA model and their ability to repair the damaged RGC in these eyes analysed. 3-4 weeks post transplantation, these animals were analysed for retinal ganglion cell function using electrophysiology and transplant cell survival and migration using immunohistochemistry. It was found that differentiated Müller stem cells were able to migrate into the GCL, IPL, and INL and express differentiated RGC markers *in vivo*. It is interesting that the cells migrated to several of the inner retinal layers and were not confined to the GCL. The transplanted cell

population though enriched for cells with the RGC phenotype was not a pure RGC precursor population and this could explain the additional migration of the cells to the IPL and the INL.

Retinal ganglion cell function can be difficult to delineate from the mass potential change that is seen in an electroretinogram (ERG) in response to flash stimulation, but recent work has shown that scotopic threshold responses (STR) can be a good indication of retinal ganglion cell function in rat full field ERGs (Bui & Fortune 2004c). The lister hooded rats were therefore analysed for their STRs without and with NMDA TA treatment and these STR responses were then compared with those of NMDA TA treated eyes which had been transplanted with the differentiated Müller stem cells.

NMDA TA treatment was found to significantly reduce the response amplitudes of the positive (pSTR) and completely erased any negative STR (nSTR) in these eyes. When Müller stem cells were transplanted in to the NMDA TA treated eyes, the ERG again showed that the pSTR was significantly reduced compared to the control eyes. However the nSTR in these eyes was significantly greater than that seen with the NMDA TA treated eyes, though still less than the control eyes. These results suggested that transplantation of differentiated Müller stem cells into the NMDA TA treated eyes was able to restore some of the nSTR lost with NMDA TA treatment. It is emphasised that this evidence is insufficient to suggest that Müller stem cells can 'replace' damaged RGC *in vivo* but constitutes some of the earliest evidence supporting the possibility that stem cell transplantation (adult human Müller stem cells in this case) can help restore lost RGC function.

8.7 Conclusion

This work has shown that adult human Müller stem cells isolated from the post mortem retina possess the same intrinsic retinal programming seen in embryonic retinal progenitors. They express markers of retinal ganglion cell competence, specification and differentiation and are regulated by the same signalling pathways crucial to embryonic retinal progenitor differentiation into RGC. Using these developmental cues, Müller stem cells can be differentiated *in vitro* into RGC precursors which express RGC specific markers, possess neural morphology and early neural functionality. To facilitate the migration and integration of these cells

upon *in vivo* grafting, it is necessary to control microglial activity and breakdown CSPG deposits. These are characteristic features of a degenerated retina and were identified as the key barriers to transplant cell migration and integration. Analysis of differentiated Müller stem cell behaviour in rat eyes treated with NMDA - Triamcinolone showed that not only are these cells able to migrate into and integrate with the ganglion cell layer, but they are also capable of restoring some degree of lost retinal ganglion cell function as seen by the recovery of nSTR on the ERG.

Müller stem cells are a good source of retinal stem cells developmentally given their retinal progenitor origins (Furukawa et al. 2000a). Because they can be isolated from the adult human retina, they also have the potential advantage of being derived from the patients own retina. Not only would the ethical dilemma of deriving stem cells from embryonic tissues be bypassed, but the fact that the cells could be derived from the patient's own retina would eliminate most major immunological issues that may affect the success of transplantation. Müller stem cells therefore would make an ideal source for repair or potentially replacement of retinal neurons. This work has defined some of the signals that could promote their differentiation towards an RGC fate and demonstrated the ability of cells thus differentiated to partially restore lost retinal ganglion cell function.

Chapter 9: Materials and Methods

9.1 Isolation and culture of Müller stem cells

9.1.1 Müller stem cell culture

Existing Müller stem cell lines at the Institute of Ophthalmology, London were used in this study (Lawrence, Singhal, Bhatia, Keegan, Reh, Luthert, Khaw, & Limb 2007d). In order to passage the cells, the media was removed and cell monolayers were dissociated with trypsin/ EDTA (Gibco™ Trypsin-EDTA (0.5% Trypsin; 5.3 mM EDTA•4Na) (10X)) followed by incubation at 37°C for 2-3 minutes. At the end of the incubation period FCS containing DMEM (Dulbecco's Modified Eagle Medium 1X with GlutaMAX, without sodium pyruvate. Cat no:61965, Invitrogen) (2.5 mls per T25 flask) was added to the cells to inactivate the trypsin. Media and cells were mixed well to dissociate the cells into a single cell suspension and then centrifuged at 1400 rpm for 5 minutes. The supernatant was discarded (thereby removing any residual trypsin) and the cell pellet resuspended in fresh media. Confluent monolayers were passaged in a 1 in 5 dilution and maintained by similar passages once a week.

Cryopreservation was carried out by resuspending the cell pellet from a T-25 flask in 1ml of a freezing mix containing 40% FCS and 10% Dimethyl Sulfoxide (DMSO, Sigma-aldrich, UK) in DMEM. The cells were transferred to a cryovial and allowed to undergo controlled freezing in an isopropanol freezing container at -80°C for 24 hours. The frozen cells were transferred to (liquid nitrogen -150°C) for long term storage.

All cells were grown in DMEM, 10% FCS and penicillin/streptomycin (Cat no: 15140-122, Invitrogen, 5mls of solution containing 10,000 units penicillin and 10,000ug streptomycin per 500mls of media) in a 37°C incubator with 5% CO_2.

9.1.2 Use of matrix substrates and growth factors to culture Müller stem cells

In order to induce differentiation, Müller stem cells were cultured on tissue culture plastic coated with various extracelluar matrix substrates. These included Laminin

(#3400-010-01, Cultrex, Trevigen), Vitronectin (Human Vitronectin, R&D Systems, Abingdon, UK Cat no: 2349-VN), Fibronectin (Sigma) and Matrigel (ECM gel, E1270, Sigma-aldrich, UK). Please note that although ECM gel was used in the experiments, it is constitutively similar to matrigel and in this work the use of the term 'matrigel' refers to the use of ECM gel. All of these substrates were reconstituted to stock concentrations as per the manufacturer's instructions and stored at -20°C. Stock solutions were then diluted in a sodium bicarbonate buffer (15mM Na_2CO_3, 35mM $NaHCO_3$, pH 9.6) to achieve solutions of working concentrations (10µg/ ml- Laminin, Fibronectin and Vitronectin and 50ug/ml- Matrigel). Working solutions were either used fresh or stored at -20°C for future use. To coat culture surfaces sufficient protein buffer solution at working concentration was added to cover the entire surface (a minimum of 1ml /T-25 flask). The flasks/ plates were then either incubated overnight at 4°C or for 2 hours at 37°C. If incubated at 4°C, the plates were transferred to 37°C for an hour prior to use. The protein buffer was then completely aspirated and cells cultured on this prepared surface.

Growth factors used were Fibroblast Growth Factor 2 (FGF2/ bFGF, F0291 Sigma-aldrich UK), Epithelial Growth Factor (EGF) (E9644, Sigma-Aldrich, UK) and Retinoic Acid (RA) (R2625, Sigma-aldrich, UK). All were reconstituted as per the manufacturer's instructions and stored in aliquots at – 20 degrees Celsius. FGF was used at a final concentration of 20 ng/ ml and RA at 50nM/ml. Depending on the experiment the growth factors were added once at the time of plating or replenished every 3 days during the experiment.

9.2 Immunostaining and Microscopy

9.2.1 Growth monitoring

Cells were followed in culture and examined under a phase contrast microscope at regular intervals. Phase images were acquired using the Leica DC viewer software and 10X or 20X phase objectives unless otherwise stated.

9.2.2 *Immunocytochemistry and immunohistochemistry*

Cells were grown as described above in Lab-Tek® glass chamber slides (16 well) (Fischer-scientific cat no: 178599 or 8 well permanox slides (Fischer-scientific cat no: 177445) for immunocytochemisty. The slides were prepared as per the experiment and density of cells plated varied accordingly. For example, when inducing neurosphere formation, cells were plated on 16 well glass chamber slides coated with laminin, matrigel or fibronectin at a density of 500 cells per well and FGF was added to the media at the time of plating. Where the neural morphology of the Müller stem cells was to be analysed, the cells were plated on permanox slides at a density of 2000 cells per well. Upon completion of experiment, or at required time points, media was removed from the wells and the cells were fixed with 4% paraformaldehyde (PFA) for 10 minutes. Slides were rinsed in PBS and cryopreserved with 30% sucrose for 20 mins. The sucrose was removed and the slides dried before either proceeding with the immunostaining or transferring to -20°C for storage and use at a later date.

If frozen, slides were defrosted and dried at room temperature for 2 hours prior to blocking. Blocking reagent was prepared in advance (Roche Cat no:1096176, 0.5% in PBS, microwaved for 10s and stirred on heater for a further 10 mins till a uniform cloudy solution was obtained. This was cooled at 4°C prior to use). Cells were blocked with this reagent for 1 hour at room temperature prior to staining. Primary antibodies were diluted appropriately in the blocking reagent and the cells were incubated for 2 hours at room temperature or overnight at 4°C in a humidified chamber to prevent drying out. A parallel secondary antibody staining only (ie no primary antibody was added) was included in each experiment to control for background staining of the secondary antibody. On completion of incubation with the primary antibody, the slides were washed in Tris Buffered Saline (TBS) at least 3 times, each wash lasting 5 minutes. Secondary antibodies (Alexa fluor, Moleclular probes, see antibody table) diluted appropriately in the blocking reagent were added and slides were incubated at room temperature for 1 hour in the dark to avoid any fluorescence excitation by light. Cells were then washed with TBS three times as before. Nuclei were counter stained with DAPI (4', 6-Diamidino-2-phenylindole dihydrochloride, Sigma, D9542), diluted 1 in 5000 with Phosphate

Buffered Saline-PBS, for a minute. After a final wash with TBS and rinse with distilled water, slides were mounted. In order to mount, all chamber cast and silicone separators were removed. This included scraping away residual adhesive on the slide with a scalpel blade to prevent uneven surface during mounting. Cells were mounted with vectashield mounting medium (Vector labs, H-1000) and sealed with nail varnish for microscopic analysis.

Immunohistochemistry of tissue sections was performed using the same protocol, but tissues were blocked with a blocking reagent consisting of PBS containing 0.3% Triton and 5% Donkey Serum (Jackson Immuno Research Laboratories, Inc. 017-000-121). The washes were performed in PBS and lasted 10 mins each.

Images were acquired either using a Leica epifluorescence microscope or a Leica TCS P2 confocal microscope. For confocal microscopy, a 40X oil immersion objective was used unless otherwise stated. All image analysis was performed using the Leica confocal software for image acquisition and analysis or the NIH image J software. Cell counts were performed using cell counter on image J.

9.3 RT-PCR

9.3.1 RNA isolation:

To isolate RNA two different kits were used. When large numbers of cells were available for RNA isolation, the RNeasy mini kit (Qiagen, 74104) was used. This kit allows for the isolation of RNA from a million cells. For substantial yields of RNA therefore, cells were grown to confluency as described above in T175 flasks. To isolate the RNA, cells were detached with 2 mls of trypsin after removing the media. The cell pellet obtained following centrifugation was washed with 500 µl of PBS to remove the medium, and centrifuged again at 3000 rpm for 5 minutes. The cell pellets were resuspended in 600ul Buffer RLT with 6 ul β mercapto-ethanol (Sigma-aldrich, M-3148) (part of the RNeasy Kit) to induce cell lysis. This solution was then either used to isolate RNA straightaway or stored at -80°C for later use. RNA isolation was performed as per manufacturer's instructions. DNase (RNase-Free DNase Set, Qiagen, 79254) treatment was applied during RNA isolation to eliminate any genomic DNA contamination of the RNA isolated. After elution of RNA from the

column in RNAse free water (30-40ul), the concentration of RNA was determined using a spectrophotometer (Eppendorf BioPhotometer or Nanodrop-1000, Thermoscientific). RNA samples were stored at -80 degrees and thawed on ice before use for RT- PCR.

When only small numbers of cells were available, RNA was isolated using the RNAqueous®-Micro Kit (Ambion AM1931, Applied Biosystems). In this case as few as 1000-10000 cells could be used for RNA isolation. RNA was isolated as per manufacturer's instructions. The RNA obtained however, was not DNAse free, and required further treatment with DNAse (RQ1 RNase –free DNase, M610A, Promega). For this procedure, 8µl of RNA were treated with 1µl of DNAse and 1 µl of DNase buffer at 37°C temperature for 30 minutes. The reaction was then stopped with 1 ul stop solution and incubation at 65°C for 10 mins. RNA was incubated on ice for a minute following this treatment and then either stored at -20°C or converted to cDNA using reverse transcription (RT).

In instances where fewer than 1000 cells were available (Eg: Low yields following cell sorting), the SuperScript CellsDirect cDNA synthesis kit (SKU# 18080-200, Invitrogen, UK) was used to isolate the RNA. This kit allows for the direct and efficient synthesis of cDNA from small amounts of RNA. cDNA synthesis was carried out as per manufacturer's instructions and the resulting cDNA used directly for PCR reactions.

9.3.2 Reverse Transcription (RT) (First strand cDNA synthesis):

First strand cDNA synthesis kit for RT-PCR (AMV) (Roche Applied Biosciences) was used to generate cDNA from isolated RNA. In each reaction, 1µg of RNA was used to generate cDNA as follows. A 20 µl reaction mix was prepared containing 10X reaction buffer, MgCl2 25mM, 10mM dNTP mix, oligo (dT)15 primer, RNase inhibitor, AMV reverse transcriptase, RNA and water (as per kit instructions). The mix was vortexed and briefly centrifuged before transfer to thermocycler. Incubations were carried out at 25 ^{0}C for 10 minutes, 42 ^{0}C for 60 minutes, 99^{0}C for 5 minutes and 4 ^{0}C for 5 minutes. The resulting product was either used immediately in PCR reactions, or stored at -20 ^{0}C for future use.

When RNA was isolated using the ambion kit, depending on the yield, the amount of RNA used for the RT reaction varied from 100ng-1µg. In all cases, when

comparing samples within a given experiment, same amounts of RNA were used for the RT reactions. This enabled the comparison of the PCR results in semi-quantitative PCR as well as in real-time quantitation.

9.3.3 PCR

Expand high fidelity plus PCR system (Cat no # 03300226001, Roche Applied Biosciences) was used to carry out the PCR. For these studies, 20 µl reaction mix was prepared on ice using 2 µl of the cDNA and reaction buffer, dNTP mix, primers, polymerase enzyme and water as per kit instructions. All primers were obtained from Invitrogen in the desalted form and reconstituted to 50µM concentration in TrisHCl-EDTA buffer. Final primer concentration used in the reaction was 0.4 µM/ml. The PCR mix was thermocycled at 94 ^{0}C (initial denaturation) for 2 minutes, 94^{0}C for 30 seconds, annealing temperature for 30 s, 72 ^{0}C for 1 minute (extension) and repeat from step 2 for 34 cycles before a final extension at 72 ^{0}C for 7 minutes and held at 4 ^{0}C. The cycling was performed using an Eppendorf mastercycler gradient thermocycler (#950000023, Eppendorf).

4 µl of PCR product with 2 µl loading dye, and 6 µl water was run on a 1% agarose gel with either 1 in 15000 SYBR gold nucleic acid gel stain(S-11494, Molecular Probes, Invitrogen) or 1 in 10000 Gel red nucleic acid gel stain(Cat no:41002, 10000X in DMSO, Biotium Inc). 1kb DNA ladder (TrackIt, Cat no:10488-085, Invitrogen) diluted 1 in 10 was run alongside the test samples. Gels were run at 100V for 35-40 minutes, visualised under a UV light and imaged using Genensnap advanced image acquisition software (Syngene). Auto exposed images were used for densitometry using image J software for semi quantitation. All bands were normalised to GAPDH loading controls.(Sambrook, Fritsch, & Maniatis 1989)

9.3.4 Real Time Quantitative PCR

For real time Quatitative PCR (QPCR), the cDNA was prepared as described previously. Given that product detection by QPCR is highly sensitive, smaller amounts of starting cDNA are required per sample and the cDNA obtained from 1µg of RNA was diluted 1 in 10 for each of the reactions.

9.3.4.1 Primer optimisation

Before comparing expression of the genes under different treatment conditions, the primers for each gene were optimised. In each QPCR, reactions were made up to 25 µl, the primers accounted for a maximum of 4 µl. For standardisation, various concentrations of the primers were tested as follows- forward to reverse in µl - 1:3, 2:2, 3:1 and 1:1(with the additional 2 µl made up of water). 6 repeats of each condition were prepared and the QPCR run to establish which set up had the best amplification and the least dimerisation. Based on the proportions, subsequent comparative QPCRs were performed.

9.3.4.2 Reaction set- up

For QPCR the SYBR Green JumpStart Taq ReadyMix for quantitative PCR mastermix (S4438, Sigma-Aldrich, UK) was used. This mastermix contains the sybrgreen tagged nucleotides and the nucleotides in a buffer that is collectively used to make up the PCR reaction along with the cDNA and the primers. Each 25µl reaction consisted of 12.5 µl of the master mix, 0.25 µl of the indicator dye (provided with the master mix), 2 µl of the cDNA, 4 µl of the primers and water to make up the remaining volume. Twelve repeats of each condition were prepared. In order to reduce pippeting errors, all 12 repeats were made up into one master mix and then divided into 25 µl samples on the QPCR plate. An example of a set up of a typical experiment where the expression of a gene (say ATOH7) was being compared in 4 different treatment conditions is described below: Four master mixes, one each for the 4 different conditions with primers for ATOH7 would be prepared. Each master mix received cDNA pertaining to the condition of interest, for eg. cDNA from cells grown on MG, LN, FN, VN. Each experiment also contained its own internal loading control where expression of house keeping genes like GAPDH, B-actin or Pgk1 was used to establish the relative levels of cDNA being loaded in each condition. Therefore along with the 4 master mixes for ATOH7 there would also be 4 master mixes for one of the above house keeping genes for the 4 different conditions. With 12 repeats for each condition and 8 different conditions overall one entire 96well plate (12 by 8) was required for an experiment of the above description.

Care was taken to arrange the samples in a manner conducive to analysis later on. Towards this, the replicates were prepared in sets of three in a row and four such rows to give a total of 12 samples for each condition. This arrangement is illustrated in Fig 9.1 and the reason such an arrangement is useful is detailed in the analysis section below.

The reactions were prepared on ice with care to prevent contamination with any substances that might contain RNases and DNases. Once ready they were stored on ice in the dark and transferred as such to the QPCR machine for the run. This was to prevent photobleaching of the light sensitive reagents in the Sybr green master mix that would interfere with the outcome of the experiment.

9.3.4.3 Real time QPCR run

The reactions were prepared and transferred as above to an applied biosystems QPCR machine. To set up the reaction, a new database was opened for a clear 96 well plate. Within the run set up, the thermal cycling parameters were set up such that there was initial denaturation at 94°C for 2 minutes followed by 40 cycles of 94°C for 15 seconds, 60°C for 30 seconds, 72°C for 1 minute and finally a stage of dissociation. The dissociation stage was always used to keep a check on the final product and ensure there was no dimerisation. The detector used was the sybrgreen detector (prp31). Data was collected between the 60°C and 72°C stage of each cycle as well as during dissociation. Ramp rates were set to 100% for all of the stages except for the last step of dissociation which was at 2%. The wells were labeled according to the samples they contained and the entire run settings were saved. The QPCR machine was then turned on and connected to the software. Prior to the run, the 96 well plate with the samples was centrifuged briefly to allow all of the reagents to settle to the bottom, sealed with adhesive film to prevent evaporation and covered with a heat mat to retain heat within the plate. Once the

	1	2	3	4	5	6	7	8	9	10	11	12
A	Nm ato h7	Nm ato h7	Nm ato h7	Ln ato h7	Ln ato h7	Ln ato h7	Mg ato h7	Mg ato h7	Mg ato h7	Vn ato h7	Vn ato h7	Vn ato h7
B	Nm ato h7	Nm ato h7	Nm ato h7	Ln ato h7	Ln ato h7	Ln ato h7	Mg ato h7	Mg ato h7	Mg ato h7	Vn ato h7	Vn ato h7	Vn ato h7
C	Nm ato h7	Nm ato h7	Nm ato h7	Ln ato h7	Ln ato h7	Ln ato h7	Mg ato h7	Mg ato h7	Mg ato h7	Vn ato h7	Vn ato h7	Vn ato h7
D	Nm ato h7	Nm ato h7	Nm ato h7	Ln ato h7	Ln ato h7	Ln ato h7	Mg ato h7	Mg ato h7	Mg ato h7	Vn ato h7	Vn ato h7	Vn ato h7
E	Nm pgk 1	Nm pgk 1	Nm pgk 1	ln pg k1	ln pg k1	ln pg k1	mg pgk 1	mg pgk 1	mg pgk 1	vn pg k1	vn pg k1	vn pg k1
F	Nm pgk 1	Nm pgk 1	Nm pgk 1	ln pg k1	ln pg k1	ln pg k1	mg pgk 1	mg pgk 1	mg pgk 1	vn pg k1	vn pg k1	vn pg k1
G	Nm pgk 1	Nm pgk 1	Nm pgk 1	ln pg k1	ln pg k1	ln pg k1	mg pgk 1	mg pgk 1	mg pgk 1	vn pg k1	vn pg k1	vn pg k1
H	Nm pgk 1	Nm pgk 1	Nm pgk 1	ln pg k1	ln pg k1	ln pg k1	mg pgk 1	mg pgk 1	mg pgk 1	vn pg k1	vn pg k1	vn pg k1

Figure 9.1: QPCR setup

Set up of a 96well plate for QPCR. Four test conditions are used here: cells cultured without matrix (NM), laminin (LN), matrigel (MG) and vitronectin (VN). For each condition 12 (3X4) replicate reactions are set up for the test gene (Atoh7) and the control gene (Pgk1). In the table above, each reaction set is coded with a different colour. The above set up allows for easy analysis of the results of the QPCR with the DART PCR software.

plate was ready the tray of the machine was opened, the tray placed in it and the run started.

9.3.4.4 QPCR analysis

Upon completion of the run which took about 2.5 to 3 hours, the tray was removed from the machine and the results analyzed. The ct (cycle at which exponential amplification of the DNA begins) values of each sample and the dissociation curves could be visualized within the software and exported in the form of images (Fig 9.2). The final analysis was performed using the DART-PCR version 1.0 software introduced by Pierson, Butler and Foster in their 2003 paper(Peirson, Butler, & Foster 2003). The raw data was imported into the spreadsheet within this software such that the values of the cycles progressed down the column and the samples themselves progressed from 1-96 across the row. Once the data had been imported in this fashion, the software could be used to analyze the results. As mentioned in the reaction set up the samples were arranged so that there were 4 rows of three each per condition, one beneath the other. In the DART PCR software, the sample set up is numbered 1, 4, 7 and 10 for the starting well of each such set. By picking 4 rows under each number one selects the entire sample set of one condition and can be analyzed as such. In this manner, by simply placing the raw data correctly, the DART PCR software can be directly used to analyze the amplification kinetics and the relative quantification of the different samples (Fig 9.3).

The software summarizes the Ct values and calculates the efficiency of amplification per data set. Using this it then generates a relative expression value (R_0) which can be compared across samples. The R_0 values of the test gene are normalized to the R_0 values of the standard (house keeping) gene in each case and the ratios thus obtained are compared across samples to get an idea of the fold change seen across samples in the gene of interest. The 12 repeats for each condition allow for internal variation thereby allowing the final difference detected to be statistically significant (Fig 9.4).

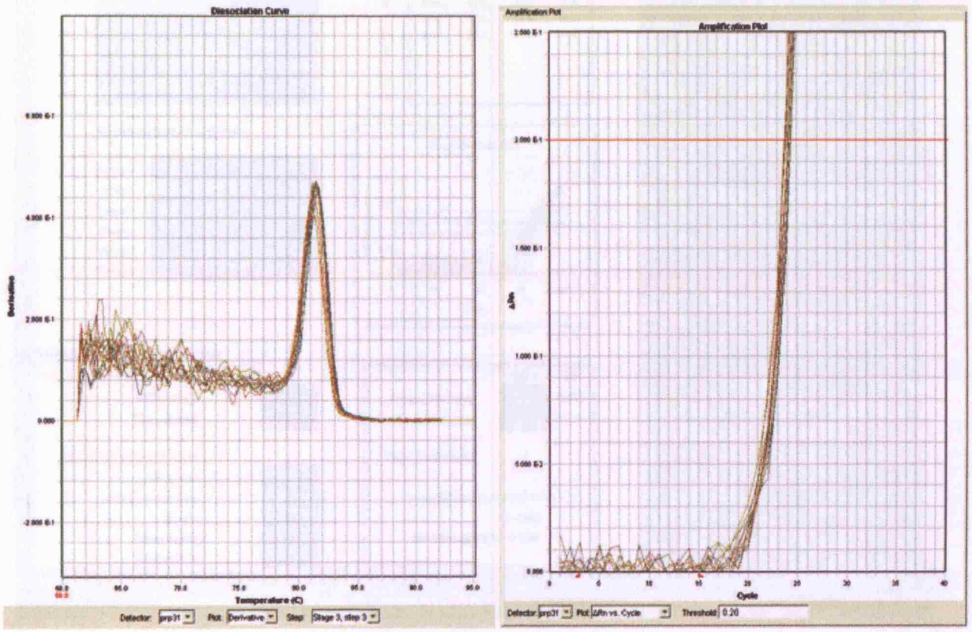

Figure 9.2: QPCR dissociation curve and amplification plot

The graph on the left shows an example of a good quality dissociation curve from a QPCR reaction. After the product is formed, it is further heated until dissociation occurs. The temperature at which dissociation occurs is plotted on the X axis. The single peak seen indicates that only one predominant product is being formed which dissociates between 90-95°C. The absence of any other peaks suggests that there is no primer dimer formation. The dissociation curve is therefore used to determine the quality of the primers. The graph on the right is an amplification plot with the Ct values plotted on the X axis. The Ct value is the cycle number at which exponential increase in product begins. In the above example this is at cycle 19.

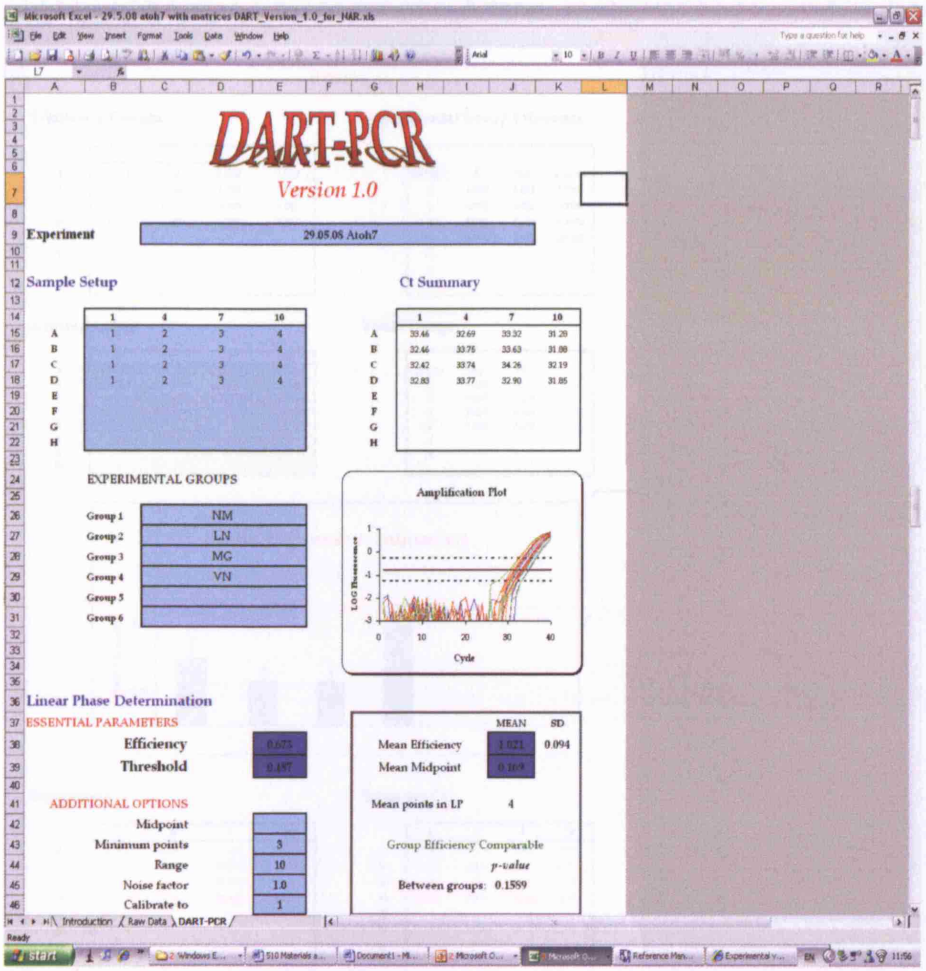

Figure 9.3: DART PCR software

Raw data from the PCR is imported into DART and shows up in the sample set up column on the top right. The corresponding CT values and amplification plots are displayed. The programme calculates the efficiency of the reactions individually and estimates comparability of the efficiencies.

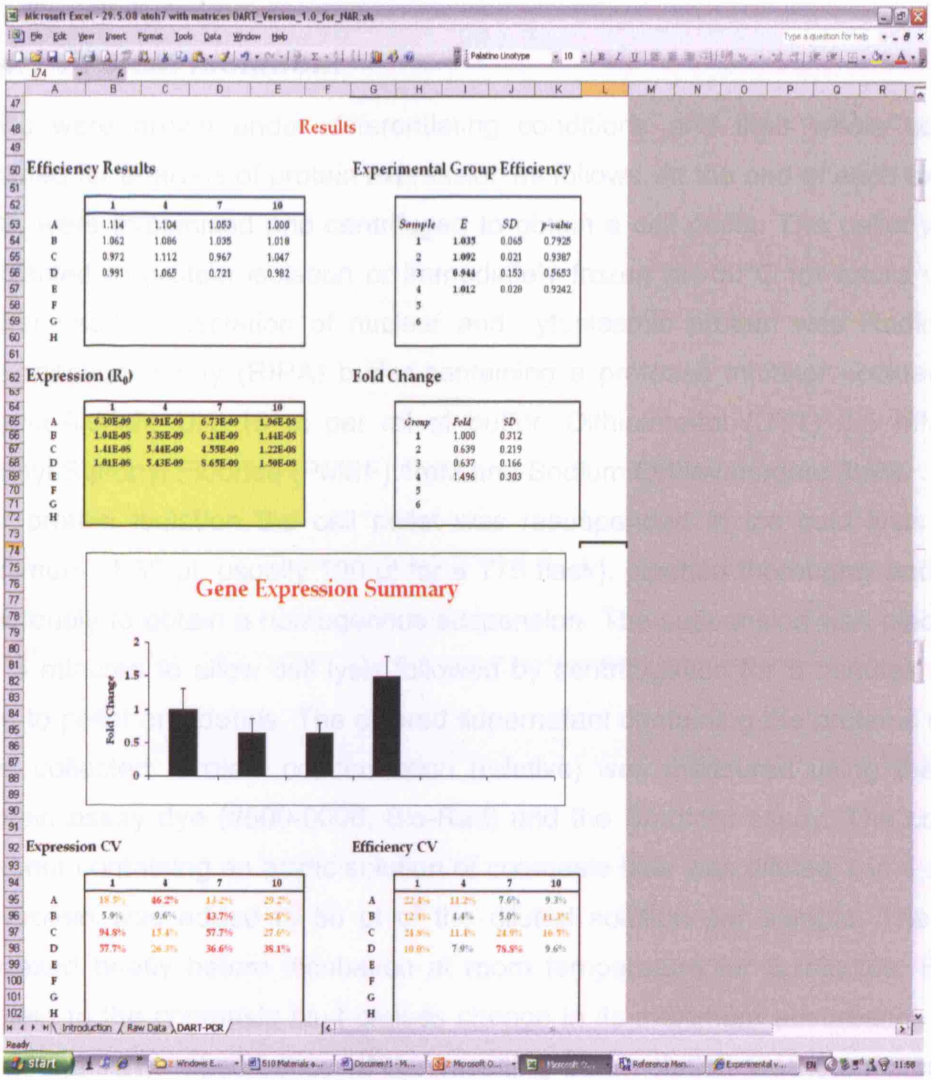

Figure 9.4: DART PCR software

Based on the efficiency the expression (R_0) values are calculated. The same analysis is carried out with the test gene and the control gene. The expression values of the test gene are divided by those of the control gene to control for loading differences if any. These values can then be charted as displayed in the gene expression summary.

9.4 Western Blotting

9.4.1 Protein isolation:

Cells were grown under differentiating conditions and their whole cell lysates isolated for analysis of protein expression as follows. At the end of each experiment, cells were trypsinised and centrifuged to obtain a cell pellet. The pellet was either subjected to protein isolation or immediately frozen at -80°C for future use. Lysis buffer used for isolation of nuclear and cytoplasmic protein was Radio Immuno Precipitation Assay (RIPA) buffer containing a protease inhibitor cocktail (P8340-Sigma-Aldrich, UK)-10 µl per ml of buffer, Dithiothreitol (DTT) 0.5 mM, Phenyl Methyl Sulfonyl Fluoride (PMSF) 1mM and Sodium Orthovanadate 3mM.

For protein isolation the cell pellet was resuspended in ice cold lysis buffer (a minimum of 50 µl, usually 100 µl for a T75 flask), pipetted thoroughly and vortexed vigorously to obtain a homogenous suspension. The suspension was placed on ice for 5 minutes to allow cell lysis followed by centrifugation for 5 minutes at 10,000 rpm to pellet any debris. The cleared supernatant containing the proteins of interest was collected. Protein concentration (relative) was measured using the Bio-Rad protein assay dye (#500-0006, Bio-Rad) and the Bradford assay. The colorimetric reagent containing an acidic solution of coomasie blue was diluted 1 in 4 and 2.5 µl of protein was added to 50 µl of the diluted solution per sample. The mix was vortexed briefly before incubation at room temperature for 5 minutes. Binding of protein to the coomasie blue causes change in its maximum absorbance form 465 to 595nm. The absorbance of the resulting blue solution was then measured at 595nm using a spectrophotometer. Protein volumes loaded onto the electophoresis gel were adjusted according to the relative absorbance readings. In addition a loading control (B-actin) was also used in each experiment to allow for further normalization of amount of protein loaded. All protein samples were aliquoted and stored at – 80°C for long term use.

9.4.2 Protein Gel Electrophoresis:

NuPAGE electrophoresis gels and buffer systems (Invitrogen, UK) were used for gel electrophoresis. Gels were selected based on the molecular weight of the protein of

interest. 10% Bis-Tris gels (NP0315, Invitrogen, UK) were used in combination with the MOPS SDS running buffer (NP0001, Invitrogen, UK) for resolution of proteins between 20 and 75 kD in size. In this work these included- Brn3 (55kD), HUD((40kD), ISL1(37kD) and β-actin (42kD). For proteins with molecular weight greater than 75kD namely Notch intra cytoplasmic domain (ICD) which is 110kD in size and full length Notch (FL notch) (250-300kD), 3-8% tris-acetate gels (EA03185BOX 1.5mmx15 well, EA0378BOX 1.5mmx10well) were used in combination with the tris –acetate running buffer system(20X, LA0041). All gels were of 1.5mm thickness but depending on the number of samples being run, the gels used contained either 10 or 15 wells. Each well is able to hold 30 µl of solution and the proteins were therefore prepared as follows. When using a 10 well gel, 30 µl of loading sample was prepared with 3 µl of reducing agent (10X), 7.5 µl of loading buffer (LDS 4X) and a maximum of 19.5 µl of protein sample. As explained before, in order to load equal amounts of protein, this volume of 19.5 µl was adjusted based on the absorption readings and the remaining volume made up with water. With the 15 well gels, 9 µl of loading buffer (slightly higher concentration than 1X in the final solution) was used with a maximum of 18µl of protein sample. This increase in loading buffer in the 15 well gels allowed for the samples to be heavier than otherwise and prevented cross contamination between samples in the closely placed adjacent lanes. The more widely spaced wells in the 10 well gels did not require this extra precaution.

The loading samples were boiled at 80^0C for 10 minutes to denature the protein. The pre prepared gels were removed from their packaging, washed in distilled water and fitted into the XCell *SureLock*™ Mini-Cell mini vertical electrophoresis system (Invitrogen, UK) after removal of the white tape seal to allow for communication of the gel with the buffer system during electrophoresis. The chamber was then locked to generate a water tight compartment for the gel and the electrodes. Into this compartment, working concentration running buffer augmented with antioxidant (500 µl/ 200mls buffer) was added. The wells were then loaded with the protein samples as well as the ladder and run at 180V for 50 minutes.

9.4.3 Gel Transfer:

Poly VinyliDene Fluoride (PVDF) membranes (Hybond-P # RPN303F, Amersham) were hydrated in absolute methanol for 2 minutes, washed in distilled water and equilibrated in working concentration transfer buffer before being applied to the gel. The transfer was carried out at 35V for 90 minutes using the XCell *SureLock*™ Mini-Cell mini transfer set up (Invitrogen, UK).

9.4.4 Immunoblotting:

Following transfer, PVDF membranes were blocked in 5% milk and 3% FBS in TBS with 0.1% Tween 20 at 37 degrees for 1 hour. Primary antibody was diluted in blocking reagent and the membrane was incubated with this overnight at 4 ^{0}C on a shaker. The next morning the membrane was washed 4-6 times over an hour with TBS with 0.1% Tween 20. The membrane was then incubated for 1 hour at room temperature in the secondary antibody (species specific peroxidase conjugated IgG, Jackson Laboratories) diluted 1 in 10,000 in the blocking reagent. On removal of the secondary antibody, the membrane was washed again over an hour with TBS with 0.1% Tween 20, and bound antibody reacted with the ECL advanced western blotting chemiluminescent immunodetection system according to the manufacturer's instructions. Images were then visualised using Hyperfilm ECL (Amersham Biosciences/ GE Healthcare). Alternatively the membrane was directly imaged using the Fuji LAS1000 image reader. Band densitometry was performed using Image J. (Walker 2002)

9.5 Cloning and transfection

9.5.1 Brn3 reporter construct

pEGFP1, a promoter less GFP vector (clonetech) with a kanamycin resistance cassette was used as a backbone (Fig 9.4). Brn3 putative promoter region (1.6 kb region upstream of human BRN3B coding sequence) was inserted into the multiple cloning site such that GFP expression was under the control of the BRN3B promoter.

A

1 TAGTTATTAC TAGCGCTACC GGACTCAGAT CTCAACACCG CGGGAAGTAT AGAGAAAATG
61 GGATCCAGAA GGAGAGGAAG TAGTGTGTGT GTGTGTGTGT GTGTGTGTGT GTGTGTGTGA
121 CAGAGAGAGA GAGATAGATA GAAAGAGATT ATCTCCTTTT GCAACTGGAA CCAAGAGTGT
181 GTGTCCATCT CTAGGAAAAG TGGTCTGCAC TGGGACTGGG ACAGAAGTGG GAGTGAAGTG
241 TCAGCTAAAA ATAGGCTCCG CACCGAGAGG CTGTGGAAAT GAAGATAAGT GAGGTTTGTG
301 CCAGCCCCCG AGGGTGTGTG TGTGTGTGTC TGTGTTGTGG GGTGTATTCA GCAGCATATG
361 CGCTGTGTAA TTTCTGACCT TCCCTCTCCC TGTCAGTTGC CCCTTCTTCC TTTGATTGTG
421 GCTAATGAAG AATAATAAAT CCAGGGGCAG GGTTTGCCAG TGGATCCTTC CAAGACTCAA
481 CTCGAACTGT ACTGGATACA GGGAGGAGGA GGAAGAGAAA AGGGGGGCAA GAGGAGCGTG
541 TGTGTGTGCC TGTGTGTATG TGTGTGTGTG TTGTGGGAGG GGTGGGGACA GCGGGGAGGG
601 GGAGGAGTCG CATGCGCACA GACGACCCGA GCCTGCTCCG CGGCTGTCCA ATCCGCTGAG
661 AGCTGCGAGA AATCGAGTGA GAGAAAGCCC TGCAGCCCCT CCGACCCCAT GTCTCTTTGG
721 CACCAGGCAC CCGCCGGGCC GTGGGGGGCT CGTAGCCGAA CGCCGACCTC CGCTCGTATT
781 GGGCTGGGAG TTCAGAGCCG CGCGCAGAAC CCGGGTTGGC CGCAACGTCT GTGTTCTCAG
841 CGGTGGCCGG GAACCTGGGA TCAGGGTCAC CTGAGCTGAC GGGGTGGGGG CGGGCCGAGT
901 GGGGTTGGAA GCCTGGAACT TAGTGGTAAG CAGGAGGCGT AGGAGGTGGC AGCCAGGTAA
961 GAGGCACTCT TACCTACCCA ACGCTGGCTT GGGCCGCAAC TTTATTTGGG AGTTTCTTTT
1021 TCCGGTGAGA CAGAGACCCG GCAGAAGAAG CGGGAGGGGC TGGAGGCTGG TCCTTAGGTA
1081 GGCACTGCCC GGCGACTGGA GCGCGGACCT GGCCATTTGG GTGGGGTTGA GTGGGGGCGC
1141 GATTGTGAGT AGCAGCCGCG GGACGCTGCG AAGGGGCGGC GGCAACAGAG CACGGGCGGG
1201 GGCAGAAAAG AGGCGGCGGA GGGCGCGGTG GGGGAGCGCG AGGCGAGTGC TGAGAGAGCA
1261 GAAAGGACTC AAGCCTGAGG GGAGTAGAGA GGAAGAAGGG GCAACGCGAG AAACCGAACA
1321 GGAGCCGGCG TTTCCTGGCA AGGGAGGGCG GAGGCGCGCG GGAGAGAGGG AGAGAGGGAG
1381 GGCGGGGGGC GCGGGGGTAG GCGCGGGGAG AGGGGAGTAT AACTCGCCGG CCGCGAGGAG
1441 CGGGGGCAGT TTCGGGTGCC GAGGTCTGCA GCTAGCGGCA AGCGGAGTCA GGCATCCGTT
1501 CAGACTGACA GCAGAGGCGG CGAAGGAGCG CGTAGCCGAG ATCAGGCGTA CAGAGTCCGG
1561 AGGCGGCGGC GGGTGAGCTC AACTTCGCAC AGCCCTTCCC AGCTCCAGCC CCGGCTGGCC
1621 CGGCACTTCT CGGAGGGTCC CGGCAGCCGG GACCAGTGAG TGCCTCTACG GACCAGCGCC
1681 CCGGCGGGCG GGAAGGTCGA CGGTACCGCG GGCCCGGGAT CCACCGGTCG CCACCATGGT

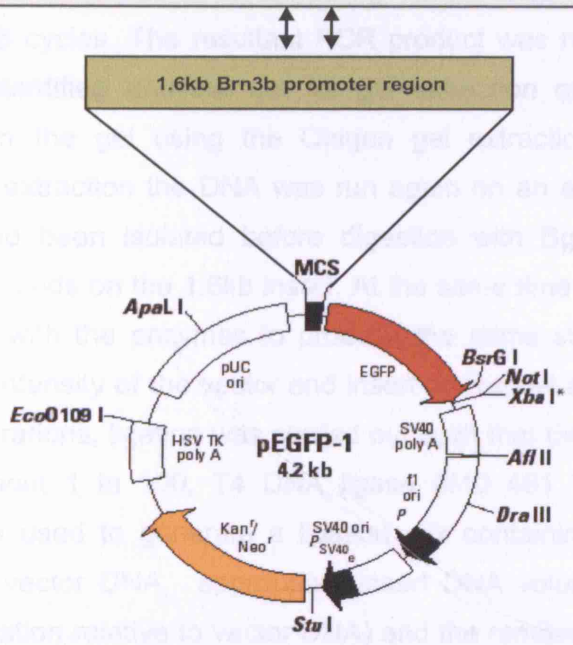

Figure 9.5: Brn3b reporter

Brn3b promoter region, 1.6kb sequence upstream of the Brn3b coding region is shown here. This region was amplified from an appropriate BACS clone and inserted into multiple cloning sequence of the pEGFP-1 vector as shown in the vector map above. The pEGFP-1 vector has a promoterless GFP coding region, and a Kanamaycin/Neomycin resistance casette.

To create the reporter, first the putative promoter region of the human BRN3B gene was identified. The UCSC genome browser was used to analyze the sequence upstream of the BRN3B coding sequence. Areas of strong conservation through species in this region were then used to ascribe a 1.6kb sequence upstream of the coding region as a putative promoter region for the gene (Fig 9.5). This sequence was then run through the FPROM Human promoter prediction software to confirm the presence of promoter motifs in this region. Following determination of this promoter sequence, primers were designed to PCR amplify the 1.6kb promoter region from a bacterial artificial chromosome (BAC) clone (CTD-2600K9, Invitrogen, UK) spanning the region such that the restriction sites of BglII and SalI were introduced upstream and downstream of the promoter region respectively. Primers to amplify the 1.6 kb genomic sequence were designed using clone-manager suite and contained the Bgl II and Sal I restriction sites (see list of primers in appendices BRN3B 4586 Bgl II F1 and BRN3B 6231 SalI R). PCR amplification of the promoter region was performed at 60°C annealing temperature with extension time of 3 minutes for 36 cycles. The resultant PCR product was run on a 1% agarose gel, 1.6kb band identified and cut out for gel extraction of the product. DNA was extracted from the gel using the Qiagen gel extraction kit (#28704, Qiagen). Following gel extraction the DNA was run again on an agarose gel to ensure the right band had been isolated before digestion with BglII and SalI enzymes to produce sticky ends on the 1.6kb insert. At the same time the backbone vector was also digested with the enzymes to produce the same sticky ends. Based on the relative band intensity of the vector and insert on the gel as well as their respective molar concentrations, ligation was carried out such that the ratio of the vector to the insert was about 1 in 100. T4 DNA ligase (#10 481 220 001, Roche applied sciences) was used to generate a ligation mix containing 1µl ligase, 10µl of 2X buffer, 1µl of vector DNA, appropriate insert DNA volume (calculated based on DNA concentration relative to vector DNA) and the remaining volume made up with water to a 20 µl reaction. The ligation mix was incubated overnight at 16 ^{0} C. The ligated product (BRN3B reporter) was transformed the next day using one shot competent E.coli (Invitrogen, UK).

9.5.2 Transformation

2.5 µl of ligation product was added to 25 µl of bacteria (One Shot Top10 competent E.coli, Invitrogen, U.K.), previously thawed on ice. The mix was allowed to stand in ice for 30 mins. Heat shock was applied at 42 ^{0}C for exactly 30 s and the bacteria replaced on ice. 125 µl of prewarmed SOC (super optimal broth with catabolite repression) media was added and the mix incubated in a 37^0 C incubator shaker at 230 rpm for 1 hr. 50-100 µl of the transformed mix was plated on to kanamycin (50 µg/ml) containing agar plates and incubated overnight at 37^0 C. A vector control with only vector and no insert was also applied. Next morning the plates were transferred to 4^{o}C storage and colonies picked in the evening for overnight inoculation into 5-6 mls of LB media with kanamycin. DNA isolated from the minipreparations was restriction digested with BglII and SalI and run on a 1% agarose gel to look for the insert of anticipated size.

Clones with the correct insert were sequenced; the DNA expanded and isolated using the nucleobond AX500 maxiprep kit (#740531, Nucleobond, Machery-Nagel). Care was taken to generate a high concentration DNA solution (at least 1 µg/µl DNA concentration so as to enable the use of very small volumes of DNA during electroporation. The DNA concentration was measured on a spectrophotometer and DNA stored at -20^{0}C.

9.5.3 Sequencing

To prepare the DNA for sequencing, a reaction mix was prepared with the following reagenst- Big dye (4 µl/rxn) and sequence buffer (2 µl/rxn) (Applied Biosystems), pEGFP sequencing primer (3.2pmol/rxn), 6 µl miniprep DNA and water to make a 20ul reaction. The sequencing reaction was run as follows: 96°C for 1 minute, 96°C for 10s, 50°C for 10s, 60°C for 4 mins and cycled for 35 cycles. The PCR product was cleaned using a mix of NaOAc 3M (2µl), EDTA 0.5M (0.59 µl) and 95% Ethanol (50 µl). 20 µl of DNA was incubated with this mix at room temperature in the dark for 15 minutes. The mix was then centrifuged at 13000 rpm for 30 minutes. 70% Ethanol (70 µl) was added and the mix centrifuged at 13000rpm again for 15 minutes. The pellet obtained at the end of this centrifugation step was dried at 65°C for 5 minutes or at room temperature for 15 minutes in the dark. The dried pellet

was then resuspended in 12 µl of formamide and sequenced on an Applied Biosystems 3730 DNA analyzer.

9.5.4 Transfection

Cells were transfected using electroporation. Low passage (P11-P25) MIO cells were grown to confluence in T 175 flasks. Once ~90% confluent cells were detached using trypsin and the cell pellet collected. Cells were resuspended in a freshly prepared electroporation buffer (containing sterile PBS 9.45mls with 0.55mls 100mM Glucose and 10ul 1M $CaCl_2$) to yield a final cell concentration of at least 10^8 cells/ml. DNA was added to this cell suspension at 10µg/ml final concentration and mixed well. The cell DNA mix was transferred to an electroporation cuvette and incubated on ice for 10 mins. The cells were then electroporated using a Biorad gene pulser II at 1.2 KV and 50 µF. Following electroporation cells were allowed to rest at 37°C for 5 minutes, resuspended in pre warmed media and plated as desired.

9.5.5 Selection of transfected cells

Post transfection cells were incubated overnight at 37^0C. The next day the supernatant along with dead cells was removed and replaced with fresh media. Since the vector contains a neomycin resistance cassette, the cells were then cultured with G418 (gentamycin) to allow only the transfected cells (which would be expected to demonstrate resistance to G418) to survive thereby positively selecting for the transfected cells. G418 was added to achieve a final concentration of 400 µg/ml and the cells were allowed to remain in culture for subsequent RNA/ protein isolation, fixing for immunostaining or FACS sorting.

9.5.6 Isolation of clones

About 1000 cells were plated following each transfection onto a 60 mm dish and G418 added to allow for selection of discrete clones. Media was changed every week at which time the dish was also examined for growing clones and their green or non green nature under an epifluorescence microscope. 3-4 weeks after plating, small to medium sized discrete clones were identifiable. These were isolated by selective dissociation within sterile clone rings using Trypsin LE solution and

transferred on to 96 well plates. The cells were pelleted by centrifugation of the plate and the supernatant replaced with fresh media. The clones were thus expanded in culture and cells were then used to isolate RNA using the SuperScript III cDNA synthesis kit (invitrogen) and PCR performed on the cDNA obtained. (Sambrook, Fritsch, & Maniatis 1989)

9.5.7 Fluorescence Assisted Cell Sorting (FACS)

FACS analysis was performed using the FACscalibur machine. Müller stem cells transfected with BRN3B reporter were cultured in 12 well plates under different culture conditions for a week. The cells were then trypsinised and resuspended in fresh culture medium without serum (500µl) for the sorting. The sort gate was set based on a control sample before the rest of the samples were run on it. The samples were prepared in triplicate, and the number of green cells in each sample were analysed based on the gating.

For Fluorescence assisted cell sorting (FACS), the same equipment was used. However the machine was set up to collect the cells passing through the sort and the sort was carried out under sterile conditions. GFP expression of transfected cells was found to be of low to moderate levels and therefore a low gate was applied to allow for maximum retrieval of green cells. Cells were retrieved in serum containing tubes. The retrieved cells were washed in media 2-3 times and the subsequent cell pellet was either used to isolate protein/ RNA or for further culture to study cell proliferation and behaviour *in vitro*.

9.6 Calcium imaging

In order to study changes in cytosolic calcium of Müller stem cells, calcium indicator dyes which change their fluorescence intensity upon calcium binding were used. These dyes require loading into the Müller stem cells prior to live cell imaging performed under an inverted fluorescence microscope with time lapse imaging capabilities to detect changes in dye fluorescence in response to stimulation with various neurotransmitter ligands.

9.6.1 Dye loading

We used the single long wavelength calcium indicator dye Fura Red (molecular probes, invitrogen). Each 50 µg vial was resuspended in 50 µl of DMSO to gain a final stock solution of 1mg/ml (which is equivalent of about 1mM/ml, Fura Red molecular weight -1089). This stock solution was diluted 1 in 500 to achieve the final concentration of 2 µM/ml used to load the dye into the cells.

Müller stem cells were plated onto coverslip bottomed 8 well chamberslides and cultured for 7 days under the different treatment conditions. At the end of 7 days the media was removed and the cells washed with 2 changes of PBS to remove all traces of serum. The Fura Red was then diluted 1 in 500 to make the 2 µM/ml working solution in serum-free DMEM. 100 µl of the working solution was added to each well and the cells incubated at 37°C for 30 minutes. At the end of this incubation period, the dye was removed from the cells and all traces of it washed away with 2 changes of PBS. 200 µl of serum containing DMEM was then added to each well and the cells recovered in this media for 30 minutes at 37°C before being imaged. Following recovery, serum containing DMEM was removed, the cells washed again with PBS and 200ul of Leibovitz -15 (L-15) medium added to each well. This optically clear medium was used for the final imaging of the cells under the microscope.

9.6.2 Stimulation and Imaging

Once loaded with the dye, cells were transferred to the microscope which had been previously prepared so that the imaging stage was at 37°C. The entire experimented was conducted with cells maintained at this temperature.

An Olympus IX81 microscope was used for these experiments in co operation with the CellˆR software. 40X oil immersion objective was used for imaging. The Fura Red was excited using the FITC 510/16 filter, given its excitation around 480nm and the emission filter used to detect Fura Red was either the 610/40 or the quad cube filter, both of which produced equally good quality images.

In each well following identification of a field, 10 readings were recorded at 1s second intervals prior to stimulation to establish a baseline. This was followed by a 2 s gap in recording at the end of which recording was recommenced at 0.5s

intervals for 1 minute (120 readings). The stimulant was added as soon as the first of the second set of recordings commenced i.e. at 12-12.5s into the entire experiment and at 0.5 seconds into the second set of recordings. At the end of the recording, regions of interest with in each cell of the field were outlined and a table of the measure of the fluorescence intensities generated. These values were then used to establish the percentage responders in each population and the kinetics of the response. One field was analysed per well and each well was counted as one experiment, thereby allowing 8 different experiments to be performed per slide (8 wells/slide)

The stock solutions of the ligands were prepared such that addition of 50 µl of the ligand to the 200 µl of the L-15 media in each well, resulted in the desirable final concentration. This volume was decided upon, following a series of trial runs to ascertain the volume of ligand solution that produced the uniform stimulation of cells without affecting the focusing of the image. Larger volumes tended to cause the image to lose focus and smaller volumes failed to spread through the entire field and often caused only localized responses. In the experiments described in the results chapter we have used final concentrations of 2mM for each of the three ligands –NMDA, McN-A343 and Nicotine (Sigma-Aldrich). Stock solutions of 10mM (NMDA-1.47mg in 1ml ultrapure water, McN-A343 mg in 1ml ultrapure water and Nicotine- mg in 1ml ultrapure water) were prepared for these ligands so that when 50µl of the stock was added to 200 µl of media (1 in 5 dilutions), a final concentration of 2mM was achieved.

9.6.3 Analysis

Once the images were acquired, the Cell^R software was used to outline each cell in the field as a region of interest (ROI) and the fluorescence values within each of these ROIs were computed by the software and displayed over time in an excel spreadsheet. Apart from the cells one ROI per field was also defined outside of a cell to allow for subtraction of the background and for bleaching effects to be taken into account in the final analysis.

The numbers generated from these spreadsheets were used to plot the individual and cumulative kinetics of the cells to a particular ligand. In performing the

experiments, we tried to analyze at least 4 different fields per cell type and ligand at one stretch and the responses of the cells from all of these 4 fields were pooled to arrive at the final response spectrum of a particular cell type. For example, control cell response to NMDA was analyzed from 4 different wells at one stretch, (about 15-20 cells per field) and the response of cells from all 4 wells pooled to define the control cell response to NMDA. The spread sheets contained fluorescence intensity (FI) in arbitrary units. These were divided by the background FI values resulting in a relative FI ratio. These values were then normalized to have a common starting point and control for variation seen due to differences in initial fluorescence intensity.

Since Fura Red undergoes a decline in fluorescence intensity, when plotted, the characteristic response curves generated from these cells constituted an initial down slope of rising cytosolic calcium followed by an upslope of recovery. In order to depict the results in the conventional up slope of response and down slope of recovery format, the values of the normalized relative FI ratios were inverted. Therefore the graphs depicted in the results of the calcium imaging experiments show conventional response curves but the y axis actually depicts 1/ relative FI.

The videos generated from the time lapse imaging were analyzed using image J. The images originally in gray scale were converted to 6 colour heat map images and then exported as such in single image and video formats. These images have been put together at respective time points to depict representative changes in fluorescence intensity with time of the different cell types in response to the various ligands.

9.7 Transplantation

9.7.1 Preparation of cells for transplants

Müller stem cells used for transplantation were transfected with an immunodeficiency virus type 1 (HIV-1) based lentiviral vector expressing low toxicity hrGFP from a spleen focus forming virus (SFFV) promoter, previously described as l-schrgfpw (Yanez-Munoz et al. 2006). The viral transfection was performed at the molecular therapy lab at the Institute of Ophthalmology. Viral transfection requires ClassIII facilities and since the author of this work was not

licensed to use these facilities, the tranfections were performed by Alexander Smith, member of a collaborating lab (headed by Prof. Robin Ali at the Institute of Ophthalmology) equipped with the facilities to carry out these transfections. The transfection efficiency was about 90 percent and the cells were subsequently cultured at high density, expanded and aliquots frozen down for future use. Prior to transplantation, green cells were placed in the required culture conditions and cultured for 7 days. On the day of the transplants the cells were examined for signs of viability, healthy growth and degree of green fluorescence. The cells were then trypsinised and spun down. Serum antibiotic free medium was then used to wash the cells thoroughly. Following cell counting and viability assays, cells were centrifuged and the cell pellet resuspended in the appropriate volume of serum antibiotic free media to obtain a final concentration of 2 x 10^4 cells/ µl. Cells were stored on ice for the duration of the transplants to slow down cellular metabolism and preserve the viability of the cells until the end of the procedure. Remaining cells were replated onto a culture flask to check for their viability and ability to attach and grow.

9.7.2 Animal models used

Lister hooded rat neonate- P2-P5 were used to study the migration of Müller stem cells in a retina conducive to transplantation.

Dystrophic RCS rats in which degeneration of retinal photoreceptors starts at the age of 3-4 weeks were used to study the behaviour of Müller stem cells in degenerating and inflamed retinae.

Lister hooded adult rat retinae treated with NMDA to selectively damage the RGC were used to study the behaviour of Müller stem cells differentiated towards an RGC fate *in vivo.*

Animals were immunosuppressed with oral CyclosporineA (Sandimmun, Sandoz, Camberley, UK, 210mg/litre of drinking water,) and Azathioprine (Sigma, UK; 20mg/litre) from 2 days before transplantation until termination of the experiment. When using additional immunosuppression, animals received oral prednisolone (Sovereign Medical, UK, 5mg/liter) in addition to Cyclosporine A and Azathioprine, together with daily intraperitoneal injections of indomethacin (0.1mg/100gm body weight) for the duration of the experiment. For transplantation into neonatal Lister

hooded pups, pregnant dams were immunosuppressed with oral Cyclosporine A and Azathioprine as above.

All rats were maintained according to the Home Office regulations for the care and use of laboratory animals and the UK Animals (Scientific Procedures) Act (1986). Dystrophic RCS rats were bred in-house and kept under 12h/12h light- dark cycle (light cycle mean illumination: 30cd/sqm.)

9.7.3 Subretinal injections

Rats were anaesthetised with an intraperitoneal injection of Ketamine HCl – 7.5mg/100g (Ketaset, Fort Dodge Animal Health, Southampton, UK) and Medetomidine HCl -5mg/100g (Domitor, Pfizer, Sandwich, UK). The pupils were dilated using 1% Tropicamide and 2.5% Phenylephrine (Chauvin Pharmaceuticals, UK). The neonates were anaesthetised with $1/10^{th}$ of the adult dose.

The LH neonates were transplanted at P2-P5. The recipients were anaesthetized and placed under the surgical microscope. The eyelids at this stage are still fused and were surgically opened along the lid crease, which is faintly but distinctly visible. The dorsolateral conjunctiva was opened with a single cut and a 33 gauge metal needle attached to a Hamilton syringe was inserted tangentially into the sclera and through the choroid till it was felt to be just beneath the retina. Cells (1 µl) were injected, the needle held in place momentarily and then withdrawn to prevent any reflux. The eyes were wiped to remove any traces of blood, the animals placed on a heating pad and the anaesthesia reversed with antisedan (0.1mg/100gm body weight). As a result of the small size of the host eye this procedure was therefore performed through external indirect visualization of the needle as opposed to direct visualization through the pupil.

Older RCS rats (3-4 wks of age) were fully developed animals and the surgical technique differed. A drop of tropicamide was used to dilate the pupil after the animal was anaesthetised. The conjunctiva was dissected dorsolateraly down to the sclera. A small amount of viscotears gel along with a coverslip was placed over the cornea and the microscope adjusted so as to focus on the retinal blood vessels which were directly visible through the dilated pupil. A 30 gauge needle (to allow for tougher tissues in the older animals) attached to a Hamilton syringe was used to penetrate the sclera and choroid for placement just beneath the retina. Cells (2 µl)

were injected and retinal detachment visualised. Any reflux/ intravitreal placement of cells was noted. The needle was held in place briefly and then withdrawn. Another 30 gauge needle was used to create a paracentesis and relieve the raised IOP which the injection may have caused.

When using chondroitinase ABC (ChABC) (Seikagaku Corporation, Tokyo, Japan) cells were prepared at twice the concentration (4x 10^4 cells/ µl) and diluted 1:1 with the enzyme (0.02units/ µl). Two µl of this mixture was injected per eye.

NMDA (N-methyl D-aspartate) (M3262, Sigma-aldrich, UK) induces selective ganglion cell damage and this property has been used to create rodent models of glaucoma. Intravitreal injection of NMDA 80 µM/ml (1µl per eye) was used to induce selective RGC death. Triamcinolone 80µgm/ml (1µl per eye) was injected along with the NMDA to control any associated activation of microglia (Gao et al. 2004a). One week after the injection, the cells were injected into the eyes intravitreally.

Intravitreal cell injections were performed following NMDA administration to target the ganglion cell layer. The eye was dissected as described previously in the adult 3-4 week old lister hooded rat. Briefly the dorsolateral conjunctiva was opened out with a single cut and subsequent blunt dissection. The 30G metal needle was inserted, under direct visualisation through the pupil, into the vitreal space and the cells injected. The needle was held in place for a moment and then retracted. A paracentesis was performed to relieve the rise in intraocular pressure.

9.7.4 Tissue analysis

At the end of the experiment, sodium pentobarbitone was used to perform terminal anaesthesia. Upper segment intracardiac perfusion was carried out using a flow pump. Briefly the abdomen was opened and the diaphragm resected to reveal the upper thoracic segment. The descending aorta was clamped using an artery clamp. The ventricle was opened using a curved small scissors and the canula inserted and held in place using a second artery clamp such that the tip sat just at the mouth of the ascending aorta. PBS perfusion was started at the rate of 30mls/min and the atrium opened to allow exit of the venous return. PBS perfusion was continued until the outflow was clear and no longer contained any blood. At this point perfusion with 4% PFA was started and about 60-100mls of PFA was perfused depending on size. Once the upper limbs were sufficiently fixed (as judged by their stiffness) perfusion

was stopped and the canulae and clamps removed. The eyes were surgically dissected out using a scalpel blade and transferred to 4% PFA for immersion fixation for a further 2 hours. They were washed with PBS and cryoprotected with 30% sucrose for storage at 4^0C. For sectioning the eyes were removed from the sucrose, placed in moulds containing OCT (optimum cutting temperature) media (VWR, UK) and slow cooled in acetone dry ice mix until frozen. These were then mounted onto a cryostat and 16-20 µm thick sections were cut and placed on slides for immunohistochemical staining and confocal imaging.

9.8 Electroretinography

Animals were dark adapted overnight and prepared in red light for electroretinography as follows. The rats were first anaesthetized with intraperitoneal injection of domitor and ketaset (same dose as that used for transplantation), with atropine. Congestion of the airways during the procedure can lead to respiratory distress. Atropine keeps airway secretions to a minimum and prevents this from happening. This made the procedure more comfortable for the rat and prevented interference of the electroretinogram with noise that can arise as a result of the aforesaid respiratory distress.

Once the animal was anaesthetized, both eyes were treated with proxymetacaine drops to anaesthetize them, phenylephrine drops to dilate the pupils and hypromellose solution to hydrate the cornea thereby preventing it from drying. Corneal moisture is essential for the successful contact with the ERG electrode. Responses from one eye were recorded at a time and the other eye was closed with a single releasable 5 o vicryl stitch through the centre of the lids. The closed eyelids were also taped over to prevent any stimulation with light while responses from the other eye were being recorded, thereby maintaining the dark adaptation.

To prevent any bias as a result of the depth of anaesthesia, the first eye recorded in each animal was alternated between the control eye and the test eye. Following this initial set up, the rat was placed into the light-tight recording chamber on a heat mat at 37°C and its head immobilized using a stabilizing metal bar.

9.8.1 ERG electrode set up

The earth electrode was set up subcutaneously at the base of the tail (Fig 9.6). The reference electrode for the ERG was placed in the cheek on the same side as the eye being recorded. The ERG recording electrode consisted of a platinum wire loop approximately the size of the corneal diameter of the rat eye (loop diameter was 2mm) and was placed such that it just touched the corneal surface thereby completing the circuitry. Following placement of the ERG electrode, the LED stimulator was placed in close proximity above the eye being tested. The recording chamber was then sealed to prevent any entry of light during the recording.

9.8.2 ERG recordings

In the experiments done here the focus was on specifically delineating scotopic threshold responses which are characteristic of retinal ganglion cell function(Bui & Fortune 2004a). Flash stimuli (3μs- 10ms duration, repetition rate 0.67Hz-0.2Hz) were presented via an LED stimulator, intensity -6.5 to -1 log cd s m^{-2}, under scotopic conditions. The higher intensities in this protocol were used to ensure that the presence of intact 'a' and 'b' waves. For each eye, first a baseline was established by measuring the ERG traces without any light stimulation. This was followed by stimulation of the retina with increasing intensities of light and measurement of the traces in response to these stimuli. 40-60 responses were measured per intensity. The responses were measured using the observer software and analyzed using the reviewer software. For cumulative analysis of data from multiple animals, results were exported to xcel spreadsheets, compiled into groups and analyzed using Prism statistical analysis software.

	Attenuations	Time	Frequency	Log intensity
1	1000	3us	0.67Hz	-6.5 log cd s m^{-2}
2	1000	10us	0.67Hz	-6.0 log cd s m^{-2}
3	300	10us	0.67Hz	-5.5 log cd s m^{-2}
4	100	10us	0.67Hz	-5.0 log cd s m^{-2}
5	10	10us	0.67Hz	-4.0 log cd s m^{-2}
6	1	10us	0.67Hz	-3.0 log cd s m^{-2}
7	1	100us	0.2Hz	-2.0 log cd s m^{-2}
8	1	1ms	0.2Hz	-1.0 log cd s m^{-2}

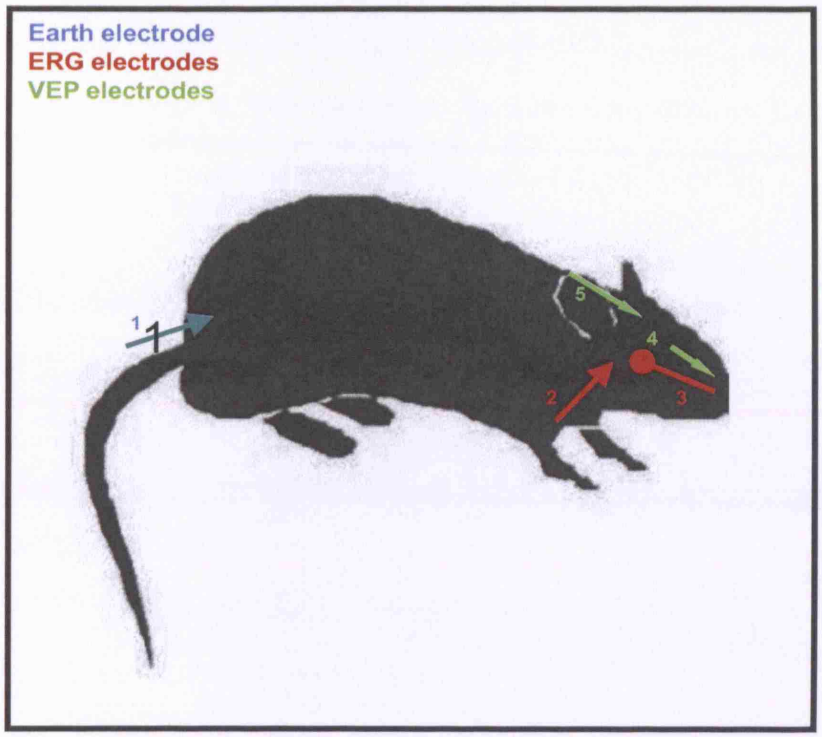

Figure 9.6: Positioning of electrodes on the rat for electrophysiology

The earth electrode is positioned just near the base of the tail in the sub cutaneous space in the direction shown by the blue arrow at position 1. The ERG reference electrode is positioned in the subcutaneous space of the cheek on the side of the eye being examined as shown by the red arrow in position 2. The ERG test electrode is a round platinum wire loop placed over the cornea as shown by the red indicator at position 3. When visual evoked potentials (VEP) were also being examined, the VEP reference electrode was placed in the midline under the skin of the nose as shown by the green arrow in position 4. The VEP test electrode is placed over the posterior surface of the contralateral cortex as shown by the green arrow in position 5. Image modified from www.braintree.gov.uk/.../Pest+Control+Rats.html

Chapter 10: References

References

Acosta, M. L., Bumsted 0'Brien, K. M., Tan, S.-S., & Kalloniatis, M. 2007, "Emergence of cellular markers and functional ionotropic glutamate receptors on tangentially dispersed cells in the developing mouse retina", *Journal of Comparative Neurology*, vol. 506, no. 3, pp. 506-523.

Adachi, M., Takahashi, K., Nishikawa, M., Miki, H., & Uyama, M. 1996, "High intraocular pressure-induced ischemia and reperfusion injury in the optic nerve and retina in rats", *Graefe's Archive for Clinical and Experimental Ophthalmology*, vol. 234, no. 7, pp. 445-451.

Ali, R. R. & Sowden, J. C. 2003, "Therapy may yet stem from cells in the retina", *British Journal of Ophthalmology*, vol. 87, no. 9, pp. 1058-1059.

Alward, W. L. M. 1999, *Glaucoma.The requisites* Mosby.

Amato, M. A., Boy, S., Arnault, E., Girard, M., Puppa, A. D., Sharif, A., & Perron, M. 2004, "Comparison of the expression patterns of five neural RNA binding proteins in the Xenopus retina", *The Journal of Comparative Neurology*, vol. 481, no. 4, pp. 331-339.

Anderson, D. H., Hageman, G. S., Mullins, R. F., Neitz, M., Neitz, J., Ozaki, S., Preissner, K. T., & Johnson, L. V. 1999, "Vitronectin Gene Expression in the Adult Human Retina", *Investigative Ophthalmology Visual Science*, vol. 40, no. 13, pp. 3305-3315.

Anthony, T. E., Klein, C., Fishell, G., & Heintz, N. 2004, "Radial glia serve as neuronal progenitors in all regions of the central nervous system", *Neuron*, vol. 41, pp. 881-890.

Aoki, H., Hara, A., Niwa, M., Motohashi, T., Suzuki, T., & Kunisada, T. 2008a, "Transplantation of cells from eye-like structures differentiated from embryonic stem cells in vitro and in vivo regeneration of retinal ganglion-like cells", *Graefe's Archive for Clinical and Experimental Ophthalmology*, vol. 246, no. 2, pp. 255-265.

Atluri, P., Fleck, M. W., Shen, Q., Mah, S. J., Stadfelt, D., Barnes, W., Goderie, S. K., Temple, S., & Schneider, A. S. 2001, "Functional Nicotinic Acetylcholine Receptor Expression in Stem and Progenitor Cells of the Early Embryonic Mouse Cerebral Cortex", *Developmental Biology*, vol. 240, no. 1, pp. 143-156.

Austin, C. P., Feldman, D. E., Ida, J. A., & Cepko, C. L. 1995a, "Vertebrate retinal ganglion cells are selected from competent progenitors by the action of Notch", *Development*, vol. 121, no. 11, pp. 3637-3650.

Baker, D.E.C., Harrison, N.J.,Maltby, E., Smith, K., Moore, H.D., Shaw, P.J., Heath, P.R.,Holden, H. & Andrews, P.W. 2007, "Adaptation to culture of human embryonic stem cells and oncogenesis *in vivo"* , *Nature Biotechnology,* vol. *25* pp. 207 - 215

Banin, E., Obolensky, A., Idelson, M., Hemo, I., Reinhardtz, E., Pikarsky, E., Ben Hur, T., & Reubinoff, B. 2006a, "Retinal Incorporation and Differentiation of Neural Precursors Derived from Human Embryonic Stem Cells", *Stem Cells*, vol. 24, no. 2, pp. 246-257.

Bao, Z. Z. & Cepko, C. L. 1997a, "The Expression and Function of Notch Pathway Genes in the Developing Rat Eye", *Journal of Neuroscience*, vol. 17, no. 4, pp. 1425-1434.

Baptiste, D. C., Powell, K. J., Jollimore, C. A. B., Hamilton, C., Levatte, T. L., Archibald, M. L., Chauhan, B. C., Robertson, G. S., & Kelly, M. E. M. 2005, "Effects of minocycline and tetracycline on retinal ganglion cell survival after axotomy", *Neuroscience*, vol. 134, no. 2, pp. 575-582.

Berardi, N., Pizzorusso, T., & Maffei, L. 2004a, "Extracellular Matrix and Visual Cortical Plasticity: Freeing the Synapse", *Neuron*, vol. 44, no. 6, pp. 905-908.

Bernardos, R. L., Lentz, S. I., Wolfe, M. S., & Raymond, P. A. 2005, "Notch-Delta signaling is required for spatial patterning and Müller glia differentiation in the zebrafish retina", *Developmental Biology*, vol. 278, no. 2, pp. 381-395.

Braam, S. R., Zeinstra, L., Litjens, S., Ward-van Oostwaard, D., van den Brink, S., van Laake, L., Lebrin, F., Kats, P., Hochstenbach, R., Passier, R., Sonnenberg, A., & Mummery, C. L. 2008, "Recombinant Vitronectin is a functionally defined substrate that supports human embryonic stem cell self renewal via AVB5 integrin ", *Stem Cells* pp. 2008-0291.

Bradbury, E. J., Moon, L. D. F., Popat, R. J., King, V. R., Bennett, G. S., Patel, P. N., Fawcett, J. W., & McMahon, S. B. 2002, "Chondroitinase ABC promotes functional recovery after spinal cord injury", *Nature*, vol. 416, no. 6881, pp. 636-640.

Brann, D. W. & Mahesh, V. B. 1991, "Endogenous excitatory amino acid regulation of the progesterone-induced LH and FSH surge in estrogen-primed ovariectomized rats.", *Neuroendocrinology*, vol. 53, no. 1, pp. 107-110.

Brown, N. L., Kanekar, S., Vetter, M. L., Tucker, P. K., Gemza, D. L., & Glaser, T. 1998, "Math5 encodes a murine basic helix-loop-helix transcription factor

expressed during early stages of retinal neurogenesis", *Development*, vol. 125, no. 23, pp. 4821-4833.

Brown, N. L., Patel, S., Brzezinski, J., & Glaser, T. 2001, "Math5 is required for retinal ganglion cell and optic nerve formation", *Development*, vol. 128, no. 13, pp. 2497-2508.

Bui, B. V., Edmunds, B., Cioffi, G. A., & Fortune, B. 2005, "The Gradient of Retinal Functional Changes during Acute Intraocular Pressure Elevation", *Investigative Ophthalmology Visual Science*, vol. 46, no. 1, pp. 202-213.

Bui, B. V. & Fortune, B. 2004a, "Ganglion cell contributions to the rat full-field electroretinogram", *The Journal of Physiology Online*, vol. 555, no. 1, pp. 153-173.

Bull, N. D. & Martin, K. R. 2007b, "Optic nerve restoration: new perspectives.", *Journal of Glaucoma*, vol. 16, no. 5, pp. 506-511.

Bull, N. D., Limb, G. A., & Martin, K. R. 2008a, "Human Müller Stem Cell (MIO-M1) Transplantation in a Rat Model of Glaucoma: Survival, Differentiation, and Integration", *Investigative Ophthalmology Visual Science*, vol. 49, no. 8, pp. 3449-3456.

Cai, J., Cheng, A., Luo, Y., Lu, C., Mattson, M. P., Rao, M. S., & Furukawa, K. 2004, "Membrane properties of rat embryonic multipotent neural stem cells", *Journal of Neurochemistry*, vol. 88, no. 1, pp. 212-226.

Calzada, J. I., Jones, B. E., Netland, P. A., & Johnson, D. A. 2002, "Glutamate-Induced Excitotoxicity in Retina: Neuroprotection with Receptor Antagonist, Dextromethorphan, but Not with Calcium Channel Blockers", *Neurochemical Research*, vol. 27, no. 1, pp. 79-88.

Campbell, K. & Gotz, M. 2002, "Radial glia: multi-purpose cells for vertebrate brain development", *Trends Neurosci*, vol. 25, pp. 235-238.

Canola, K., Angenieux, B., Tekaya, M., Quiambao, A., Naash, M. I., Munier, F. L., Schorderet, D. F., & Arsenijevic, Y. 2007, "Retinal Stem Cells Transplanted into Models of Late Stages of Retinitis Pigmentosa Preferentially Adopt a Glial or a Retinal Ganglion Cell Fate", *Investigative Ophthalmology Visual Science*, vol. 48, no. 1, pp. 446-454.

Carlson, M. E. & Conboy, I. M. 2007a, "Regulating the Notch pathway in embryonic, adult and old stem cells", *Current Opinion in Pharmacology*, vol. 7, no. 3, pp. 303-309.

Carnevale, D., DeSimone, R., & Minghetti, L. 2007, "Microglia-neuron interaction in inflammatory and degenerative diseases: role of cholinergic and

noradrenergic systems.", *CNS Neurological Disorders and Drug Targets*, vol. 6, no. 6, pp. 388-397.

Cepko, C. L., Austin, C. P., Yang, X., Alexiades, M., & Ezzeddine, D. 1996, "Cell fate determination in the vertebrate retina", *Proceedings of the National Academy of Sciences of the United States of America*, vol. 93, no. 2, pp. 589-595.

Chacko, D. M., Das, A. V., Zhao, X., James, J., Bhattacharya, S., & Ahmad, I. 2003b, "Transplantation of ocular stem cells: the role of injury in incorporation and differentiation of grafted cells in the retina", *Vision Research*, vol. 43, no. 8, pp. 937-946.

Chen, L. F., Yin, Z. Q., Chen, S., & Chen, Z. S. 2008, "Cultured stem cells from embryonic rat retina differentiate and produce action potentials in vitro.", *Investigative Ophthalmology Visual Science*, vol. ahead of print.

Chen, L., Yang, P., & Kijlstra, A. 2002, "Distribution, markers, and functions of retinal microglia", *Ocular Immunology & Inflammation*, vol. 10, no. 1, pp. 27-39.

Chidlow, G. & Osborne, N. N. 2003, "Rat retinal ganglion cell loss caused by kainate, NMDA and ischemia correlates with a reduction in mRNA and protein of Thy-1 and neurofilament light", *Brain Research*, vol. 963, no. 1-2, pp. 298-306.

Ciulla, T. A., Criswell, M. H., Danis, R. P., & Hill, T. E. 2001, "Intravitreal Triamcinolone Acetonide Inhibits Choroidal Neovascularization in a Laser-Treated Rat Model", *Archives of Ophthalmology*, vol. 119, no. 3, pp. 399-404.

Coles, B. L. K., Ang+¬nieux, B., Inoue, T., Rio-Tsonis, K., Spence, J. R., McInnes, R. R., Arsenijevic, Y., & van der Kooy, D. 2004, "Facile isolation and the characterization of human retinal stem cells", *Proceedings of the National Academy of Sciences of the United States of America*, vol. 101, no. 44, pp. 15772-15777.

Cunningham, M. A., Edelman, J. L., & Kaushal, S. 2008, "Intravitreal Steroids for Macular Edema: The Past, the Present, and the Future", *Survey of Ophthalmology*, vol. 53, no. 2, pp. 139-149.

D'Cruz, P. M., Yasumura, D., Weir, J., Matthes, M. T., Abderrahim, H., LaVail, M. M., & Vollrath, D. 2000, "Mutation of the receptor tyrosine kinase gene Mertk in the retinal dystrophic RCS rat", *Human Molecular Genetics*, vol. 9, no. 4, pp. 645-651.

Das, A. V., Edakkot, S., Thoreson, W. B., James, J., Bhattacharya, S., & Ahmad, I. 2005a, "Membrane properties of retinal stem cells/progenitors.", *Progress in Retinal Eye Research*, vol. 24, no. 6, pp. 663-681.

Das, A. V., James, J., Bhattacharya, S., Imbalzano, A. N., Antony, M. L., Hegde, G., Zhao, X., Mallya, K., Ahmad, F., Knudsen, E., & Ahmad, I. 2007, "SWI/SNF Chromatin Remodeling ATPase Brm Regulates the Differentiation of Early Retinal Stem Cells/Progenitors by Influencing BRN3B Expression and Notch Signaling", *Journal of Biological Chemistry*, vol. 282, no. 48, pp. 35187-35201.

Das, A. V., Mallya, K. B., Zhao, X., Ahmad, F., Bhattacharya, S., Thoreson, W. B., Hegde, G. V., & Ahmad, I. 2006, "Neural stem cell properties of Müller glia in the mammalian retina: Regulation by Notch and Wnt signaling", *Developmental Biology*, vol. 299, no. 1, pp. 283-302.

de Kozak, Y., Cotinet, A., Goureau, O., Hicks, D., & Thillaye-Goldenberg, B. 1997a, "Tumor necrosis factor and nitric oxide production by resident retinal glial cells from rats presenting hereditary retinal degeneration.", *Ocul Immunol Inflamm*, vol. 5, no. 2, pp. 89-94.

Deschenes-Furry, J., Perrone-Bezzozero, N., & Jasmin, B. J. 2006, "The RNA-binding protein HUD:a regulator of neuronal differentiation,maintenance and plasticity", *Bioessays*, vol. 28, no. 8, pp. 822-833.

Doetsch, F. 2003, "The glial identity of neural stem cells", *Nat Neurosci*, vol. 6, pp. 1127-1134.

Dong, X., Pulido, J., Qu, T., & Sugaya, K. 2003, "Differentiation of human neural stem cells into retinal cells.", *Neuroreport*, vol. 14 , no. 1, pp. 143-146.

Dorsky, R. I., Rapaport, D. H., & Harris, W. A. 1995, "Xotch inhibits cell differentiation in the xenopus retina", *Neuron*, vol. 14, no. 3, pp. 487-496.

Ekstrom, P. & Johansson, K. 2003a, "Differentiation of ganglion cells and amacrine cells in the rat retina: correlation with expression of HuC/D and GAP-43 proteins", *Developmental Brain Research*, vol. 145, no. 1, pp. 1-8.

Elshatory, Y., Deng, M., Xie, X., & an, L. 2007a, "Expression of the LIM-homeodomain protein ISL1 in the developing and mature mouse retina", *Journal of Comparative Neurology*, vol. 503, no. 1, pp. 182-197.

Elshatory, Y., Everhart, D., Deng, M., Xie, X., Barlow, R. B., & Gan, L. 2007b, "Islet-1 Controls the Differentiation of Retinal Bipolar and Cholinergic Amacrine Cells", *Journal of Neuroscience*, vol. 27, no. 46, pp. 12707-12720.

Esteve, P. & Bovolenta, P. 2006a, "Secreted inducers in vertebrate eye development: more functions for old morphogens", *Current Opinion in Neurobiology*, vol. 16, no. 1, pp. 13-19.

Ever, L. & Gaiano, N. 2005, "Radial 'glial' progenitors: neurogenesis and signaling", *Curr Opin Neurobiol*, vol. 15, pp. 29-33.

Fausett, B. V. & Goldman, D. 2006, "A role for alpha1 tubulin-expressing Müller glia in regeneration of the injured zebrafish retina", *J Neurosci*, vol. 26, pp. 6303-6313.

Faux, C. H., Turnley, A. M., Epa, R., Cappai, R., & Bartlett, P. F. 2001, "Interactions between Fibroblast Growth Factors and Notch Regulate Neuronal Differentiation", *Journal of Neuroscience*, vol. 21, no. 15, pp. 5587-5596.

Fischer, A. J. & Reh, T. A. 2001, "Müller glia are a potential source of neural regeneration in the postnatal chicken retina", *Nat Neurosci*, vol. 4, pp. 247-252.

Fischer, A. J. & Reh, T. A. 2003a, "Potential of Müller glia to become neurogenic retinal progenitor cells", *Glia*, vol. 43, pp. 70-76.

Fischer, A. J. 2005, "Neural regeneration in the chick retina", *Progress in Retinal and Eye Research*, vol. 24, no. 2, pp. 161-182.

Fischer, A. J., McGuire, C. R., Dierks, B. D., & Reh, T. A. 2002, "Insulin and Fibroblast Growth Factor 2 Activate a Neurogenic Program in Müller Glia of the Chicken Retina", *Journal of Neuroscience*, vol. 22, no. 21, pp. 9387-9398.

Fischer, A. J. & Reh, T. A. 2002, "Exogenous Growth Factors Stimulate the Regeneration of Ganglion Cells in the Chicken Retina", *Developmental Biology*, vol. 251, no. 2, pp. 367-379.

Fortune, B., Bui, B. V., Morrison, J. C., Johnson, E. C., Dong, J., Cepurna, W. O., Jia, L., Barber, S., & Cioffi, G. A. 2004, "Selective Ganglion Cell Functional Loss in Rats with Experimental Glaucoma", *Investigative Ophthalmology Visual Science*, vol. 45, no. 6, pp. 1854-1862.

Fox, V., Gokhale, P. J., Walsh, J. R., Matin, M., Jones, M., & ANDREWS, P. W. 2008, "Cell-Cell Signaling Through NOTCH Regulates Human Embryonic Stem Cell Proliferation", *Stem Cells*, vol. 26, no. 3, pp. 715-723.

Furukawa, T., Mukherjee, S., Bao, Z. Z., Morrow, E. M., & Cepko, C. L. 2000a, "rax, Hes1, and notch1 Promote the Formation of Müller Glia by Postnatal Retinal Progenitor Cells", *Neuron*, vol. 26, no. 2, pp. 383-394.

Gaiano, N., Nye, J. S., & Fishell, G. 2000, "Radial Glial Identity Is Promoted by Notch1 Signaling in the Murine Forebrain", *Neuron*, vol. 26, no. 2, pp. 395-404.

Gal, A., Li, Y., Thompson, D. A., Weir, J., Orth, U., Jacobson, S. G., Apfelstedt-Sylla, E., & Vollrath, D. 2000, "Mutations in MERTK, the human orthologue of the RCS rat retinal dystrophy gene, cause retinitis pigmentosa", *Nat Genet*, vol. 26, no. 3, pp. 270-271.

Gamm, D., Wang, S., Lu, B., Girman, S., Holmes, T., Bischoff, N., Shearer, R., Sauve`, Y., Capowski, E., Svendsen, C., & Lund, R. 2007, "Protection of visual functions by human neural progenitors in a rat model of retinal disease.", *PLoS ONE*, vol. 2, no. E338.

Gan, L., Wang, S. W., Huang, Z., & Klein, W. H. 1999a, "POU Domain Factor Brn-3b Is Essential for Retinal Ganglion Cell Differentiation and Survival but Not for Initial Cell Fate Specification", *Developmental Biology*, vol. 210, no. 2, pp. 469-480.

Gan, L., Xiang, M., Zhou, L., Wagner, D. S., Klein, W. H., & Nathans, J. 1996a, "POU domain factor Brn-3b is required for the development of a large set of retinal ganglion cells", *Proceedings of the National Academy of Sciences*, vol. 93, no. 9, pp. 3920-3925.

Gao, H., Qiao, X., Gao, R., Mieler, W. F., McPherson, A. R., & Holz, E. R. 2004a, "Intravitreal triamcinolone does not alter basal vascular endothelial growth factor mRNA expression in rat retina", *Vision Research*, vol. 44, no. 4, pp. 349-356.

Ghai, K., Stanke, J. J., & Fischer, A. J. 2008, "Patterning of the circumferential marginal zone of progenitors in the chicken retina", *Brain Research*, vol. 1192, pp. 76-89.

Gong, J., Sagiv, O., Cai, H., Tsang, S. H., & Del Priore, L. V. 2008a, "Effects of extracellular matrix and neighboring cells on induction of human embryonic stem cells into retinal or retinal pigment epithelial progenitors", *Experimental Eye Research*, vol. 86, no. 6, pp. 957-965.

Graziadei, G. A. & Grasiadei, P. P. 1979, "Neurogenesis and neuron regeneration in the olfactory system of mammals. II. Degeneration and reconstitution of the olfactory sensory neurons after axotomy.", *J Neurocytol*, vol. 8, no. 2, pp. 197-213.

Graziadei, P. P., Levine, R. R., & Graziadei, G. A. 1978, "Regeneration of olfactory axons and synapse formation in the forebrain after bulbectomy in neonatal mice.", *Proc Natl Acad Sci U S A*, vol. 75, no. 10, pp. 5230-5234.

Grunder, T., Kohler, K., Kaletta, A., & Guenther, E. 2000, "The distribution and developmental regulation of NMDA receptor subunit proteins in the outer and inner retina of the rat.", *Journal of Neurobiology*, vol. 44, no. 3, pp. 333-342.

Gruter, O., Kostic, C., Crippa, S. V., Perez, M.-T. R., Zografos, L., Schorderet, D. F., Munier, F. L., & Arsenijevic, Y. 2005a, "Lentiviral vector-mediated gene transfer in adult mouse photoreceptors is impaired by the presence of a physical barrier", *Gene Ther*, vol. 12, no. 11, pp. 942-947.

Gu, P., Harwood, L. J., Zhang, X., Wylie, M., Curry, W. J., & Cogliati, T. 2007, "Isolation of retinal progenitor and stem cells from the porcine eye.", *Molecular Vision*, vol. 13, pp. 1045-1057.

Harada, T., Harada, C., Kohsaka, S., Wada, E., Yoshida, K., Ohno, S., Mamada, H., Tanaka, K., Parada, L. F., & Wada, K. 2002a, "Microglia-Müller Glia Cell Interactions Control Neurotrophic Factor Production during Light-Induced Retinal Degeneration", *Journal of Neuroscience*, vol. 22, no. 21, pp. 9228-9236.

Hartfuss, E., Galli, R., Heins, N., & Gotz, M. 2001, "Characterization of CNS precursor subtypes and radial glia", *Dev Biol*, vol. 229, pp. 15-30.

Haupt, C. & Huber, A. B. 2008, "How axons see their way--axonal guidance in the visual system.", *Front Biosci.*, vol. 13, pp. 3136-3149.

Hill, A. J., Zwart, I., Tam, H. H., Chan, J., Navarrete, C., Jen, L. S., & Navarrete, R. 2008a, "Human umbilical cord blood-derived mesenchymal stem cells do not differentiate into neural cells types or integrate into the retina after intravitreal grafting in neonatal rats.", *Stem Cells and Development*, vol. ahead of print.

Hiscott, P., Sheridan, C., Magee, R. M., & Grierson, I. 1999a, "Matrix and the retinal pigment epithelium in proliferative retinal disease", *Progress in Retinal and Eye Research*, vol. 18, no. 2, pp. 167-190.

Hobert, O. & Westphal, H. 2000, "Functions of LIM-homeobox genes", *Trends in Genetics*, vol. 16, no. 2, pp. 75-83.

Hollyfield, J. G. 1968, "Differential addition of cells to the retina in Rana pipiens tadpoles", *Developmental Biology*, vol. 18, no. 2, pp. 163-179.

Huang, W. C., Kuo, W. C., Cherng, J. H., Hsu, S. H., Chen, P. R., Huang, S. H., Huang, M. C., Liu, J. C., & Cheng, H. 2006, "Chondroitinase ABC promotes axonal re-growth and behavior recovery in spinal cord injury", *Biochemical and Biophysical Research Communications*, vol. 349, no. 3, pp. 963-968.

Hyatt, G. A. & Dowling, J. E. 1997a, "Retinoic acid. A key molecule for eye and photoreceptor development", *Investigative Ophthalmology Visual Science*, vol. 38, no. 8, pp. 1471-1475.

Hyatt, G. A., Schmitt, E. A., Fadool, J. M., & Dowling, J. E. 1996, "Retinoic acid alters photoreceptor development in vivo", *Proceedings of the National Academy of Sciences of the United States of America*, vol. 93, no. 23, pp. 13298-13303.

Inatani, M., Honjo, M., Otori, Y., Oohira, A., Kido, N., Tano, Y., Honda, Y., & Tanihara, H. 2001a, "Inhibitory Effects of Neurocan and Phosphacan on Neurite Outgrowth from Retinal Ganglion Cells in Culture", *Investigative Ophthalmology Visual Science*, vol. 42, no. 8, pp. 1930-1938.

Inatani, M., Tanihara, H., Oohira, A., Honjo, M., Kido, N., & Honda, Y. 2000, "Upregulated Expression of Neurocan, a Nervous Tissue Specific Proteoglycan, in Transient Retinal Ischemia", *Investigative Ophthalmology Visual Science*, vol. 41, no. 9, pp. 2748-2754.

Jaissle, G. B., Szurman, P., & Bartz-Schmidt, K. U. 2004, "Nebenwirkungen und Komplikationen der intravitrealen Triamcinolonacetonid-Therapie", *Der Ophthalmologe*, vol. 101, no. 2, pp. 121-128.

Jonas, J. B., Degenring, R. F., Kamppeter, B. A., Kreissig, I., & Akkoyun, I. 2004, "Duration of the effect of intravitreal triamcinolone acetonide as treatment for diffuse diabetic macular edema", *American Journal of Ophthalmology*, vol. 138, no. 1, pp. 158-160.

Jonas, J. B., Harder, B. r., & Kamppeter, B. A. 2004, "Inter-eye difference in diabetic macular edema after unilateral intravitreal injection of triamcinolone acetonide", *American Journal of Ophthalmology*, vol. 138, no. 6, pp. 970-977.

Jones, L. L., Margolis, R. U., & Tuszynski, M. H. 2003, "The chondroitin sulfate proteoglycans neurocan, brevican, phosphacan, and versican are differentially regulated following spinal cord injury", *Experimental Neurology*, vol. 182, no. 2, pp. 399-411.

Jones, L. L., Sajed, D., & Tuszynski, M. H. 2003a, "Axonal Regeneration through Regions of Chondroitin Sulfate Proteoglycan Deposition after Spinal Cord Injury: A Balance of Permissiveness and Inhibition", *Journal of Neuroscience*, vol. 23, no. 28, pp. 9276-9288.

Jones, L. L. & Tuszynski, M. H. 2002a, "Spinal Cord Injury Elicits Expression of Keratan Sulfate Proteoglycans by Macrophages, Reactive Microglia, and Oligodendrocyte Progenitors", *Journal of Neuroscience*, vol. 22, no. 11, pp. 4611-4624.

Jones, L. L., Yamaguchi, Y., Stallcup, W. B., & Tuszynski, M. H. 2002a, "NG2 Is a Major Chondroitin Sulfate Proteoglycan Produced after Spinal Cord Injury and Is Expressed by Macrophages and Oligodendrocyte Progenitors", *Journal of Neuroscience*, vol. 22, no. 7, pp. 2792-2803.

Katoh, M. & Katoh, M. 2006, "Notch ligand, JAG1, is evolutionarily conserved target of canonical WNT signaling pathway in progenitor cells", *International Journal of Molecular Medicine*, vol. 17, no. 4, pp. 681-685.

Keithley, E. M., Erkman, L., Bennett, T., Lou, L., & Ryan, A. F. 1999, "Effects of a hair cell transcription factor, Brn-3.1, gene deletion on homozygous and heterozygous mouse cochleas in adulthood and aging", *Hearing Research*, vol. 134, no. 1-2, pp. 71-76.

Kim, B. G., Dai, H. N., Lynskey, J. V., McAtee, M., & Bregman, B. S. 2006, "Degradation of chondroitin sulfate proteoglycans potentiates transplant-mediated axonal remodeling and functional recovery after spinal cord injury in adult rats.", *J Comp Neurol.*, vol. 497, no. 2, pp. 182-198.

Kim, Y. H., Choi, M. Y., Kim, Y. S., Park, C. H., Lee, J. H., Chung, I. Y., Yoo, J. M., Choi, W. S., Cho, G. J., & Kang, S. S. 2007a, "Triamcinolone acetonide protects the rat retina from STZ-induced acute inflammation and early vascular leakage", *Life Sciences*, vol. 81, no. 14, pp. 1167-1173.

Kim, Y. H., Chung, I. Y., Choi, M. Y., Kim, Y. S., Lee, J. H., Park, C. H., Kang, S. S., Roh, G. S., Choi, W. S., Yoo, J. M., & Cho, G. J. 2007c, "Triamcinolone suppresses retinal vascular pathology via a potent interruption of proinflammatory signal-regulated activation of VEGF during a relative hypoxia", *Neurobiology of Disease*, vol. 26, no. 3, pp. 569-576.

Kohzaki, K., Vingrys, A. J., & Bui, B. V. 2008, "Early Inner Retinal Dysfunction in Streptozotocin-Induced Diabetic Rats", *Investigative Ophthalmology Visual Science*, vol. 49, no. 8, pp. 3595-3604.

Kokkinopoulos, I., Pearson, R. A., MacNeil, A., Dhomen, N. S., MacLaren, R. E., Ali, R. R., & Sowden, J. C. 2008, "Isolation and characterisation of neural progenitor cells from the adult Chx10orJ/orJ central neural retina", *Molecular and Cellular Neuroscience*, vol. 38, no. 3, pp. 359-373.

Konstantopoulos, A., Williams, C. P. R., Newsom, R. S., & Luff, A. J. 2006, "Ocular morbidity associated with intravitreal triamcinolone acetonide", *Eye*, vol. 21, no. 3, pp. 317-320.

Kubrusly, R. C. C., da Cunha, M. C. C., Reis, R. A. d. M., Soares, H., Ventura, A. L. c. M., Kurtenbach, E., de Mello, M. C. F., & de Mello, F. G. 2005, "Expression of functional receptors and transmitter enzymes in cultured Müller cells", *Brain Research*, vol. 1038, no. 2, pp. 141-149.

Lam, T. T., Abler, A. S., Kwong, J. M. K., & Tso, M. O. M. 1999a, "N-Methyl-D-Aspartate (NMDA)-Induced Apoptosis in Rat Retina", *Investigative Ophthalmology Visual Science*, vol. 40, no. 10, pp. 2391-2397.

Lamba, D. A., Karl, M. O., Ware, C. B., & Reh, T. A. 2006, "Efficient generation of retinal progenitor cells from human embryonic stem cells", *Proceedings of the National Academy of Sciences*, vol. 103, no. 34, pp. 12769-12774.

Landers, R. A., Rayborn, M. E., Myers, K. M., & Hollyfield, J. G. 1994, "Increased Retinal Synthesis of Heparan Sulfate Proteoglycan and HNK-1 Glycoproteins Following Photoreceptor Degeneration", *Journal of Neurochemistry*, vol. 63, no. 2, pp. 737-750.

Lawrence, J. M., Singhal, S., Bhatia, B., Keegan, D. J., Reh, T. A., Luthert, P. J., Khaw, P. T., & Limb, G. A. 2007a, "MIO-M1 cells and Similar Müller Glial Cell Lines Derived from Adult Human Retina Exhibit Neural Stem Cell Characteristics", *Stem Cells* pp. 2006-0724.

Lebrun-Juleien, F. & DiPolo, A. 2008, "Molecular and cell-based approaches for neuroprotection in glaucoma.", *Optometry and Visual Science*, vol. 85, no. 6, pp. 417-424.

Lecchi, M., McIntosh, M., Bertrand, S., Safran, A. B., & Bertrand, D. 2005, "Functional properties of neuronal nicotinic acetylcholine receptors in the chick retina during development", *Europoean Journal of Neuroscience*, vol. 21, no. 11, pp. 3182-3188.

Levine, E. M., Fuhrmann, S., & Reh, T. A. 2000, "Soluble factors and the development of rod photoreceptors", *Cellular and Molecular Life Sciences (CMLS)*, vol. 57, no. 2, pp. 224-234.

Levkovitch-Verbin, H., Quigley, H. A., Martin, K. R. G., Valenta, D., Baumrind, L. A., & Pease, M. E. 2002a, "Translimbal Laser Photocoagulation to the Trabecular Meshwork as a Model of Glaucoma in Rats", *Investigative Ophthalmology Visual Science*, vol. 43, no. 2, pp. 402-410.

Lewis, G. P., Erickson, P. A., Guerin, C. J., Anderson, D. H., & Fisher, S. K. 1992, "Basic fibroblast growth factor: a potential regulator of proliferation and intermediate filament expression in the retina", *Journal of Neuroscience*, vol. 12, no. 10, pp. 3968-3978.

Limb, G. A., Salt, T. E., Munro, P. M. G., Moss, S. E., & Khaw, P. T. 2002a, "In Vitro Characterization of a Spontaneously Immortalized Human Müller Cell Line (MIO-M1)", *Investigative Ophthalmology Visual Science*, vol. 43, no. 3, pp. 864-869.

Little, C. W., Castillo, B., DiLoreto, D. A., Cox, C., Wyatt, J., del Cerro, C., & del Cerro, M. 1996a, "Transplantation of human fetal retinal pigment epithelium rescues photoreceptor cells from degeneration in the Royal College of Surgeons rat retina", *Investigative Ophthalmology Visual Science*, vol. 37, no. 1, pp. 204-211.

Liu, L., Wang, C., Ni, X., & Sun, J. 2007, "A rapid inhibition of NMDA receptor current by corticosterone in cultured hippocampal neurons", *Neuroscience Letters*, vol. 420, no. 3, pp. 245-250.

Lopez, T., Lopez-Colome, A. M., & Ortega, A. 1997, "NMDA receptors in cultured radial glia.", *FEBS Lett.*, vol. 405, no. 2, pp. 245-248.

Louvi, A. & Artavanis-Tsakonas, S. 2006a, "Notch signalling in vertebrate neural development", *Nat Rev Neurosci*, vol. 7, no. 2, pp. 93-102.

Luke, M., Januschowski, K., Beutel, J., Warga, M., Grisanti, S., Peters, S., Schneider, T., Lnke, C., Bartz-Schmidt, K. U., & Szurman, P. 2008, "The effects of triamcinolone crystals on retinal function in a model of isolated perfused vertebrate retina", *Experimental Eye Research*, vol. 87, no. 1, pp. 22-29.

Lund, R. D., Kwan, A. S. L., Keegan, D. J., Sauve, Y., Coffey, P. J., & Lawrence, J. M. 2001a, "Cell Transplantation as a Treatment for Retinal Disease", *Progress in Retinal and Eye Research*, vol. 20, no. 4, pp. 415-449.

Lund, R. D., Ono, S. J., Keegan, D. J., & Lawrence, J. M. 2003, "Retinal transplantation: progress and problems in clinical application", *Journal of Leukocyte Biology*, vol. 74, no. 2, pp. 151-160.

Lund, R. D., Adamson, P., Sauve, Y., Keegan, D. J., Girman, S. V., Wang, S., Winton, H., Kanuga, N., Kwan, A. S. L., Beauchene, L., Zerbib, A., Hetherington, L., Couraud, P. O., Coffey, P., & Greenwood, J. 2001b, "Subretinal transplantation of genetically modified human cell lines attenuates loss of visual function in dystrophic rats", *Proceedings of the National Academy of Sciences*, vol. 98, no. 17, pp. 9942-9947.

Lund, R. D., Wang, S., Lu, B., Girman, S., Holmes, T., Sauve, Y., Messina, D. J., Harris, I. R., Kihm, A., Harmon, A. M., Chin, F. Y., Gosiewska, A., & Mistry, S. K. 2007a, "Cells Isolated from Umbilical Cord Tissue Rescue Photoreceptors and Visual Functions in a Rodent Model of Retinal Disease", *Stem Cells*, vol. 25, no. 4, p. 1089.

MacLaren, R. E., Pearson, R. A., MacNeil, A., Douglas, R. H., Salt, T. E., Akimoto, M., Swaroop, A., Sowden, J. C., & Ali, R. R. 2006a, "Retinal repair by transplantation of photoreceptor precursors", *Nature*, vol. 444, no. 7116, pp. 203-207.

MacNeil, A., Pearson, R. A., MacLaren, R. E., Smith, A. J., Sowden, J. C., & Ali, R. R. 2007, "Comparative Analysis of Progenitor Cells Isolated from the Iris, Pars Plana, and Ciliary Body of the Adult Porcine Eye", *Stem Cells*, vol. 25, no. 10, pp. 2430-2438.

Mankowska, A., Rejdak, R., Oleszczuk, A., Kiczynska, M., Lekawa, A., Choragiewicz, T., & Zagorski, Z. 2008, "Decrease of the postoperative inflammatory reaction during pars plana vitrectomy (PPV) after administration of triamcinolone acetonide.", *Klinika Oczna*, vol. 110, no. 4-6, pp. 151-154.

Martinez-Morales, J. R., Del Bene, F., Nica, G., Hammerschmidt, M., Bovolenta, P., & Wittbrodt, J. 2005, "Differentiation of the Vertebrate Retina Is Coordinated by an FGF Signaling Center", *Developmental Cell*, vol. 8, no. 4, pp. 565-574.

Martins, R. A., Linden, R., & Dyer, M. A. 2006, "Glutamate regulates retinal progenitors cells proliferation during development.", *Europoean Journal of Neuroscience*, vol. 24, no. 4, pp. 969-980.

Martins, R. A. P. & Pearson, R. A. 2008a, "Control of cell proliferation by neurotransmitters in the developing vertebrate retina", *Brain Research*, vol. 1192, pp. 37-60.

Martinez-Morales, J. R., Marti¦, E., Frade, J. M., & Rodri¦guez-Te¦bar, A. 1995, "Developmentally regulated vitronectin influences cell differentiation, neuron survival and process outgrowth in the developing chicken retina", *Neuroscience*, vol. 68, no. 1, pp. 245-253.

Mascarelli, F., Tassin, J., & Courtois, Y. Effect of FGFs on adult bovine Müller cells: proliferation, binding and internalization. Growth factors 4[2], 81-95. 1991. Ref Type: Journal (Full)

Massey, J. M., Hubscher, C. H., Wagoner, M. R., Decker, J. A., Amps, J., Silver, J., & Onifer, S. M. 2006a, "Chondroitinase ABC Digestion of the Perineuronal Net Promotes Functional Collateral Sprouting in the Cuneate Nucleus after Cervical Spinal Cord Injury", *Journal of Neuroscience*, vol. 26, no. 16, pp. 4406-4414.

Matter, J. M., Matter-Sadzinski, L., & Ballivet, M. 1995a, "Activity of the beta 3 nicotinic receptor promoter is a marker of neuron fate determination during retina development", *Journal of Neuroscience*, vol. 15, no. 9, pp. 5919-5928.

Matter-Sadzinski, L., Puzianowska-Kuznicka, M., Hernandez, J., Ballivet, M., & Matter, J. M. 2005a, "A bHLH transcriptional network regulating the specification of retinal ganglion cells", *Development*, vol. 132, no. 17, pp. 3907-3921.

McCaffery, P., Lee, M. O., Wagner, M. A., Sladek, N. E., & Drager, U. C. 1992a, "Asymmetrical retinoic acid synthesis in the dorsoventral axis of the retina", *Development*, vol. 115, no. 2, pp. 371-382.

Mellough, C. B., Cui, Q., & Harvey, A. R. 2007, "Treatment of adult neural progenitor cells prior to transplantation affects graft survival and integration in a neonatal and adult rat model of selective retinal ganglion cell depletion", *Restorative Neurology and Neuroscience*, vol. 25, no. 2, pp. 177-190.

Mellough, C. B., Cui, Q., Spalding, K. L., Symons, N. A., Pollett, M. A., Snyder, E. Y., Macklis, J. D., & Harvey, A. R. 2004, "Fate of multipotent neural precursor cells transplanted into mouse retina selectively depleted of retinal ganglion cells", *Experimental Neurology*, vol. 186, no. 1, pp. 6-19.

Merkle, F. T., Tramontin, A. D., Garcia-Verdugo, J. M., & Alvarez-Buylla, A. 2004, "Radial glia give rise to adult neural stem cells in the subventricular zone", *Proc Natl Acad Sci USA*, vol. 101, pp. 17528-17532.

Michailov, G. V., Sereda, M. W., Brinkmann, B. G., Fischer, T. M., Haug, B., Birchmeier, C., Role, L., Lai, C., Schwab, M. H., & Nave, K. A. 2004, "Axonal Neuregulin-1 Regulates Myelin Sheath Thickness", *Science*, vol. 304, no. 5671, pp. 700-703.

Mizumoto, H., Mizumoto, K., Whiteley, S. J. O., Shatos, M., Klassen, H., & Young, M. J. 2001, "Transplantation of Human Neural Progenitor Cells to the Vitreous Cavity of the Royal College of Surgeons Rat", *Cell Transplantation*, vol. 10, pp. 223-233.

Moore, K. B., Mood, K., Daar, I. O., & Moody, S. A. 2004, "Morphogenetic Movements Underlying Eye Field Formation Require Interactions between the FGF and ephrinB1 Signaling Pathways", *Developmental Cell*, vol. 6, no. 1, pp. 55-67.

Morgenstern, D. A., Asher, R. A., & Fawcett, J. W. 2002, "Chapter 22 Chondroitin sulphate proteoglycans in the CNS injury response," in *Progress in Brain Research*
Spinal Cord Trauma: Regeneration, Neural Repair and Functional Recovery, Volume 137 edn, L. McKerracher, ed., Elsevier, pp. 313-332.

Mori, T., Buffo, A., & Gotz, M. 2005, "The novel roles of glial cells revisited: the contribution of radial glia and astrocytes to neurogenesis", *Curr Top Dev Biol*, vol. 69, pp. 67-99.

Morrison, J. C., MOORE, C. G., Deppmeier, L. M. H., Gold, B. G., Meshul, C. K., & Johnson, E. C. 1997a, "A Rat Model of Chronic Pressure-induced Optic Nerve Damage", *Experimental Eye Research*, vol. 64, no. 1, pp. 85-96.

Mu, X., Fu, X., Beremand, P. D., Thomas, T. L., & Klein, W. H. 2008a, "Gene regulation logic in retinal ganglion cell development: ISL1 defines a critical branch distinct from but overlapping with Pou4f2", *Proceedings of the National Academy of Sciences*, vol. 105, no. 19, pp. 6942-6947.

Mu, X., Fu, X., Sun, H., Beremand, P. D., Thomas, T. L., & Klein, W. H. 2005, "A gene network downstream of transcription factor Math5 regulates retinal progenitor cell competence and ganglion cell fate", *Developmental Biology*, vol. 280, no. 2, pp. 467-481.

Mu, X. & Klein, W. H. 2004a, "A gene regulatory hierarchy for retinal ganglion cell specification and differentiation", *Seminars in Cell & Developmental Biology*, vol. 15, no. 1, pp. 115-123.

Murphy, S., Pearce, B., & Morrow, C. 1986, "Astrocytes have both M1 and M2 muscarinic receptor subtypes", *Brain Research*, vol. 364, no. 1, pp. 177-180.

Naskar, R., Wissing, M., & Thanos, S. 2002a, "Detection of Early Neuron Degeneration and Accompanying Microglial Responses in the Retina of a Rat Model of Glaucoma", *Investigative Ophthalmology Visual Science*, vol. 43, no. 9, pp. 2962-2968.

Nelson, B. R., Hartman, B. H., Georgi, S. A., Lan, M. S., & Reh, T. A. 2007a, "Transient inactivation of Notch signaling synchronizes differentiation of neural progenitor cells", *Developmental Biology*, vol. 304, no. 2, pp. 479-498.

Newman, E. & Reichenbach, A. 1996, "The Mnller cell: a functional element of the retina", *Trends in Neurosciences*, vol. 19, no. 8, pp. 307-312.

Ng, T. F. & Streilein, J. W. 2001, "Light-Induced Migration of Retinal Microglia into the Subretinal Space", *Investigative Ophthalmology Visual Science*, vol. 42, no. 13, pp. 3301-3310.

Nucci, C., Tartaglione, R., Rombolα, L., Morrone, L. A., Fazzi, E., & Bagetta, G. 2005, "Neurochemical Evidence to Implicate Elevated Glutamate in the Mechanisms of High Intraocular Pressure (IOP)-induced Retinal Ganglion Cell Death in Rat", *NeuroToxicology*, vol. 26, no. 5, pp. 935-941.

Ohzeki, T., Machida, S., Takahashi, T., Ohtaka, K., & Kurosaka, D. 2007, "The Effect of Intravitreal N -Methyl-dl -Aspartic Acid on the Electroretinogram in Royal College of Surgeons Rats", *Japanese Journal of Ophthalmology*, vol. 51, no. 3, pp. 165-174.

Ooto, S., Akagi, T., Kageyama, R., Akita, J., Mandai, M., Honda, Y., & Takahashi, M. 2004, "Potential for neural regeneration after neurotoxic injury in the adult mammalian retina", *Proc Natl Acad Sci USA*, vol. 101, pp. 13654-13659.

Pan, L., Deng, M., Xie, X., & Gan, L. 2008a, "ISL1 and BRN3B co-regulate the differentiation of murine retinal ganglion cells", *Development*, vol. 135, no. 11, pp. 1981-1990.

Pan, L., Yang, Z., Feng, L., & Gan, L. 2005, "Functional equivalence of Brn3 POU-domain transcription factors in mouse retinal neurogenesis", *Development*, vol. 132, no. 4, pp. 703-712.

Pearson, R., Catsicas, M., Becker, D., & Mobbs, P. 2002a, "Purinergic and Muscarinic Modulation of the Cell Cycle and Calcium Signaling in the Chick Retinal Ventricular Zone", *Journal of Neuroscience*, vol. 22, no. 17, pp. 7569-7579.

Peirson, S. N., Butler, J. N., & Foster, R. G. 2003, "Experimental validation of novel and conventional approaches to quantitative real-time PCR data analysis", *Nucleic Acids Research*, vol. 31, no. 14, p. e73.

Perron, M. & Harris, W. A. 2000, "Retinal stem cells in vertebrates", *BioEssays*, vol. 22, no. 8, pp. 685-688.

Pfaff, S. L., Mendelsohn, M., Stewart, C. L., Edlund, T., & Jessell, T. M. 1996, "Requirement for LIM Homeobox Gene ISL1 in Motor Neuron Generation Reveals a Motor Neuron- Dependent Step in Interneuron Differentiation", *Cell*, vol. 84, no. 2, pp. 309-320.

Pizzorusso, T., Medini, P., Berardi, N., Chierzi, S., Fawcett, J. W., & Maffei, L. 2002a, "Reactivation of Ocular Dominance Plasticity in the Adult Visual Cortex", *Science*, vol. 298, no. 5596, pp. 1248-1251.

Poenie, M. 2006, "Fluorescent Calcium Indicators Based on BAPTA," in *Calcium Signaling*, 2 edn, J. W. J. Putney, ed., CRC Press, pp. 1-50.

Porrello, K. & LaVail, M. M. 1986, "Immunocytochemical localization of chondroitin sulfates in the interphotoreceptor matrix of the normal and dystrophic rat retina.", *Current Eye Research*, vol. 5, no. 12, pp. 981-993.

Pow, D. V., Crook, D. K., & Wong, R. O. 1994, "Early appearance and transient expression of putative amino acid neurotransmitters and related molecules in the developing rabbit retina: an immunocytochemical study.", *Visual Neuroscience*, vol. 11, no. 6, pp. 1115-34.

Puro, D. G., Yuan, J. P., & Sucher, N. J. 1996, "Activation of NMDA receptor-channels in human retinal Müller glial cells inhibits inward-rectifying potassium currents.", *Visual Neuroscience*, vol. 13, no. 2, pp. 319-326.

Qiu, G., Seiler, M. J., Mui, C., Arai, S., Aramant, R. B., Juan, J., & Sadda, S. 2005, "Photoreceptor differentiation and integration of retinal progenitor cells transplanted into transgenic rats", *Experimental Eye Research*, vol. 80, no. 4, pp. 515-525.

Quigley, H. A. & Iglesia, D. S. 2003, "Stem cells to replace the optic nerve", *Eye*, vol. 18, no. 11, pp. 1085-1088.

Ramon, Y. & Cajal, S. 1972, "The Structure of the Retina".

Raymond, P., Barthel, L., Bernardos, R., & Perkowski, J. 2006, "Molecular characterization of retinal stem cells and their niches in adult zebrafish", *BMC Developmental Biology*, vol. 6, no. 1, p. 36.

Rhodes, K. E. & Fawcett, J. W. 2004, "Chondroitin sulphate proteoglycans: preventing plasticity or protecting the CNS?", *Journal of Anatomy*, vol. 204, no. 1, pp. 33-48.

Robson, J. G., Saszik, S. M., Ahmed, J., & Frishman, L. J. 2003, "Rod and cone contributions to the a-wave of the electroretinogram of the macaque", *The Journal of Physiology Online*, vol. 547, no. 2, pp. 509-530.

Rodrigues, E. B. 2007, "Inflammation in dry age-related macular degeneration.", *Ophthalmologica*, vol. 221, no. 3, pp. 143-152.

Ronchini, C. & Capobianco, A. J. 2001, "Induction of Cyclin D1 Transcription and CDK2 Activity by Notchic: Implication for Cell Cycle Disruption in Transformation by Notchic", *Molecular and Cellular Biology*, vol. 21, no. 17, pp. 5925-5934.

Roque, R. S., Imperial, C. J., & Caldwell, R. B. 1996a, "Microglial cells invade the outer retina as photoreceptors degenerate in Royal College of Surgeons rats.", *Investigative Ophthalmology Visual Science*, vol. 37, no. 1, pp. 196-203.

Roque, R. S., Rosales, A. A., Jingjing, L., Agarwal, N., & Al Ubaidi, M. R. 1999a, "Retina-derived microglial cells induce photoreceptor cell death in vitro", *Brain Research*, vol. 836, no. 1-2, pp. 110-119.

Roth, D. B., Realini, T., Feuer, W. J., Radhakrishnan, R., Gloth, J., Heimmel, M. R., Fechtner, R. D., Yarian, D. L., & Green, S. N. 2008, "Short-term complications of intravitreal injection of triamcinolone acetonide.", *Retina*, vol. 28, no. 1, pp. 66-70.

Sakaguchi, D. S., Van Hoffelen, S. J., & Young, M. J. 2003a, "Differentiation and Morphological Integration of Neural Progenitor Cells Transplanted into the Developing Mammalian Eye", *Annals of the New York Academy of Sciences*, vol. 995, no. 1, pp. 127-139.

Sakaki, Y., Fukuda, Y., & Yamashita, M. 1996, "Muscarinic and purinergic Ca2+ mobilizations in the neural retina of early embryonic chick", *International Journal of Developmental Neuroscience*, vol. 14, no. 6, pp. 691-699.

Sambrook, J., Fritsch, E. F., & Maniatis, T. 1989, *Molecular Cloning: A Laboratory Manual*, 3 edn, Cold Spring Harbor Laboratory.

Saszik, S. M., Robson, J. G., & Frishman, L. J. 2002, "The scotopic threshold response of the dark-adapted electroretinogram of the mouse", *The Journal of Physiology Online*, vol. 543, no. 3, pp. 899-916.

Scheer, N., Groth, A., Hans, S., & Campos-Ortega, J. A. 2001a, "An instructive function for Notch in promoting gliogenesis in the zebrafish retina", *Development*, vol. 128, no. 7, pp. 1099-1107.

Schipke, C. G., Ohlemeyer, C., Matyash, M., Nolte, C., Kettenmann, H., & Kirchhoff, F. 2001a, "Astrocytes of the mouse neocortex express functional N-methyl-D-aspartate receptors", *The FASEB Journal* pp. 00-0439fje.

Schneider, M. L., Turner, D. L., & Vetter, M. L. 2001, "Notch Signaling Can Inhibit Xath5 Function in the Neural Plate and Developing Retina", *Molecular and Cellular Neuroscience*, vol. 18, no. 5, pp. 458-472.

Segal, M. & Auerbach, J. M. 1995, "Imaging of intracellular calcium in hippocampal slices: methods, limitations and achievements," in *Brain slices in basic and clinical research*, A. Schurr & B. Rigor, eds., CRC Press, pp. 89-98.

Selles-Navarro, I., Ellezam, B., Fajardo, R., Latour, M., & McKerracher, L. 2001a, "Retinal Ganglion Cell and Nonneuronal Cell Responses to a Microcrush Lesion of Adult Rat Optic Nerve", *Experimental Neurology*, vol. 167, no. 2, pp. 282-289.

Shaikh, S., Ho, S., Engelmann, L. A., & Klemann, S. W. 2006, "Cell viability effects of triamcinolone acetonide and preservative vehicle formulations", *British Journal of Ophthalmology*, vol. 90, no. 2, pp. 233-236.

Shen, Y., Liu, X. L., & Yang, X. L. 2006a, "N -Methyl-d -aspartate receptors in the retina", *Molecular Neurobiology*, vol. 34, no. 3, pp. 163-179.

Shortt, A. J., Secker, G. A., Notara, M. D., Limb, G. A., Khaw, P. T., Tuft, S. J., & Daniels, J. T. 2007, "Transplantation of Ex Vivo Cultured Limbal Epithelial Stem Cells: A Review of Techniques and Clinical Results", *Survey of Ophthalmology*, vol. 52, no. 5, pp. 483-502.

Srinivasan, B., Roque, C. H., Hempstead, B. L., Al Ubaidi, M. R., & Roque, R. S. 2004, "Microglia-derived Pronerve Growth Factor Promotes Photoreceptor Cell Death via p75 Neurotrophin Receptor", *Journal of Biological Chemistry*, vol. 279, no. 40, pp. 41839-41845.

Stenkamp, D. L., Gregory, J. K., & Adler, R. 1993a, "Retinoid effects in purified cultures of chick embryo retina neurons and photoreceptors", *Investigative Ophthalmology Visual Science*, vol. 34, no. 8, pp. 2425-2436.

Stockton, R. A. & Slaughter, M. M. 1989, "B-wave of the electroretinogram. A reflection of ON bipolar cell activity", *The Journal of General Physiology*, vol. 93, no. 1, pp. 101-122.

Sucher, N. J., Lipton, S. A., & Dreyer, E. B. 1997, "Molecular basis of glutamate toxicity in retinal ganglion cells", *Vision Research*, vol. 37, no. 24, pp. 3483-3493.

Sugioka, M., Fukuda, Y., & Yamashita, M. 1998, "Development of glutamate-induced intracellular Ca^{2+} rise in the embryonic chick retina", *Journal of Neurobiology*, vol. 34, no. 2, pp. 113-125.

Suzuki, T., Akimoto, M., & Imai, H. 2007, "Chondroitinase ABC treatment enhances synaptogenesis between transplant and host neurons in model of retinal degeneration.", *Cell Transplantation*, vol. 16, no. 5, pp. 493-503.

Szurman, P., Sierra, A., Kaczmarek, R., Jaissle, G. B., Wallenfels-Thilo, B., Grisanti, S., Lnke, M., Bartz-Schmidt, K. U., & Spitzer, M. S. 2007, "Different biocompatibility of crystalline triamcinolone deposits on retinal cells in vitro and in vivo", *Experimental Eye Research*, vol. 85, no. 1, pp. 44-53.

Takahashi, M., Palmer, T. D., Takahashi, J., & Gage, F. H. 1998a, "Widespread Integration and Survival of Adult-Derived Neural Progenitor Cells in the Developing Optic Retina", *Molecular and Cellular Neuroscience*, vol. 12, no. 6, pp. 340-348.

Takatsuka, K., Hatakeyama, J., Bessho, Y., & Kageyama, R. 2004, "Roles of the bHLH gene Hes1 in retinal morphogenesis", *Brain Research*, vol. 1004, no. 1-2, pp. 148-155.

Tanigaki, K., Nogaki, F., Takahashi, J., Tashiro, K., Kurooka, H., & Honjo, T. 2001, "Notch1 and Notch3 Instructively Restrict bFGF-Responsive Multipotent Neural Progenitor Cells to an Astroglial Fate", *Neuron*, vol. 29, no. 1, pp. 45-55.

Taupin, P. 2006, "The therapeutic potential of adult neural stem cells.", *Curr Opin Mol Ther.*, vol. 8, no. 3, pp. 225-231.

Thanos, C. & Richter, W. 1993a, "The migratory potential of vitally labelled microglial cells within the retina of rats with hereditary photoreceptor dystrophy.", *Int J Dev Neurosci.*, vol. 11, no. 5, pp. 671-680.

The Lung Health Study Research Group 2000, "Effect of Inhaled Triamcinolone on the Decline in Pulmonary Function in Chronic Obstructive Pulmonary Disease", *The New England Journal of Medicine*, vol. 343, no. 26, pp. 1902-1909.

Thor, S. & Thomas, J. B. 1997, "The Drosophila islet Gene Governs Axon Pathfinding and Neurotransmitter Identity", *Neuron*, vol. 18, no. 3, pp. 397-409.

Tian, N. & Slaughter, M. M. 1995, "Correlation of dynamic responses in the ON bipolar neuron and theb-wave of the electroretinogram", *Vision Research*, vol. 35, no. 10, pp. 1359-1364.

Tokunaga, A., Kohyama, J., Yoshida, T., Nakao, K., Sawamoto, K., & Okano, H. Mapping spatio-temporal activation of Notch signaling during neurogenesis and gliogenesis in the developing mouse brain. Journal of Neurochemistry 90[1], 142-154. 2004.
Ref Type: Journal (Full)

Tropepe, V., Coles, B. L., Chiasson, B. J., Horsford, D. J., Elia, A. J., McInnes, R. R., & van der Kooy, D. 2000, "Retinal Stem Cells in the Adult Mammalian Eye", *Science*, vol. 287, no. 5460, pp. 2032-2036.

Turner, E. E., Jenne, K. J., & Rosenfeld, M. G. 1994, "Brn-3.2: A Brn-3-related transcription factor with distinctive central nervous system expression and regulation by retinoic acid", *Neuron*, vol. 12, no. 1, pp. 205-218.

Uchihhori, Y. & Puro, D. G. 1993, "Glutamate as a neuron-to-glial signal for mitogenesis: role of glial N-methyl-D-aspartate receptors.", *Brain Research*, vol. 613, no. 2, pp. 212-220.

Uhlin-Hansen, L. & Kolset, S. O. 1988a, "Cell density-dependent expression of chondroitin sulfate proteoglycan in cultured human monocytes", *Journal of Biological Chemistry*, vol. 263, no. 5, pp. 2526-2531.

Vaegan & Millar, T. J. 1994, "Effect of kainic acid and NMDA on the pattern electroretinogram, the scotopic threshold response, the oscillatory potentials and the electroretinogram in the urethane anaesthetized cat", *Vision Research*, vol. 34, no. 9, pp. 1111-1125.

Van Der Zee, E. A., De Jong, G. I., Strosberg, A. D., & Luiten, P. G. 1993, "Muscarinic acetylcholine receptor-expression in astrocytes in the cortex of young and aged rats.", *Glia*, vol. 8, no. 1, pp. 42-50.

Verkhratsky, A. & Kirchhoff, F. 2007, "NMDA Receptors in Glia", *The Neuroscientist*, vol. 13, no. 1, pp. 28-37.

Wakabayashi, K., Gieser, J., & Sieving, P. A. 1988, "Aspartate separation of the scotopic threshold response (STR) from the photoreceptor a-wave of the cat and monkey ERG", *Investigative Ophthalmology Visual Science*, vol. 29, no. 11, pp. 1615-1622.

Wakakura, M., Utsunomiya-Kawasaki, I., & Ishikawa, S. 1998a, "Rapid increase in cytosolic calcium ion concentration mediated by acetylcholine receptors in cultured retinal neurons and M++Iler cells", *Graefe's Archive for Clinical and Experimental Ophthalmology*, vol. 236, no. 12, pp. 934-939.

Walker, J. M. 2002, *The Protein Protocols Handbook*, 2 edn, Humana Press.

Wang, S. W., Gan, L., Martin, S. E., & Klein, W. H. 2000, "Abnormal Polarization and Axon Outgrowth in Retinal Ganglion Cells Lacking the POU-Domain Transcription Factor Brn-3b", *Molecular and Cellular Neuroscience*, vol. 16, no. 2, pp. 141-156.

Wang, S. W., Kim, B. S., Ding, K., Wang, H., Sun, D., Johnson, R. L., Klein, W. H., & Gan, L. 2001a, "Requirement for math5 in the development of retinal ganglion cells", *Genes and Development*, vol. 15, no. 1, pp. 24-29.

Watanbe, M., Sawai, H., & Fukuda, Y. 1997, "Survival of axotomized retinal ganglion cells in adult mammals.", *Clin Neurosci*, vol. 4, no. 5, pp. 233-239.

Wojciechowski, A. B., Englund, U., Lundberg, C., Wictorin, K., & Warfvinge, K. 2002a, "Subretinal Transplantation of Brain-derived Precursor Cells to Young RCS Rats Promotes Photoreceptor Cell Survival*", *Experimental Eye Research*, vol. 75, no. 1, pp. 23-37.

Wong, R. O. 1995, "Effects of glutamate and its analogs on intracellular calcium levels in the developing retina.", *Visual Neuroscience*, vol. 12, no. 5, pp. 907-917.

Wong, R. O. 1998, "Calcium imaging and multielectrode recordings of global patterns of activity in the developing nervous system.", *Histochem J.*, vol. 30, no. 3, pp. 217-229.

Wurziger, K., Lichtenberger, T., & Hanitzsch, R. 2001, "On-bipolar cells and depolarising third-order neurons as the origin of the ERG-b-wave in the RCS rat", *Vision Research*, vol. 41, no. 8, pp. 1091-1101.

Xiang, M., Gan, L., Li D, Zhou, L., Chen, Z.-Y., Wagner, D., O'Malley, B. W., Klein, W. H., & Nathans, J. 1998, "Role of the Brn-3 family of POU-domain genes in the development of the auditory/vestibular, somatosensory, and visual systems.", *Cold Spring Harbor Symp.Quant.Biol.*, vol. 62, pp. 325-335.

Xiang, M., Zhou, L., Macke, J. P., Yoshioka, T., Hendry, S. H., Eddy, R. L., Shows, T. B., & Nathans, J. 1995a, "The Brn-3 family of POU-domain factors: primary structure, binding specificity, and expression in subsets of retinal ganglion cells and somatosensory neurons", *Journal of Neuroscience*, vol. 15, no. 7, pp. 4762-4785.

Xiang, M. 1998a, "Requirement for Brn-3b in Early Differentiation of Postmitotic Retinal Ganglion Cell Precursors", *Developmental Biology*, vol. 197, no. 2, pp. 155-169.

Xiang, M., Gan, L., Zhou, L., Klein, W. H., & Nathans, J. 1996, "Targeted deletion of the mouse POU domain gene Brn-3a causes a selective loss of neurons in the brainstem and trigeminal ganglion, uncoordinated limb movement, andáimpairedásuckling", *Proceedings of the National Academy of Sciences*, vol. 93, no. 21, pp. 11950-11955.

Xiang, M., Zhou, L., Nathans, J.1996 "Similarities and differences among inner retinal neurons revealed by the expression of reporter transgenes controlled by Brn-3a, Brn-3b, and Brn-3c promotor sequences." *Vis*ual *Neurosci*ence vol.*13*, no.*5*, pp.*955-62.*

Xiang, M., Zhou, L., Peng, Y.-W., Eddy, R. L., Shows, T. B., & Nathans, J. 1993, "Brn-3b: a POU domain gene expressed in a subset of retinal ganglion cells", *Neuron*, vol. 11, no. 4, pp. 689-701.

Yanez-Munoz, R. J., Balaggan, K. S., MacNeil, A., Howe, S. J., Schmidt, M., Smith, A. J., Buch, P., MacLaren, R. E., Anderson, P. N., Barker, S. E., Duran, Y., Bartholomae, C., von Kalle, C., Heckenlively, J. R., Kinnon, C., Ali, R. R., & Thrasher, A. J. 2006, "Effective gene therapy with nonintegrating lentiviral vectors", *Nat Med*, vol. 12, no. 3, pp. 348-353.

Yang, Z., Ding, K., Pan, L., Deng, M., & Gan, L. 2003a, "Math5 determines the competence state of retinal ganglion cell progenitors", *Developmental Biology*, vol. 264, no. 1, pp. 240-254.

Yao, S., Chen, S., Clark, J., Hao, E., Beattie, G. M., Hayek, A., & Ding, S. 2006, "Long-term self-renewal and directed differentiation of human embryonic stem cells in chemically defined conditions", vol. 103, no. 18, pp. 6907-6912.

Young, M. J., Ray, J., Whiteley, S. J. O., Klassen, H., & Gage, F. H. 2000a, "Neuronal Differentiation and Morphological Integration of Hippocampal Progenitor Cells Transplanted to the Retina of Immature and Mature Dystrophic Rats", *Molecular and Cellular Neuroscience*, vol. 16, no. 3, pp. 197-205.

Yurco, P. & Cameron, D. A. 2005, "Responses of Müller glia to retinal injury in adult zebrafish", *Vision Res*, vol. 45, pp. 991-1002.

Zeng, H. y., Zhu, X. a., Zhang, C., Yang, L. P., Wu, L. m., & Tso, M. O. M. 2005, "Identification of Sequential Events and Factors Associated with Microglial Activation, Migration, and Cytotoxicity in Retinal Degeneration in rd Mice", *Investigative Ophthalmology Visual Science*, vol. 46, no. 8, pp. 2992-2999.

Zhang, X., Bao, S., Lai, D., Rapkins, R. W., & Gillies, M. C. 2008, "Intravitreal Triamcinolone Acetonide Inhibits Breakdown of the Blood-Retinal Barrier Through Differential Regulation of VEGF-A and Its Receptors in Early Diabetic Rat Retinas", *Diabetes*, vol. 57, no. 4, pp. 1026-1033.

Zhang, Y., Rauch, U., & Perez, M. T. 2003, "Accumulation of Neurocan, a Brain Chondroitin Sulfate Proteoglycan, in Association with the Retinal Vasculature in RCS Rats", *Investigative Ophthalmology Visual Science*, vol. 44, no. 3, pp. 1252-1261.

Zhao, X., Das, A. V., Bhattacharya, S., Thoreson, W. B., Sierra, J. R., Mallya, K. B., & Ahmad, I. 2008, "Derivation of Neurons with Functional Properties from Adult Limbal Epithelium: Implications in Autologous Cell Therapy for Photoreceptor Degeneration", *Stem Cells* pp. 2007-0727.

Zubair, M., Watanabe, E., Fukada, M., Noda, M. 2002 "Genetic labelling of specific axonal pathways in the mouse central nervous system." European Journal of Neuroscience, Vol. 15, pp. 807-814

Chapter 11: Appendices

11.1 Tables

11.1.1 Primary antibodies

Antibody	Raised in	Supplier	Catalogue no.	Dilution
B-actin	mouse	Sigma	A5316 (clone-AC-74)	1/5000 (wb)
BrdU	mouse	Novocastra	NC1-BrdU	1/300
BRN3B	goat	Santa Cruz	N-15 sc-31987	1/200 (wb)
CD44 (anti human)	mouse	Serotec	MCA89T	1/1000
Chondroitin Sulphate Proteoglycan (CS56)	mouse	Sigma	C-8035	1/200
CRALBP	rabbit	Saari	Gift	1/500
ED1	mouse	Serotec	MCA 341R	1/1000
GFP	rabbit	MBL	598	1/500
HUD	rabbit	Santa Cruz	sc-2536	1/500
ISL1	mouse	DSHB	39.4D5	1/50, 1/100 (wb)
Ki67	mouse	Novocastra		1/1000
Nestin	mouse	Chemicon	MAB5326	1/500
Neurocan	mouse	DSHB	IF6	1/100
Neurofilament 200	mouse	DSHB	RT97	1in 2
Notch 1	rabbit	Santa Cruz	C-20 sc-6014	1/100 (wb)
Notch1 activated or Cleaved Notch 1 (Val1744)	rabbit	Cell Signaling	#2421	1 in 50
Notch 1(bTan20)	rat	DSHB	bTan20	1 in 20
Stub antibody (CS)	mouse	Gift (Fawcett J)	-	1 in 50
Sox2	rabbit	Chemicon	AB5603	1/200
Versican	mouse	DSHB	12C5	1/100
Vimentin	rabbit	Santa Cruz	sc-5565	1/500

11.1.2 Primers

Gene	Accession no.	Sequence	cDNA position	Annealing Temp.	Product size	Source
ATOH7 F	NM_145178	ACTGCCTTCGACCGCTTAC	172	60		
ATOH7 R		CAGAGCCATGATGTAGCTCAG	276	60	105	primer bank (id:21553337a1)
B-ACTIN F	NM_001101	CATGTACGTTGCTATCCAGGC	393	60		
B-ACTIN R		CTCCTTAATGTCACGCACGAT	642	60	250	primer bank (id:4501885a1)
BRN3B F	NM_004575	CAGGTTCGAGTCCCTCACAC	903	60		
BRN3B R		ATGGCAAAGTAGGCTTCGAGC	1100	60	198	primer bank (id:4758948a2)
GAPDH-2 F (qpcr)	AC002389	CCAGTGCAAAGAGCCCAAAC	444	60		
GAPDH-2 R (qpcr)		GCACGGACACTCACAATGTTC	668	60	225	primer bank (id:2282013a2)
HES1 F	NM_005524.2	AAGATAGCTCGCGGCATTCCA	200	60		
HES1 R		CGTTCATGCACTCGCTGAAG	358	60	160	self
HES5 F	NM_001010926.2	AAGCTGGAGAAGGCCGACAT	244	60		
HES5 R		CGAGTAGCCTTCGCTGTAGT	360	60	116	self
HEY2F	NM_012259	CAACCCCTTGTCGCCTCTC	620	60		
HEY2R		CCG TGG ATG GCA TTC GGA G	730	60	111	primer bank (id:6912414a3)
HUD F	NM_021952.2	GAAACTGTCCTTCTCCCATGC	310	64		
HUD R		GATTGAGGCAGAGCTCGGAC	611	64	301	self
ISL1 F	NM_002202	CAGGTTGTACGGGATCAAATGC	207	60		
ISL1 R		CACACAGCGGAAACACTCGAT	315	60	109	primer bank (id:4504737a2)
NOTCH1 F	NM_017617	GCTGGACTGGTGAGGACTG	977	60		
NOTCH1 R		AGCCCTCGTTACAGGGGTT	1153	60	180	primer bank (id:27894368a3)
PGK-1 F (qpcr)	NM_000291	TTAAAGGGAAGCGGGTCGTTA	41	60		
PGK-1 R (qpcr)		TCCATTGTCCAAGCAGAATTTGA	162	60	122	primer bank (id:4505763a1)
TLE1F	NM_005077	CAGTTCCCCTTACGCCTCAC	419	60		
TLE1R		ATCGTGGTGCTTCTTGTCATC	561	60	143	Primer bank (id:21541824a3)
TLE4 F	NM_007005	ACAGAGATGCAGCGGCATTA	1009	60		
TLE4 R		TTCCACAGCCTGCACCACTT	1173	60	165	self
Cloning primers						
BRN3B 4586 BGL II F		TACCAGATCT-CAACACCGCGGGAAGTATAG				
BRN3B 6248 SAL I R		AATTGTCGAC-CGCTGGTCCGTAGAGGCACTCA			1.6KB	
pEGFP1 sequencing primer		CTCTGACTTGAGCGTCGATT	3981	60		

11.2 Publications

1. Lawrence JM, **Singhal S**, Bhatia B, Keegan DJ, Reh TA, Luthert PJ, Khaw PT, Limb GA.
   MIO-M1 cells and similar Müller glial cell lines derived from adult human retina exhibit neural stem cell characteristics.
   Stem Cells 2007 Aug; 25(8):2033-43.

2. **Singhal S**, Lawrence JM, Bhatia B, Ellis JS, Kwan AS, Macneil A, Luthert PJ, Fawcett JW, Perez MT, Khaw PT, Limb GA.
   Chondroitin sulfate proteoglycans and microglia prevent migration and integration of grafted Müller stem cells into degenerating retina.
   Stem Cells 2008 Apr; 26(4):1074-82.

STEM CELLS
TISSUE-SPECIFIC STEM CELLS

MIO-M1 Cells and Similar Müller Glial Cell Lines Derived from Adult Human Retina Exhibit Neural Stem Cell Characteristics

JEAN M. LAWRENCE,[a] SHWETA SINGHAL,[a] BHAIRAVI BHATIA,[a] DAVID J. KEEGAN,[a] THOMAS A. REH,[b] PHILIP J. LUTHERT,[a] PENG T. KHAW,[a] GLORIA ASTRID LIMB[a]

[a]Ocular Repair and Regeneration Biology Unit, Departments of Cell Biology and Pathology, Institute of Ophthalmology and Moorfields Eye Hospital, London, United Kingdom; [b]Department of Biological Structure, University of Washington, Seattle, Washington, USA

Key Words. Adult stem cells • Cellular proliferation • Glial differentiation • Glia • Neural differentiation • Retinal transplantation Stem/progenitor cell • Tissue-specific stem cells

ABSTRACT

Growing evidence suggests that glial cells may have a role as neural precursors in the adult central nervous system. Although it has been shown that Müller cells exhibit progenitor characteristics in the postnatal chick and rat retinae, their progenitor-like role in developed human retina is unknown. We first reported the Müller glial characteristics of the spontaneously immortalized human cell line MIO-M1, but recently we have derived similar cell lines from the neural retina of several adult eye donors. Since immortalization is one of the main properties of stem cells, we investigated whether these cells expressed stem cell markers. Cells were grown as adherent monolayers, responded to epidermal growth factor, and could be expanded indefinitely without growth factors under normal culture conditions. They could be frozen and thawed without losing their characteristics. In the presence of extracellular matrix and fibroblast growth factor-2 or retinoic acid, they acquired neural morphology, formed neurospheres, and expressed neural stem cell markers including βIII tubulin, Sox2, Pax6, Chx10, and Notch 1. They also expressed markers of postmitotic retinal neurons, including peripherin, recoverin, calretinin, S-opsin, and Brn3. When grafted into the subretinal space of dystrophic Royal College of Surgeons rats or neonatal Lister hooded rats, immortalized cells migrated into the retina, where they expressed various markers of retinal neurons. These observations indicate that adult human neural retina harbors a population of cells that express both Müller glial and stem cell markers and suggest that these cells may have potential use for cell-based therapies to restore retinal function. STEM CELLS *2007;25:2033–2043*

Disclosure of potential conflicts of interest is found at the end of this article.

INTRODUCTION

Müller cells constitute the main glial population of the retina [1]. They share a lineage with retinal neurons, and both Müller cells and neurons share a common progenitor that is multipotent at all stages of retinal histogenesis [2]. This evidence derives from examination of the progeny of a single mouse retinal progenitor cell transfected with a retrovirus, which generated clones containing up to three types of neurons, whereas others contained a combination of neurons and Müller glia, Müller glia alone, or a single type of neuron [2]. For several decades, it has been known that fish and amphibians are capable of regenerating neural retina [3], and previous studies have indicated that Müller cells may regenerate chick [4] and rat retina [5]. More recent findings have shown that, in the adult zebra fish, Müller glia form the retinal stem cell niche and are able to generate retinal stem cells in the regenerating retina [6]. Furthermore, Müller glia from the adult rat retina have been more recently shown to exhibit neural stem cell properties [7].

Müller cells have a structural role in the retina in addition to providing metabolic support to neurons and blood vessels. They are easily characterized by their phenotypic characteristics in vitro, including the presence of intracellular glycogen granules and the expression of epidermal growth factor receptor (EGF-R), vimentin, cellular retinaldehyde binding protein (CRALBP), and glutamine synthetase [8, 9]. They also express the glutamate transporter GLAST and depolarize in response to L-glutamate without changes in membrane resistance, consistent with the electrogenic uptake of this amino acid [10]. We first described the Müller cell characteristics of the spontaneously immortalized human cell line MIO-M1 [11], but our recent work has revealed that many similar cell lines can be derived from the adult human retina. Since immortalization is one of the characteristics of stem cells, and based on recent evidence that postnatal Müller cells in zebra fish and rat exhibit progenitor characteristics in experimental models of retinal injury, we investigated whether the immortalized human cell lines that we have obtained from the neural retina of adult human eyes have stem cell characteristics. On this basis, we examined whether MIO-M1 cells and similar cell preparations express markers of neural progenitors, whether they are capable of differentiating into retinal neurons in vitro, and whether they have the potential to migrate and differentiate, a property of neural and retinal stem cells [12–16], when grafted into the subreti-

Correspondence: Gloria Astrid Limb, Ph.D., Ocular Repair and Regeneration Biology Unit, Departments of Cell Biology and Pathology, Institute of Ophthalmology, 11 Bath Street, London EC1V 9EL, U.K. Telephone: 020 7608-6974; Fax: 020 7608-4034; e-mail: g.limb@ucl.ac.uk Received November 8, 2006; accepted for publication May 9, 2007; first published online in STEM CELLS *EXPRESS* May 24, 2007. 1066-5099/2007/$30.00/0 doi: 10.1634/stemcells.2006-0724

Table 1. Primer sequences used for reverse transcription-polymerase chain reaction analysis

Human genes	Primer sequences (5′–3′)	Product size (bp)	Annealing temperature (°C)
CRALBP	**F: ATG TCA GAA GGG GTG GG** **R: TCA GAA GGC TGT GTT CTC A**	**953**	**60**
Glutamine synthetase	F: ATGCTGGAGTCAAGATTGCG R: TCATTGAGAAGACACGTGCG	535	60
Sox2	**F: GG CAG CTA CAG CAT GAT GC** **R: TC GGA CTT GAC CAC CGA AC**	**236**	**60**
Chx10	F: A GCT AGA GGA GCT GGA GAA G R: CA TGA TGC CAT CCT TGG CTG	258	62
Pax6	**F: AG ATG AGG CTC AAA TGC GAC** **R: GT TGG TAG ACA CTG GTG CTG**	**302**	**60**
Notch 1	F: GTCGGACTGGTGAGGACTG R: AGCCCTCGTTACAGGGGTT	177	60
S-opsin	**F: TAGCAGGTCTGGTTACAGGATG** **R: GAGACGCCAATACCAATGGTC**	**148**	**60**
Calretinin	F: ATC CTG CCA ACC GAA GAG AAC R: GCA GGA AGT TTT CCT GGA CAG	291	64
Recoverin	**F: AG CTG CAG CTG AAC ACC AAG** **R: TCG TCT GGA AGG AGC TTC AC**	**384**	**62**

Abbreviations: bp, base pairs; CRALBP, cellular retinaldehyde binding protein; F, forward; R, reverse.

nal space of the dystrophic Royal College of Surgeons (RCS) rat, a model of retinal degeneration, or the neonatal Lister hooded rat.

MATERIALS AND METHODS

Isolation of Müller Cells from the Adult Neural Retina

Müller cells were isolated as previously described by us and others [9, 11, 17, 18] from the neural retina of cadaveric donor eyes with no eye disease (age range 18 months to 83 years old). Upon approval of the ethics committee of the local health authority, eyes consented for research were obtained from Moorfields Hospital Eye Bank between 24 and 48 hours postmortem. After removal of the cornea and the lens by holding the optic nerve on the upright position, vitreous and retina were gently dislodged from the eyecup with a pair of small forceps, leaving behind the retinal pigment epithelium (RPE) and choroid. The retina was then carefully cut from the optic nerve and placed in a Petri dish. Using a surgical blade, the neural retina was excised approximately 4 mm away from the ciliary body (supplemental online Fig. A). This was done to avoid contamination with retinal stem cells reported in this region [19]. Since separation of the retina from the ciliary body and the vitreous may potentially dislodge cells from the ciliary body that could contaminate cell preparations obtained from the neural retina, we obtained small fragments of neural retina from two eyes without disturbing the ciliary body. For this purpose, we made four radial cuts through the sclera and the vitreous (the deepest one in the superior pole) to obtain a flattened structure. Then, using a punch cutter 1 cm in diameter, we cut a section of retina attached to vitreous, RPE, and choroid from the posterior section of the eye. Retina was then carefully dissected from these small fragments (supplemental online Fig. B). To isolate the Müller cells, neural retina was rinsed with phosphate-buffered saline (PBS), placed in Trypsin-EDTA (5% trypsin, 2% EDTA; Gibco-BRL, Gaithersburg, MD, http://www.gibcobrl.com), homogenized by vigorous pipetting, and incubated in the same solution for 20 minutes at 37°C. Large tissue debris was then removed by filtration through a stainless steel sieve. Dissociated cells were washed and cultured in tissue culture flasks (Becton, Dickinson and Company, Franklin Lakes, NJ, http://www.bd.com) coated with 10 $\mu g/cm^2$ fibronectin (Sigma-Aldrich, St. Louis, http://www.sigmaaldrich.com) in the presence of 40 ng/ml epidermal growth factor (EGF; Sigma) in Dulbecco's modified Eagle's medium (DMEM) containing L-Glutamax I (Gibco-BRL) and 10% fetal calf serum (FCS; Gibco-BRL). The original medium was maintained until the first colonies were formed, after which it was replaced weekly with fresh medium without EGF. After 2–3 weeks, cells were detached by incubation with Trypsin-EDTA (5.0 g/l trypsin, 2.0 g/l EDTA) (Sigma) for 3 minutes at 37°C. Cells were then expanded in culture and examined for their characteristic morphology, electron-microscopic features, and expression of CRALBP (antibody kindly provided by Professor J. Saari, University of Washington), cytokeratin 8/18 (CAM 5.2 antibody from Becton, Dickinson), fibroblast surface protein (antibody from Abcam, Cambridge, U.K., http://www.abcam.com), vimentin (antibody from Dako, Glostrup, Denmark, http://www.dako.com), glial fibrillary acidic protein (GFAP), EGF-R, and glutamine synthetase (antibodies from Santa Cruz Biotechnology Inc., Santa Cruz, CA, http://www.scbt.com) using our methods previously described [11]. Cells isolated from whole neural retina or retinal sections obtained by punch cutting through the vitreous and sclera yielded similar cell preparations that exhibited Müller cell characteristics and spontaneous immortalization.

Expression of mRNA Coding for Markers of Neural Retinal Stem Cells and Mature Retinal Neurons by Immortalized Cells

Following trypsinization of Müller cell monolayers, total cellular RNA was isolated from cell pellets using the RNeasy system (Qiagen, Hilden, Germany, http://www1.qiagen.com) according to the manufacturer's instructions. Cells used to isolate RNA were derived from passages 8–45. For the reaction, 1 μg of total RNA was reverse-transcribed in 20-μl reactions consisting of 5 mM $MgCl_2$, 1 mM deoxynucleoside-5′-triphosphate (dNTP), 1 U/μl RNase inhibitor, 0.8 U/μl AMV reverse transcriptase (Roche Diagnostics, Basel, Switzerland, http://www.roche-applied-science.com), and 80 ng/μl oligo(dT)-15 primers (Roche) in 10 mmol/l Tris/HCl buffer containing 50 mM KCl. The mixture was incubated as follows: 10 minutes at 25°C, 60 minutes at 42°C, 5 minutes at 99°C, and 5 minutes at 4°C in a thermal cycler (Eppendorf AG, Hamburg, Germany, http://www.eppendorf.de). Polymerase chain reaction (PCR) amplification was then performed using our published methods [20] and specific primers for CRALBP, glutamine synthetase, Notch 1, Sox2, Chx10, Pax6, calretinin, S-opsin, and recoverin. Sequences were derived from the human genome sequence, GenBank (Table 1). The amplification was performed in a final volume of 50 μl by addition of 1.5 mM $MgCl_2$, 0.2 mM dNTP, 2.5 U Expand HiFi Taq DNA polymerase (Roche), 0.4 μM primers in 50 mM KCl, and 10 mM Tris/HCl, pH 8.0. The mixture was initially incubated at 94°C for 2 minutes followed by 30–34 cycles

under the following conditions: 94°C for 30 seconds, annealing temperature for 30 seconds, 72°C for 1 minute, and one cycle of 72°C for 5 minutes. PCR products were then analyzed by agarose gel electrophoresis (1%) containing 25 ng/ml ethidium bromide (Sigma).

Differentiation of MIO-M1 Cells and Other Cell Lines into Neural Phenotypes

The Müller cell line MIO-M1 and similar immortalized cells, named as MIO-M2, MIO-M3, MIO-M4, etc., were maintained in culture as previously described [11]. In more detail, cells were maintained as monolayers cultured in the presence of DMEM containing L-Glutamax I and 10% FCS. Upon confluence, cells were detached using Trypsin-EDTA (5% trypsin, 2% EDTA) and seeded at a 1:6 dilution of the original flask. For dedifferentiation studies, cells were cultured at a density of 500–800 cells per cm^2 in DMEM containing 10% FCS on cell culture slides coated with 50 μg/ml extracellular matrix (ECM) gel or 10 μg/ml fibronectin (Sigma). Fibroblast growth factor-2 (FGF2) or retinoic acid (RA) (Sigma) were then added to the medium to achieve concentrations of 40 ng/ml and 500 nM, respectively. Cells were cultured for 3–7 days at 37°C with replenishment of medium and growth factors every 2 days. To assess the clonality of the cells, a mixture of cells transfected with enhanced green fluorescent protein (EGFP) (see below) was mixed with nontransfected cells at a ratio of 1:1 and the formation of green or nongreen neurospheres examined after 4 days in culture using the same culture conditions as above. Acquisition of neural morphology was examined by phase contrast microscopy using the Leica imaging system DC200 (Heerbrugg, Switzerland, http://www.leica.com) and confocal microscopy (see below). To examine the expression of markers of retinal stem cells, slides were fixed in 4% paraformaldehyde in PBS, pH 7.4, and stained with the following antibodies: rabbit polyclonal anti-Notch 1, sonic hedgehog (Shh), Pax6 (Santa Cruz Biotechnology), Sox2 (Chemicon, Temecula, CA, http://www.chemicon.com), goat polyclonal anti-Chx10 (Santa Cruz Biotechnology), monoclonal anti-nestin and anti-βIII tubulin (Chemicon), and rabbit polyclonal anti-cyclin D (Santa Cruz Biotechnology). Cells were also labeled with fluorescent peanut agglutinin (Vector Laboratories, Burlingame, CA, http://www.vectorlabs.com). Specificity of staining for Sox2, Pax6, Shh, and Chx10 was confirmed by overnight incubation of the corresponding blocking peptides (catalog numbers: sc-17319P, sc-7750P, sc-1194P, and sc-21692P, respectively; Santa Cruz Biotechnology) with the primary antibodies at a ratio of 10:1 by weight. Additional controls included the omission of primary antibodies and the use of IgG isotypes from the same species in which the primary antibodies were raised. To determine the expression of retinal neural phenotypes, cells were stained with monoclonal antibodies to cone/rod peripherin (clone 5, kind gift from Professor R. Molday, University of British Columbia); polyclonal anti-protein kinase C (PKC) (Santa Cruz Biotechnology); polyclonal anti-calretinin identifying ganglion cells and major retinal neurons (Swant, Bellinzona, Switzerland, http://www.swant.com); polyclonal anti-HuD and Brn3 identifying ganglion and amacrine cells (Santa Cruz Biotechnology); and polyclonal anti-160 kDa neurofilament protein identifying major retinal neurons (Chemicon). Binding of primary antibodies was detected with donkey anti-IgG labeled with Alexa Fluor 488 or 546 reacting with the species in which the primary antibody was raised (Molecular Probes, Eugene, OR, http://probes.invitrogen.com). Slides were costained with 4,6-diamidino-2-phenylindole (Sigma) to visualize cell nuclei. Fluorescent images were recorded using a confocal microscope (LSM 510; Carl Zeiss, Jena, Germany, http://www.zeiss.com).

To assess the percentage of cells expressing the different markers, following fixation and immunostaining of cells cultured in 96-well plates, positively stained cells were counted using the Cellomics ArrayScan VTI HCS automated reader (Cellomics, Pittsburgh, http://www.cellomics.com). Using the integrated reader's software, over 5,000 cells from five replicates were analyzed in each group. Results were expressed as the percentage of positive cells.

Western Blot Analysis

Subconfluent cell monolayers of Müller cell lines cultured on either uncoated tissue culture flasks or culture flasks coated with fibronectin (FN) or ECM gel in the presence or absence of RA or FGF2 extracellular matrix proteins were lysed with Laemmli buffer, followed by centrifugation of the lysates at 13,000 rpm for 5 minutes and storage of the supernatants at −85°C until use. Western blotting of cell lysates (1.5 mg/ml) was performed as previously described [20] using the same antibodies used for immunostaining, secondary antibodies coupled to horseradish peroxidase (Jackson Immunoresearch Laboratories, West Grove, PA, http://www.jacksonimmuno.com), and enhanced chemiluminescence reagent (Amersham Biosciences, Piscataway, NJ, http://www.amersham.com). The images were analyzed using a Fuji image reader LAS-1000 Pro, version 2.1 (Fuji, Bedford, U.K., http://www.fujifilm.com).

Retinal Transplantation

The use of animals in this study was in accordance with the Home Office regulations for the care and use of laboratory animals and the U.K. Animals (Scientific Procedures) Act (1986). RCS rats were bred in-house, and Lister hooded rats were purchased from Harlan (Indianapolis, http://www.harlan.com) or Charles River Laboratories (Wilmington, MA, http://www.criver.com). Animals were kept under a 12-hour/12-hour light-dark cycle (light cycle mean illumination: 30 cd/m^2). To trace the transplanted cells, spontaneously immortalized Müller cells were transfected with a retroviral vector harboring EGFP protein (Clontech, Palo Alto, CA, http://www.clontech.com) using Lipofectamine 2000 (Invitrogen, Carlsbad, CA, http://www.invitrogen.com) according to the manufacturer's instructions and our published methods. Three cell lines (MIO-M1, MIO-M4, and MIO-M7) obtained from whole neural retinae were used for the transplantation studies. Dissociated cells (2×10^4 cells in 2 μl) were grafted into the subretinal space of 3–4-week-old dystrophic RCS rats susceptible to retinal degeneration [21, 22] as previously described [23]. Adult animals were anesthetized using a mixture of medetomine hydrochloride and ketamin reversed with atipamezole hydrochloride. Sham-injected rats received DMEM without cells. All injections were given in a single eye, with the contralateral eyes used as untreated controls. Animals were immunosuppressed with oral cyclosporine A (210 mg/l drinking water) from day 2 before transplantation until termination of the experiment. For transplants into neonatal Lister hooded rats, the dams were maintained on oral cyclosporine and azathioprine immediately after the birth of the rat pups. Each experimental group consisted of 6–8 animals. Under terminal anesthesia and following intracardial perfusion with 4% paraformaldehyde in PBS, eyes were enucleated. After washing in PBS, eyes were cryoprotected in 30% sucrose. Frozen sections 15-μm thick were cut, and the fate of the transplanted cells was investigated by confocal microscopy of retinal sections costained with monoclonal antibody to GFP and antibodies to neural retinal markers as above. Nontransfected donor cells were identified using antibodies to human mitochondria (Chemicon).

RESULTS

Establishment and Characterization of Immortalized Müller Cell Lines from Adult Human Retina

Similar to the protocols used to grow the Müller cell line MIO-M1 [11], cell colonies formed after 2–3 weeks in culture were dissociated, expanded in the absence of EGF, and examined for Müller characteristics at the time of the first passage and after 20 passages. Cells that continued dividing after twenty passages (approximately 100 divisions) were considered immortalized. To date, out of 15 eye donors, we have generated 12 cell lines with similar characteristics. Six of the cell lines have undergone 20 passages (approximately 100 divisions), four of the cell lines (MIO-M3 to M6) 57 passages (approximately 285 divisions), one cell line (MIO-M2) 102 passages (approximately 510 passages), and the previously published cell line MIO-M1

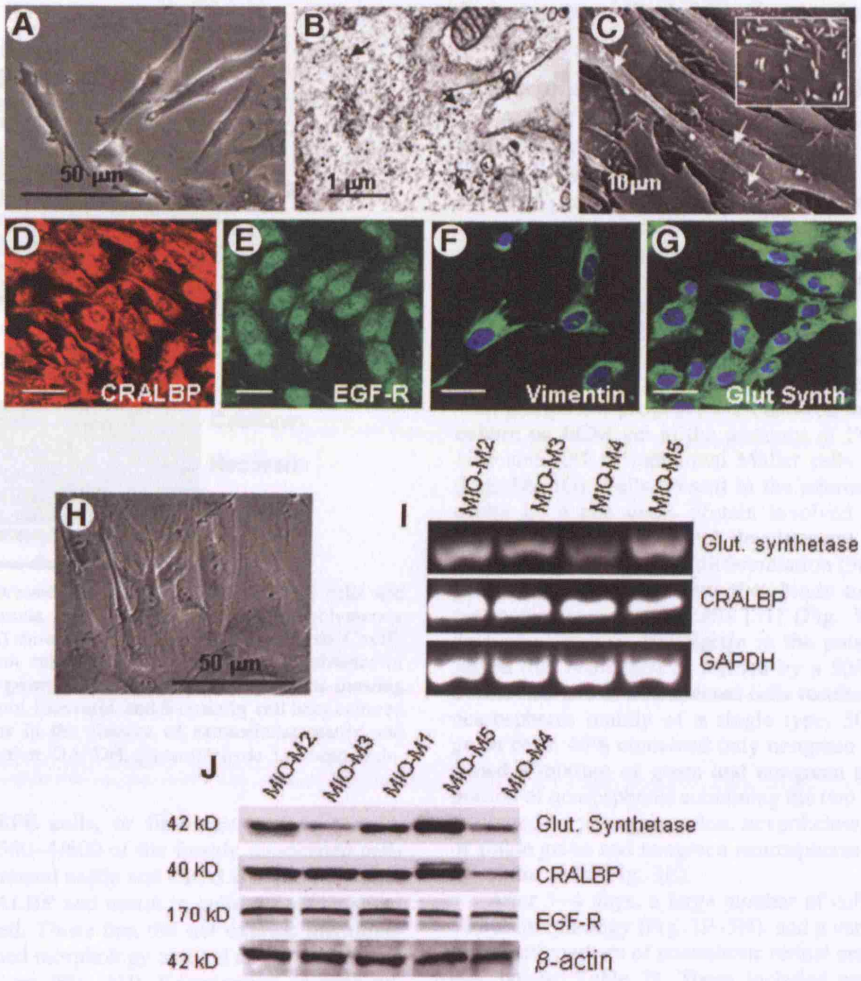

Figure 1. Confirmation of Müller cell phenotypes in spontaneously immortalized human cells derived from the adult neural retina. **(A):** Characteristic Müller cell bipolar morphology under standard in vitro culture conditions observed under a phase contrast microscope. **(B):** Transmission electron-microscope image showing intracellular accumulation of glycogen granules (black arrows). **(C):** Scanning electron-microscope image showing characteristic microvilli on apical surface (white arrows). Inset shows a magnification of these microvilli. **(D–G):** Immunostaining of cells in culture for various Müller cell markers confirming the expression of CRALBP, EGF-R, vimentin, and glutamine synthetase. Nuclei are stained with 4,6-diamidino-2-phenylindole (blue). **(H):** Characteristic morphology of retinal cells that do not express EGF-R or nestin and that do not maintain their growth in vitro. **(I):** Reverse transcription-polymerase chain reaction products showing that different cell lines express CRALBP and glutamine synthetase, the well known markers of Müller glia. **(J):** Western blotting of cell lysates from different cell lines showing the corresponding bands for glutamine synthetase, CRALBP, and EGF-R. Bars in confocal images denote 50 μm. Abbreviations: CRALBP, cellular retinaldehyde binding protein; EGF-R, epidermal growth factor receptor; GAPDH, glyceraldehyde-3-phosphate dehydrogenase; Glut., glutamine; Glut Synth, glutamine synthetase.

[11] has undergone 120 passages (approximately 600 divisions). Although Müller glia that became immortalized in vitro are responsive to EGF, the first two cell lines established in our laboratory did not have EGF in culture at any time. However, we found that faster colonies were formed when EGF was added to the primary culture and that, once we dissociate the first colonies for expansion, EGF is not necessary to maintain cell growth. These cell lines have been frozen and thawed several times without losing their characteristics, and all cells examined after 50 passages exhibit the same features of cells tested at passages 1 and 20. We were also able to grow cells with immortalized characteristics from two eyes in which we sectioned the neural retina by punch cutting through the vitreous and sclera without disturbing the eye anatomy. This was done to avoid any potential contamination with cells from the ciliary body. The natures of the immortalized cell preparations obtained from adult neural retina were identified by gene expression and immunostaining for Müller cell markers as well as by their phenotypic characteristics using phase contrast, transmission, and scanning electron microscopy using standard techniques in our laboratory [11]. Subconfluent immortalized cells exhibited bipolar morphology, irregular membrane appearance, and formation of cytoplasmic projections (Fig. 1A), which are well recognized features of Müller cells in culture [9, 11, 17, 18]. They also contained cytoplasmic glycogen granules as observed by transmission electron microscopy (Fig. 1B) and displayed microvillous projections on their apical surface as observed by scanning electron microscopy (Fig. 1C), as previously described for Müller glia [11]. Immunocytochemical staining confirmed that these cells expressed well characterized markers of Müller cells, including CRALBP, EGF-R, vimentin, and glutamine synthetase [8, 9, 17, 24] (Fig. 1D–1G). Only a small proportion of these cells (<5%) expressed GFAP (not shown), which is in accordance with previous reports that GFAP is found at low levels or is completely absent in mammalian Müller cells [25], and none of the cell preparations expressed cytokeratin 8 or 18,

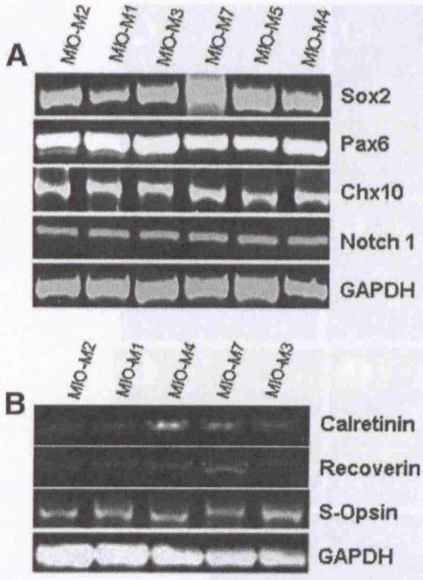

Figure 2. mRNA expression of markers of neural stem cells and postmitotic retinal neurons. **(A):** Reverse transcription-polymerase chain reaction (RT-PCR) showing the expression of Sox2, Pax6, Chx10, and Notch 1 by different cell lines' cells cultured in the absence of extracellular matrix and growth factors. **(B):** RT-PCR products showing the expression of calretinin, recoverin, and S-opsin by cell lines cultured under normal conditions in the absence of extracellular matrix and growth factors. Abbreviation: GAPDH, glyceraldehyde-3-phosphate dehydrogenase.

known markers of RPE cells, or fibroblast surface protein. Interestingly, only 1/500–1/600 of the freshly dissociated cells from the retina coexpressed nestin and CRALBP, and only cells that coexpressed CRALBP and nestin in culture became spontaneously immortalized. Those that did not express this molecule acquired a flattened morphology and did not proliferate for more than 4–6 passages (Fig. 1H). Examination of gene expression by reverse transcription (RT)-PCR confirmed that these cells express mRNA coding for glutamine synthetase and CRALBP (Fig. 1I). In addition, Western blot analysis of cell lysates showed that bands of molecular weights 42 kDa, 40 kDa, and 170 kDa corresponding to glutamine synthetase, CRALBP, and EGF-R, respectively (Fig. 1J), were obtained by immunoblotting with the corresponding antibodies. Cells obtained from punch cutting through the sclera and vitreous exhibited similar characteristics to the cells obtained by dislodging the whole vitreous body with the retina. When cultured in the absence of extracellular matrix and growth factors, all cell lines permanently expressed Müller glial markers.

Gene Expression of Retinal Stem Cell Markers by Spontaneously Immortalized Cell Lines

Investigation of the expression of various markers of retinal stem cells was performed by RT-PCR of mRNA extracted from different cell lines cultured on tissue culture flasks in the absence of extracellular matrix and without the addition of growth factors. Expression of mRNA coding for Sox2, Pax6, Chx10, and Notch 1 was observed in all cell lines examined. Figure 2A shows the expression of mRNA by 6 of the 12 cell lines established in our laboratory. Similarly, mRNA coding for markers of postmitotic retinal neurons, including calretinin, recoverin, and S-opsin, was also observed in cells cultured under the above conditions (Fig. 2B). Variations in the levels of expression of these factors were observed among cell lines, and further studies will elucidate the significance of these differences.

Differentiation of Immortalized Cell Lines

We induced differentiation of the different immortalized cell lines using conditions known to promote neural retinal differentiation [19, 26–28]. Culture of cells at a low density (500–800 cells per cm^2) on ECM gel in the presence of FGF2 or RA caused individual cells to form neurospheres, which could be examined for multipotentiality. Confirmation of clonality was achieved by limiting the dilution of cells dissociated from neurospheres so that a single cell placed in a tissue-culture well could multiply until confluence. Cells originating from a single clone were then dissociated and repeatedly cultured at low density (as above) to induce new formation of neurospheres with pluripotent progeny. We observed that, after 3–4 days of culture on ECM gel in the presence of FGF2 or RA, between 10% and 20% of individual Müller cells formed neurospheres (Fig. 3A–3D). Cells present in the neurospheres expressed (a) cyclin D, a cell cycle protein involved in the regulation of proliferation during retinal development [29]; (b) nestin, an early marker of neuronal differentiation [30]; and (c) binding of peanut agglutinin, a lectin that binds to glycoconjugates of pluripotent neural stem cells [31] (Fig. 3B–3D). Following 4 days of culture on fibronectin in the presence of RA, we observed that neurospheres formed by a 50/50 mixture of EGFP transfected and nontransfected cells resulted in the formation of neurospheres mainly of a single type: 50.3% contained only green cells, 46% contained only nongreen cells, and 3.7% contained a mixture of green and nongreen cells. The small proportion of neurospheres containing the two types of cells may be attributed to cell aggregation; nevertheless, the high proportion of single green and nongreen neurospheres confirms the clonality of the cells (Fig. 3E).

After 3–4 days, a large number of cells (>70%) exhibited neural morphology (Fig. 3F–3H), and a variable proportion also expressed markers of postmitotic retinal neurons at 4 and 7 days (see below; Table 2). These included expression of PKC (a marker of bipolar cells), peripherin (a marker of photoreceptor cells), HuD and Brn3 (markers of ganglion cells), 160 kDa neurofilament protein (a marker of ganglion, amacrine, and horizontal cells), and calretinin (a marker of ganglion, amacrine, and horizontal cells) (Fig. 3I–3N) [32–35]. Cells cultured under the same conditions for 4–7 days also expressed βIII tubulin, a marker of immature neurons (Fig. 3O) [36]. Acquisition of neural markers has been examined in 10 of the 12 spontaneously immortalized human cell lines established in our laboratory, and all have the ability to differentiate into cells expressing markers of retinal neurons.

Influence of Growth Factors and Extracellular Matrix on Müller Cell Differentiation

Depending on the growth factor used for differentiation of cells cultured on ECM gel, there was variability in the proportion of cells expressing markers of retinal progenitors and mature retinal neurons as well as in the pattern of staining for various progenitor and mature retinal markers (Table 2; Fig. 4A). Staining for Pax6, a progenitor and amacrine cell marker [37], was observed in cells cultured with FGF2 and RA, but very little or no staining was observed in cells cultured in the absence of these factors (Fig. 4A–4C). Staining for Sox2, a transcription factor and progenitor marker [38], was characteristically associated with cytoplasmic and neurite extensions on cells cultured with FGF2 (Fig. 4D), but nuclear staining was observed in 25%–30% of cells cultured in the presence of RA (Fig. 4E). In the absence of ECM gel and growth factors, the majority of cells

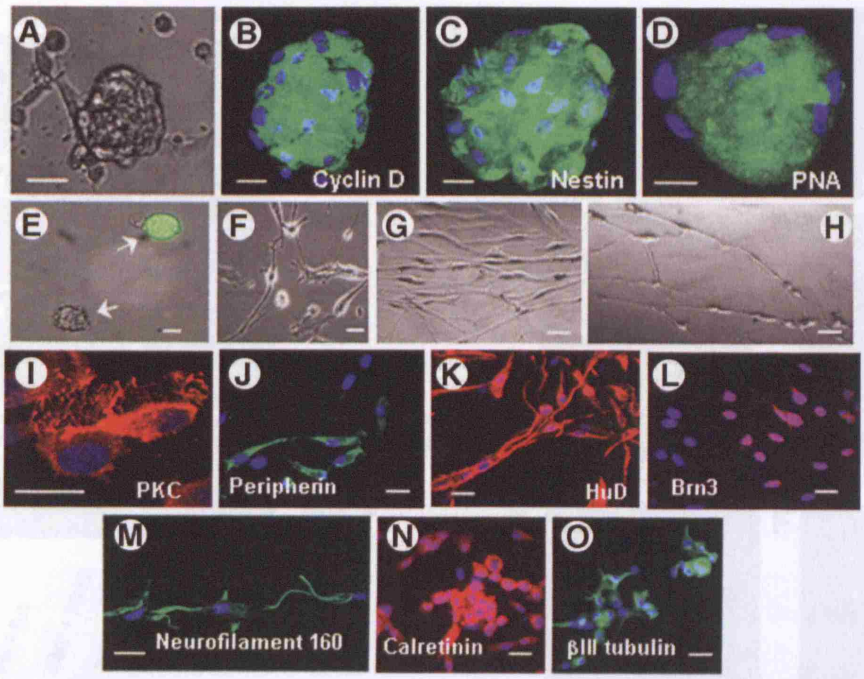

Figure 3. Dedifferentiation of Müller progenitor cells following short-term culture under various conditions. **(A–D):** Neurospheres derived from individual Müller cells after 3 days of culture on basement membrane protein in the presence of fibroblast growth factor-2 (FGF2). **(A):** Characteristic neurosphere as observed under phase light microscopy. **(B–D):** Cells forming neurospheres express markers of neural progenitors including cyclin D, nestin, and binding of PNA. **(E):** Cells contained in a mixture of enhanced green fluorescent protein transfected and nontransfected cells gave rise to neurospheres of a single cell type, confirming their clonality. **(F–H):** Cells cultured for 4 days on extracellular matrix gel in the presence of FGF2 exhibit a characteristic neuronal morphology. **(I–O):** Cells cultured for 4 days with FGF2 acquire markers of differentiated retinal neurons. They express PKC, peripherin, HuD, Brn3, 160 kDa neurofilament, calretinin, and βIII tubulin. Bars denote 50 μm. Nuclei are stained with 4,6-diamidino-2-phenylindole (blue). Abbreviations: PKC, protein kinase C; PNA, peanut agglutinin.

Table 2. Percentage of cells expressing markers of various cell types upon differentiation on extracellular matrix with addition of growth factors

		Variations in culture conditions		
Antibody	**Cell marker**	**ECM + FGF2 (%)**	**ECM + RA (%)**	**No ECM or growth factors (%)**
Markers of neural progenitors—4 days in culture				
Sox2	Progenitor	75 ± 8.5[a]	59 ± 6.4	86 ± 7.0
Pax6	Amacrine/progenitor	40 ± 4.1[a,b]	19 ± 7.4[b]	5 ± 1.5
Shh	Progenitor	40 ± 7.1[b]	38 ± 8.2[b]	10 ± 3.0
Chx10	Bipolar/progenitor	15 ± 2.4[a,b]	5.0 ± 2.2	3 ± 0.8
Markers of postmitotic retinal neurons and Müller glia—7 days in culture				
CRALBP	Müller glia	12 ± 2.0[b]	15 ± 5.0[b]	74 ± 4.0
HuD	Ganglion	37 ± 6.3[b]	35 ± 8.2[b]	5 ± 2.0
PKC	Bipolar	33 ± 2.4[a,b]	17 ± 3.0[b]	7 ± 2.0
Peripherin	Photoreceptors	29 ± 3.6[b,c]	14 ± 4.6	2 ± 0.6

The figures indicate the proportion of cells immunostaining for each of the molecules investigated (± SEM) following 4 days (neural progenitor markers) and 7 days (postmitotic neural retinal markers) in culture on ECM gel in the presence of FGF2 or RA. Figures do not equal 100% because some of the staining marked overlapping cell populations.

[a] $p < .01$ versus percentage of positive cells cultured in the presence of RA.

[b] $p < .01$ versus percentage of positive cells cultured in the absence of ECM gel and growth factors.

[c] $p < .05$ versus percentage of positive cells cultured in the presence of RA.

Abbreviations: CRALBP, cellular retinaldehyde binding protein; ECM, extracellular matrix; FGF2, fibroblast growth factor-2; PKC, protein kinase C; RA, retinoic acid; Shh, sonic hedgehog.

expressed cytoplasmic Sox2 (Fig. 3F). Staining for the signaling protein Shh, a key regulator of neural development [39], was predominantly perinuclear in cells cultured with FGF2, but less dense perinuclear and cytoplasmic staining was observed in cells cultured with RA (Fig. 4G, 4H). Staining for Chx10, a progenitor and amacrine cell marker [40, 41], was mainly observed in the cytoplasm of a small proportion of cells cultured with FGF2, but weak or no staining for this molecule was observed on a very small number of cells cultured in the presence of RA (Fig. 4J, 4K). In the absence of extracellular matrix

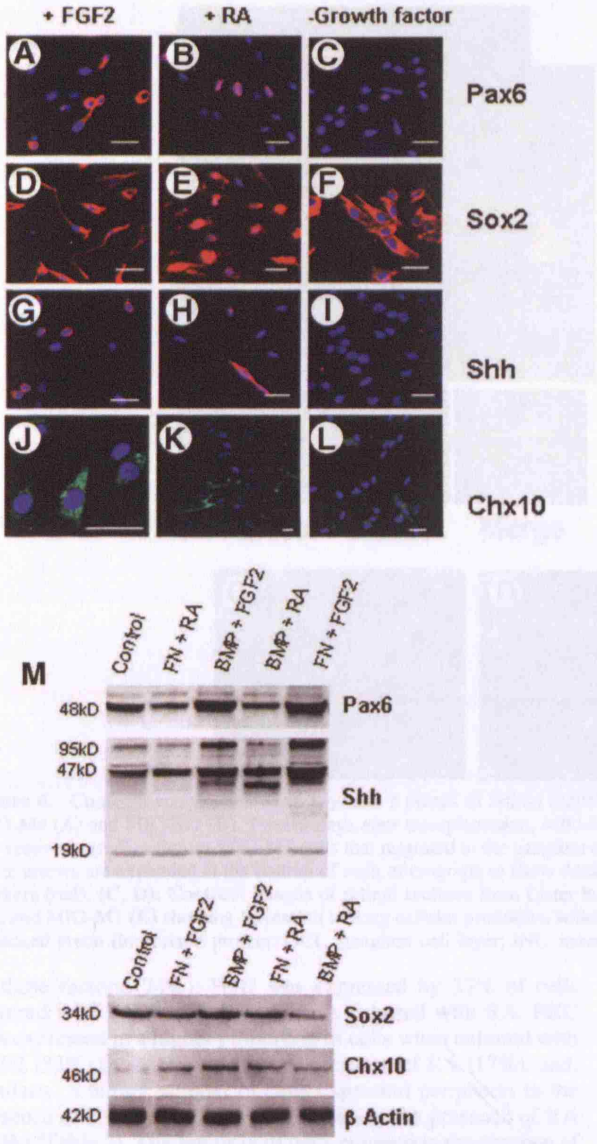

Figure 4. Confocal photomicrographs of cells stained for markers of neural progenitors. Only positive cells are shown to illustrate the pattern of expression of these factors under different conditions. Cells were cultured on extracellular matrix (ECM) gel with FGF2 or RA for 5 days. Nuclei are stained with 4,6-diamidino-2-phenylindole (blue). Perinuclear **(A)** and nuclear **(B)** staining for Pax6 in cells cultured with FGF2 or RA. **(D):** Cytoplasmic and dendrite staining for Sox2 on cells cultured with FGF2 and **(E)** nuclear localization of this factor in cells cultured with RA. Perinuclear **(G)** and cytoplasmic **(H)** staining for Shh in cells cultured with FGF2 and RA, respectively. **(J):** Cytoplasmic staining for Chx10 in cells cultured with FGF2 and **(K)** weak staining for the same molecule in cells cultured with RA. **(C, F, I, L):** With the exception of Sox2, which was expressed by most cells cultured in the absence of growth factors, the proportion of cells staining for Pax6, Shh, and Chx10 under these control conditions was much reduced. **(M):** Western blots of Müller cell lysates cultured in the presence of FN or ECM gel with FGF2 or RA. The bands show molecular weights corresponding to Pax6, Shh, Chx10, Sox2, and the control protein β actin. Bars in confocal images denote 50 μm. Abbreviations: BMP, basement membrane protein; FGF2, fibroblast growth factor-2; FN, fibronectin; RA, retinoic acid; Shh, sonic hedgehog.

and growth factors, a very small proportion of cells expressed Shh and Chx10 (Fig. 4I, 4L). Table 2 shows the variations in the

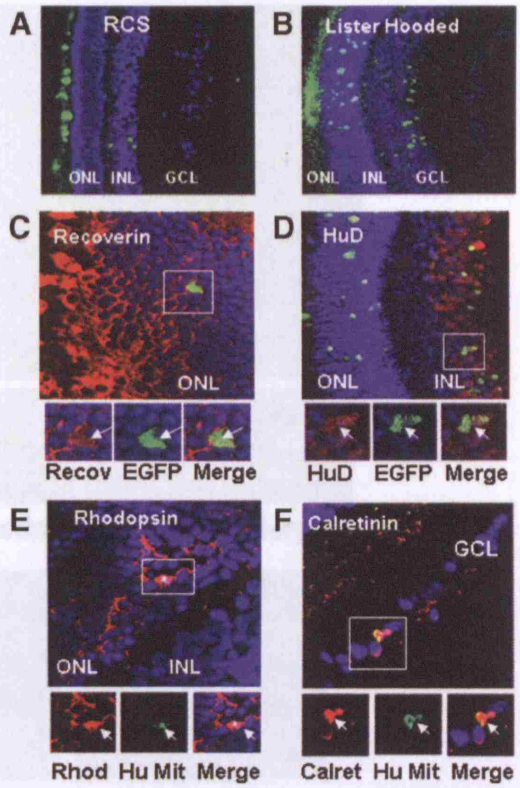

Figure 5. Confocal images of retinal sections from RCS and Lister hooded rats grafted with the immortalized Müller cell line MIO-M1. **(A):** More cells (green) migrate into the neonatal Lister hooded rat retina than into **(B):** the degenerating retina of the RCS rat 14 days after transplantation. **(C, D):** Confocal images of retinal sections from neonatal Lister hooded rats stained for recoverin and HuD. Two weeks after grafting, cells that migrated to the ONL expressed recoverin (red), whereas cells that migrated to the inner nuclear layer expressed HuD (red). **(E, F):** Confocal images of retinal sections from RCS rats stained for rhodopsin and calretinin. Nine days after transplantation, cells that migrated into the ONL could be seen expressing rhodopsin (red), whereas cells that migrated into the GCL could be seen expressing calretinin (red). Areas enclosed in white boxes are expanded at the bottom of each confocal micrograph to show individual and dual staining for either EGFP (green) transfected cells (Lister hooded) or human mitochondria (green) (RCS rats) and the corresponding neural markers (red). Nuclei are stained with 4,6-diamidino-2-phenylindole (blue). Abbreviations: Calret, calretinin; EGFP, enhanced green fluorescent protein; GCL, ganglion cell layer; Hu Mit, human mitochondria; INL, inner nuclear layer; ONL, outer nuclear layer; RCS, Royal College of Surgeons; Recov, recoverin; Rhod, rhodopsin.

proportion of cells staining for the various markers examined. When cultured with FGF2, 75% expressed Sox2 when compared with 59% of cells cultured with RA ($p < .01$). A higher number of cells expressed Pax6 when cultured with FGF2 (40%) compared with RA (19%) ($p < .01$), and a similar number of cells expressed Shh when cultured in the presence of FGF2 or RA (40% and 38%, respectively). Although a small proportion of cells expressed Chx10 in the presence of FGF2 (15%), this was significantly higher ($p < .05$) than in the presence of RA (5%). Variations in the proportion of cells expressing markers of postmitotic retinal neurons were also observed when cells were cultured for 7 days in the presence of different growth factors (Table 2). A significant decrease in the number of cells expressing CRALBP was observed when cells were cultured in the presence of FGF2 or RA (12% and 15%, respectively) when compared with cells cultured in the absence

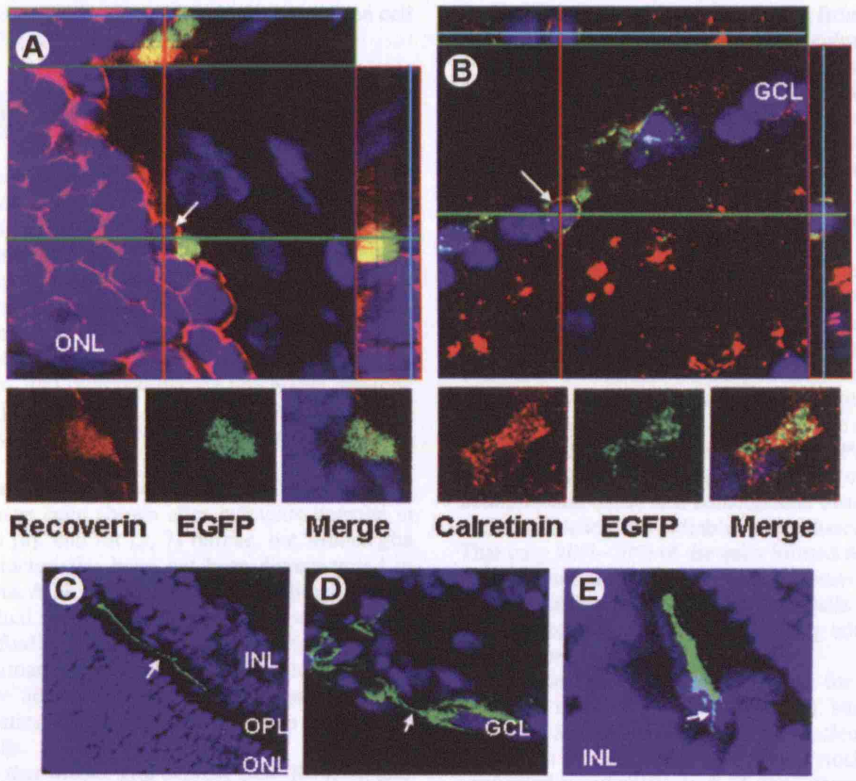

Figure 6. Confocal analysis showing *x*, *y*, and *z* planes of retinal sections from Lister hooded rats grafted with the immortalized Müller cell lines MIO-M4 **(A)** and MIO-M7 **(B)**. Twelve days after transplantation, MIO-M4 cells that migrated to the outer nuclear layer costained for EGFP (green) and recoverin (red), whereas MIO-M7 cells that migrated to the ganglion cell layer costained for EGFP (green) and calretinin (red). Cells marked with white arrows are expanded at the bottom of each micrograph to show details of individual and dual staining for EGFP and the corresponding neuronal markers (red). **(C, D):** Confocal images of retinal sections from Lister hooded rats grafted with the immortalized cell lines MIO-M4 **(C)**, MIO-M7 **(D)**, and MIO-M1 **(E)** showing formation of long cellular processes, which in some cases resemble axonal formation (arrows). Abbreviations: EGFP, enhanced green fluorescent protein; GCL, ganglion cell layer; INL, inner nuclear layer; ONL, outer nuclear layer; OPL, outer plexiform layer.

of these factors (74%). HuD was expressed by 37% of cells cultured with FGF2 and 35% of cells cultured with RA. PKC was expressed in a higher proportion of cells when cultured with FGF2 (33%) ($p < .01$) than in the presence of RA (17%), and, similarly, a higher number of cells expressed peripherin in the presence of FGF2 (29%) ($p < .01$) than in the presence of RA (14%) (Table 2). The majority of cells cultured in the absence of ECM gel and growth factors also maintained the expression of Sox2 (86%) after 7 days, but very few cells expressed markers of retinal neurons (Table 2). Confirmation of the specificity of staining for Sox2, Pax6, Shh, and HuD was achieved by blocking the activity of these antibodies by overnight incubation with their corresponding blocking peptides. Using this approach, complete depletion of immunoreactivity was achieved, resulting in negative staining for these molecules (not shown). Lack of immunoreactivity was also observed when the primary antibody was omitted or when control isotype antibodies were used. Western blot analysis of cell lysates following culture on ECM gel or FN in the presence or absence of FGF2 or RA showed that bands of molecular weights 48 kDa, 47 kDa, 46 kDa, and 34 kDa corresponding to Pax6, Shh, Sox2, and Chx10, respectively, were obtained by immunoblotting with the corresponding antibodies. In addition, immunoblotting with the anti-Shh antibody yielded bands of approximately 19 kDa (corresponding to the secreted N-terminal domain of Shh) and 95 kDa (which appears to be a Shh dimer) (Fig. 4M). Equal amounts of protein were applied to the blots, which were controlled by immunodetection with anti-β actin antibodies (Fig. 4M).

Retinal Grafting of Immortalized Cells with Müller and Stem Cell Characteristics

We investigated the biological activity of human Müller glia with neural stem cell characteristics by examining their ability to migrate into the retina and to express markers of retinal neurons in vivo, following grafting of dissociated cells into the subretinal space of the dystrophic RCS rat, a model of retinal degeneration [22] and neonatal Lister hooded rats. Confocal microscopy examination of retinal sections showed that transplanted cells could be observed in the outer and inner nuclear cell layers 9–14 days after grafting. We observed better migration of the Müller cell line MIO-M1 into the neonatal retina of Lister hooded rats than into the dystrophic retina of the RCS rat (Fig. 5A, 5B). Cells that migrated into the photoreceptor cell layer stained for recoverin and rhodopsin (Fig. 5C, 5E), markers of photoreceptor cells [31], whereas cells that migrated to the inner nuclear layer expressed HuD, a marker of major retinal neurons found in this layer [42] (Fig. 5D). Cells that had migrated to the ganglion cell layer also stained for calretinin (Fig. 5F), a marker of ganglion cells and amacrine cells [32] that may be found in this layer. As shown in Figure 6, subretinal injection of the Müller cell lines MIO-M4 and MIO-M7 also yielded similar results to those obtained with the Müller cell line MIO-M1. Following 12 days after subretinal injection of the MIO-M4 cell line, cells costaining for EGFP and recoverin were observed in the outer nuclear cell layer (Fig. 6A). Similarly, MIO-M7 cells that migrated to the ganglion cell layer costained for EGFP and calretinin. Cells with long processes, in some

cases resembling axons, were observed with all of the three cell lines investigated (Figs 6C, 6D).

DISCUSSION

Glial cells have the role of stem cells in the adult and embryonic brain in various species, and it is suggested that differentiation along the glial lineage may be a default state of development reflected in the progression of stem cells along the neuroepithelial to radial glia to astrocyte lineage [43]. Stem cells are thought to have an undifferentiated phenotype, but a population of glia retains neural progenitor ability in the central nervous system of different species [44]. This is illustrated by observations that radial glia, astrocytes, and oligodendrocyte precursors generate neurons [43, 45–49], for which it has been proposed that progression along a glial pathway is related to neuronal production [43].

The presence and neural regenerative ability of Müller glia in postnatal retina have been shown after cytotoxic damage in chick [4], zebra fish [6], and rat [5, 7] retinae, but Müller glia with progenitor characteristics have not been demonstrated in the adult human retina. Although there are obvious limitations to the study of individual cell progenies during human development, the present findings that a small proportion of cells isolated from the human neural retina becomes spontaneously immortalized in vitro and exhibits both Müller glia and neural stem cell characteristics suggest that adult human retina may also harbor these cells.

It is well known that Müller glia express EGF-R [8, 9], and studies have shown that overexpression of EGF-R by neural progenitors in vivo enhances glial cell differentiation [50]. Observations that EGF-R was localized to the cytoplasm and nuclei of immortalized Müller glia are in agreement with those previously reported that intracellular expression of EGF-R strongly correlates with highly proliferating activities of tissues [51–53]. This is in accordance with our observations that the immortalized cells reported in this study are highly proliferative. EGF responsiveness has been shown to correlate with EGF-R expression [53, 54] and may explain our observations that initial exposure to EGF by cells expressing EGF-R induces rapid proliferation. Expression of cyclin D by cells present in neurospheres is in agreement with observations that this cell cycle regulatory protein is found in the cytoplasm of proliferating cells [55] and neurons during development [56].

All the spontaneously immortalized cell lines we have established not only express mRNA for well known markers of Müller glia but also express proteins (as determined by immunostaining and Western blotting) that are characteristically expressed by these cells, including CRALBP, glutamine synthetase, vimentin, and EGF-R [1, 9, 11, 25]. In addition, electrophysiological studies on the first characterized cell line (MIO-M1) showed that they depolarized in response to glutamate without change in membrane resistance, a well known feature of mammalian Müller cells [10]. Other investigations on the cell line MIO-M1 have shown that, in response to proinflammatory factors, these cells produce matrix metalloproteinases 1, 2, and 9 [20, 57] as well as hepatocyte growth factor and vascular endothelial growth factor [58], which are known features of mature cells. These observations indicate that these cells not only possess features of mature Müller glia but also of neural stem cells when exposed to various extracellular matrix and growth factors in vitro.

As for the requirements for in vitro isolation and establishment of immortalized cell lines with Müller and stem cell characteristics, it is important to emphasize that, in our study, we did not derive the immortal cells from neurospheres grown under conditions normally used to culture retinal stem cells. Unlike previous reports in which retinal stem cells were derived from the ciliary body as sphere colonies in the absence of FCS [19], the cells reported in this study were grown as monolayers of adherent cells obtained from the neural retina and cultured in the presence of FCS. Using the culture conditions used by other investigators to grow neurospheres from the ciliary body [19], we were unable to grow these from the neural retina, which is in agreement with that previously reported [19]. Here, we show that factors present in FCS do not induce differentiation of neural retinal cells with stem cell and Müller glia characteristics, but that presence of extracellular matrix and neurogenic factors such as FGF2 and RA induce their differentiation. It is unlikely that the cell lines that we have established are derived from the ciliary body, as the human eye is a large organ in comparison with the eyes of fish and rodents, where Müller glia with stem cell characteristics have been identified. Potential contamination with cells from the ciliary body was avoided by removing the neural retinal tissue at a considerable distance from this region, which is clearly identifiable when dissecting the human eye. That only 10%–20% of the cells formed neurospheres under the culture conditions used to induce expression of neural markers may be explained by the fact that cells were cultured in the presence of FCS, which, by promoting adherence, might inhibit neurosphere formation.

Nuclear and cytoplasmic staining for Sox2 is found in the inner cell mass of the blastocyst [59], supporting our observations that Sox2 is expressed in the nucleus and cytoplasm of a population of Müller glia. Immunocytochemical studies were confirmed by identification of gene expression using RT-PCR analysis as well as by Western blots of cell lysates, which yielded corresponding molecular weights. Sox2 expression is associated with dividing stem cells and precursors of the central nervous system [38, 59] and has been shown to maintain neurogenesis in the adult mouse brain [60]. It is therefore possible that this factor may maintain the neurogenic properties of the spontaneously immortalized cells from the adult human retina. Shh is implicated in regulating adult neural stem cell proliferation [61], and it is a mitogenic factor for retinal progenitors [39], suggesting that it may promote the proliferation of stem cells with Müller characteristics isolated from the adult human retina. Chx10 constitutes an early marker of the developing retina and is required for retinal progenitor cell proliferation as well as formation of bipolar cells [40, 41]. In the mouse and chick, Chx10 is expressed in nearly all retinal progenitors but is absent from all postmitotic cells types except bipolar interneurons and a subset of Müller glia [41], which is in agreement with our findings that immortal cells expressing Müller glial characteristics express this protein. The Notch 1 signaling pathway is important at several stages of retinal development including the differentiation of retinal ganglion cells and Müller glia [62, 63]. Expression of this molecule by the cell lines reported in this study further indicates that they have neural stem cell characteristics. In our study, it is of interest that human-derived cells with Müller characteristics not only express genes coding for neural stem cells but also genes coding for proteins expressed by mature retinal neurons, such as Calretinin, recoverin, and S-opsin. Although a very small number of cells cultured under nondifferentiating conditions expressed markers of retinal neurons, as judged by immunohistochemical staining, a greater number of cells cultured in the presence of ECM and FGF2 or RA expressed neural retinal markers (Table 2). These observations highlight the proneural ability of the immortalized cells reported in this study. Immunohistochemical staining showed that HuD was expressed at both nuclear and cytoplasmic levels, which is in accordance with what is described by others, that

intracellular trafficking of HuD is important for neuronal differentiation [64, 65]. Extracellular matrix proteins have been recognized to play a very important role not only in the maintenance of the stem cell niche [66, 67] but also in the tissue-specific stem cell differentiation [68]. It is therefore of interest that, when cultured in the presence of ECM and growth factors, cells with Müller and stem cell characteristics are induced to express stem cell and neural markers in different proportions (Table 2; Fig. 3). We did not investigate the differentiation of Müller glia into astrocytes. However, under the experimental conditions used, we did not observe cells expressing the astrocyte marker GFAP. Differentiation of retinal stem cells into astrocytes has not been carefully investigated and it may be due to the scarcity of these cells in the neural retina [69]. Further studies using different matrix substrates and growth or differentiation factors may help to clarify this issue.

Although Müller glial cell proliferation (reactive gliosis) has been shown to occur during degenerative retinal processes [1], neurogenesis occurring in these conditions has not been demonstrated in the adult human retina. It is possible to speculate that if neural progenitors are harbored in the adult retina, these may have the potential to regenerate neurons. However, as there is no evidence that postdevelopmental neurogenesis may occur in the human eye, the possibility arises that this process is suppressed in vivo by unidentified factors present in the adult eye. Investigations into the feasibility of activating neurogenesis mediated by Müller progenitors in vivo may have the potential to develop into treatments for endogenous replacement of dysfunctional neurons.

To date, attempts to regenerate murine retina by transplantation of brain-derived or retinal progenitors have produced mixed results, and better migration and integration of stem cells have been shown when brain- or retinal-derived neural progenitors are transplanted into immature or injured retina [12, 70, 71]. Our study showed that migration and survival of cells with Müller and stem cell characteristics was better in normal neonatal retina than in the degenerating retina of the RCS rat, indicating that developmental cues may be beneficial to cell integration. The migration and acquisition of neural retinal markers in vivo by our immortalized human retinal cells closely resemble that observed with other neural progenitors [13, 15, 16]. At present, there are many limitations to the effective delivery of stem cells to regenerate retina [13, 15, 16], but the fact that cells with Müller glia and stem cell characteristics can be easily grown from human cadaveric retina, cryopreserved, and renewed for long periods of time without losing their phenotypic or genetic characteristics suggests that, once other obstacles in the retina itself can be overcome, these cells may have potential for clinical application and may merit further investigations.

ACKNOWLEDGMENTS

This work was supported by the Medical Research Council (MRC) (Grant number 67386), the Helen Hamlyn Trust (in memory of Paul Hamlyn), the Wellcome Trust (Grant reference 062290), the Henry Smith Charity, and the Michael and Ilse Katz Foundation, U.K. We thank Dr. James Ellis for help with tissue processing. We are also very grateful to Professor A.R. Venkitaraman from the Hutchison MRC Research Centre for allowing us to use the Cellomics ArrayScan VTI automated reader. This research has been partly funded by The Department of Health's National Institute for Health Research Biomedical Research Centre at Moorfields Eye Hospital and the UCL Institute of Ophthalmology, U.K. S.S. is supported by the Inlaks Foundation and the Henry Smith Trust.

DISCLOSURE OF POTENTIAL CONFLICTS OF INTEREST

The authors indicate no potential conflicts of interest.

REFERENCES

1 Newman E, Reichenbach A. The Muller cell: A functional element of the retina. Trends Neurosci 1996;19:307–312.
2 Turner DL, Cepko CL. A common progenitor for neurons and glia persists in rat retina late in development. Nature 1987;328:131–136.
3 Raymond PA, Hitchcock PF. Retinal regeneration: Common principles but a diversity of mechanisms. Adv Neurol 1997;72:171–184.
4 Fischer AJ, Reh TA. Muller glia are a potential source of neural regeneration in the postnatal chicken retina. Nat Neurosci 2001;4:247–252.
5 Ooto S, Akagi T, Kageyama R et al. Potential for neural regeneration after neurotoxic injury in the adult mammalian retina. Proc Natl Acad Sci U S A 2004;101:13654–13659.
6 Raymond PA, Barthel LK, Bernardos RL et al. Molecular characterization of retinal stem cells and their niches in adult zebrafish. BMC Dev Biol 2006;6:36.
7 Das AV, Mallya KB, Zhao X et al. Neural stem cell properties of Muller glia in the mammalian retina: Regulation by Notch and Wnt signaling. Dev Biol 2006;299:283–302.
8 Lillien L. Changes in retinal cell fate induced by overexpression of EGF receptor. Nature 1995;377:158–162.
9 Sarthy VP, Brodjian SJ, Dutt K et al. Establishment and characterization of a retinal Muller cell line. Invest Ophthalmol Vis Sci 1998;39212–216.
10 Bouvier M, Szatkowski M, Amato A et al. The glial cell glutamate uptake carrier countertransports pH-changing anions. Nature 1992;360:471–474.
11 Limb GA, Salt TE, Munro PM et al. In vitro characterization of a spontaneously immortalized human Muller cell line (MIO-M1). Invest Ophthalmol Vis Sci 2002;43:864–869.
12 Guo Y, Saloupis P, Shaw SJ et al. Engraftment of adult neural progenitor cells transplanted to rat retina injured by transient ischemia. Invest Ophthalmol Vis Sci 2003;44:3194–3201.
13 Klassen HJ, Ng TF, Kurimoto Y et al. Multipotent retinal progenitors express developmental markers, differentiate into retinal neurons, and preserve light-mediated behavior. Invest Ophthalmol Vis Sci 2004;45:4167–4173.
14 Meyer JS, Katz ML, Maruniak JA et al. Embryonic stem cell-derived neural progenitors incorporate into degenerating retina and enhance survival of host photoreceptors. STEM CELLS 2006;24:274–283.
15 Van Hoffelen SJ, Young MJ, Shatos MA et al. Incorporation of murine brain progenitor cells into the developing mammalian retina. Invest Ophthalmol Vis Sci 2003;44:426–434.
16 Warfvinge K, Kiilgaard JF, Lavik EB et al. Retinal progenitor cell xenografts to the pig retina: Morphologic integration and cytochemical differentiation. Arch Ophthalmol 2005;123:1385–1393.
17 Lewis GP, Kaska DD, Vaughan DK et al. An immunocytochemical study of cat retinal Muller cells in culture. Exp Eye Res 1988;47:855–868.
18 Roque RS, Agarwal N, Wordinger RJ et al. Human papillomavirus-16 E6/E7 transfected retinal cell line expresses the Muller cell phenotype. Exp Eye Res 1997;64:519–527.
19 Coles BL, Angenieux B, Inoue T et al. Facile isolation and the characterization of human retinal stem cells. Proc Natl Acad Sci U S A 2004;101:15772–15777.
20 Limb GA, Daniels JT, Pleass R et al. Differential expression of matrix metalloproteinases 2 and 9 by glial Muller cells: Response to soluble and extracellular matrix-bound tumor necrosis factor-alpha. Am J Pathol 2002;160:1847–1855.
21 LaVail MM, Sidman RL, Gerhardt CO. Congenic strains of RCS rats with inherited retinal dystrophy. J Hered 1975;66:242–244.
22 D'Cruz PM, Yasumura D, Weir J et al. Mutation of the receptor tyrosine kinase gene Mertk in the retinal dystrophic RCS rat. Hum Mol Genet 2000;9:645–651.
23 Lawrence JM, Keegan DJ, Muir EM et al. Transplantation of Schwann cell line clones secreting GDNF or BDNF into the retinas of dystrophic Royal College of Surgeons rats. Invest Ophthalmol Vis Sci 2004;45:267–274.
24 Okada M, Matsumura M, Ogino N et al. Muller cells in detached human retina express glial fibrillary acidic protein and vimentin. Graefes Arch Clin Exp Ophthalmol 1990;228:467–474.

25 Lewis GP, Guerin CJ, Anderson DH et al. Rapid changes in the expression of glial cell proteins caused by experimental retinal detachment. Am J Ophthalmol 1994;118:368–376.
26 Kelley MW, Turner JK, Reh TA. Regulation of proliferation and photoreceptor differentiation in fetal human retinal cell cultures. Invest Ophthalmol Vis Sci 1995;36:1280–1289.
27 Klassen H, Ziaeian B, Kirov II et al. Isolation of retinal progenitor cells from post-mortem human tissue and comparison with autologous brain progenitors. J Neurosci Res 2004;77:334–343.
28 Yang P, Seiler MJ, Aramant RB et al. In vitro isolation and expansion of human retinal progenitor cells. Exp Neurol 2002;177:326–331.
29 Dyer MA, Cepko CL. Regulating proliferation during retinal development. Nat Rev Neurosci 2001;2:333–342.
30 Rietze RL, Valcanis H, Brooker GF et al. Purification of a pluripotent neural stem cell from the adult mouse brain. Nature 2001;412:736–739.
31 Seiler MJ, Aramant RB. Photoreceptor and glial markers in human embryonic retina and in human embryonic retinal transplants to rat retina. Brain Res Dev Brain Res 1994;80:81–95.
32 Osborne NN, Larsen AK. Antigens associated with specific retinal cells are affected by ischaemia caused by raised intraocular pressure: Effect of glutamate antagonists. Neurochem Int 1996;29:263–270.
33 Fisher SK, Lewis GP. Muller cell and neuronal remodeling in retinal detachment and reattachment and their potential consequences for visual recovery: A review and reconsideration of recent data. Vision Res 2003;43:887–897.
35 Liu W, Khare SL, Liang X et al. All Brn3 genes can promote retinal ganglion cell differentiation in the chick. Development 2000;127: 3237–3247.
36 Meyer JS, Katz ML, Maruniak JA et al. Neural differentiation of mouse embryonic stem cells in vitro and after transplantation into eyes of mutant mice with rapid retinal degeneration. Brain Res 2004;1014: 131–144.
37 Marquardt T, Shery-Padan R, Andrejewski N et al. Pax6 is required for the multipotent state of retinal progenitor cells. Cell 2001;105:43–55.
38 Ellis P, Fagan BM, Magness ST et al. SOX2, a persistent marker for multipotential neural stem cells derived from embryonic stem cells, the embryo or the adult. Dev Neurosci 2004;26:148–165.
39 Moshiri A, Reh TA. Persistent progenitors at the retinal margin of ptc+/− mice. J Neurosci 2004;24:229–237.
40 Chen CM, Cepko CL. Expression of Chx10 and Chx10–1 in the developing chicken retina. Mech Dev 2000;90:293–297.
41 Rowan S, Chen CM, Young TL et al. Transdifferentiation of the retina into pigmented cells in ocular retardation mice defines a new function of the homeodomain gene Chx10. Development 2004;131:5139–5152.
42 Fischer AJ, Skorupa D, Schonberg DL et al. Characterization of glucagon-expressing neurons in the chicken retina. J Comp Neurol 2006;496: 479–494.
43 Doetsch F. The glial identity of neural stem cells. Nat Neurosci 2003;6: 1127–1134.
44 Doetsch F, Scharff C. Challenges for brain repair: Insights from adult neurogenesis in birds and mammals. Brain Behav Evol 2001;58: 306–322.
45 Belachew S, Chittajallu R, Aguirre AA et al. Postnatal NG2 proteoglycan-expressing progenitor cells are intrinsically multipotent and generate functional neurons. J Cell Biol 2003;161:169–186.
46 Doetsch F, Caille I, Lim DA et al. Subventricular zone astrocytes are neural stem cells in the adult mammalian brain. Cell 1999;97:703–716.
47 Kondo T, Raff M. Oligodendrocyte precursor cells reprogrammed to become multipotential CNS stem cells. Science 2000;289:1754–1757.
48 Laywell ED, Rakic P, Kukekov VG et al. Identification of a multipotent astrocytic stem cell in the immature and adult mouse brain. Proc Natl Acad Sci U S A 2000;97:13883–13888.
49 Noctor SC, Flint AC, Weissman TA et al. Neurons derived from radial glial cells establish radial units in neocortex. Nature 2001;409:714–720.
50 Sun Y, Goderie SK, Temple S. Asymmetric distribution of EGFR receptor during mitosis generates diverse CNS progenitor cells. Neuron 2005;45:873–886.
51 Dumstrei K, Nassif C, Abboud G et al. EGFR signaling is required for the differentiation and maintenance of neural progenitors along the dorsal midline of the Drosophila embryonic head. Development 1998;125: 3417–3426.
52 Lin SY, Makino K, Xia W et al. Nuclear localization of EGF receptor and its potential new role as a transcription factor. Nat Cell Biol 2001; 3:802–808.
53 Marti U, Ruchti C, Kampf J et al. Nuclear localization of epidermal growth factor and epidermal growth factor receptors in human thyroid tissues. Thyroid 2001;11:137–145.
54 Jorissen RN, Walker F, Pouliot N et al. Epidermal growth factor receptor: Mechanisms of activation and signalling. Exp Cell Res 2003;284: 31–53.
55 De Falco M, Fedele V, De LL et al. Evaluation of cyclin D1 expression and its subcellular distribution in mouse tissues. J Anat 2004;205: 405–412.
56 Coyle-Rink J, Del VL, Sweet T et al. Developmental expression of Wnt signaling factors in mouse brain. Cancer Biol Ther 2002;1:640–645.
57 Limb GA, Matter K, Murphy G et al. Matrix metalloproteinase-1 associates with intracellular organelles and confers resistance to lamin A/C degradation during apoptosis. Am J Pathol 2005;166:1555–1563.
58 Hollborn M, Tenckhoff S, Jahn K et al. Changes in retinal gene expression in proliferative vitreoretinopathy: Glial cell expression of HB-EGF. Mol Vis 2005;11:397–413.
59 Avilion AA, Nicolis SK, Pevny LH et al. Multipotent cell lineages in early mouse development depend on SOX2 function. Genes Dev 2003; 17:126–140.
60 Ferri AL, Cavallaro M, Braida D et al. Sox2 deficiency causes neurodegeneration and impaired neurogenesis in the adult mouse brain. Development 2004;131:3805–3819.
61 Bambakidis NC, Wang RZ, Franic L et al. Sonic hedgehog-induced neural precursor proliferation after adult rodent spinal cord injury. J Neurosurg 2003;99(suppl 1):70–75.
62 Ahmad I, Zaqouras P, Rtavanis-Tsakonas S. Involvement of Notch-1 in mammalian retinal neurogenesis: Association of Notch-1 activity with both immature and terminally differentiated cells. Mech Dev 1995;53: 73–85.
63 Silva AO, Ercole CE, McLoon SC. Regulation of ganglion cell production by Notch signaling during retinal development. J Neurobiol 2003; 54:511–524.
64 Kasashima K, Terashima K, Yamamoto K et al. Cytoplasmic localization is required for the mammalian ELAV-like protein HuD to induce neuronal differentiation. Genes Cells 1999;4:667–683.
65 Lee VM, Sechrist JW, Bronner-Fraser M et al. Neuronal differentiation from postmitotic precursors in the ciliary ganglion. Dev Biol 2002;252: 312–323.
66 Hall PE, Lathia JD, Miller NG et al. Integrins are markers of human neural stem cells. STEM CELLS 2006;24:2078–2084.
67 Spradling A, Drummond-Barbosa D, Kai T. Stem cells find their niche. Nature 2001;414:98–104.
68 Philp D, Chen SS, Fitzgerald W et al. Complex extracellular matrices promote tissue-specific stem cell differentiation. STEM CELLS 2005;23: 288–296.
69 MacLaren RE. Development and role of retinal glia in regeneration of ganglion cells following retinal injury. Br J Ophthalmol 1996;80: 458–464.
70 Nishida A, Takahashi M, Tanihara H et al. Incorporation and differentiation of hippocampus-derived neural stem cells transplanted in injured adult rat retina. Invest Ophthalmol Vis Sci 2000;41:4268–4274.
71 Sakaguchi DS, Van Hoffelen SJ, Young MJ. Differentiation and morphological integration of neural progenitor cells transplanted into the developing mammalian eye. Ann N Y Acad Sci 2003;995:127–139.

See www.StemCells.com for supplemental material available online.

MIO-M1 Cells and Similar Müller Glial Cell Lines Derived from Adult Human Retina Exhibit Neural Stem Cell Characteristics

Jean M. Lawrence, Shweta Singhal, Bhairavi Bhatia, David J. Keegan, Thomas A. Reh, Philip J. Luthert, Peng T. Khaw and Gloria Astrid Limb

Stem Cells 2007;25;2033-2043; originally published online May 24, 2007;
DOI: 10.1634/stemcells.2006-0724

STEM CELLS
TRANSLATIONAL AND CLINICAL RESEARCH

Chondroitin Sulfate Proteoglycans and Microglia Prevent Migration and Integration of Grafted Müller Stem Cells into Degenerating Retina

SHWETA SINGHAL,[a] JEAN M. LAWRENCE,[a] BHAIRAVI BHATIA,[a] JAMES S. ELLIS,[a] ANTHONY S. KWAN,[a] ANGUS MACNEIL,[a] PHILIP J. LUTHERT,[a] JAMES W. FAWCETT,[b] MARIA-THEREZA PEREZ,[c,d] PENG T. KHAW,[a] G. ASTRID LIMB[a]

[a]Institute of Ophthalmology and Moorfields Eye Hospital, London, United Kingdom; [b]Centre for Brain Repair, University of Cambridge, Cambridge, United Kingdom; [c]Department of Ophthalmology, Lund University, Lund, Sweden; [d]Department of Ophthalmology, Glostrup Hospital, Glostrup, Denmark

Key Words. Adult stem cells • Cell migration • Stem cell transplantation • Experimental models • Tissue regeneration Tissue-specific stem cells

ABSTRACT

At present, there are severe limitations to the successful migration and integration of stem cells transplanted into the degenerated retina to restore visual function. This study investigated the potential role of chondroitin sulfate proteoglycans (CSPGs) and microglia in the migration of human Müller glia with neural stem cell characteristics following subretinal injection into the Lister hooded (LH) and Royal College of Surgeons (RCS) rat retinae. Neonate LH rat retina showed minimal baseline microglial accumulation (CD68-positive cells) that increased significantly 2 weeks after transplantation ($p < .001$), particularly in the ganglion cell layer (GCL) and inner plexiform layer. In contrast, nontransplanted 5-week-old RCS rat retina showed considerable baseline microglial accumulation in the outer nuclear layer (ONL) and photoreceptor outer segment debris zone (DZ) that further increased ($p < .05$) throughout the retina 2 weeks after transplantation. Marked deposition of the N-terminal fragment of CSPGs, as well as neurocan and versican, was observed in the DZ of 5-week-old RCS rat retinae, which contrasted with the limited expression of these proteins in the GCL of the adult and neonate LH rat retinae. Staining for CSPGs and CD68 revealed colocalization of these two molecules in cells infiltrating the ONL and DZ of the degenerating RCS rat retina. Enhanced immune suppression with oral prednisolone and intraperitoneal injections of indomethacin caused a reduction in the number of microglia but did not facilitate Müller stem cell migration. However, injection of cells with chondroitinase ABC combined with enhanced immune suppression caused a dramatic increase in the migration of Müller stem cells into all the retinal cell layers. These observations suggest that both microglia and CSPGs constitute a barrier for stem cell migration following transplantation into experimental models of retinal degeneration and that control of matrix deposition and the innate microglial response to neural retina degeneration may need to be addressed when translating cell-based therapies to treat human retinal disease. STEM CELLS *2008;26:1074–1082*

Disclosure of potential conflicts of interest is found at the end of this article.

INTRODUCTION

Stem cell-based therapies provide a hope for restoration of sight in individuals whose retinal function has been irreversibly damaged by disease. Transplantation of neural stem cells and retinal progenitors has been extensively performed in various experimental models of retinal disease, with several studies yielding a mixed success to date [1–7]. However, before this procedure can be translated into human therapies, many problems need to be solved to promote adequate cell survival, differentiation, and functional integration of grafted cells into the retina. Studies involving retinal transplantation of brain-derived precursor cells into Royal College of Surgeons (RCS) rats have been shown to promote photoreceptor cell survival, but although the transplanted cells migrate to the photoreceptor layer in some instances, they do not express retinal-specific markers [8–10]. It has been suggested that either specific retinal precursors are needed for functional and morphological regeneration, or specific cues, such as retinal injury, are needed for appropriate migration and differentiation of transplanted cells. These views have been confirmed by observations that brain progenitors and ocular stem cells show improved migration, although not optimal integration and differentiation into retinal neurons when transplanted into injured retina [11, 12]. It has also been shown that neonate retina provides an amenable environment for stem cell transplantation [12, 13] and that the ontogenic stage of transplanted retinal precursors determines the ability of these cells to integrate into degenerated retina [14].

Müller glial cells have shown neural regenerative ability in the postnatal retina of zebrafish, chick, and rat [15–17], and a population of Müller glia with neural stem cell characteristics

Correspondence: G. Astrid Limb, M.Sc., Ph.D., Ocular Repair and Regeneration Biology Unit, Departments of Cell Biology and Pathology, Institute of Ophthalmology, 11 Bath Street, London EC1V 9EL, United Kingdom. Telephone: 020-7608-6974; Fax: 020-7608-4034; e-mail: g.limb@ucl.ac.uk Received October 30, 2007; accepted for publication January 20, 2008; first published online in STEM CELLS *EXPRESS* January 24, 2008. 1066-5099/2008/$30.00/0 doi: 10.1634/stemcells.2007-0898

has recently been identified in the adult human eye [18]. These cells have the potential to be used in cell-based therapies to treat retinal disease, but like other stem cells used for experimental transplantation to regenerate retina, when grafted into neonate and degenerated retina, they show limited migration and integration [18].

Retinal degeneration is characterized by formation of glial scarring [19] and severe microglial activation [20–22], which may contribute to the lack of migration, integration, and differentiation of transplanted stem cells. Adult CNS neurons that retain the ability to grow following injury are unable to extend processes beyond the injury-induced glial scar due to the presence of inhibitory proteins such as the chondroitin sulfate proteoglycans (CSPGs) aggrecan, versican, and neurocan [23, 24]. These proteins, which inhibit axon guidance [25], have been identified in the human retina and appear during normal development [26]. Their response to retinal injury has not been widely investigated, but deposition of CSPGs has been shown to inhibit regeneration of the injured rat optic nerve [27]. Degradation of CSPGs using enzymatic digestion by chondroitinase enhances neurite outgrowth and axon regeneration in injured brain [28] and spinal cord [29–31], and it is possible that similar treatments may facilitate functional integration of stem cells transplanted into the retina.

On the basis of the above evidence, we investigated whether CSPG deposition and macrophage/microglia accumulation may prevent the successful migration and integration of Müller glial stem cells when transplanted into the subretinal space of the dystrophic RCS rat, an experimental model of retinal degeneration. Since neonatal retina is known to provide a permissible environment for stem cell transplantation [12, 13], we compared the response of the dystrophic 5-week-old RCS rat retina with that of the neonate Lister hooded rat. We also examined whether CSPG degradation and microglial inhibition could facilitate migration and integration of the grafted cells.

MATERIALS AND METHODS

Animals and Immunosuppression

Dystrophic RCS rats and neonatal Lister hooded rats were used in the study. All rats were maintained according to the Home Office regulations for the care and use of laboratory animals and the U.K. Animals (Scientific Procedures) Act (1986). Dystrophic RCS rats were bred in-house, kept under a 12-hour/12-hour light-dark cycle (light cycle mean illumination, 30 cd/m^2), and transplanted at the age of 5–6 weeks (35–40 days), by which time the retinal degeneration is well established. Lister hooded rats were purchased from Harlan (Harlan UK Ltd., Oxon, U.K., http://www.harlaneurope.com/main-uk.htm). Animals were normally immunosuppressed with oral cyclosporine A (210 mg/l of drinking water; Sandimmun; Sandoz, Camberley, U.K., http://www.sandoz.com) and azathioprine (20 mg/l; Sigma-Aldrich, Gillingham, U.K., http://www.sigmaaldrich.com) from 2 days before transplantation until termination of the experiment. When using additional immunosuppression, animals received oral prednisolone (5 mg/l; Sovereign Medical, Bishops Stortford, U.K., http://www.sovereignmedical.org/) in addition to cyclosporine A and azathioprine, together with daily intraperitoneal injections of indomethacin (0.1 mg per 100 g of body weight) for the duration of the experiment. For transplantation into neonatal Lister hooded pups, pregnant dams were immunosuppressed with oral cyclosporine A and azathioprine as described above.

Isolation and Preparation of Müller Cells with Stem Cell Characteristics

Isolation of Müller stem cells from the neural retina of donor human eyes consented for research was performed as previously described [32]. Briefly, neural retina sectioned at least 2 mm away from the ora serrata was incubated in trypsin-EDTA (0.5% trypsin/0.2% EDTA; Invitrogen, Paisley, U.K., http://www.invitrogen.com) for 20 minutes at 37°C. After vigorous trituration, released cells were washed and suspended in Dulbecco's modified Eagle's medium (DMEM) containing GlutaMAX-I (Invitrogen), 10% fetal calf serum (Invitrogen), and 40 ng/ml epidermal growth factor (EGF; Sigma-Aldrich). Cells were plated onto fibronectin-coated tissue culture dishes and cultured for 2–3 weeks until formation of adherent cell colonies. Colonies were detached and transferred onto new culture dishes, and culture was continued in the above medium without EGF. Upon reaching confluence, cells were examined for their stem cell characteristics as previously described [18]. Cells that underwent more than 50 passages without losing their stem cell characteristics were used for transplantation.

Preparation of Cells for Transplantation

Müller stem cells used for transplantation were transfected with an immunodeficiency virus type 1 (HIV-1)-based, lentiviral vector-expressing, low-toxicity humanized R. reniformis green fluorescent protein from a spleen focus-forming virus promoter, previously described as l-schrgfpw [33]. Confluent cells plated in a 12-well culture dish were infected with l-schrgfpw at a multiplicity of infection of one transducing unit per cell in the presence of polybrene (10 μg/ml; Chemicon, Temecula, CA, http://www.chemicon.com). Using this method, more than 80% of Müller stem cells expressed green fluorescent protein (GFP) 1 week after infection. The transfected cells were grown to confluence in a 25-cm^2 flask, and green fluorescent cells were selected by fluorescence-activated cell sorting using a FACSCalibur (BD Biosciences, Oxford, U.K., http://www.bdbiosciences.com). To ensure that the lentiviral vector did not modify the stem cell characteristics of the transfected cells, they were examined for the expression of stem cell markers and sphere formation as previously described [18]. Three days prior to transplantation, lentivirus-GFP-transfected cells were plated onto a 75-cm^2 flask and allowed to reach approximately 70% confluence. On the day of the transplant, cells were trypsinized, counted, and resuspended in serum-free medium to a concentration of 2×10^4 cells per microliter.

Subretinal Transplantation

Rats were anesthetized with an intraperitoneal injection of ketamine HCl 7.5 mg/100 g (Ketaset; Fort Dodge Animal Health, Southampton, U.K., http://www.fortdodge.eu/) and medetomidine HCl −5 mg/100 g (Domitor; Pfizer, Sandwich, U.K., http://www.pfizer.com). The pupils were dilated using 1% tropicamide and 2.5% phenylephrine (Chauvin Pharmaceuticals, Surrey, U.K.) before injection of 2 μl of the cell suspension into the subretinal space of adult dystrophic RCS rats ($n = 9$) using a 30-gauge metal needle attached to a Hamilton syringe, under direct visualization with a Leitz operating microscope. Sham-injected rats received DMEM without cells ($n = 6$). Neonatal Lister hooded rats (postnatal day 2) were anesthetized with 1/10th the adult dose of ketamine (0.75 mg/100 g) and medetomidine (0.5 mg/100 g) by intraperitoneal injection. The lids were opened surgically, and 1 μl of cell suspension ($n = 11$) or medium ($n = 9$) was injected into the subretinal space using a 32-gauge metal needle attached to a 2.5-μl Hamilton syringe. When treating RCS retinae with chondroitinase ABC ($n = 8$), cells were suspended at a concentration of 4×10^4 cells per microliter. Prior to transplantation, 1 μl of the cell suspension was mixed with 1 μl (0.01U) of chondroitinase ABC (ChABC; Seikagaku, Tokyo, http://www.seikagaku.co.jp/english), and the mixture was injected into the subretinal space as indicated above.

Tissue Processing and Immunohistochemistry

Two weeks post-transplantation, rats were terminally anesthetized with intraperitoneal sodium pentobarbitone and perfused transcardially with phosphate-buffered saline (PBS) followed by 4% paraformaldehyde (PFA) in 0.1 M phosphate buffer. Eyes were excised, postfixed in PFA for 1 hour, cryoprotected with 30% sucrose overnight, and embedded in optimal cutting temperature compound (VWR, Lutterworth, U.K., http://uk.vwr.com/app/Home). Cryostat

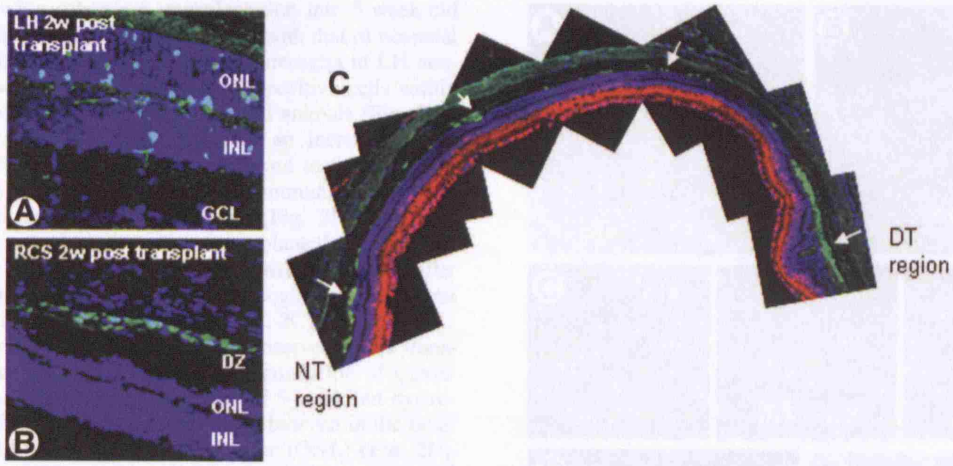

Figure 1. Migration of Müller stem cells following subretinal transplantation into the neonate LH and dystrophic RCS rats. **(A):** Migration of Müller stem cells (green fluorescent protein [GFP]-labeled) into the INL and ONL 2 w after transplantation into a 3-day-old LH rat. **(B):** Müller stem cells (GFP-labeled) remained in the subretinal space 2 w after transplantation into a 5-w-old RCS rat. **(C):** Montage of whole retina to show widespread Müller stem cell migration along the subretinal space 5 w after subretinal injection into a 5-w-old RCS rat. Red staining indicates reactivity to an antibody against the neural marker HuD. Cell nuclei were stained with 4′,6-diamidino-2-phenylindole (blue). Abbreviations: DT, dorso temporal; DZ, debris zone; GCL, ganglion cell layer; INL, inner nuclear layer; LH, Lister hooded; NT, naso temporal; ONL, outer nuclear layer; RCS, Royal College of Surgeons; w, week(s).

sections 14 μm thick were placed onto precharged slides, and the slides were air-dried prior to storage at −80°C. Sections with visible transplants (in eyes that underwent cellular transplantation) (untreated RCS, $n = 4$; neonatal Lister hooded, $n = 6$; ChABC-treated RCS, $n = 5$) and sections with visible transplant sites (in sham-operated eyes) (RCS, $n = 3$; Lister hooded, $n = 3$) were selected for immunostaining. Sections from two different unoperated eyes in each group were used as controls.

Dried slides were blocked with 5% donkey serum in PBS/0.3% Triton and reacted with primary antibodies diluted in the same blocking solution overnight at room temperature (RT). The primary antibodies used were CSPG (CS56; monoclonal; 1:200; Sigma-Aldrich); neurocan (IF6; monoclonal; 1:100; Developmental Studies Hybridoma Bank, Iowa City, IA, http://www.uiowa.edu/~dshbwww); versican (12C5; monoclonal; 1:100; Developmental Studies Hybridoma Bank); ED1 (anti-rat-CD68; monoclonal, 1:1,000; Serotec Ltd., Oxford, U.K., http://www.serotec.com), a marker for rat macrophage/microglia; and 2B6 (Seikagaku), an antibody that recognizes an epitope exposed following chondroitinase ABC degradation of chondroitin-4-sulfate. After incubation with primary antibodies overnight at RT, sections were washed in PBS and incubated with the relevant Alexa Fluor secondary antibodies (mouse, rabbit, or goat 488 or 555, raised in donkey; Invitrogen) diluted 1:500 in PBS plus 2% donkey serum for 1.5 hours at RT. After washing, sections were counterstained with 4′,6-diamidino-2-phenylindole (Sigma-Aldrich) washed with Tris buffer (0.05 M; pH 7.4), and mounted in Vectashield (Vector Laboratories, Peterborough, U.K., http://www.vectorlabs.com). Sections were also processed in parallel with secondary antibodies alone, which served as negative controls.

Macrophage/microglial infiltration was determined by costaining of retinal sections with a mouse monoclonal antibody to CD68 antigen (ED1; Serotec). Antibody reactivity was determined by visualization with 3,3′-diaminobenzidine (DAB; Sigma-Aldrich) enhanced with aqueous 1% nickel ammonium sulfate and aqueous 1% cobalt chloride by a modification of published methods [34] as follows. Sections were blocked and incubated with the anti-CD68 antibody overnight at RT, using the same blocking solution used with other antibodies in the study (described above), with the addition of 0.5% bovine serum albumin (Sigma-Aldrich). After washing, sections were incubated in biotinylated horse anti-mouse secondary antibody, rat-adsorbed (1:150, Vector Laboratories), followed by streptavidin-horseradish peroxidase (Vector Laboratories). They were then developed with 25 seconds of incubation in DAB solution (0.05% in 0.1 M PBS with 1% nickel ammonium sulfate and 1% cobalt chloride in hydrogen peroxide), and cells expressing CD68 were detected by their characteristic brown-black staining under Nomarski illumination.

To identify other markers in sections stained for CD68, slides were then washed, blocked, and incubated with other primary antibodies (described above) and detected with fluorescence-labeled antibodies. Sections were photographed using a Zeiss LSM 510 confocal microscope, and images were analyzed using the Zeiss LSM Image Browser software (Carl Zeiss, Oberkochen, Germany, http://www.zeiss.com).

RESULTS

Migration and Integration of Müller Stem Cells Following Subretinal Grafts into Neonate Lister Hooded and RCS Rats

Two weeks after transplantation of Müller stem cells into the subretinal space of neonate (2 days old) Lister hooded (LH) rats, migration of cells into the inner and outer retinal cell layers was often observed. However, relatively few cells migrated, and this migration occurred only into the area adjacent to the transplantation site (Fig. 1A). In contrast, 2 weeks after transplantation of these cells into the subretinal space of 4–5-week-old RCS rats (the age at which the photoreceptor cell layer has been reduced to about half of its normal thickness), cells accumulated at the interface between the outer segment debris zone (DZ) and the retinal pigment epithelium and often gave the appearance of small-cell aggregates or cell debris (Fig. 1B). Cells rarely migrated into the retina. Examination of the whole RCS retina 2 weeks after transplantation showed that cells migrated predominantly along the subretinal space lining the DZ (Fig. 1C). It was of interest that cells that had been grafted in the subretinal space of the dorsotemporal region were often seen along the entire subretinal space, but not within the retina itself (Fig. 1C).

Microglia Response to Retinal Transplantation of Müller Stem Cells

Since microglia are known to migrate and proliferate within the degenerating retina of the RCS rat [20–22], we investigated whether these cells play a role in the inhibition of Müller cell

migration following subretinal transplantation into 5-week-old RCS rats. We also compared this response with that of neonatal LH rats. Examination of the presence of microglia in LH neonate retina showed only occasional CD68-positive cells within the ganglion cell layer (GCL) of 2-day-old animals (Fig. 2A). However, 3 weeks after transplantation, an increase in the number of CD68-positive cells was observed in the GCL and inner plexiform layer of LH rats, despite immune suppression with oral cyclosporine and azathioprine (Fig. 2B). Confocal examination of retinal sections from transplanted neonatal LH rats stained for CD68 and GFP showed that although Müller stem cells had migrated into the retina, microglial reactivity was often associated with the grafted cells (Fig. 2C).

Unlike the mild microglia activation observed in the transplanted neonatal LH retina, a marked accumulation of CD68-positive cells was observed in the retina of 5-week-old dystrophic RCS rats. Numerous microglia were observed in the outer segment DZ and in the outer nuclear layer (ONL) (Fig. 2D). Two weeks after Müller stem cell injection into the subretinal space, adult RCS rat retina showed a more severe and widespread migration of microglia (Fig. 2E), despite immune suppression with oral cyclosporine and azathioprine. Quantitative comparison of the infiltrating microglia in the LH and RCS rat prior to and following transplantation showed that the degenerating RCS rat retina harbored significantly higher numbers of microglia than the normal LH rat retina ($p < .01$) (Fig. 2F) and that Müller stem cell transplantation caused a marked increase in the number of microglia in both the LH ($p < .001$) and RCS ($p < .05$) rat retinae (Fig. 2G).

Confocal microscopy of transplanted retinal sections costained for CD68 and GFP showed that Müller stem cells that had not migrated into the retina and that lined the outer segment DZ were closely associated to microglia, as judged by the colocalization of CD68 and GFP (Fig. 3A). Moreover, aggregates of grafted Müller stem cells, frequently observed in the subretinal space of the transplanted RCS rat, were always surrounded by microglia (Fig. 3B). To promote cell migration by diminishing microglial activation, animals were given oral prednisolone and daily intraperitoneal injections of indomethacin, in addition to oral cyclosporine and azathioprine, for the duration of the experiment. As observed in Figure 3C, although microglial numbers appeared comparatively reduced with additional prednisolone and indomethacin treatment, transplanted cells continued to be associated with microglia and remained in the DZ, unable to migrate into the retina. Although better migration of transplanted cells into the retina of the neonate LH rat was generally observed, on occasions when trauma to the retina occurred as a result of the transplantation procedure, severe microglia accumulation at the site of the injection also prevented Müller stem cells from migrating into the retina of these animals (Fig. 3D).

Expression of CSPGs in the Normal and Degenerated Rat Retina and Association of These Proteins with Microglia

Immunostaining of the unoperated 5-week-old RCS rat retina for the CSPG N-terminal region (common to all CSPGs) revealed marked expression of this molecule in the outer segment DZ (Fig. 4A). Strong staining for neurocan and versican was also observed in the same region in unoperated (Fig. 4A) and sham-operated animals (not shown). This contrasted with the expression of these proteins observed in the neonate LH rat, where staining for these molecules was detected only in the ganglion cell region (Fig. 4B).

Costaining for CSPGs and CD68 in retinal sections from 5-week-old RCS rats showed that microglia were localized mainly at the sites where accumulation of CSPGs could be

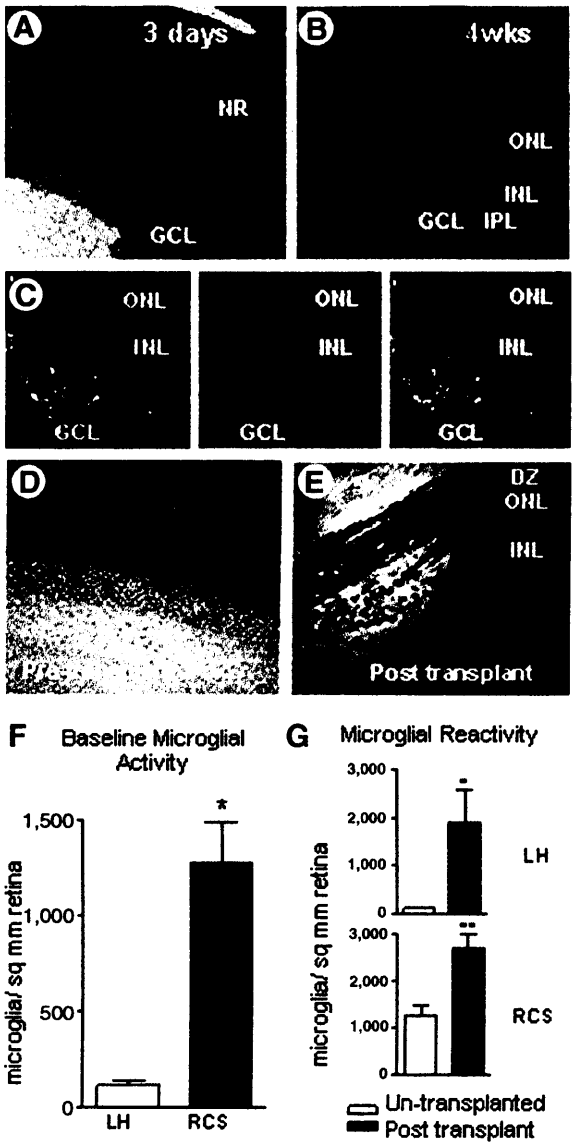

Figure 2. Distribution of microglia in the LH and RCS rat retina before and after Müller cell transplantation. **(A):** Neonate LH rat retina (3-day-old animal) showing minimal microglia reactivity as judged by CD68-positive cells (black) in the GCL. **(B):** Microglia accumulation (black staining) in the GCL and IPL of an LH rat retina 2 wks after neonatal transplantation. **(C):** Müller stem cell (green fluorescent protein-labeled) migration into the GCL 2 wks after transplantation into the neonate LH rat retina (left). Middle panel shows Nomarski illumination of the same section, demonstrating accumulation of CD68-positive microglia (black) in the GCL. Right panel illustrates Nomarski illumination of the same section, showing association of microglia with transplanted Müller stem cells. **(D):** Nomarski illumination of a nontransplanted RCS rat retina at 5 wks of age showing severe infiltration of microglia in the outer segment DZ and the ONL. **(E):** Nomarski illumination of RCS rat retina 2 wks after transplantation in a 5-wk-old animal. Microglia (black) can be observed thorough all retinal cell layers. **(F):** Histogram shows a significantly higher number of microglia in 5-wk-old RCS rat retina compared with the neonatal LH retina (*, $p = .0055$). Results are the mean ± SE of the mean of three different experiments. **(G):** Following Müller stem cell transplantation, there was a significant increase in microglial accumulation in both the LH (*, $p < .001$, transplanted vs. nontransplanted retina) and the RCS (**, $p < .05$, transplanted vs. nontransplanted) rat retinae. Results are the mean ± SE of the mean of three different experiments. Abbreviations: DZ, debris zone; GCL, ganglion cell layer; INL, inner nuclear layer; IPL, inner plexiform layer; LH, Lister hooded; NR, neural retina; ONL, outer nuclear layer; RCS, Royal College of Surgeons; wks, weeks.

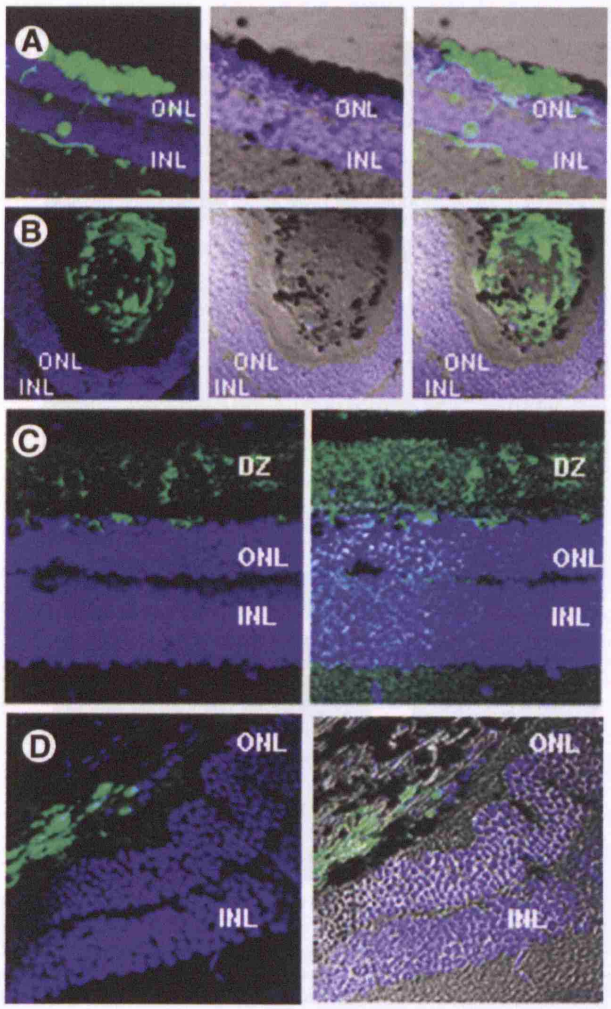

Figure 3. Microglia associates with aggregates of Müller stem cells. **(A):** Left panel shows accumulation of Müller stem cells (green fluorescent protein-labeled) in the subretinal space 2 weeks after transplantation in a 5-week-old Royal College of Surgeons (RCS) rat. Middle panel shows Nomarski illumination to identify CD68-positive cells (black) in the same retinal section. Right panel shows Nomarski illumination to identify colocalization of transplanted cells with microglia. **(B):** Left panel shows a large cluster of Müller stem cells in the subretinal space 2 weeks after transplantation in a 5-week-old RCS rat. Middle panel shows Nomarski illumination of the same section indicating localization of CD68-positive microglia around the transplanted cells (black). Right panel shows microglia (black) surrounding the transplanted cells and resembling a granuloma-type structure. **(C):** Retinal section of an RCS rat treated with oral prednisolone and intraperitoneal indomethacin in addition to cyclosporine A and azathioprine. Left panel shows limited migration of grafted cells into the DZ and reduced infiltration of microglia in the same region as that observed under Nomarski illumination in the right panel. **(D):** Retinal section of a Lister hooded rat 2 weeks after neonatal transplantation in which retinal damage occurred. Animal was not treated with additional microglial suppression. Left panel shows lack of migration and accumulation of Müller stem cells in the subretinal space of the damaged retina. Right panel shows microglia accumulation (black) around the transplant, as observed under Nomarski illumination. Abbreviations: DZ, debris zone; INL, inner nuclear layer; ONL, outer nuclear layer.

observed (Fig. 4C). Furthermore, microglia observed outside the DZ and infiltrating the ONL costained for the N terminus of CSPGs, as well as neurocan and versican, suggesting that microglia may constitute a source of CSPGs in the degenerating RCS rat retina (Fig. 4C).

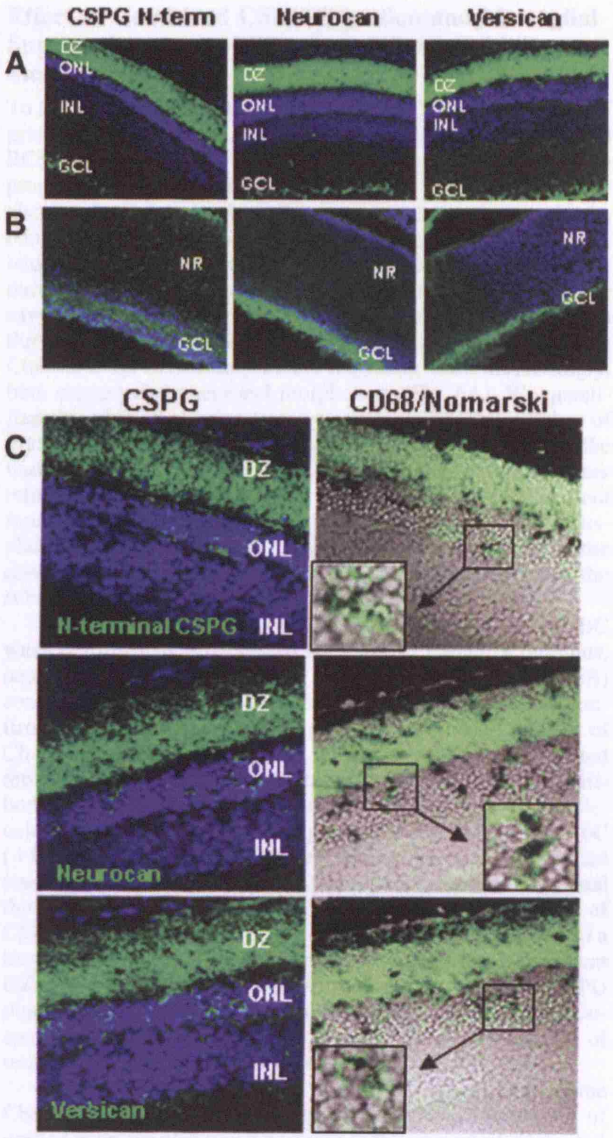

Figure 4. Expression of CSPGs in the retina of nontransplanted Lister hooded (LH) and dystrophic Royal College of Surgeons (RCS) rats and CSPG colocalization with microglia. **(A):** Confocal images showing accumulation of the N-terminal region of CSPGs, neurocan, and versican (green staining) in the DZ of retinal sections from a nontransplanted 5-week-old RCS rat. **(B):** Retinal sections of nontransplanted neonate LH rat retina showing expression of CSPGs in the inner plexiform layer and developing GCL. **(C):** Confocal retinal images of nontransplanted 5-week-old RCS rats showing accumulation of the N-term of CSPGs, neurocan, and versican (green fluorescence) on the left, and colocalization of these proteins with CD68-positive microglia (black) as observed under Nomarski illumination on the right. Cells surrounded by squares are magnified in the insets to show details of microglial colocalization with CSPGs. Abbreviations: CSPG, chondroitin sulfate proteoglycan; DZ, debris zone; GCL, ganglion cell layer; INL, inner nuclear layer; NR, neural retina; N-term, N terminus; ONL, outer nuclear layer.

Inhibition of Müller Stem Cell Migration by CSPGs

To elucidate the role of CSPGs on the inhibition of Müller stem cell migration and integration 3 weeks after transplantation into the subretinal space of 5-week-old RCS rats, we examined retinal sections of grafted animals for the expression of CSPGs and CD68. Confocal microscopic analysis of grafted RCS rat retinae showed that Müller stem cells that

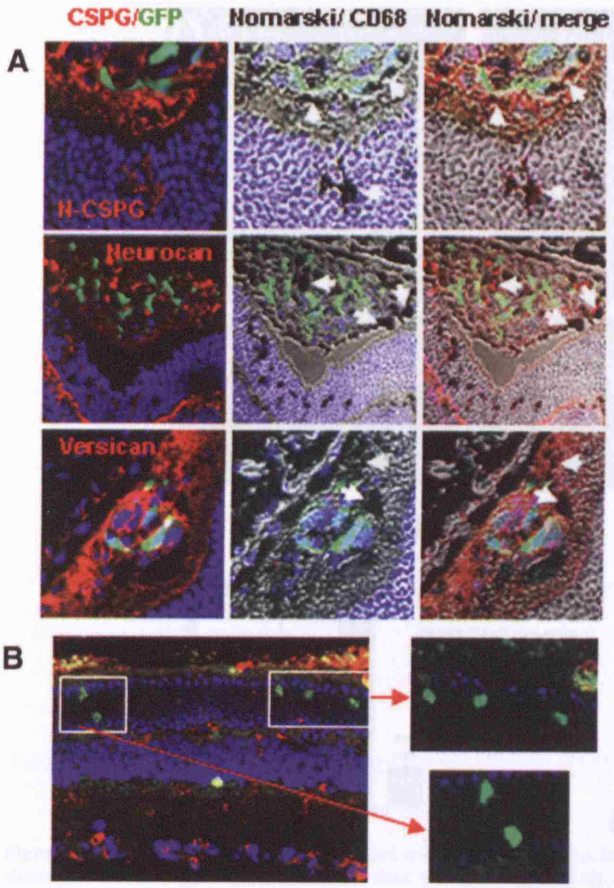

Figure 5. Inhibition of Müller stem cell migration by chondroitin sulfate proteoglycans. **(A):** Confocal images of retinal sections from 7-week-old Royal College of Surgeons (RCS) rats 2 weeks after subretinal transplantation of Müller stem cells. Sections in the left column show the transplanted cells (GFP-labeled) surrounded by N-CSPG, neurocan, and versican (red). The middle column shows the same sections under Nomarski illumination to illustrate the accumulation of CD68-reactive microglia (black). The column on the right shows the merged images under Nomarski illumination illustrating colocalization of CD68-positive cells and CSPGs (red) surrounding the transplanted cells (GFP-labeled). Nuclei were stained with 4′,6-diamidino-2-phenylindole (blue). **(B):** Confocal image of a 7-week-old RCS rat retina 2 weeks after transplantation in the presence of chondroitinase ABC. Staining for the N terminus of CSPGs (red) showed that cells that had migrated (GFP) were not surrounded by these extracellular matrix proteins. Migratory cells are shown within white squares, and their magnification is indicated by red arrows. Abbreviations: CSPG, chondroitin sulfate proteoglycan; GFP, green fluorescent protein; N-CSPG, N-terminal chondroitin sulfate proteoglycan.

failed to migrate into the retina were often surrounded by the N terminus of CSPGs, neurocan, and versican (Fig. 5A). CSPGs often formed a pericellular cuffing with severe microglial activation. Colocalization of microglia with all the CSPGs investigated was observed in all specimens examined (Fig. 5A). This spatial correlation of ECM proteins and CD68 expression around the transplanted cells suggests that in addition to CSPGs accumulating in the degenerating retina, CSPGs released by activated microglia are also likely to contribute to the inhibition of cell migration and integration. Further confirmation that absence of CSPGs facilitates migration of the transplanted cells was shown by observations that areas of cell migration did not stain for CSPGs in retina treated with ChABC at the time of transplantation (Fig. 5B).

Effect of Combined CSPG Digestion and Microglial Suppression on the Migration of Grafted Müller Stem Cells

To further characterize the contribution of CSPG to inhibition of graft cell migration and integration, we transplanted 5-week-old RCS rats with Müller stem cells together with ChABC to promote matrix degradation and promote cell migration. We also used enhanced microglial suppression on these animals, combining oral cyclosporine A, azathioprine, and prednisolone with daily intraperitoneal injections of indomethacin for the duration of the experiment. Two weeks post-transplantation, we saw a dramatic improvement in the migration of grafted cells through the entire thickness of the retina in eyes treated with ChABC (Fig. 6A). Many of the migrating cells, interestingly, bore characteristic neuronal morphology (Fig. 6A). We quantified this change in migration by counting the total number of grafted cells detected in the retina and classifying them on the basis of their localization to the subretinal space or to the inner retinal layers beyond the ONL. Almost 80% of the cells were found to have migrated into the inner retinal layers when transplanted in conjunction with ChABC. This was in contrast to the control animals, where almost all of the cells remained in the subretinal space (t test; $n = 4$; $p = .0011$).

Reduction in CSPG expression in eyes treated with ChABC was confirmed by a decreased staining for CSPG N terminus, neurocan, and versican in the outer segment DZ (Fig. 6B) compared with untreated retinae (Fig. 4A). In addition, to confirm that reduction in CSPG expression was indeed a result of ChABC digestion, we stained untreated and ChABC-treated retinal sections with the chondroitin sulfate (CS) stub IB5 antibody, which detects CS stub epitopes exposed on CSPG molecules by ChABC enzymatic digestion. As seen in Figure 6C (+ChABC), the ChABC-treated retinae showed widespread staining for the stub antibody throughout the whole retinal thickness, indicating that CSPGs were reduced as a result of ChABC digestion. Interestingly, untreated retinae also showed a localized staining for the CS stub epitopes in the outer segment DZ (Fig. 6C, −ChABC), suggesting that some degree of CSPG digestion also occurs during photoreceptor degeneration. Despite the ChABC enzymatic activity, the retinal architecture of treated animals appeared to be well preserved (Fig. 6A).

With the use of enhanced microglial suppression in the ChABC-treated animals, in addition to improved migration of grafted cells, we also saw a decrease in the amount of microglial accumulation (Fig. 6A). Quantitative analysis showed that the number of microglia within the retinae of animals treated with ChABC and enhanced immune suppression was significantly lower than in animals transplanted without additional immune suppression (Bonferroni $p < .001$) (Fig. 6D). In addition, the number of Müller stem cells present within the retinae of animals treated with ChABC combined with enhanced microglial suppression was significantly higher than in the animals treated without ChABC ($p < .001$) (Fig. 6E). Despite the reduction in microglial infiltration, many cells that had migrated and acquired neural morphology were colocalized (although less frequently) with CD68-positive cells (Fig. 6A).

DISCUSSION

Successful migration and integration of stem cells to restore tissue function may depend on the appropriate interaction of the host environment with the transplanted cells. Various studies have shown that when stem cells are transplanted to regenerate retina, migration and integration of grafted cells is better in an immature retina or in a retina subject to acute injury [11, 27].

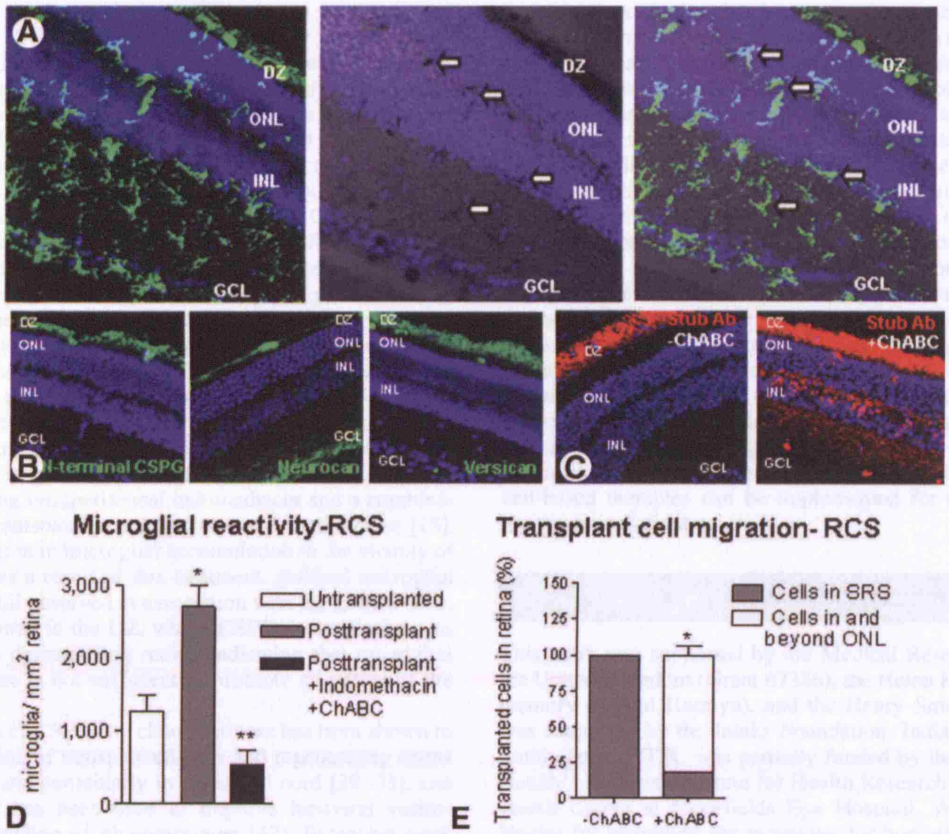

Figure 6. Digestion of CSPGs and enhanced microglial suppression facilitates migration of grafted Müller stem cells. **(A):** Micrograph on the left shows a confocal image of a retinal section from a 7-week-old RCS rat 2 weeks after Müller stem cell transplantation in the presence of ChABC and enhanced immune suppression for the duration of the experiment. Transplanted cells (green fluorescent protein [GFP]-labeled) were observed throughout the whole width of the retina. Middle panel shows the same retinal section under Nomarski illumination to illustrate retinal infiltration by CD68-positive cells (black; arrows). Right panel shows the same section under Nomarski illumination to illustrate the colocalization of CD68-positive microglia with the migrated cells (GFP-labeled; arrows). **(B):** Confocal images from retinal sections of a 7-week-old RCS rat 2 weeks after injection of ChABC. Sections stained for CSPGs showed a marked reduction in the expression of the N-terminal region of CSPGs, neurocan, and versican (green fluorescence). **(C):** Left panel shows a retinal section of a 5-week-old nontransplanted RCS rat staining for the stub epitope. Spontaneous degradation of CSPGs is shown by the red staining. Right panel shows a retinal section of a 7-week-old rat 2 weeks after subretinal injection of ChABC. Red staining indicates the exposure of the stub epitope upon degradation of CSPGs by this matrix-degrading enzyme. **(D):** Histogram shows that subretinal injection of Müller stem cells into RCS rats induced a marked increase in the number of infiltrating microglia (*, $p < .05$ vs. nontransplanted animals) and that enhanced immune suppression induced a significant reduction in the number of infiltrating retinal microglia (**, $p < .001$ vs. transplanted animals). **(E):** Histogram depicting increased migration of Müller stem cells into the inner retinal layers when transplanted with ChABC. No cells were detected beyond the ONL in the control animals (−ChABC), whereas nearly 80% of cells migrated beyond the INL into the inner retinal layers with ChABC (*, $p = .001$). Results are the mean ± SEM of four different experiments. Abbreviations: ChABC, chondroitinase ABC; DZ, debris zone; GCL, ganglion cell layer; INL, inner nuclear layer; ONL, outer nuclear layer; RCS, Royal College of Surgeons; Ab, antibody.

However, little consideration has been given to the migration and integration of stem cells in long-standing retinal degeneration and inflammation. It is important to understand that tissue that needs repair has often undergone a series of inflammatory and degenerative changes, which may limit the functional integration of grafted stem cells. The present observations confirm previous reports that the neonatal retina provides a permissive environment in which stem cells can migrate and integrate. However, our results show that although grafted Müller stem cells migrated into the neonate LH retina, they were often found in association with cells expressing CD68, a marker of macrophage/microglia. Although recent evidence suggests that microglia not only promote neurotoxicity but also have a neuroprotective role and enhance nerve repair [35], it might be possible to speculate that they closely associate with the transplanted cells to promote their migration and survival. However, the present observations that extensive microglial activation was frequently associated with poor migration and survival of Müller stem cells strongly suggest that microglia may have been responsible for inhibiting cell graft migration and integration.

In accordance with previous studies, considerable microglial activation was seen in the degenerating retina of the dystrophic RCS rat prior to transplantation [20–22]. It is therefore likely that pre-existing activated microglia may constitute a first line of response to retinal stem cell transplantation, as they may be ready to exert their cytotoxic and phagocytic functions [35]. Stem cell clusters were often seen in the subretinal space of the RCS rat, densely surrounded by microglia and resembling granuloma-like structures. These clusters were not observed in the neonate LH rat retina, indicating that in the absence of microglia, the grafted cells were able to migrate into the retina. It is possible that the xenograft nature of the transplant (human cells to rat retina) further enhanced the microglia response, but allogeneic transplantation of Müller stem cells in the RCS rat retina resulted in similar microglia reactivity (data not shown).

CSPGs are produced during glial scarring in the central nervous system [24], and their role as inhibitory axon guidance molecules [25, 36] is well documented. We observed, in accordance with other studies, that the retina of the dystrophic RCS rat shows heavy accumulation of the N terminus of chondroitin sulfate proteoglycans [37], neurocan [38], and versican. Our results further demonstrated that microglia, which are known to produce CSPGs in vitro [39] and in vivo upon spinal cord injury [40, 41], also express the N-terminal fraction of CSPGs, as well as neurocan and versican in the degenerating RCS rat retina. Significantly, costaining of retinal sections from transplanted RCS rat retinae for CSPGs and CD68 expression showed that microglia surrounding the grafted cells stained for CSPGs. These observations suggest that one of the mechanisms by which microglia might be inhibiting stem cell migration and integration into the damaged retina is by releasing CSPGs.

Since stem cell migration from the subretinal space into the damaged or injured retina is crucial to retinal repair, we aimed to facilitate cell migration by inhibiting the microglial response in RCS rats using intraperitoneal indomethacin and a combination of oral prednisolone, cyclosporine, and azathioprine [18]. Despite a reduction in microglial accumulation in the vicinity of the transplants as a result of this treatment, residual microglial reactivity was still observed in association with the grafted cells. Microglia remained in the DZ, where CSPG accumulation was observed in the degenerating retina, indicating that microglial suppression alone is not sufficient to promote migration of the grafted cells.

Degradation of CSPGs by chondroitinase has been shown to promote migration of transplanted cells and regenerating axons through glial scars, particularly in the spinal cord [29–31], and in the retina it has been used to improve lentiviral vector-mediated transduction of photoreceptors [42]. Extensive work on the role of CSPG in neuronal plasticity has also revealed that the deposition of this extracellular matrix protein is inhibitory to the formation of new neuronal synaptic connections and is a mechanism by which the mature mammalian nervous system protects itself from the formation of aberrant neuronal synapses when injured [43]. In addition, ChABC has been shown to restore synaptic plasticity by breaking down the CSPG-rich perineural nets in the visual cortex of mature rats [44, 45], and more recent research showed that this enzyme causes improved synapse formation of transplanted photoreceptor precursors with host neurones [46]. On this basis, the role of ChABC might extend beyond its effect on cell migration by facilitating neurite extension of the transplanted cells, as suggested by the observation that Müller stem cells also adopted a neuronal morphology when grafted in the presence of this enzyme.

The present observations that ChABC, in conjunction with oral azathioprine/cyclosporine and intraperitoneal indomethacin, was able to dramatically improve migration of transplanted Müller stem cells into the retina strongly indicate that abnormal deposition of extracellular matrix and activation of the innate inflammatory responses constitute major barriers to retinal stem cell transplantation. Development and refinement of approaches to simultaneously modify the extracellular matrix and suppress microglia reactivity may therefore help to overcome the present limitations to achieve integration of stem cells into degenerated retina. However, further investigation is needed before effective cell-based therapies can be implemented for the treatment of human retinal disease.

ACKNOWLEDGMENTS

This work was supported by the Medical Research Council of the United Kingdom (Grant 67386), the Helen Hamlyn Trust (in memory of Paul Hamlyn), and the Henry Smith Charity. S.S. was supported by the Inlaks Foundation, India, and the Henry Smith Trust. P.T.K. was partially funded by the Department of Health's National Institute for Health Research Biomedical Research Centre at Moorfields Eye Hospital. We thank Dr. A. Vugler for providing the technique for horseradish peroxidase detection of CD68.

DISCLOSURE OF POTENTIAL CONFLICTS OF INTEREST

The authors indicate no potential conflicts of interest.

REFERENCES

1 Takahashi M, Palmer TD, Takahashi J et al. Widespread integration and survival of adult-derived neural progenitor cells in the developing optic retina. Mol Cell Neurosci 1998;12:340–348.
2 Qiu G, Seiler MJ, Mui C et al. Photoreceptor differentiation and integration of retinal progenitor cells transplanted into transgenic rats. Exp Eye Res 2005;80:515–525.
3 Lund RD, Adamson P, Sauve Y et al. Subretinal transplantation of genetically modified human cell lines attenuates loss of visual function in dystrophic rats. Proc Natl Acad Sci U S A 2001;98:9942–9947.
4 Lund RD, Wang S, Lu B et al. Cells isolated from umbilical cord tissue rescue photoreceptors and visual functions in a rodent model of retinal disease. STEM CELLS 2007;25:1089.
5 Dong X, Pulido J, Qu T et al. Differentiation of human neural stem cells into retinal cells. Neuroreport 2003;14:143–146.
6 Canola K, Angenieux B, Tekaya M et al. Retinal stem cells transplanted into models of late stages of retinitis pigmentosa preferentially adopt a glial or a retinal ganglion cell fate. Invest Ophthalmol Vis Sci 2007;48:446–454.
7 Banin E, Obolensky A, Idelson M et al. Retinal incorporation and differentiation of neural precursors derived from human embryonic stem cells. STEM CELLS 2006;24:246–257.
8 Gamm D, Wang S, Lu B et al. Protection of visual functions by human neural progenitors in a rat model of retinal disease. PLoS ONE 2007;2:e338.
9 Mizumoto H, Mizumoto K, Whiteley SJO et al. Transplantation of human neural progenitor cells to the vitreous cavity of the Royal College of Surgeons rat. Cell Transplant 2001;10:223–233.
10 Wojciechowski AB, Englund U, Lundberg C et al. Subretinal transplantation of brain-derived precursor cells to young RCS rats promotes photoreceptor cell survival. Exp Eye Res 2002;75:23–37.
11 Chacko DM, Das AV, Zhao X et al. Transplantation of ocular stem cells: The role of injury in incorporation and differentiation of grafted cells in the retina. Vision Res 2003;43:937–946.
12 Young MJ, Ray J, Whiteley SJO et al. Neuronal differentiation and morphological integration of hippocampal progenitor cells transplanted to the retina of immature and mature dystrophic rats. Mol Cell Neurosci 2000;16:197–205.
13 Sakaguchi DS, Van Hoffelen SJ, Young MJ. Differentiation and morphological integration of neural progenitor cells transplanted into the developing mammalian eye. Ann NY Acad Sci 2003;995:127–139.
14 MacLaren RE, Pearson RA, MacNeil A et al. Retinal repair by transplantation of photoreceptor precursors. Nature 2006;444:203–207.
15 Fischer AJ, Reh TA. Muller glia are a potential source of neural regeneration in the postnatal chicken retina. Nat Neurosci 2001;4:247–252.
16 Ooto S, Akagi T, Kageyama R et al. Potential for neural regeneration after neurotoxic injury in the adult mammalian retina. Proc Natl Acad Sci U S A 2004;101:13654–13659.
17 Raymond P, Barthel L, Bernardos R et al. Molecular characterization of retinal stem cells and their niches in adult zebrafish. BMC Dev Biol 2006;6:36.
18 Lawrence JM, Singhal S, Bhatia B et al. MIO-M1 cells and similar muller glial cell lines derived from adult human retina exhibit neural stem cell characteristics. STEM CELLS 2007;25:2033–2043.
19 Lewis GP, Fisher SK. Up-regulation of glial fibrillary acidic protein in response to retinal injury: Its potential role in glial remodeling and a comparison to vimentin expression. Int Rev Cytol 2003;230:263–290.
20 de Kozak Y, Cotinet A, Goureau O et al. Tumor necrosis factor and nitric

oxide production by resident retinal glial cells from rats presenting hereditary retinal degeneration. Ocul Immunol Inflamm 1997;5:89–94.
21 Thanos C, Richter W. The migratory potential of vitally labelled microglial cells within the retina of rats with hereditary photoreceptor dystrophy. Int J Dev Neurosci 1993;11:671–680.
22 Roque RS, Imperial CJ, Caldwell RB. Microglial cells invade the outer retina as photoreceptors degenerate in Royal College of Surgeons rats. Invest Ophthalmol Vis Sci 1996;37:196–203.
23 Jones LL, Margolis RU, Tuszynski MH. The chondroitin sulfate proteoglycans neurocan, brevican, phosphacan, and versican are differentially regulated following spinal cord injury. Exp Neurol 2003;182:399–411.
24 Morgenstern, Daniel A, Asher, RA et al. Chondroitin sulphate proteoglycans in the CNS injury response. In: McKerracher L, ed. Progress in Brain Research Spinal Cord Trauma: Regeneration, Neural Repair and Functional Recovery. Amsterdam, NL: Elsevier, 2002:313–332.
25 Jones LL, Sajed D, Tuszynski MH. Axonal regeneration through regions of chondroitin sulfate proteoglycan deposition after spinal cord injury: A balance of permissiveness and inhibition. J Neurosci 2003;23:9276–9288.
26 Inatani M, Tanihara H. Proteoglycans in retina. Prog Retin Eye Res 2002;21:429–447.
27 Sellés-Navarro I, Ellezam B, Fajardo R et al. Retinal ganglion cell and nonneuronal cell responses to a microcrush lesion of adult rat optic nerve. Exp Neurol 2001;167:282–289.
28 Cafferty WBJ, Yang SH, Duffy PJ et al. Functional axonal regeneration through astrocytic scar genetically modified to digest chondroitin sulfate proteoglycans. J Neurosci 2007;27:2176–2185.
29 Bradbury EJ, Moon LDF, Popat RJ et al. Chondroitinase ABC promotes functional recovery after spinal cord injury. Nature 2002;416:636–640.
30 Huang WC, Kuo WC, Cherng JH et al. Chondroitinase ABC promotes axonal re-growth and behavior recovery in spinal cord injury. Biochem Biophys Res Commun 2006;349:963–968.
31 Kim BG, Dai HN, Lynskey JV et al. Degradation of chondroitin sulfate proteoglycans potentiates transplant-mediated axonal remodeling and functional recovery after spinal cord injury in adult rats. J Comp Neurol 2006;497:182–198.
32 Limb GA, Salt TE, Munro PMG et al. In vitro characterization of a spontaneously immortalized human muller cell line (MIO-M1). Invest Ophthalmol Vis Sci 2002;43:864–869.
33 Yáñez-Munoz RJ, Balaggan KS, MacNeil A et al. Effective gene therapy with nonintegrating lentiviral vectors. Nat Med 2006;12:348–353.
34 Green MA, Sviland L, Malcolm AJ et al. Improved method for immunoperoxidase detection of membrane antigens in frozen sections. J Clin Pathol 1989;42:875–880.
35 Bessis A, Béchade C, Bernard D et al. Microglial control of neuronal death and synaptic properties. Glia 2007;55:233–238.
36 Inatani M, Honjo M, Otori Y et al. Inhibitory effects of neurocan and phosphacan on neurite outgrowth from retinal ganglion cells in culture. Invest Ophthalmol Vis Sci 2001;42:1930–1938.
37 Porrello K, LaVail MM. Immunocytochemical localization of chondroitin sulfates in the interphotoreceptor matrix of the normal and dystrophic rat retina. Curr Eye Res 1986;5:981–993.
38 Zhang Y, Rauch U, Perez MT. Accumulation of neurocan, a brain chondroitin sulfate proteoglycan, in association with the retinal vasculature in RCS rats. Invest Ophthalmol Vis Sci 2003;44:1252–1261.
39 Uhlin-Hansen L, Kolset SO. Cell density-dependent expression of chondroitin sulfate proteoglycan in cultured human monocytes. J Biol Chem 1988;263:2526–2531.
40 Jones LL, Yamaguchi Y, Stallcup WB et al. NG2 is a major chondroitin sulfate proteoglycan produced after spinal cord injury and is expressed by macrophages and oligodendrocyte progenitors. J Neurosci 2002;22:2792–2803.
41 Jones LL, Tuszynski MH. Spinal cord injury elicits expression of keratan sulfate proteoglycans by macrophages, reactive microglia, and oligodendrocyte progenitors. J Neurosci 2002;22:4611–4624.
42 Grüter O, Kostic C, Crippa SV et al. Lentiviral vector-mediated gene transfer in adult mouse photoreceptors is impaired by the presence of a physical barrier. Gene Ther 2005;12:942–947.
43 Rhodes KE, Fawcett JW. Chondroitin sulphate proteoglycans: Preventing plasticity or protecting the CNS? J Anat 2004;204:33–48.
44 Berardi N, Pizzorusso T, Maffei L. Extracellular matrix and visual cortical plasticity: Freeing the synapse. Neuron 2004;44:905–908.
45 Pizzorusso T, Medini P, Berardi N et al. Reactivation of ocular dominance plasticity in the adult visual cortex. Science 2002;298:1248–1251.
46 Suzuki T, Akimoto M, Imai H. Chondroitinase ABC treatment enhances synaptogenesis between transplant and host neurons in model of retinal degeneration. Cell Transplant 2007;16:493–503.

Chondroitin Sulfate Proteoglycans and Microglia Prevent Migration and Integration of Grafted Müller Stem Cells into Degenerating Retina

Shweta Singhal, Jean M. Lawrence, Bhairavi Bhatia, James S. Ellis, Anthony S. Kwan, Angus MacNeil, Philip J. Luthert, James W. Fawcett, Maria-Thereza Perez, Peng T. Khaw and G. Astrid Limb

Stem Cells 2008;26;1074-1082; originally published online Jan 24, 2008;
DOI: 10.1634/stemcells.2007-0898